CANADIAN THESES

THÈSES CANADIENNES

NOTICE

AVIS

THIS DISSERTATION
HAS BEEN MICROFILMED
EXACTLY AS RECEIVED

LA THÈSE A ÉTÉ
MICROFILMÉE TELLE QUE
NOUS L'AVONS REÇUE

BRAIDED FLUVIAL ARCHITECTURE WITHIN A RAPIDLY SUBSIDING BASIN: THE PENNSYLVANIAN CUMBERLAND GROUP SOUTHWEST OF SAND RIVER, NOVA SCOTIA

by

Carlos J. Salas

A thesis submitted to the School of Graduate Studies in partial fulfillment of the requirements for the degree of Master of Science in Geology

UNIVERSITY OF OTTAWA
OTTAWA, CANADA, 1986

ISBN 0-315-33246-8

ACKNOWLEDGEMENTS:

Innumerable people have aided in the completion of this thesis (scientifically and otherwise), and it is difficult to name all of them without leaving somebody out. Nevertheless I will make a feeble attempt.

I would like to thank Dr. B.R. Rust for his helpful advise in many matters, supervision, and financial support. Drs. W.L. Duke and R.G. Walker are acknowledged for their help in finding proper methods for analysing cyclicity.

Special thanks are warranted to M.J. Shields for his great field work (on very dull "nanoprojects"), perseverance and companionship. I would also like to thank Joanne Wallace for her field work, typing and for sticking with me through thick and thin.

Many thanks also go out to the always helpful Edward Hearn for his sage advice on many matters, and for making the G.A.C. talk in Fredericton a success. I would also like to thank Sue Meunier for the use of the "good" typewriter.

My colleages Iain, Penny, Geof, Gary, Susie, Dana, Margie and the "baseball boys" are thanked for all their help throughout the years on all matters. Last but not least I would like to thank Art Rupp and Charlie Bruce for putting a pot of gold at the end the rainbow!

TABLE OF CONTENTS:

FIGURES

TABLES

APPENDICES

ABSTRACT

The Pennsylvanian Cumberland Group consists of five distinctive units comprising two coarse units overlain by a finer grained succession. It is divided into: i) the Lower Coarse Unit; ii) the Middle Coal-bearing Unit; iii) the Middle Non-coal bearing Unit; iv) the Upper Coarse Unit; and v) the Upper Fine Unit. The Upper Coarse; Middle Non-coal bearing and Lower Coarse Units are the subject of this present investigation. These units were deposited within a rapidly subsiding intermontane basin by a series of alluvial fans, transverse braidplains and trunk braidplains.

The Lower Coarse Unit comprises poorly sorted matrix-supported conglomerates, rims the basin margin and is interpreted as alluvial fan deposits derived from the adjacent uplands (Cobequid and Caledonian Highlands). The Middle Fine Unit consists of grey mudstones, and thin coals, thought to have been deposited on wetlands marginal to the alluvial fans.

The Upper Coarse Unit can be subdivided into deposits from an axial trunk braidplain and a subordinate transverse braidplain. The axial trunk braidplain shows contrasting fluvial architecture in the proximal and distal reaches. The proximal reaches are coarser grained (conglomeratic), display thick amalgamated cycles (10m to 40m) which coarsen- and

thicken upsection. With increasing distality cycles become finer grained, bedding thickness decreases and three dominant fluvial architectural styles are displayed, indicative of different avulsive/abandonment mechanisms. The cycles are marked by conglomeratic/sandstone coarsening/fining-upward cycles and coarsening-upward cycles. The CUFU cycles average 10m thick, have sharp lower contacts with the underlying fine member. They FU in the upper metre and are sharply overlain by a fine member. Paleocurrents in the lower part of the cycle diverge from those of the underlying cycles and the overlying in-channel deposits. This feature together with the nature of the facies associations suggest that allocyclically-induced avulsion was marked by sheet (crevasse)-splays prograding into the adjacent wetlands. Splay progradation was followed by in-channel deposition of trough crossbeds and finally a short period of gradual abandonment resulting in the CUFU cycles. CU cycles differ by lacking a period of gradual abandonment - hence they are sharply overlain by fine members, suggestive of avulsion.

The fluvial architecture of the tranverse braidplain is quite different from that of the axial system. The cycles are thinner, have a very well developed fining-upward motif, thicker fine members and gradational contacts, indicative of gradual channel abandonment rather than avulsion. Differences in architectural styles are ascribed to differing sedimentation rates.

Vertical and lateral facies associations within the study area show that an initial fanglomerate stage resulted from uplift (or back-stepping) in the Cobequid Highlands. This was followed by progressive onlapping of the basin margin by a trunk river. Sediment loading along the basin axis created flexural upwarp in the adjacent uplands and initiated the progradation of detritus shed from the Cobequid Highlands in the form of a transverse braidplain.

1.0 INTRODUCTION

1.1 Location and Access

The Cumberland Group is located in northwest Nova Scotia and outcrops along the east coast of Chignecto Bay (Bay of Fundy) between Joggins and Squally Point (Figs.1,2). This study concentrated on the continuously exposed 25km coastal section between Sand River and Squally Point. The whole section can be examined (from north to south) by entering the following access points: i) Sand River; ii) Two Mile Brook; iii) Birch Cove; iv) Pollys Flats; v) Edgetts Beach; vi) West Apple River (see access map Fig.1). Care should be taken when examining these sections due to the diurnal 20m tides - the largest in the world. Lumbering roads leading to the aforementioned access points are in very poor condition and should not be attempted without, at the very least a small front wheel drive vehicle (a four wheel drive would be the best suited).

1.2 Regional Geology

The Cumberland Basin is a major basin contained within the much larger Fundy Rift Zone of the Maritime Provinces. The basin covers approximately 1036 square kilometres and extends along the Isthmus of Chignecto in a northeasterly direction up to Prince Edward Island, which it probably

LOCATION AND ACCESS MAP

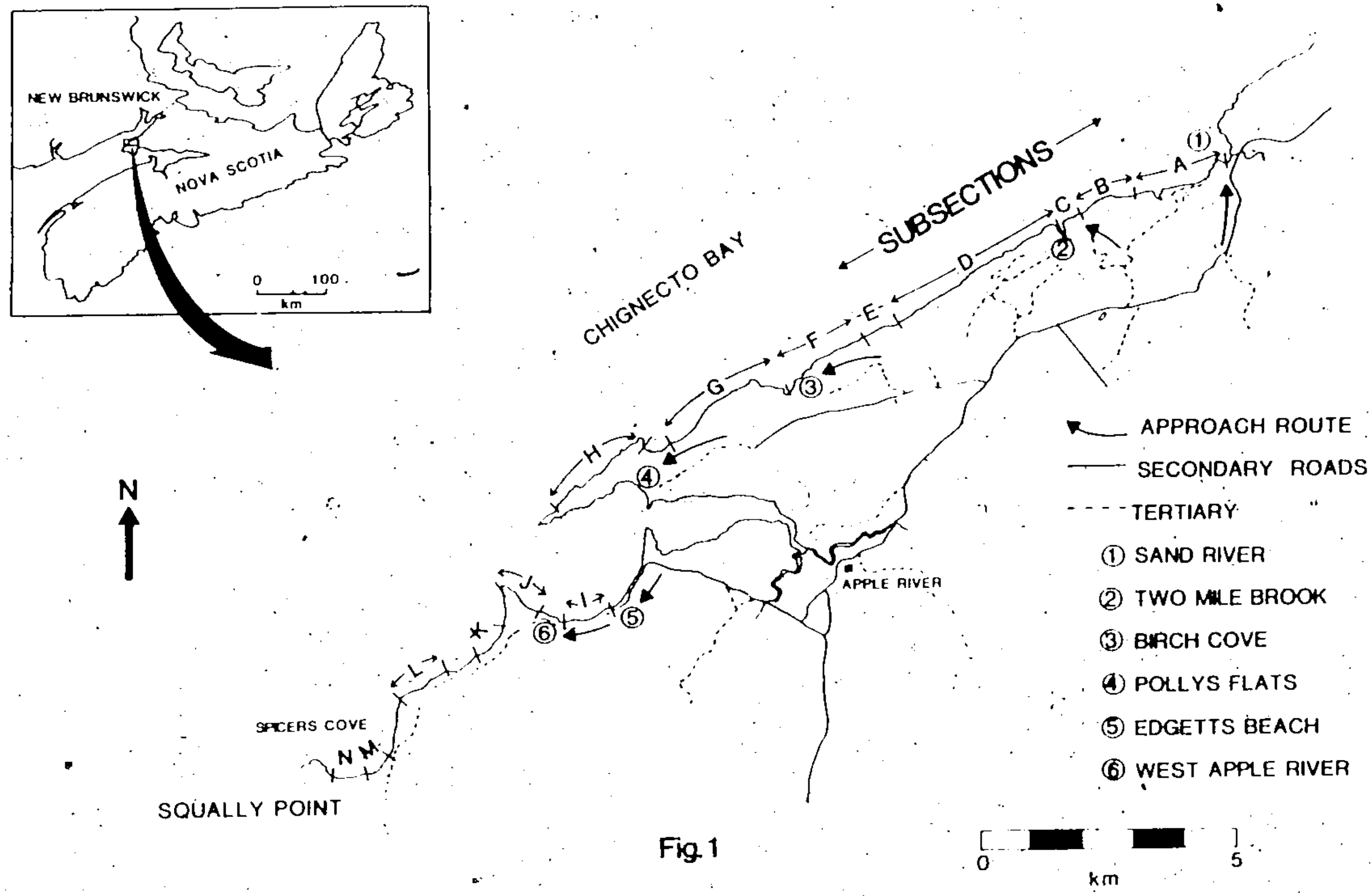

Fig. 1

Fig. 2 GEOLOGY OF THE CUMBERLAND GROUP (after Calder, 1982)

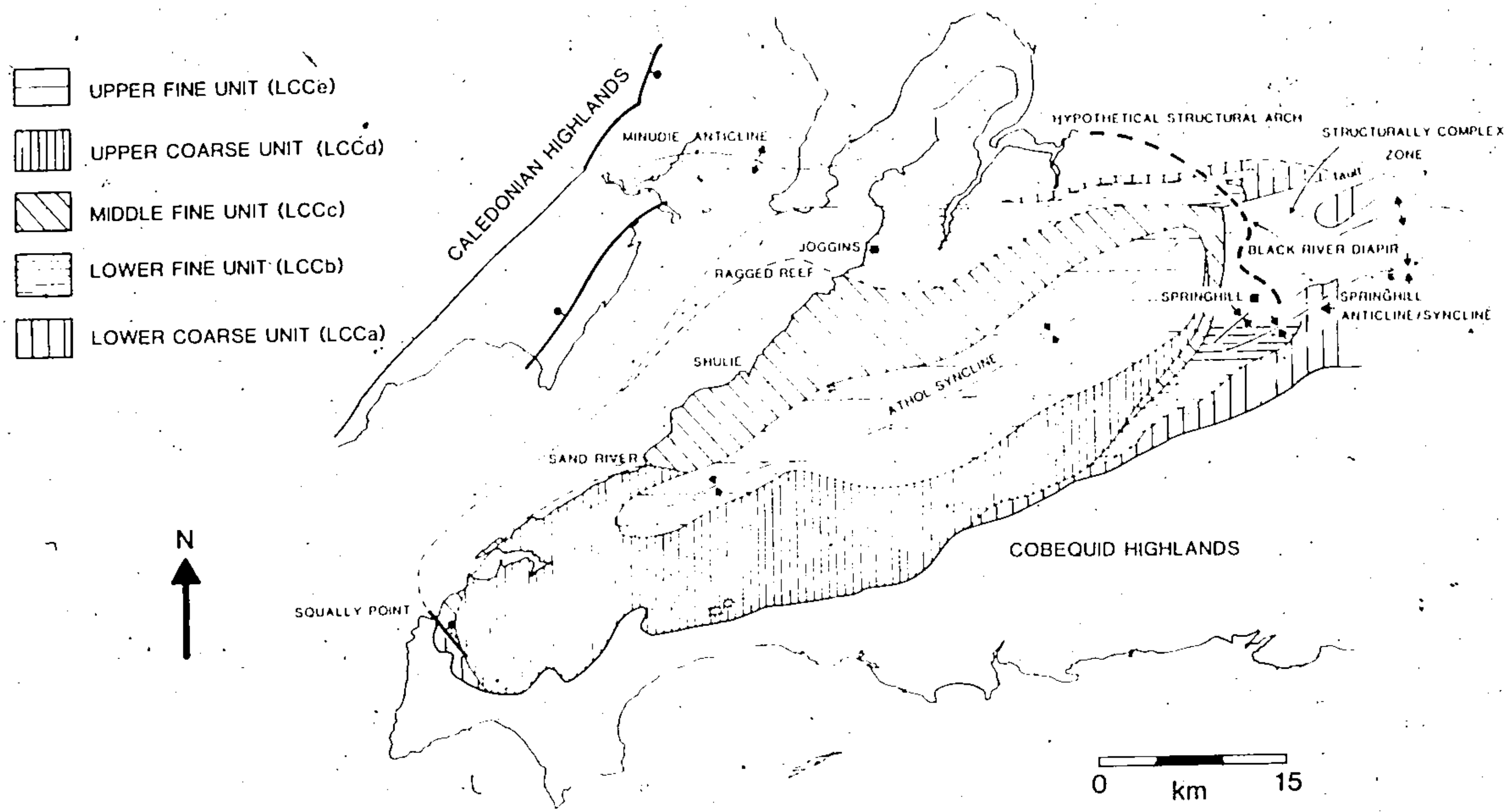

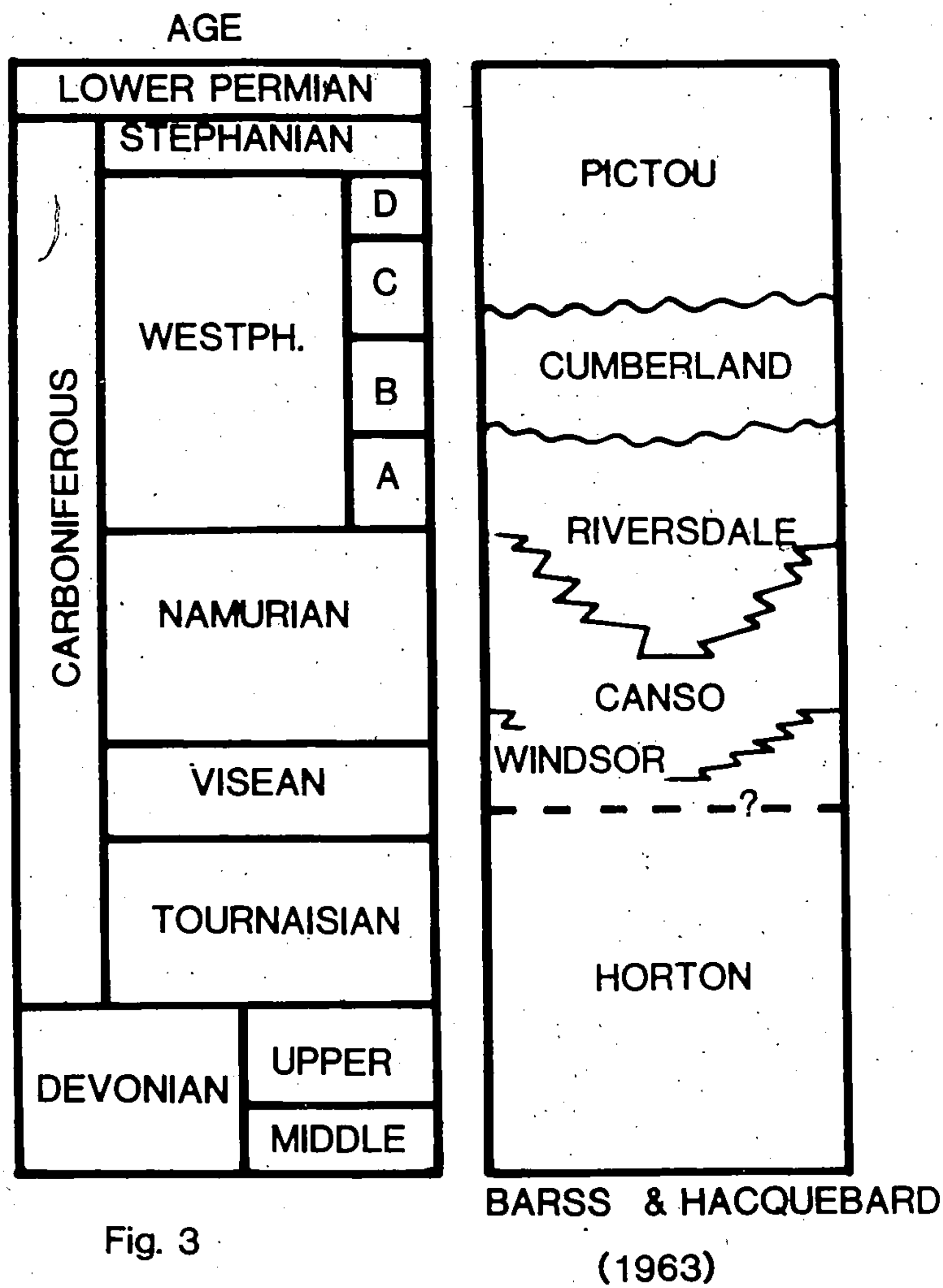
AGE
LOWER PERMIAN
STEPHANIAN
CARBONIFEROUS
WESTPH.
D
C
B
A
NAMURIAN
VISEAN
TOURNAISIAN
DEVONIAN
UPPER
MIDDLE
PICTOU
CUMBERLAND
RIVERSDALE
CANSO
WINDSOR
?
HORTON
BARSS & HACQUEBARD
(1963)

Fig. 3

underlies (Copeland,1958). The basin axis is marked by the Athol syncline and lesser folds which are found in the northeast part of the basin. The northwestern Minudie anticline and Springhill anticline/syncline are thought to be due to diapirs from the underlying Windsor Group (Copeland,1958). Gravimetric work by Garland (1953) in this region has shown that a northwesterly trending arch may exist between these two structures, possibly due to interconnection of the diapirs. The presence of a syndepositional arch is corroborated by the lack of Cumberland strata north of the Minudie anticline and the unconformity with the underlying Riversdale Group. The basin is bounded to the south and northwest by the Cobequid and Caledonian Highlands respectively (Fig.2). The Cobequid Highlands are an accreted terrane (Keppie,1985) composed primarily of Proterozoic and Early Paleozoic sediments, metasediments, felsic plutonic and volcanic rocks. The Caledonian Highlands are principally of Proterozoic age and comprise metasediments felsic/intermediate volcanics and minor Mississippian sediments. The Caledonian Highlands may also be an accreted terrane (Giles and Ruitenberg,1977).

The Cumberland Basin is thought to have been created during the Lower Devonian Acadian Orogeny (Hacquebard and Donaldson,1964). The non-marine Horton Group (Tournaisian) was the first deposit (Fig.3) within the basin and comprises continental sediments and volcanics. It is exposed along the coast north of Joggins. During the Visean stage a marine transgression deposited the associated carbonates and evaporites of the Windsor Group - the only marine sediments within the basin (Hacquebard,1972). A regression ,initiated during the late Visean, reinstated non-marine conditions which persisted during the rest of the Paleozoic and deposited the Canso and Riversdale Groups. A late phase of the Acadian Orogeny, during Westphalian A time caused transpression in southern New Brunswick, and resulted in a zone of extension between the sinistral Harvey-Hopewell Fault (see Fig.86, Belt,1968) and the dextral Cobequid-Chedabucto Fault (Bradley,1982). This formed a southerly dipping homocline (half graben) whose exact configuration with respect to the surrounding basin margin is difficult to discern due to the lack of seismic data. The few seismic lines that have been shot in this area have been hampered by poor resolution because of the presence of igneous basement close to the surface (R. Leatherbarrow, pers. comm. 1985). The initiation of extensional tectonics between the Harvey-Hopewell and Cobequid-Chedabucto Faults during the Westphalian A resulted in the deposition of the first Cumberland Group sediments (Fig.3).

1.3 Previous Work and Stratigraphy

The Cumberland Group has been known primarily for its coal as far back as the eighteenth century, when coal was mined at Joggins by French settlers from Fort Beausejour (near present day Amherst, Nova Scotia). The first published account of the basin was by T.C. Haliburton (1829) who described the Joggins section. More detailed work was completed by Sir Charles Lyell (1843) and subsequently by the first Director of the Geological Survey of Canada, Sir William Logan (1845), who subdivided the group into five divisions. Further work was done on this section in 1853 by Lyell and Dawson. Fletcher (1908) was the first to measure the section from Shulie to Spicer's Cove but aside from Fletcher, and this study, no detailed work has been done south of Sand River. Since the early twentieth century, work on the Cumberland Group has been sporadic and only concerned with the coal-bearing strata of Joggins and Springhill (Bell,1944; Copeland,1958; Hacquebard and Donaldson,1964; Way,1968; Duff and Walton,1973; Kaplan and Donahue,1980; Calder,1984; Rust et al.,1984).

Bell (1914) was the first to subdivide the group into formations based on lithologies: the upper Shulie Formation comprising sandstones and shales and the lower Joggins Formation comprising basal conglomerates overlain by coal-bearing mudstones, passing up into conglomerates, sandstones and shales. The contact between the formations was defined at the base of the upper conglomeratic facies. In 1944 Bell abandoned the formational names, stating that "this division was of little practical value for mapping purpose(s)" and redefined the Cumberland Group to include strata that lie unconformably or disconformably above the Riversdale Group and unconformably below the Pictou Group (Fig.3). Shaw (1951) subdivided the basin into five facies based on lithology - two coarse clastic facies overlain by finer grained units, with the middle fine facies subdivided into a coal-bearing and non coal-bearing facies. These facies are considered to be a series of interfingering wedges not bound by time planes. Subsequent workers (Calder,1982; Donohoe and Wallace,1982) have followed this five-fold subdivision of the basin. No attempts have been made to define formations in this study due to the diachronous nature, lateral/vertical variability, and lack of inland exposure of the studied units. This study will use the same basic nomenclature proposed by Shaw (1951), and modified by Calder (1982), with only a slight modification. Shaw's (1951) use of the word "facies" is not in accordance with the normal definition of the word (c.f. Middleton,1978) and hence it will replaced by the term "stratigraphic unit".

The five stratigraphic units are characterized by the following:

<u>Lower Coarse Unit:</u>

The Lower Coarse Unit (LCCa of Calder,1982) is exposed around the periphery of the basin where it offlaps from the adjacent highlands. It attains a maximum thickness of 1300m proximal to the Cobequid Highlands, near Springhill (Copeland,1958; Bell,1958). Grain size and angularity trends imply that this facies thins toward the interior of the basin (Copeland,1958; Calder,1984). In this study it is exposed north of Squally Point.

Lower Fine Unit:

The Lower Fine Unit (LCCb) is the most economically important and hence the most studied unit, comprising mudstones, minor limestones, sandstones and thick coals. This unit is best developed in the northern part of the basin (eg. Joggins and Springhill). The contact with the overlying non coal-bearing Middle Fine Unit (LCCc) has been placed at the highest known coal horizon (Hacquebard and Donaldson,1964). Shaw (1951) was able to trace this horizon from Joggins to Springhill using aerial photographs and noted that it closely matched the inferred junction with the two coarse units - hence it is postulated that the top of the Lower Fine Unit approaches a time line (Haquebard and Donaldson,1964). The Lower Fine Unit is dated as Westphalian B.

Middle Fine Unit:

The Middle Fine Unit (LCCc) comprises sandstones, mudstones and minor conglomerates, and is best developed along the coast between Shulie and Ragged Reef. The only southerly exposure of this unit is at Spicer's Cove, where several coal seams are found. These coal seams have been dated by Hacquebard (1960) and Hacquebard and Donaldson

(1964) as Westphalian C typical of the Lonchopteris zone of the Morien Group, which is the Sydney Coalfield equivalent of the Pictou Group (i.e. the Cumberland Group is partly equivalent with the Pictou Group). The Cumberland-Pictou boundary may be diachronous throughout Nova Scotia (G. Yeo, pers. comm., 1986).

Upper Coarse Unit:

The Upper Coarse Unit (LCCd) consists of conglomerates, sandstones, and minor mudstones and can be seen on the coast between Sand River and Spicer's Cove. This unit is found only in the southern limb of the Athol syncline. It has been argued that this unit continuously onlaps the basement margin (i.e. the Cobequid Highlands, Copeland, 1958; Haquebard and Donaldson, 1964; Calder, 1982;1984, pers. comm.) - this is regarded by this author as a moot point and will be discussed in section 10.3.

Upper Fine Unit:

The Upper Fine Unit (LCCd) is the uppermost unit comprising reddish siltstones and sandstones, and is only found along the axis of the Athol syncline.

1.4 Method of Study

Mapping commenced at Sand River and proceeded southwesterly along the coast to Squally Point, where the Cumberland Group lies with angular nonconformity on the underlying undifferentiated volcanics of the Fountain Lake Group (part of the Cobequid Highlands). A total of fourteen

GENERAL STRATIGRAPHY

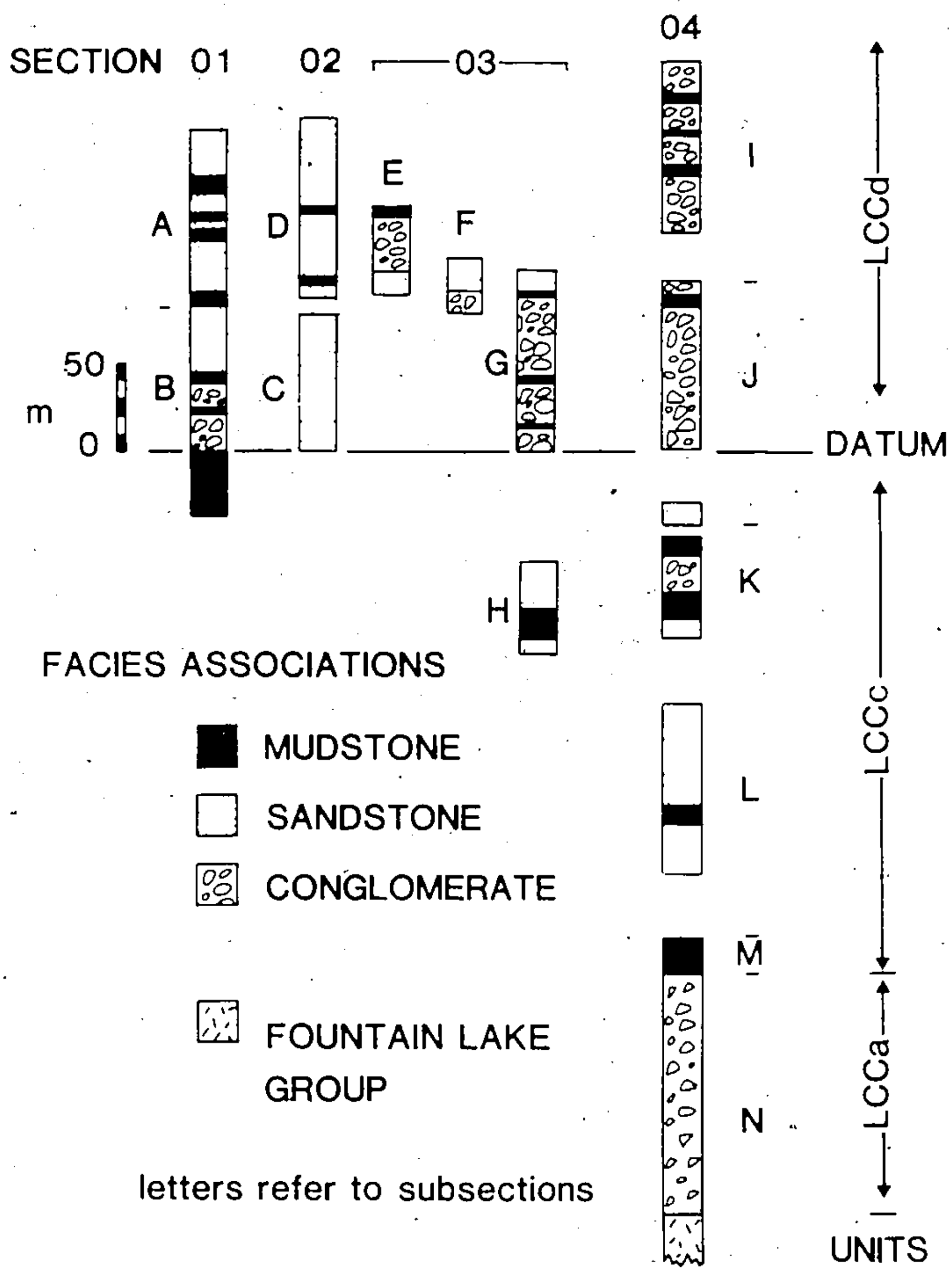

Fig. 4

after Calder, 1982

subsections were delineated and labelled A through N (Fig. 4). These sections are shown in Appendices 2-8. Units within each subsection are numerically coded beginning at one, whereas cycles are noted by the subsection letter and a roman numeral (eg. AIV). Cycles are always numbered in stratigraphically ascending order (eg. AIV overlies AIII), whereas units are numbered according to which was encountered first while mapping (i.e dependant on northerly or southerly dip of strata). The fourteen subsections were compiled into four laterally equivalent sections: section 01 comprising subsections A and B; section 02 made up of subsections C and D; section 03 comprising subsections E,F,G, and H and section 04 consisting of subsections I through N. The lateral correlation of these sections is based on facies, facies associations, clast provenance studies, petrology and aerial photography (Fig.4). The datum used for correlation was the contact between the Upper Coarse Unit and the Middle Fine Unit (Calder,1982).

The understanding of controls on cyclicity was aided by choosing appropriate mapping techniques. Each cycle was mapped and the following characteristics were noted wherever possible: vertical and lateral facies trends (including vertical and lateral variations in set size); vertical and lateral paleocurrent trends; relationships between coarse and fine members; log orientation and clast analysis. Clast analysis involved the systematic measurement of apparent A and B axis length, angularity, and determination of lithology for one hundred clasts (discussed further in section 8.2.1). Each sample locality was also photographed in order to measure the percentage of matrix. Each coarse and fine member was sampled for later petrographic analysis (note: thin sections were only made for strategic cycles). Sampled locations are shown in App.1. A glossary of some terms specifically used in this study can be seen in App.17.

1.5 Aims of Study

Very little work other than reconnaissance mapping has been done since Fletcher (1908) measured the section south of Sand River. The aims of this study are:

i) Paleogeographical and depositional modelling of the sediments deposited in this part of the basin.

ii) Determination of controls on fluvial architecture within a rapidly subsiding basin.

iii) Introduction of some alternative methods for the study of sedimentation and tectonics.

2.0 FACIES DESCRIPTIONS

2.1 Introduction

Subdivision of units into lithofacies was aided by using an expanded version of Miall's (1977,1978) and Rust's (1978b) fluvial facies classification. The addition of subscripts to the facies codes allowed: i) a more rapid and efficient way of mapping the sediments; ii) reinforcement of subtle, yet important, differences within sequences dominated by one lithofacies. Hence, subsequent analysis of facies and facies associations was able to draw, where necessary, on a much greater data base. The first three sections are composed of twelve major lithofacies, described herewith.

2.2 Mudrock Lithofacies (F)

2.2.1 Fm-Massive Mudstones

Massive mudstones (Fm) comprise between 5.5% to 9.5% of the measured sections. The average thickness is 1.28m (n=45 s=1.09) and ranges between 0.2m to 4.7m. Massive mudstones, as the name implies, are massive with scoured upper and erosive lower bounding surfaces and lack any visible sedimentary or biogenic structures. Fm can be subdivided into red massive mudstones, grey massive mudstones, and mottled massive mudstones.

Red massive mudstones range from argillaceous siltstones to claystones and make up 50% of the Fm occurrences. Red massive mudstones are commonly associated with other Fm-type lithofacies and low energy sandstone lithofacies (eg. Sr, Sm). Grey massive mudstones make up 27.5% of the Fm occurrences and consists of argillaceous siltstones to claystones. Macerated carbonaceous plant fragments, of <u>Sigallaria</u> <u>sp</u>. and <u>Calamites</u> <u>sp</u>. affinities, are commonly interspersed throughout the units. Grey massive mudstones are found most commonly (in 53% of the cases) as thin units (< 0.20m) underlying thick sheet channel sandstones or conglomerates and overlying red mudstones. This is attributed to reduction of the previously oxidized red massive mudstone by reducing waters within the sheet channel unit. Similar occurrences have been reported by Rust et al. (1984) in the Middle Fine Unit (LCCc) of the Cumberland Group around McCarren Creek (3km south of Joggins).

Mottled massive mudstones comprise claystones to argillaceous siltstones and constitute 22.5% of the total Fm. Mottling is in the form of grey and red amorphous patches within red and grey massive mudstones respectively,and often is associated with rhizoliths. Carbonaceous fragments are found within the grey mottles but are rare in the red mottles. Mottling can be attributed to either reduction of the oxidized mudstones around roots or syngenetic percolation of reducing waters into subaerially exposed mudrocks

(Gibling, 1978).

2.2.2 Fl- Laminated Mudrocks

Laminated mudrocks (Fl) comprise 0% to 4.2% of measured sections. Fl is composed of argillaceous siltstones and claystones, and is internally stratified by either low flow regime plane beds or small-scale ripple cross-lamination (ripple sets rarely exceeding 0.01m in thickness). Fl units have planar non-erosive upper and lower bounding surfaces and usually contain small macerated plant fragments. Fl is intimately associated with the other mudstone lithofacies (Fm, Fr) and commonly passes laterally into one of them. Fl can be subdivided into red laminated mudrocks grey laminated mudrocks and mottled laminated mudrocks. The interpretation of colour variation is the same as that put forward under lithofacies Fm.

2.2.3 Fr- Rooted Mudstones

Rooted mudstones (Fr) constitute between 0% to 11% of the measured sections (average 4.1%). Fr is composed of argillaceous siltstone-claystone with varying amounts of rhizoliths (Fig.5), Stigmaria roots being the most common. Fr

Fig.5. Rhizoliths in lithofacies Sm (in cycle GII at loc.27). Scale on notebook is in tenths of a foot.

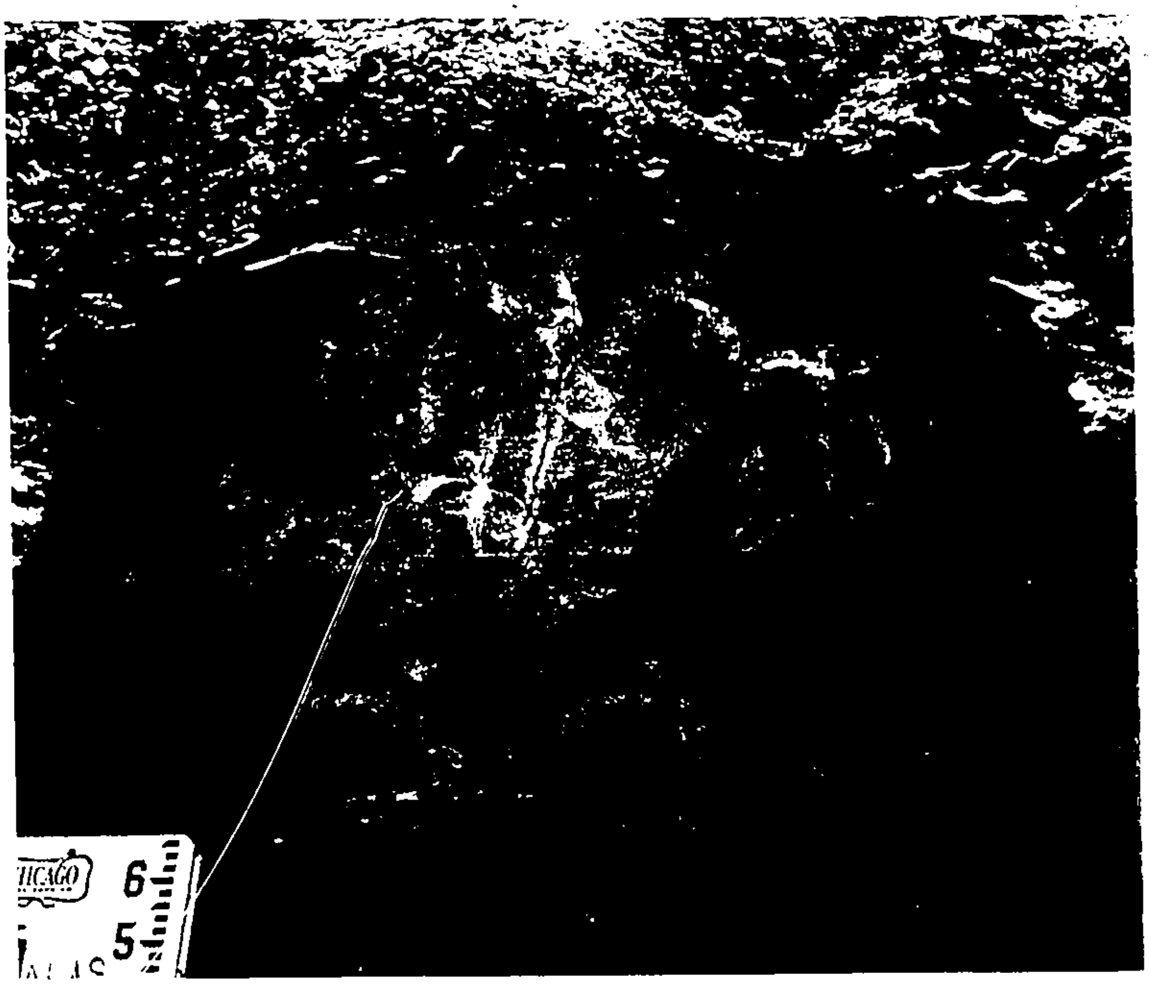
CHICAGO
6
5

units have an average thickness of 1.39m (n=14, s=0.51) and range from 0.5m to 2.3m. Fr can also be subdivided into red rooted mudstones, grey rooted mudstones, and mottled rooted mudstones. Red rooted mudstones are the most common, making up 47.4% of the total Fr occurrences followed by mottled rooted mudstones (36.8%) and grey rooted mudstones (15.8%). These ratios may indicate that an oxidation continuum exists between these subfacies that relates to subaerial exposure time. Hence the predominance of red rooted mudstones may indicate either prolonged subaerial exposure between channel avulsions or the prevalence of well drained soil conditions (Bown and Kraus, 1981). The absence of desiccation cracks and calcretes suggests either that high deposition rates proximal to channel margins prohibited calcrete growth (Leeder, 1975); or that calcrete growth was inhibited by a humid climate (Allen, 1974). A humid paleoclimate is postulated from the abundance of rooted horizons, carbonized flora, rare raindrop imprints (Fig.6), and lack of desiccation cracks.

The percentage of Fr increases from sections 03 to 01 (i.e. from south to north), and also upsection, denoting progressive changes in fluviatile style due to overriding allocyclic controls (Miall, 1980). This will be further discussed in section 6.2.

Fig.6. Raindrop imprints in cycle BI (1.71km NE of loc.1). Molds are found underneath hammer while original imprints are to the right. Hammer head is 0.15m.

2.3 Sandstone Lithofacies (S)

2.3.1 Sm, Sr- Massive , Ripple Cross-laminated Sandstones

Massive sandstones (Sm) are a very minor facies comprising an average of 0.5% of the measured sections, with a maximum of 11.8% per sector. Unit thicknesses range from 0.2m to 2.2m, with a mean of 1.03 (n=3, s=1.04). Sm is characteristically very fine-grained (4.0ϕ to 3.0ϕ), very well sorted sandstone, lacking visible sedimentary or biogenic structures. Sm units are sharp-based and generally fine upwards into siltstones/mudstones and laterally into Sr or lower flow regime plane beds. Sm is prevalent in heterolithic assemblages. Red and grey mottling is common in this facies and along with its massive nature suggests that these are overbank deposits which have been severely root turbated by plants.

Ripple cross-laminated sandstones (Sr) constitute an average of 2.7% of the measured sections and range between 1.4% to 5.1% per section. Sr units have a mean thickness of 1.05m (n=29, s=0.56) and range between 0.3m to 2.5m. Sr ranges from very fine grained (4.0ϕ to 2.5ϕ) to lower fine grained , very well sorted sandstones with small-scale cross laminae in sets rarely exceeding 0.02m thick. Foresets are occasionally draped with thin mudstone laminae and fragmented organic material. The lack of three dimensional exposures did not allow positive identification of the ripple types, but the irregular cut-and-fill nature of the cross-laminae suggests that the ripples are not regular, and most probably are asymmetric linguiod types (Allen, 1968). A small percentage (10.3%) of the Sr occurrences are type B climbing ripple drift (Jopling and Walker, 1968). Sr units have sharp non-erosional bases and may grade upward into mudstones. Upper contacts may be erosional in nature; Sr is also laterally transitional into lower and upper flow regime plane beds and occasionally into St. Sr is found in heterolithic overbank assemblages (40% of occurrences), or the top of sheet sandstones or conglomerates (40%) and at the base of sheet sandstones (20%) - rarely in the middle of a cycle. Percentages of Sr increase up-section and laterally from section 03 to 01, implying a progressive change in fluviatile style due to allocyclic controls (further discussion in 6.2).

2.3.2 Sl, Sh - Low Angle Cross-Stratified and Plane-bedded Sandstones

Low angle stratified sandstone (Sl) constitutes 0.5% of the sections, ranging from 0%-1.8%. Sl units have a mean thickness of 0.9m (n=2) and range from 0.8m to 1.0m. Sl is composed of very well sorted, fine to very fine grained (4.0Ø to 2.5ϕ) sandstone, with strata inclined at angles much less than the angle of repose (less than 10^{o} by definition; Miall, 1978). Parting lineation is a common internal structure and indicates supercritical flow conditions (Crowell,1959; Allen 1982). Sl is found most commonly at the top of sandstone/conglomeratic fining-upward cycles and is laterally and vertically transitional to Sh and Sh/F respectively. Sl is interpreted as formed by scour filling under supercritical flow conditions. Sl is also intimately associated with Sp, St and Gp bar complexes which will be discussed under lithofacies Gp.

Plane-bedded sandstones (Sh) make up an average of 2.8% of measured sections and range between 1.2% to 6.9%. Sh units range from 0.6m to 2.0m in thickness with a mean of 1.48m (n=19,s=1.02). Sh is composed of very fine to fine grained (4.0ϕ to 2.5ϕ), very well sorted sandstones and can be divided into two subfacies - the subfacies distinction is between lineated (Sh(u)) and non-lineated (Sh(l) plane beds, interpreted as upper flow regime and lower flow regime respectively. Sh(u) is the most common of the two (78.9% of occurrences) and is denoted by straight, concordant, non-undulating laminae arranged in thin to medium-sized beds with bedding surfaces displaying parting lineation (Crowell, 1959). Sh(u) is found at the top of sandstone/conglomeratic fining-upward cycles and is commonly laterally and vertically transitional to St, Sr, Sh(l), or F. Sh(u) is also found as topsets in Gp-, Sp-type bar complexes (discussed in lithofacies Gp). Sh(l) comprises 21.1% of Sh occurrences and is differentiated on the basis of no parting lineations, and presence of undulating sandstone laminae commonly intercalated with thin discontinuous lutite laminae. Sh(l) is found associated with heterolithic overbank assemblages and in the upper parts of cycles. No consistent lateral or vertical trends were noticed in Sh.

2.3.3 Sp: Planar-Tabular Cross-Stratified Sandstones

The nature of Sp and its facies associations makes an estimate of its abundance very difficult. Sp is associated with conglomeratic lithofacies Gp and Gt, pebbly sandstones (St(c)) and can be divided into two types.

Type 1 Sp has low angle (commonly $<15^{0}$) planar foresets with parting lineation, which are laterally equivalent to and/or onlap Gp, Gt or St(c) (Fig.7a). Lateral contacts between the different facies types may or may not be marked by reactivation surfaces. The lower bounding contact of Sp is delineated by an intraclast or pebbly lag; the upper bounding surface may be erosional (Se) or may have Sh/Sl topsets, upstream from the Sp foresets, and overlying the core Gt, Gp, or St(c). In many cases these topsets are laterally continuous and gradational into Sp foresets. The

TYPE 1 and 2 Sp BAR COMPLEXES

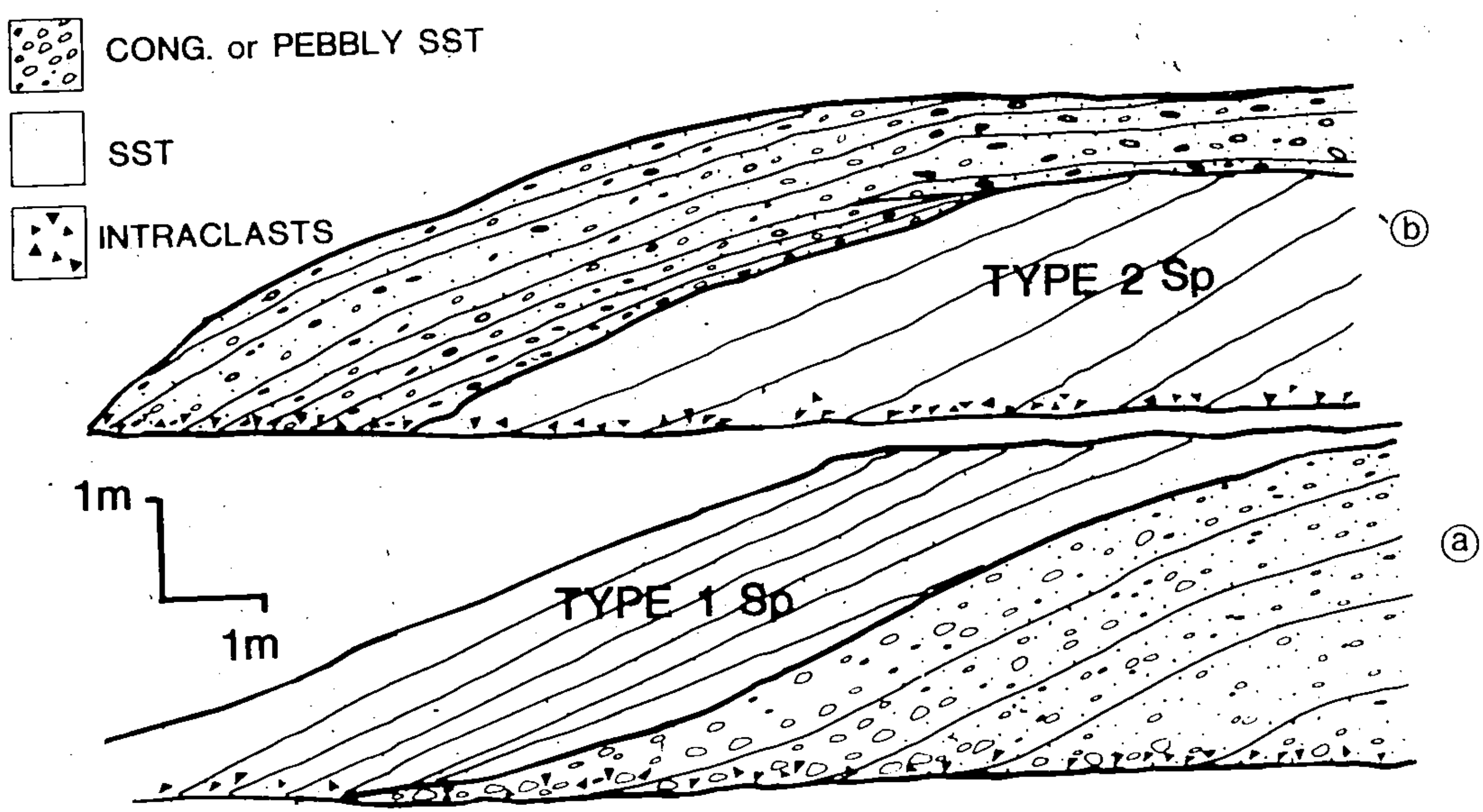

Fig. 7

entire complex comprises a single set ranging between 0.8m to 3.5m and is most often found at the base of sheet channel sandstones or conglomerates scouring into the underlying mudstones. Sp-type bar complexes are commonly laterally persistant over 20m.

The second type of Sp set has low angle (commonly <15^{0}) planar foresets that are laterally equivalent to and/or are onlapped by Gp, Gt or St(c) (Fig.7b). The most common lateral associations are Sp-> Gp-> Gt, Sp->St(c), or Sp->Gt; contacts between facies may be gradational or may be marked by reactivation surfaces. The lower bounding surface of Sp is intra-and extraclast strewn while the upper bounding surface, upstream from the Sp foresets, may be erosional (Se) and overlain by Sh/Sl or Gl (low angle stratified gravel topsets belonging to the offlapping coarser-grained facies). In many cases, topsets belonging to the offlapping coarser-grained facies are laterally traceable into foresets (Fig.7b). The bar complex comprises a single Sp set with a mean thickness of 0.8m with a range of 0.7m to 3.0m. Type 2 Sp is also commonly found at the base of sheet channel sandstones or conglomerates.

Types 1 and 2 Sp are interpreted respectively as the result of waning and waxing flows. A flood to waning stage origin is hypothesized for type 1 Sp due to : i) large size of the bedforms (average thickness 2.0m, range 1.0m to 4.0m);

ii) positioning beneath erosively-based sheet-channel sands; iii) erosive lower bounding surface (created during flood stage); iv) large paleocurrent deviation from the overlying strata; v) decrease in grain size from the coarser grained "core" facies to the offlapping Sp. A mechanism for the formation of type 1 Sp would necessitate a large flood to avulse a large channel over overbank deposits (Coleman, 1969; Rust and Jones, 1985, pers. comm.) hence creating an erosional surface (Se); and the large scale Sp complex. During waning stages competence would decrease, making transportation of pebbles by suspension or traction and the formation of coarse-grained cross-strata impossible. Under these conditions only sand-sized particles could be carried by traction thereby allowing the formation of only planar cross-strata (Allen, 1982). The presence of reactivation surfaces between Sp and the coarse-grained core suggests fluctuating stage conditions (Collinson, 1970).

Type 2 Sp is interpreted as the result of waxing flows (rising stage) which had sufficient stream power to carry pebbles in suspension/saltation and to create flow separation (Jopling,1965) over the core Sp, thus allowing the formation of gravelly trough or planar cross-strata. Complexes with connected foresets and topsets are interpreted as compound bars (Allen, 1983) which need currents in the range of 1-2 ms^{-1} depending on grain size.

2.3.4 St- Trough Crossbedded Sandstones and Pebbly Sandstones

Trough crossbedded sandstones are ubiquitous and comprise 26.9% to 88.8% (mean of 59.7%) of the measured sections. The mean thickness of St cosets is 3.14m (n=101 s=3.15) with a range from 0.3m to 40m. St is subdivided into four subfacies dependent on the percentage of pebbles with "a" axes >0.01m: i)St-trough cross-strata (0%); ii) St(d)-dispersed pebble trough cross-strata (<5% pebbles); iii) St(m)- matrix-supported pebbly trough cross-strata (>50%matrix); iv)St(c)-pebbly clast-supported trough cross-strata (>50% clasts, note that grain size makes it St(c) and not Gt). Set thickness is variable from 3.0m to 0.2m, most often lying in the tens of centimetre range. Variation of set thickness between the four subfacies was studied in a laterally extensive unit (D7). After application of a student-t test no significant difference was found at the 85% confidence level between sets belonging to the same lithofacies at different localities. Set thickness between different lithofacies showed contrasting results. Comparison of St and Gt set thicknesses showed that in 86% of the cases Gt thickness is greater than St at the 95% confidence level (Table 1). Set thickness rarely decreases upward in sheet channel units which are greater than 5m thick, and more commonly decreases upward in thinner units. The decrease in set size is marked only in the upper quarter of the cycle.

TABLE 1: COMPARATIVE THICKNESSES OF St AND Gt SET SETS AT VARIOUS LOCALITIES

CYCLE	UNIT	COM.	X_1	X_2	S_1	S_2	N_1	N_2	t	SIG
DIV	D7	Gt>St	0.74	0.71	0.33	0.63	30	46	0.302	-
DV	D9	Gt>St	1.19	0.90	0.67	0.39	16	8	1.08	85%
E	TOTAL	Gt>St	0.73	0.40	0.32	0.22	3	11	1.91	99%
F	TOTAL	Gm>St	0.72	0.40	0.29	0.24	15	22	3.55	99.9%
GIV	G4	Gt>St	0.98	0.53	0.53	0.18	5	21	3.06	99.9%
GII	G6	Gt>St	1.39	0.56	0.98	0.24	6	8	2.13	99.0%
GI	G8	Gt>St	1.01	0.46	0.69	0.19	18	65	5.62	99.9%
G	TOTAL	Gt>St	1.39	0.83	0.98	0.42	6	12	1.59	99.0%
H	TOTAL	Gt>St	1.30	0.40	0.76	0.10	9	3	1.86	99.0%

COM. = pair of sets being compared

X_1 = mean of thicker set (m)

X_2 = mean of smaller set (m)

S_1 = standard deviation of larger set (m)

S_2 = standard deviation of smaller set (m)

N_1, N_2 = number of observations for larger and smaller sets.

t = t-test result

SIG = statistical significance

Trough cross-strata commonly show tangential foresets with mean apparent dips ranging between 21.8° and 24.5° (n=66). St(c) foresets display a closed framework fabric which probably indicates that matrix infiltration occurred as backflow transported sand up the foreset slope. Carbonized logs (Stigmaria, Calamites) are common on foresets and assume orientations sub-parallel or tranverse to flow (Fig 8). The lack of any systematic trends in log orientation casts doubt on the practicality of using logs for paleocurrent studies in St cosets. Penecontemporaneous deformation is commonly associated with fossil logs and can be explained by compaction of the organic material by overlying sediments.

St commonly takes the form of low angle (less than 15°) cross-strata. In transverse sections they appear as low angle trough cross-strata with a width of 2m to 10m and a set thickness of 0.3m. The cross-sets are erosively based, displaying pebble and rip-up clast lags (up to 0.30m thick) sharply and concordantly overlain by well sorted sandstone foresets (Fig.9). The sharp contact between the thick pebbly lag and the overlying foreset sandstones requires a mechanism for its formation. The consistently large width/depth ratio and trough shape of the structure suggest formation by migration of a low amplitude/large wavelength dunes (not sandwaves since flow separation is needed to form a scour in front of the bedform), which created a pebbly bottomset lag. This bottomset lag could be further thickened by overpassing

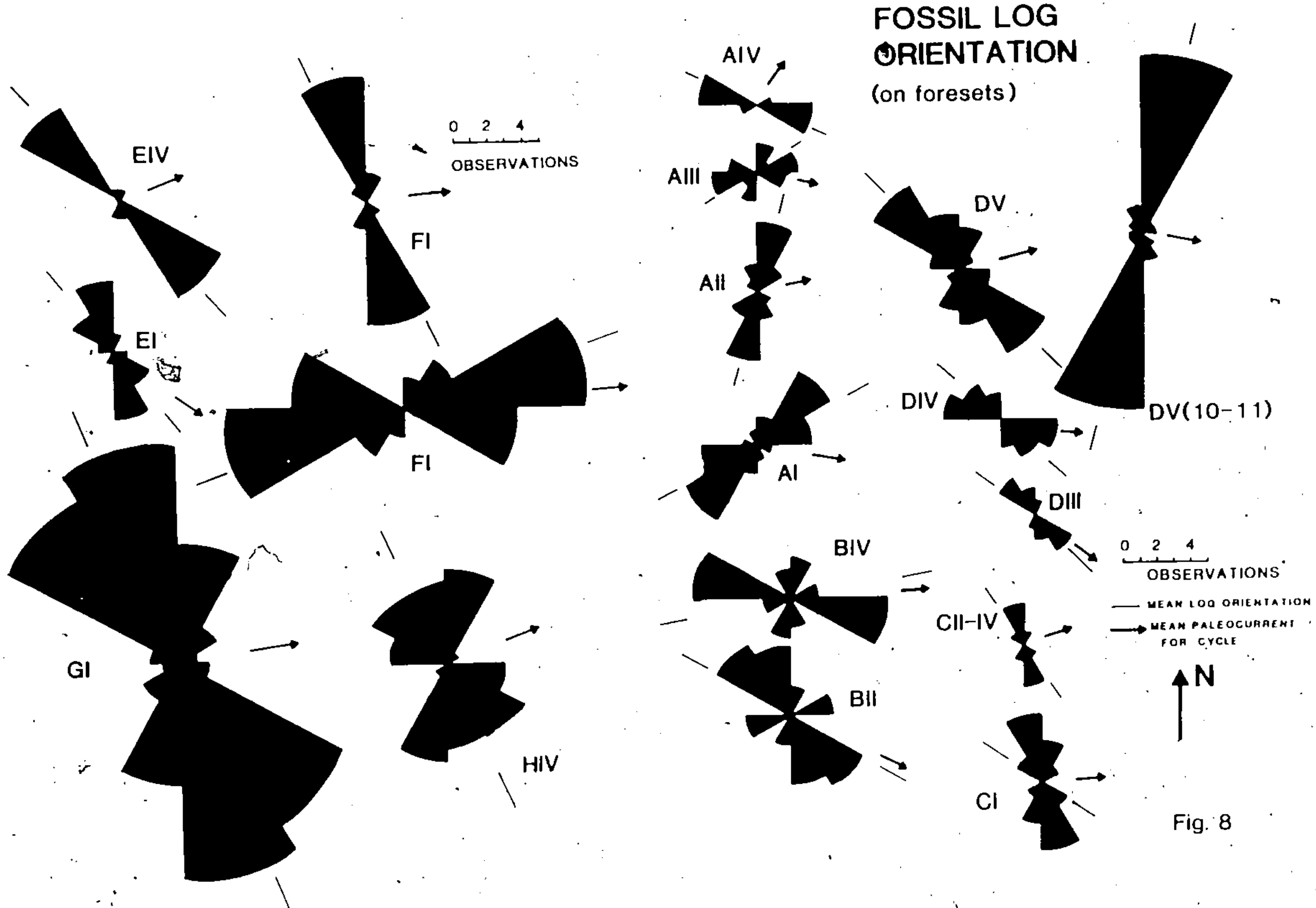
FOSSIL LOG ORIENTATION
(on foresets)
0 2 4
OBSERVATIONS
EIV
FI
EI
FI
GI
HIV
AIV
AIII
AII
AI
BIV
BII
DV
DV(10-11)
DIV
DIII
CII-IV
CI
0 2 4
OBSERVATIONS
MEAN LOG ORIENTATION
MEAN PALEOCURRENT FOR CYCLE
N

Fig. 8

Fig.9. Scale is 1.0m.

Fig. 9 Low angle St at loc.8

of pebbles along the back of the bedform and avalanching into the lag-laden trough. This mechanism has been proposed by Allen (1983, 1984b) to explain coarser-grained foresets within compound bars in the Lower Devonian Brownstones. The formation of low amplitude/large wavelength dunes and the overpassing of pebbles demands upper flow regime conditions ($1\text{-}2ms^{-1}$).

There is a lateral increase in St(c) from section 01 to 02, and an upward decrease within both sections. St(c) is replaced by its conglomeratic equivalent, Gt, in section 03. Vertical and lateral lithofacies changes follow the continuum St-> St(d)-> St(m)-> St(c).

2.4 CONGLOMERATIC LITHOFACIES

2.4.1 Gp-Planar Cross-Stratified Conglomerates

Gp is very similar to Sp in its facies associations and differs only in grain size. Gp is found only in section 03 and is estimated to constitute up to 10% of conglomeratic lithofacies. Sets range in thickness from 0.8m to 2.5m averaging 1.0m. Gp is associated with lithofacies Sp, St(c) and Gt, and like Sp can be subdivided into two types:

Type 1- low angle ($<15^{0}$) planar foresets which are laterally equivalent and/or onlap Gt, St(c), Sp (Fig.10a).

TYPE 1 and 2 Gp BAR COMPLEXES

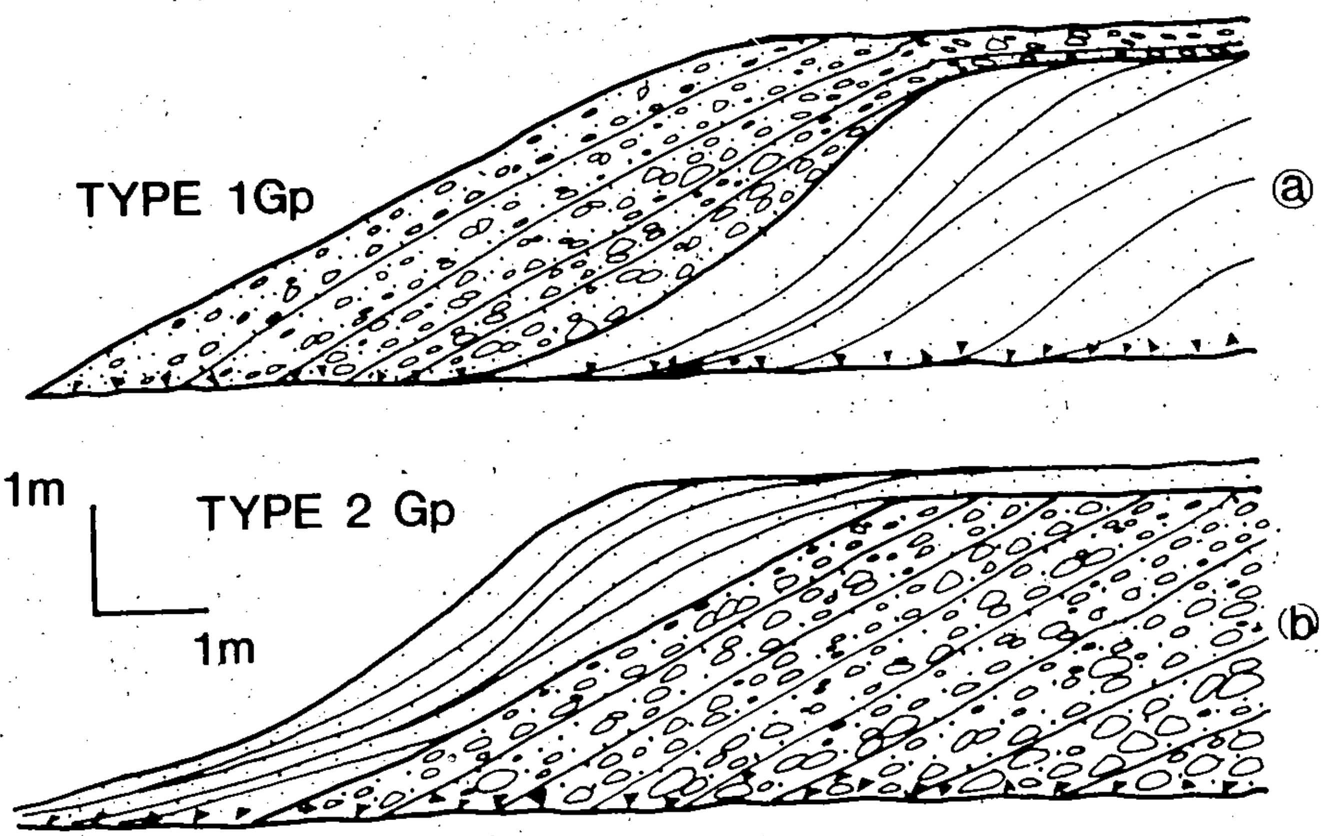

Fig. 10

Lateral contacts may or may not have reactivation surfaces; the lower bounding surface is non-erosive, while the upper bounding surface may be erosional (Se) or capped by Sh/Sl or Gm/Gl topsets upstream from the Gp foresets, and overlying the core Gt, St(c), Sp (Fig.10a). This type of complex is commonly found at the base of sandstone/conglomeratic sheet sandstones scouring into the underlying mudstones.

Type 2- In the second type, low angle (<15^{0}) planar foresets are laterally equivalent and/or are onlapped by St(c), Gt, or Sp (Fig.10b) with or without reactivation surfaces. In many cases topsets (Sh/Sl, Gm/Gl) belonging to the offlapping lithofacies are continuous with the foresets.

Unlike type 1 and 2 Sp, type 1 and 2 Gp cannot be simply interpreted as deposits from waning and waxing flows since the classification in both cases is based on the upstream or downstream positioning of the planar cross-strata with respect to the other lithofacies, and not on hydraulics. The following Gp associations can be interpreted as waning and waxing flow deposits respectively: waning - Gp-> St(c), Gp-> Sp; waxing - St(c)-> Sp, Gp-> Gt. Conceivably type 1 Gp could pass into type 2 Gp during waning stages.

2.4.2 Gt-Trough Crossbedded Conglomerates

Trough crossbedded conglomerates (Gt) are almost exclusively found in section 03 and comprise 37.9% of the section (range 28.4% to 51.1% between subsections). Gt units average 11.6m in thickness, ranging from 2.5m to 34.0m. Gt can be differentiated into two subfacies dependant on whether it is matrix-supported (>50% matrix, note: grain size >0.01m defines it as Gt(m) not St(c) or St(m)) - Gt(m), or clast-supported (>50% clasts) - Gt(c). Sorting and grain size is quite variable and will be discussed in section 8. Mean foreset dips down the trough axis range from 18.9^{0} to 25.9^{0}. Comparison of apparent foreset dips in Gt and St from sections 02 and 03 show no significant difference at the 95% confidence level (F-test). Foresets commonly have carbonized tree trunks arranged subparallel or transverse to the paleocurrent direction. Mean set thicknesses vary from 0.79m to 1.39m and most often are in the one metre range. Set thickness decreases upward in thin (<5m) sheet channel units but rarely does so in thick amalgamated units. Gt set thicknesses are invariably larger than St (Table 1), the difference increasing from section 02 (subsection D) to 03 from 0.10m to 0.55m, and decreasing upsection in 03 (from 0.55m to 0.23m).

Larger Gt sets are interpreted to have been formed by migration of sinuous-crested dunes in deep first order channels (Williams and Rust, 1969). Flow was competent enough to transport gravel while flow in shallower second order (or third order) channels was less competent, and hence was only able to create smaller sandy bedforms. An alternative explanation is based on the intimate faciës association between Gt and St which suggests that these are stage controlled features. Vertical and lateral decreases in the set size difference between St and Gt are due to allocyclic controls on grain size and fluvial channel style i.e. an upward and lateral increase in distal nature.

Gt is vertically and laterally associated with Gm, Gp, Sp and Sh. The most common association is interbedded Gt and Gm (Gt/Gm), followed by interbedded Gt and St (Gt/St).

2.4.3 Gm/Gl- Horizontally Stratified and Low Angle Stratified Conglomerates

Horizontally stratified conglomerates (Gm) are almost exclusively found in section 03. Gm is most commonly interbedded with Gt (Gm/Gt), with which it makes up 55.5% of section 03. Gm/Gt units average 11.8m in thickness (n=6, s=12.2) and range from 1.2m to 34.0m.

Gm occurs with erosive and non-erosive bases. Erosively-based Gm units infill large scours which dip $<10^{\circ}$, commonly

$<5^{0}$ and cross-cut each other. Pebble imbrication is well developed with AB planes dipping upslope within the scour. Gm beds range from 0.3 to 1.1m in thickness (mean=0.71m, s=0.29, n=15) and are 73.3% (n=15) normally graded, 20% ungraded and in few cases show inverse grading. All beds have a closed-framework fabric. Thin sandstone lenses of St or Sh (<0.5m thick and laterally extensive up to 5m) with non-erosional bases and hummocky tops are commonly interspersed with Gm. This type of Gm is interpreted as deposited within wide shallow channels and on longitudinal bars during flood stage. Sandstone lenses draped on top of Gm units denote low stage deposition on the flanks of scours or longitudinal bars (Williams and Rust,1969; Rust and Koster,1984).

The non-erosively based Gm is closely associated with large scale Gt. This facies association takes the form of laterally extensive (up to 20m) large-scale Gt sets overlain by non-erosively based medium-sized Gm units (up to 0.4m thick; Fig.11). In some cases the Gm units drape over the Gt foresets creating low angle stratification (Gl). This facies association is attributed to deposition by migrating linguoid gravelly bars (Bluck,1979; Hazeldine,1983). The advancing bar front (foreset) creates Gt and the suprabar platform (topset) deposits Gm, while a rise in stage might cause offlapping of the topset to create Gl.

Gm is most common above the lower third of section 03

Fig.11. Gravelly linguoid bar deposit of large Gt set (under notebook, 0.19m long) overlain by suprabar platform deposit comprising Gm (unit G-8, cycle GI, at loc.22).

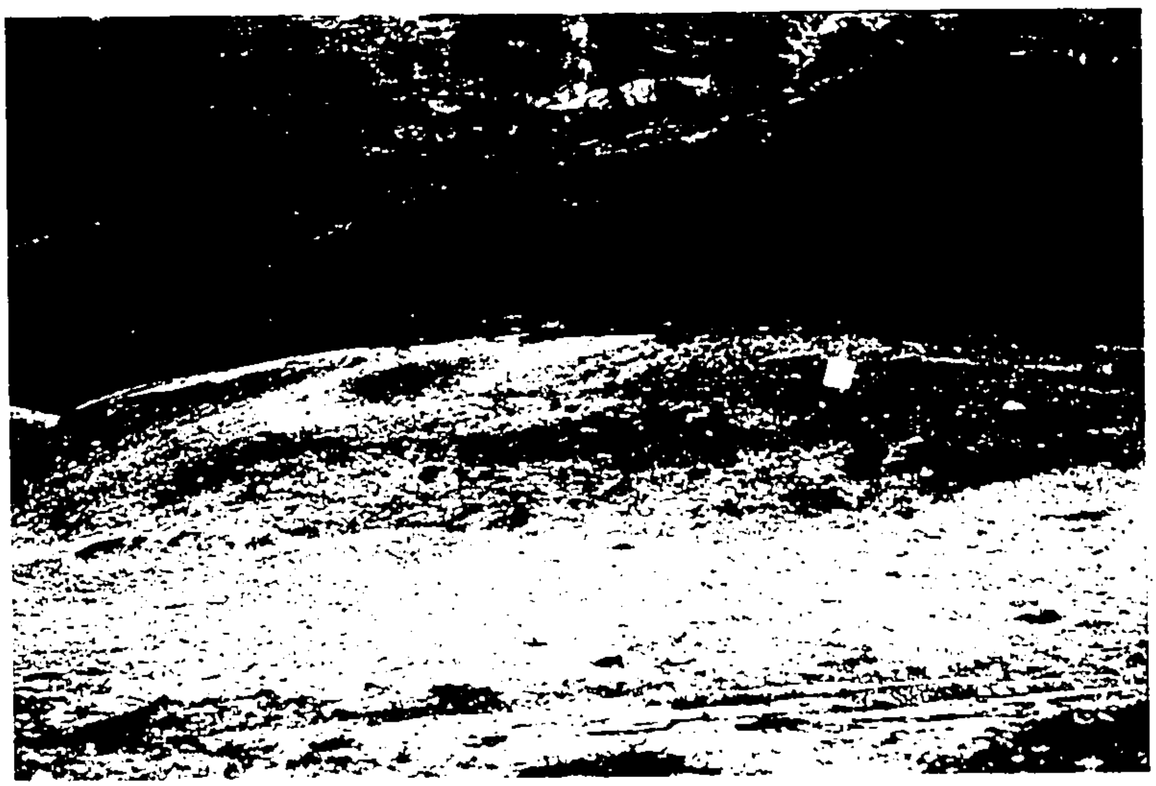

and decreases in abundance upwards.

2.4.4 Se- Erosional Surface

Erosional surfaces are very common in all three sections. Se is marked by laterally extensive (often>50m) clast-strewn surfaces commonly several clasts thick. Clasts may be of intra- or extrabasinal affinities, the former marking amalgamation surfaces between fining-upward cycles. Se is less than 0.2m thick with a maximum relief of 4.0m and generally has a planar convex shape (Allen,1983). Mudstone rip-up clasts within Se are well-rounded and grey regardless of the colour of the underlying mudstone. Erosional surfaces are interpreted as scoured surfaces caused by channel switching, channel avulsion, or bedform migration. The former two are differentiated from the latter by their lateral extent, commonly showing an order of magnitude in difference.

3.0 FACIES ASSOCIATIONS

3.1 Introduction

Sections 01, 02 and 03 comprise three major facies associations, namely the heterolithic-, sandstone-, and conglomeratic facies associations. The facies associations are arranged into cycles, a cycle being defined by a sharp-based coarse member (contact erosional or non-erosional) comprising sandstone/conglomeratic facies associations (i.e. in-channel deposits) and an overlying fine member comprising a heterolithic facies assemblage (i.e. overbank deposits; terminology of Collinson, 1978). Cycles from sections 01 and 02 have a sandstone facies assemblage coarse member and become fine member poor downsection and towards section 03. The cycles are 5m to 40m thick, sheet-like, laterally extensive and fine-upwards. The conglomeratic facies association is most prominent in section 03 and displays thick amalgamated (17m to 50m) sheet-like, laterally extensive sequences which fine upwards in only the upper few metres.

3.2 Heterolithic Facies Association

The heterolithic facies association consists of interbedded lithofacies Fm, Fr, Sr, with minor Fl and Sm and ranges in thickness from 0.2m to 26.4m with a mean of 4.36m (n=27, s=5.55). On average it comprises 92.2% mudstone and 7.8% sandstone lithotypes (n=27, s=14.1%); the percentage of sandstone varies from 0% to 48.1% and increases with increasing thickness of the assemblage.

Fm and Fr are the major components of the heterolithic facies association. Fm and Fr commonly grade vertically and laterally into each other, but rarely show preferred facies transitions within a unit, except that Fm(g) commonly underlies sandstone/conglomeratic units. However there are some vertical and lateral trends in these lithofacies. An upward increase in the moving percentage of Fr along with a decrease in the moving percentage of Fm and Fl is noted in section 01 (Fig.12) and is attributed to an allocyclically-controlled upward change in fluviatile style (discussion in section 6.2).

Sandstone beds (Sr and Sm) within the heterolithic assemblage are thin, laterally extensive (over hundreds of metres), sharp-based and often fine-upwards into silty and argillaceous sandstones indicating episodic deposition under waning flows- typical of overbank sedimentation. Sr is the predominant sandstone lithofacies within the heterolithic facies assemblage, although interbeds rarely number more than three.

Thick heterolithic facies assemblages (eg. BI, HII, see

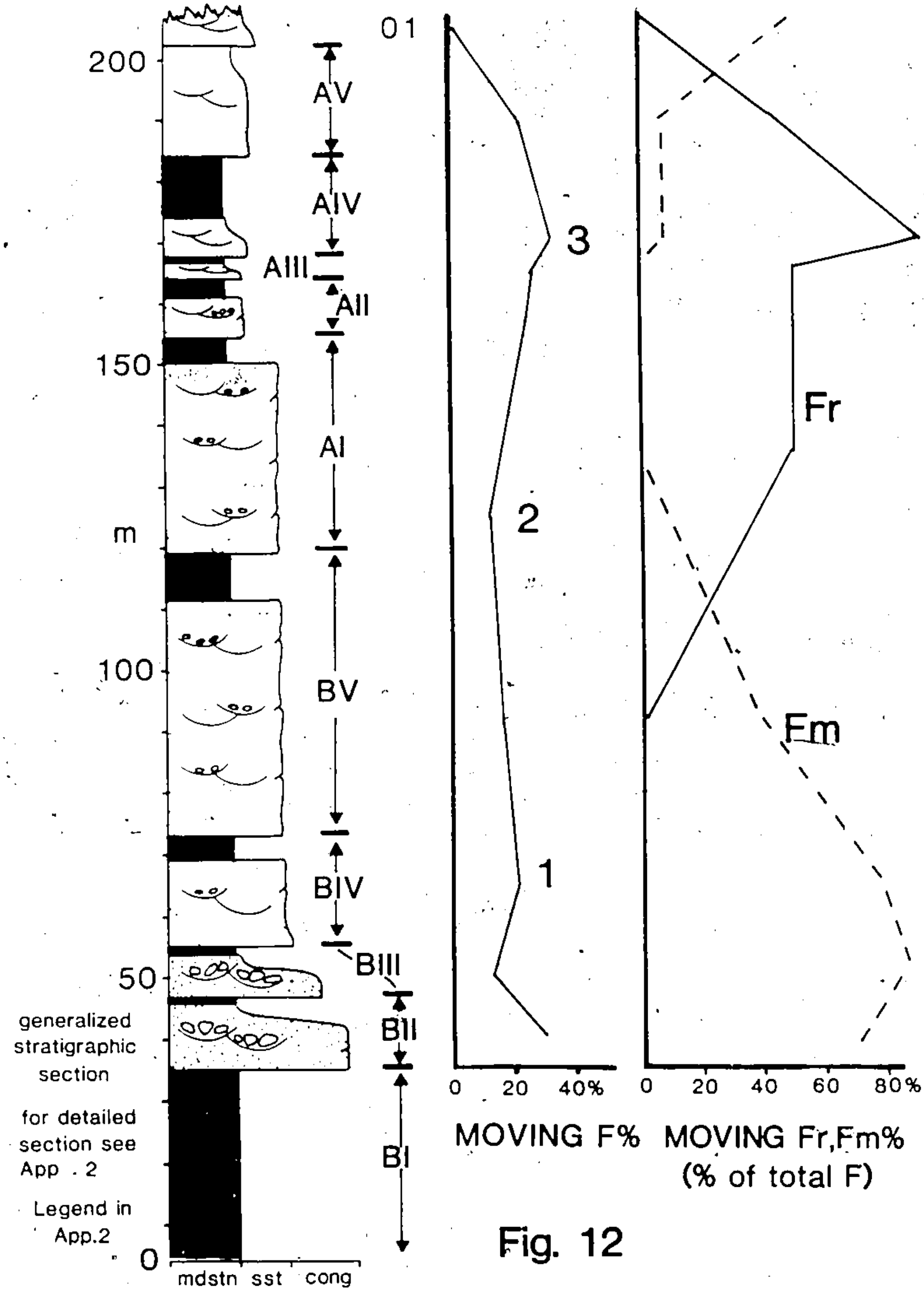
01
200
150
m
100
50
0
AV
AIV
AIII
AII
AI
BV
BIV
BIII
BII
BI
generalized stratigraphic section
for detailed section see App . 2
Legend in App.2
mdstn sst cong
3
2
1
0 20 40%
MOVING F%
Fr
Fm
0 20 40 60 80%
MOVING Fr,Fm%
(% of total F)

Fig. 12

Apps.2,4 respectively) are rarer and have a greater proportion of sandstone ranging from 20.7% to 48.1%. Sandstone beds can be divided into thin and thick varieties, both types displaying a laterally extensive sheet-like character. The thick beds (>1.0m) are sharp-based, often scouring into the underlying mudstones, fine upwards and are internally stratified with decimetre-scale St (with copious plant fragments) at the base, passing up into Sr. Thin beds (<1m) are also sharp-based and may fine, or coarsen-up or show no vertical grain size difference. Thick sandstone beds may be interpreted as either thick overbank sandstone deposits or minor anabranching braided channels within the floodplain. Thinner sandstone/mudstone FU cycles are due to episodic overbank sedimentation.

The most common facies association within thick heterolithic facies assemblages is Sr->Fm->Fr. The sequence fines upward and ranges in thickness from 1m to 4m. These sequences are interpreted in terms of episodic floodplain deposition followed by a lowering of the water table and colonization by plants. Lower water tables must have persisted for prolonged periods in order to allow the high abundance of Fr (13.6% to 23.1%) and red mudstones. The intimate lateral and vertical facies association between Fr and mottled Fm suggests that mottling was a pedogenic process genetically related to rooting (Bown and Kraus, 1981). In conclusion, thick heterolithic facies assemblages indicate that periodic overbank deposition was interspersed with long periods of relatively low water tables.

The heterolithic facies assemblage is horizontally stratified, fines upward, with a lower non-erosive base showing negligible relief. Occasionally, lower surfaces are inclined ($<20^{0}$) and infilled with a coarsening-upward heterolithic facies assemblage (Fig.13). This sequence is attributed to a sudden channel avulsion followed by infilling from a prograding source into ponded waters. This is suggestive of a crevasse-splay building into overbank lakes (Gersib and McCabe,1981, Fig.11; Boothroyd and Nummedal,1978,Fig.13a). An exposure in section 03 (cycle EV) shows two isolated fixed channels with steep sides, approximately 10m wide, 2m deep (5:1 width/depth ratio) infilled with mudstones/pebbly sandstones and enclosed in a heterolithic facies assemblage (Fig.14). The mudstone-filled channel is interpreted as the result of a sudden avulsive event followed by deposition by suspension. The pebbly sandstone-filled channel is thought to be a crevasse-splay channel also formed and abandoned by avulsion.

Vertical trends in the heterolithic facies association (which includes all previously discussed lithofacies in the heterolithic facies assemblage)are plotted as the moving average of the percentage of heterolithic facies comprising a cycle. Such trends for the sections 01 and 02 are plotted in Figs.12,15 and show a close similarity in shape, the difference being that section 01 has a greater overall

Fig:13. Inclined erosional surface cuts into sandstone (continues to the left underneath talus) overlain by a CU heterolithic assemblage (see text for explanation). Loc. 0.95km south of Sand River. Scale is 1.0m.

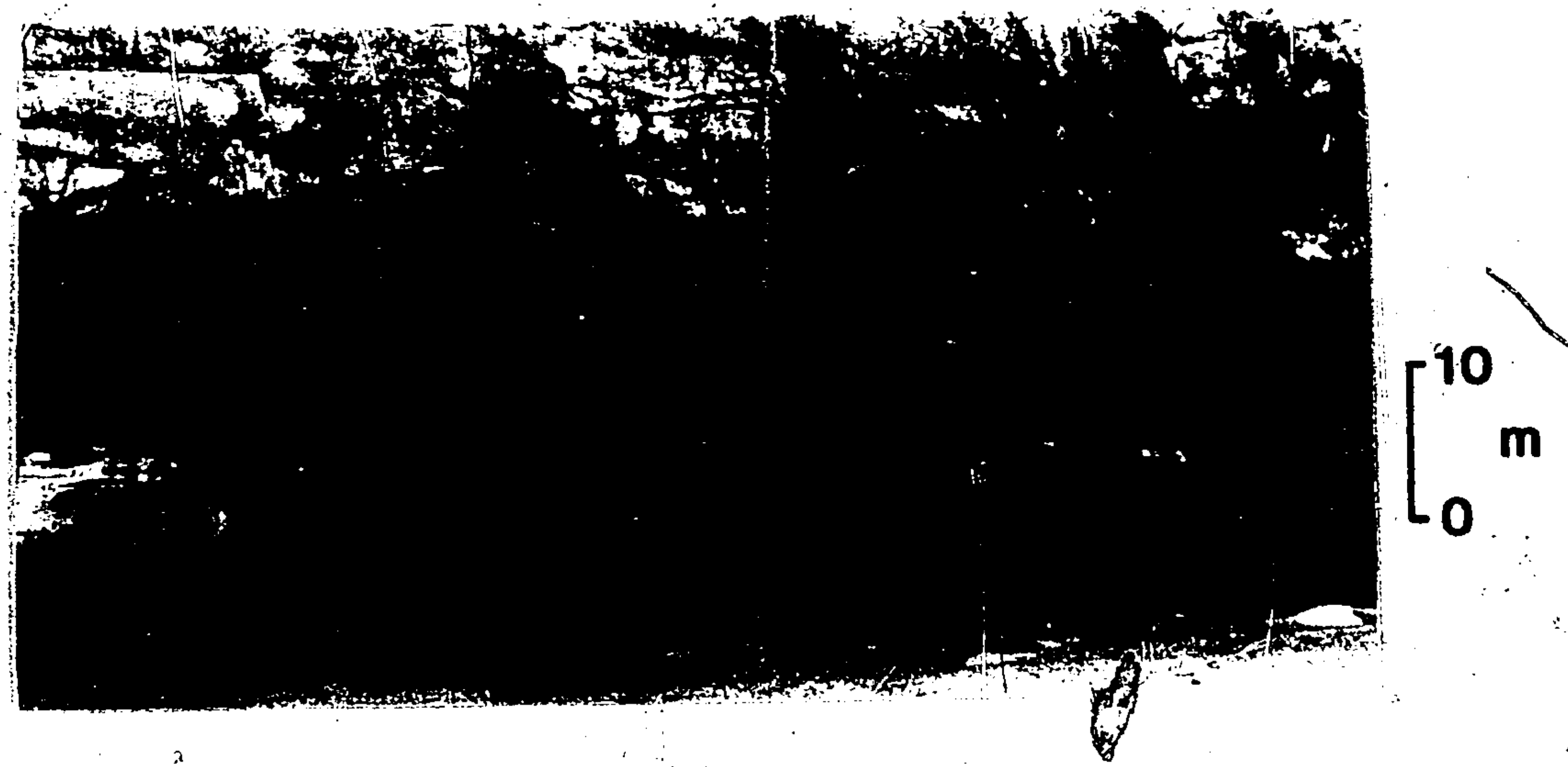

Fig. 14 Mudstone-filled channel within cycle EV at loc 11.

Fig.15

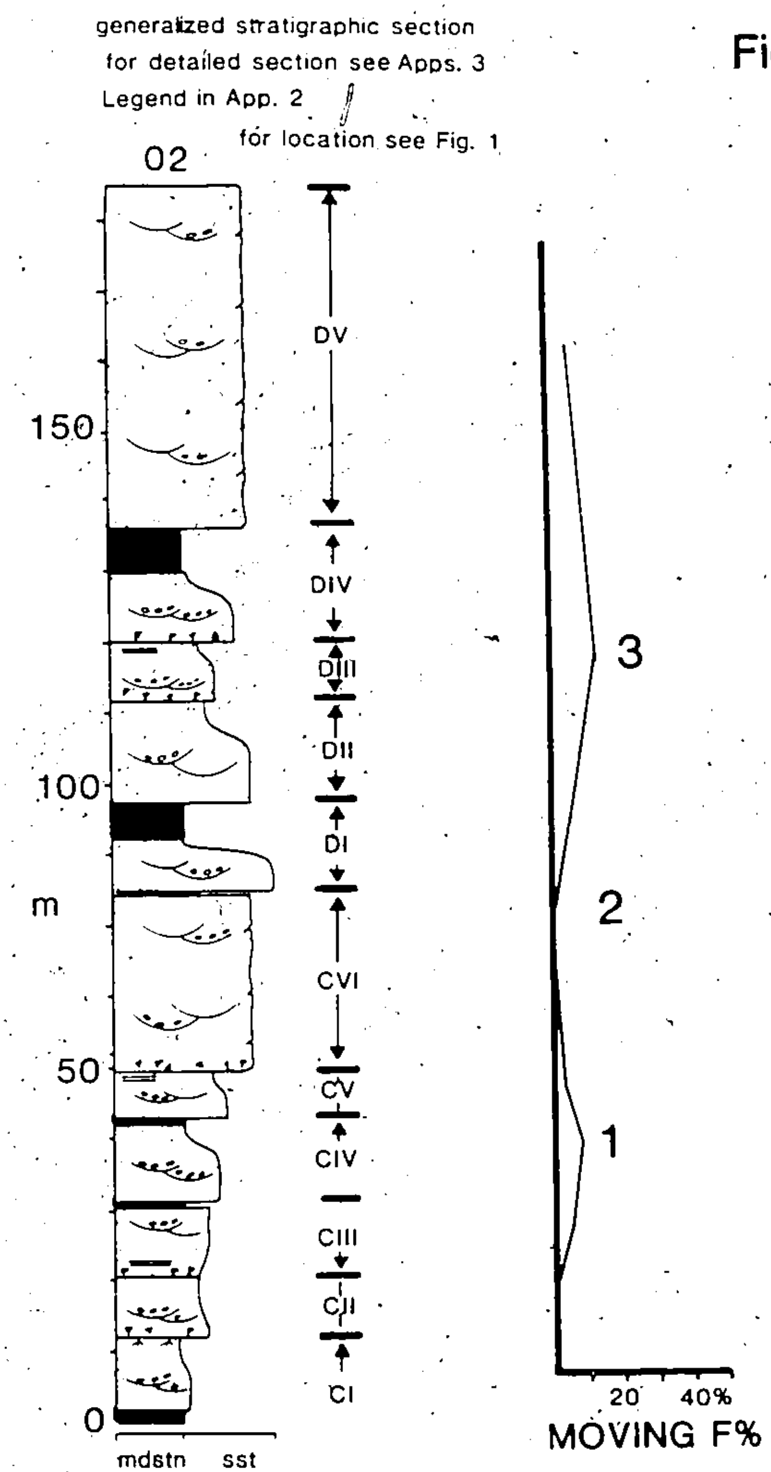
generalized stratigraphic section
for detailed section see Apps. 3
Legend in App. 2
for location see Fig. 1
02
150
100
m
50
0
mdstn
sst
DV
DIV
DIII
DII
DI
CVI
CV
CIV
CIII
CII
CI
3
2
1
20
40%
MOVING F%

percentage of mudstones. Three points of inflection can be identified (labelled in Fig.12) in both sections, the first indicating a maximum in the moving percentage, the second a minimum, while the third peak shows an overall maximum. The three correlative peaks correspond to synchronous deposition of allocyclically-controlled thick heterolithic assemblages (note that there is an offset between the peaks and the mudstone units due to the nature of the moving average). The significance of these peaks will be discussed in chapter 6. Units corresponding to these peaks can be traced laterally for over 7.5km.

Section 03 is also marked by low percentages of heterolithic assemblages and shows two small peaks in the moving average (Fig.16), labelled "0" and "1". Peak 1 is correlative with peak 1 of sections 01 and 02 (see Fig.12).

3.2.1 Summary

The heterolithic facies assemblage overlies the sandstone/conglomeratic facies assemblage in a fining-upward sequence (sensu Heward,1978). Units of the heterolithic facies association are concordantly bedded with a non-erosive lower contact and scoured upper contact, and comprise interbedded Fm, Fr, with minor Sr. The sequence averages 4.36m in thickness (range 0.2m to 26.4m); and has a 12:1 mudstone to sandstone ratio.

Trends in the abundance of heterolithic facies

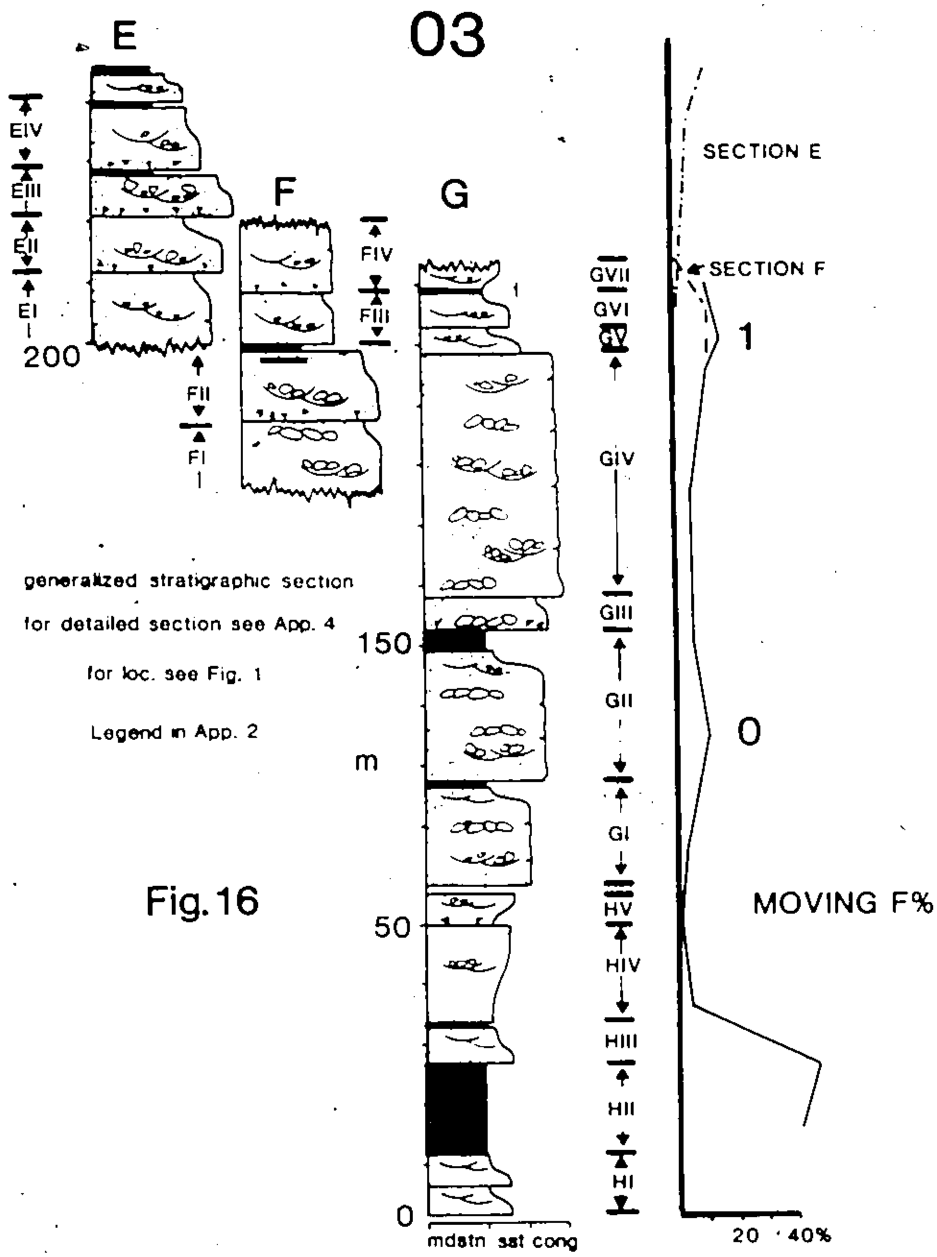

03
E
F
G
EIV
EIII
EII
EI
FIV
FIII
FII
FI
GVII
GVI
GV
GIV
GIII
GII
GI
HV
HIV
HIII
HII
HI
200
150
50
0
m
mdstn sst cong
SECTION E
SECTION F
1
0
MOVING F%
20 40%
generalized stratigraphic section
for detailed section see App. 4
for loc. see Fig. 1
Legend in App. 2

Fig.16

associations show: i) a decrease downsection and towards section 03; ii) three peaks in the moving percentage which can be correlated between sections 01 and 02; iii) sections 01 and 02 show an upward decrease in Fl and Fm and an upward increase in Fr.

3.2.2 Interpretations

The general fining-upward nature of the heterolithic assemblage, its lateral extent, high ratio of mudstone/sandstone (12:1), sheet-like geometry of fine member, and abundance of Fr and Fm are indicative of sudden avulsion followed by suspension deposition into newly created floodplains. Periodic breaching of vegetated leveed channel margins created crevasse- or sheet splays (Boothroyd and Nummedal, 1978; Gersib and McCabe,1981) allowing the influx of sheet-like, sharp-based, FU sandstones into the distal reaches and channelized sandbodies proximal to the crevasse-splay (Bridge,1984). Progradation of crevasse-splays into parts of the floodplain created coarsening-upward sequences. The vast majority of sediments, though, would have been deposited into adjacent floodplains by suspension deposition from overbank floods. The large areal expanse of the floodplain would have been most conducive to deposition from suspension (to form Fm), while traction currents accumulated Fl in a limited area close to the channel margins. Subsequent lowering of stage, and hence of the water table, would have allowed colonization by plants and creation of Fr (Walker and

Cant, 1984). As the length of subaerial exposure was increased pedogenic processes started and grey Fr became oxidixed to mottled Fr and finally to red Fr. Hence the predominance of red mudstones (Fm, Fr) indicates that alternating periods of overbank deposition and a low water table must have existed in order to achieve the necessary thickness of Fm/Fr and the red colour. Further evidence of fluctuating stage conditions is seen in the abundance of rill and slumped blocks (Gibling and Rust, 1984). The presence of rill and slump blocks and vertical stepped bases in the overlying sandstones/conglomerates also implies that channel banks must have been cohesive. This may have been partly due to stabilization by plants.

The absence of calcretes suggests that high deposition rates may have inhibited calcrete growth (Leeder,1975); this may have been further hampered by a humid climate (Allen,1978) which is postulated for the Cumberland Group (Duff and Walton,1973; Rust et al. 1984; D'Orsay and van de Poll,1985). A humid climate is also postulated in this study from the abundance of rooted horizons, carbonized flora, rare raindrop imprints, and lack of desiccation cracks.

Vertical and lateral trends in the percentage of the heterolithic facies association show an upward and northeasterly increase (from section 03 to 01)- indicating an increasingly distal nature in those directions. An upward increase in Fr (in section 01) along with a decrease in Fm, and an increase in stepped channel bases (discussed in section 3.3) denotes a change in fluviatile style towards further channel stability, problably induced by allocyclic controls. Allocyclic controls, rather than autocyclic, are also invoked for correlative peaks in the moving percentage of heterolithic facies assemblage due to their lateral extent and thickness (see section 3.2), an unlikely characteristic of autocyclically-controlled deposits. These conclusions were based on the area over which correlations were possible.

3.3 Sandstone Facies Association (Sections 01 and 02)

The sandstone facies association, found primarily in sections 01 and 02, is made up of interbedded St(c), St(m), St(d), St, Sp, Sh, and Sr and occurs as sequences that range in thickness from 4.7m to 49.5m with a mean of 14.4m (n=22, s=12.5m). The assemblage is composed entirely of sandstones, pebbly sandstones with thin minor laterally discontinuous mudstone interbeds, and internal erosion surfaces (Se). The abundance of pebbly sandstones decreases in the upper half of sections 01 and 02 (subsections A and D respectively) and laterally towards section 01.

The sandstone facies assemblage is laterally extensive; sequences ranging between 10m and 40m can be traced for over 7.5km. They are sheet-like in geometry, with erosional concordant lower contact and concordant non-erosional upper contacts. The sandstone facies association is commonly bounded on the top and bottom by the heterolithic facies assemblage- the sandstone facies coarse member and its overlying fine member defining a complete cycle. Complete cycles are most prevalent in section 01 averaging 18.6m thick (n=11, s=11.8m) and displaying a fining-upward trend in 40% of the coarse members. Those fining-upward coarse members occur in the upper and lower parts of section 01 (eg. cycles BII, BIII, AIII, AIV, see App.2) whereas the middle section shows no fining-upward trends. Amalgamated cycles become more common in section 02 (45.5%), where they have a mean thickness of 15.8m (n=11, s=12.4) and demonstrate fining-upward trends in 73.7% of the coarse members.

Coarsening-upward trends in the lower two metres of cycles are quite common in section 01 (60% of the cycles displaying it), with half then proceeding to fine-up. This trend diminishes towards section 02 with only 18.2% displaying this property. The lower two metres of these cycles comprise Sr or decimetre-scale St, which is commonly overlain by Se, and finally the rest of the coarse member.

Fining-up (FU) coarse members in section 01 exhibit the following facies associations: an erosional planar concordant base (Se) -> a thin 1m to 2m unit of fine-grained medium-scale St or Sr (present in half of the cycles) -> Se -> interbedded medium to large-scale St(c)/St (or Gt in cycles BI and BII see App.2), with minor Sp -> a thin to medium-sized unit of Sh. An upward decrease in the size of sedimentary structures is noted in FU coarse members. FU coarse members in section 02 are more prevalent and differ from section 01 by the absence of the basal St/Sr unit (observed in only 18.2% of cycles) and the greater proportion of St(c) compared to St.

Non-FU amalgamated coarse members in sections 01 and 02 (eg: cycles BV, AI, CVI, see Apps. 2,3) reveal the ensuing facies associations: Se -> a thick series of interbedded St(c)/St and minor Sp with multiple, internal, discordant, laterally discontinuous erosional surfaces (Se). Non-FU amalgamated coarse members are much thicker than FU coarse members and often create laterally extensive cliffs..

The internal geometry is difficult to delineate due to the complex cross-cutting relationships shown by the sandstone facies association and the freshly exposed cliff surfaces which do not allow etching out of structures. Channel geometry is best ascertained in thick amalgamated cycles (eg. BV, AI, CVI, DII, DIII, DIV, DV) where low angle concave-up erosional surfaces are exposed. Cycle DII displays a well-defined shallow convex-down channel with gently inclined channel sides and infilled with large-scale Gt and St (Fig.17). The apparent width is over 30m, with a depth of 2.0m, giving a width/depth ratio greater than 15:1. Internal erosion surfaces are more common in thicker amalgamated cycles than in thinner FU ones.

Fig. 17 Shallow channel in cycle DII infilled with Gt and St at loc.1

Basal contacts with the heterolithic assemblage are indicators of stage and flow conditions and can be divided into four categories: i) slumped channel margin blocks; ii) sole marks; iii) stepped channel bases; iv) "overhanging " sandstone/mudstone contacts.

Channel margin slump blocks up to 1m in length are common, and are composed of a heterolithic assemblage or mudstone, the latter being more prevalent. Sandstone molds of slumped intraclasts display rill molds on the downcurrent side (Fig.18) and have been interpreted by Gibling and Rust (1984) as rill marks formed on slumped cohesive channel margin blocks during a lowering of stage. An alternative possibility is that they are formed by channelization of water from dewatering of the slumped mudblock (B.R. Rust, per. comm.,1985). Further work must be done on these features in order to understand their origin.

Flute marks are the most common of the sole marks, showing a spectrum of shapes, mostly elongate (0.05m-0.50m), bilaterally symmetrical and widely scattered. Kolking structures (Harvey,1980) are commonly seen on soles of beds. Guttercasts are also quite common (Fig.19), some scouring as deep as one metre, and often traceable for upwards of one metre. Kolking structures have been interpreted as forming under rising flood stage by kolks (Matthes,1947), a form of

Fig.18. Rill molds in unit D-2 (cycle DI), 0.57km north of loc.1. Scale divisions are 0.10m.

Fig.19. Guttercast (within sandstone), 0.50km south of Sand River. Approximately 0.65m wide and 0.40m deep and overlies overbank mudstones.

macroturbulence generated by high energy flows with low suspended sediment, and bed roughness elements capable of creating flow separation (Baker,1973; Jackson,1976a). Bed roughness elements capable of initiating flow separation include dunes, logs, or bank slumps (Harvey,1980) all of which are present. High energy flows needed for the formation of kolks are postulated from large-scale (often larger than 2.5m) cross-strata at the base of cycles, and the presence of compound bars (terminology of Allen,1984). Guttercasts also have a similar origin (Whitaker, 1973), differing only in that the macroturbulence (helicoidal flow) proceeds downcurrent hence creating the elongated furrow.

Stepped channel bases (Fig.20) are most common in the upper half of sections 01 and 02 (subsections A and B) and are characterized by near vertical steps, the top step often marked by a laterally continuous internal erosional surface. Unfortunately the sections did not allow viewing of the lateral extent of these features. Stepped bases have been reported in braided fluvial deposits of the Carboniferous Morien Group (Gibling and Rust,1984), and interpreted as falling stage features although there lacked internal erosion surfaces. Stepped bases have also been anhotated in recent anastomosed rivers (Smith, 1983) and in an ancient example within the Cumberland Group around McCarren Creek by Rust et al. (1984). In both cases the stepped bases and internal erosion surfaces are attributed to vertical accretion on a low gradient plain within a rapidly subsiding

Fig. 20 Northerly stepping channel base (cycle BI) at One Mile Brook.

basin. The presence of rilled blocks (i.e. blocks with surficial rills), abundant rooted horizons, near vertical stepped bases, and planar concordant mudstone/sandstone contacts suggests that muds were very cohesive, hence the possibility of incision during falling stage (sensu stricto) may not be appropriate and a vertically accreting explanation is favoured.

A variation of stepped channel bases are "overhanging" sandstone/mudstone contacts (noted in six examples). These are distinguished from stepped bases by a "z-shaped" contact rather than a vertical one, with the mudstone unit "overhanging" the sandstone (Fig.21). The upper dipping contact between both units ranges from 47^{0} to 67^{0} and is planar in nature. The upper contact may continue as an internal erosion surface (Fig.21b).The height of the structure ranges from 0.2m to 2.0m, and averages 1.0m. The overhang (width of the "z") averages 0.6m with a maximum of 1.0m.

Some "overhanging" mudstone contacts are marked by an erosional surface cutting down into the adjacent mudstones (Fig.21b). This surface can be traced laterally up into the overhanging contact between the mudstones and the sandstones. The overhanging contact can be explained simply by avulsion (Fig.22,A1,A2) and subsequent mudstone infilling of a channel. It may very well be that most of these types of contacts are formed in this manner, but that poor exposure

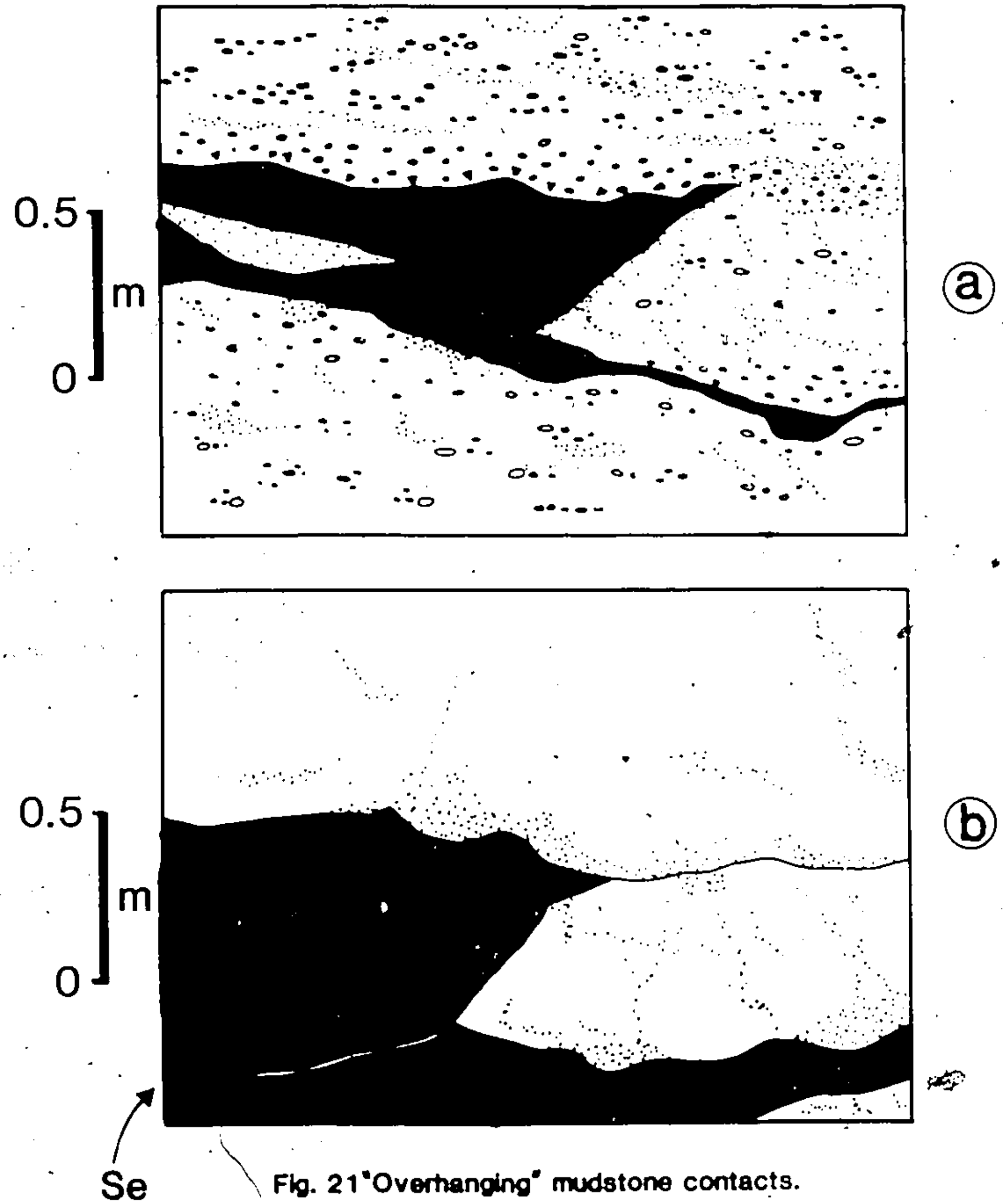

Fig. 21 "Overhanging" mudstone contacts.

ⓐ–cycle DIV at loc. 7

ⓑ–cycle DV at loc. 7

and the homogeneity of mudstones does not allow detection of the erosional surface.

The majority of the observed cases do not show observable erosional surfaces cutting down into the adjacent mudstones (Fig.21a). If these mudstones are indeed lacking erosional surfaces (as observed) then an alternate explanation for these structures is needed. This explanation would require a mechanism for the formation of a planar steeply dipping contact that was overhanging at the time of formation. As with stepped channel bases their formation may be related to either a falling stage or vertical accretion. The former is not favoured, firstly because it is unlikely that a channel could deeply undercut the cohesive banks during falling stage; and secondly it would not explain these features on a small scale (those <0.2m). A rising stage-vertically accreting explanation may be more appropriate.

It is envisaged that overhanging sandstone/mudstone contacts could be created on stepped channel bases by fracturing of the channel margin during flood stage and plucking of a block during low stage (Fig.22B). Fracture patterns needed for their formation could be produced by either tensionally-induced fractures (eg. plumose fractures) or current shearing. The former has been described in the Carboniferous Morien Group of Nova Scotia (Gibling and Rust,1984) as a causative agent for bank collapse but it is unlikely that plumose fractures were responsible in this

Fig.22. Formation of "overhanging" mudstone contacts.

- A1 - downcutting of channel into underlying overbank mudstones
- A2 - subsequent channel abandonment and mudstone infilling
- B - calving of mudstone block due to vigourous current shearing during flood stage

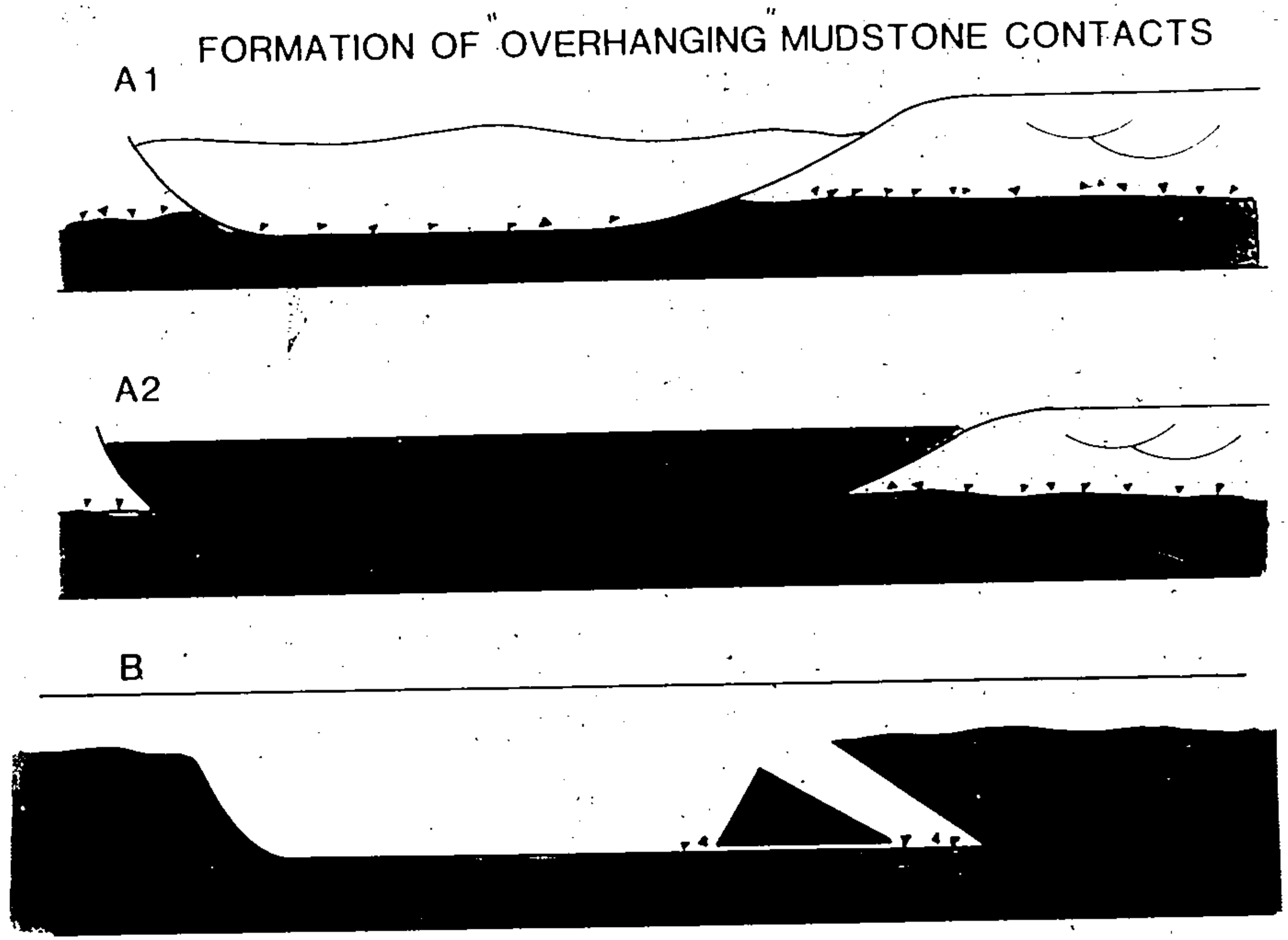

Fig. 22

study since they were not seen. In addition the fanning-out pattern of the fractures would create a curvilinear contact (on a large surface) rather than a rectilinear one (Bankwitz,1965). Other types of tensional fracture could allow the outward collapse of bank material, but not explain why the contact consistently dips between 47^{o} and 67^{o}. An alternative explanation involves vigourous current shearing at flood stage, which would create synthetic planar fractures (consistent with the dips seen on the planar surfaces) on the side of the channel margin (Fig.22B). Further current shearing during low stage could pluck away the block and leave the overhanging bank. Allen (1969) has shown experimentally that supercritical flows over weakly cohesive muds may create mass shearing; given the abundance of upper flow regime structures seen overlying the heterolithic assemblage, a current shearing phenomenom may be the cause of some planar overhanging sandstone /mudstone contacts (i.e. those lacking erosional surfaces).

Vertical trends in the sandstone facies association plotted as the moving average of the percentage of sandstone facies comprising a cycle are shown in Figs.23,24. Trends for section 01 and 02 show an antithetic relationship between the moving percentage of heterolithic facies and sandstone facies. The antithetic peaks from the moving percentage of heterolithic facies (Figs.12,15) are also labelled one, two, three in Figs.23,24, and like the former can be laterally

Fig. 23

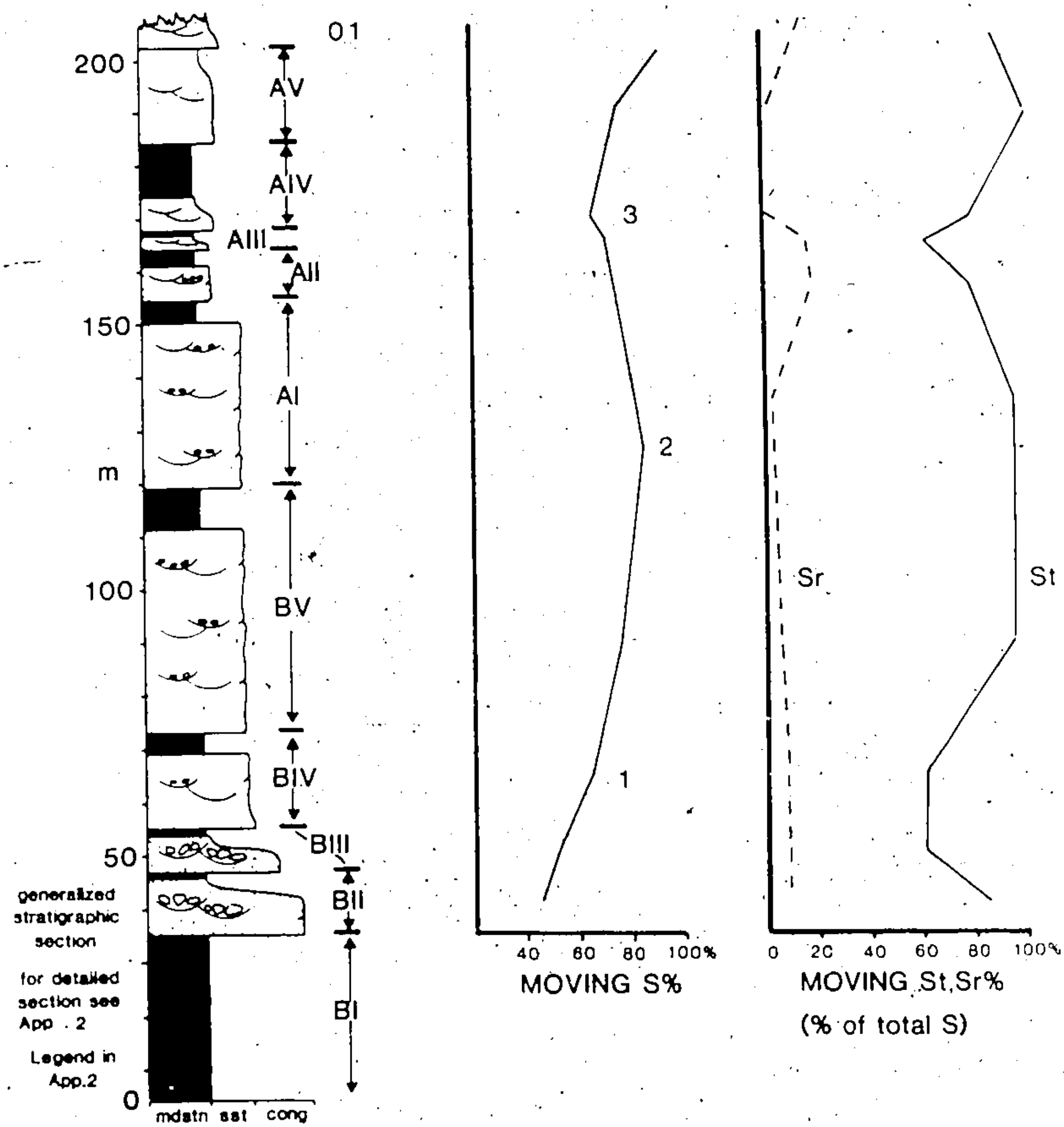

01
200
150
m
100
50
0
AV
AIV
AIII
AII
AI
BV
BIV
BIII
BII
BI
generalized stratigraphic section
for detailed section see App. 2
Legend in App.2
mdstn sst cong
3
2
1
40 60 80 100%
MOVING S%
Sr
St
0 20 40 60 80 100%
MOVING St,Sr%
(% of total S)

Fig. 24

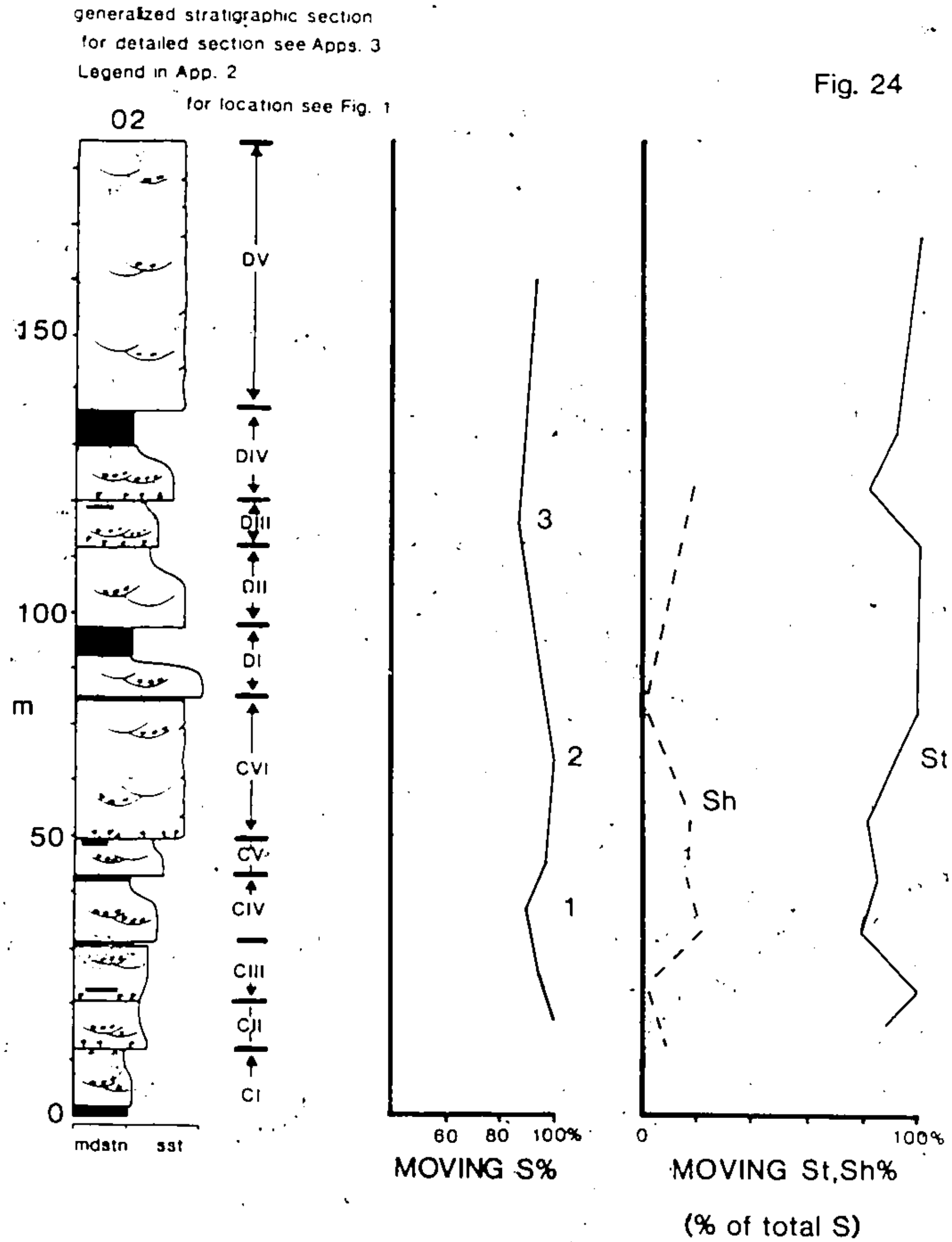
generalized stratigraphic section
for detailed section see Apps. 3
Legend in App. 2
for location see Fig. 1
02
150
100
m
50
0
mdstn sst
DV
DIV
DIII
DII
DI
CVI
CV
CIV
CIII
CII
CI
3
2
1
60 80 100%
MOVING S%
Sh
St
0
100%
MOVING St,Sh%
(% of total S)

correlated. Peaks in the moving percentage are attributed to tectonic control and will be discussed in section 6.2.

Vertical trends for the major lithofacies (St, Sh, Sr) comprising the sandstone facies assemblage are plotted beside the moving average of sandstone facies (Figs.23,24). St is the major component showing similar trends to the moving percentage of sandstone facies (S%) in both sections. Sh(u) and Sr are minor facies, the former being prevalent in section 02 and the latter being most common in section 01.

The predominance of either Sr or Sh is indicative of channel style and channel margin morphology. Sr is a low flow regime bedform and necessitates low stream power and shallow depths for its formation. In modern braided rivers Sr is commonly found near channel margins (Williams and Rust,1969) or bartops (Cant and Walker,1978). Its presence at the base of cycles in section 01 may represent gradual lateral encroachment of a channel upon its marginal sediments or avulsion into adjacent floodplains (discussed further in section 7.4).Sh is an upper flow regime bedform whose formation is controlled by velocity, depth, Froude number, and ratio between tractive and suspended load (Middleton,1977; Englelund and Fredsøe, 1974). Sh is often found on bartops or channel margins where the depth decreases enough to allow its formation. The increasing proportion of Sh from section 01 to 02 indicates increasingly proximal conditions (Smith,1970) and a decrease in sinuosity (Allen,1970), both of which can be corroborated with paleocurrent data (discussed in 7.5).

3.3.1 Sandstone Facies Association (Section 03)

The sandstone facies association is located above and below the conglomeratic facies association in section 03. Those sandstone facies association units lying above conglomeratic units are marked by an overall FU trend whereas those underlying conglomeratic units show a CU trend.

The upper sandstone facies association in section 03 is very similar to that of sections 01 and 02, differing only in coarser grain size and a predominance of pebbly clast-supported sandstone lithologies (pebbles with "a" axis <0.01m). Mean thickness for the coarse member of cycles from the upper sandstone facies association is 6.5m (n=6, s=3.1m). The major facies include St(c), St, Sh with minor Sr. Most sandstone assemblages are arranged in FU cycles (80% of them) with only one cycle showing CU in the lower two metres. Amalgamation is displayed in only 20% of the cycles.

Coarse members display the following facies associations : Se -> St(c) decreasing upwards in set size and often interbedded with lensoid beds of St -> small to medium scale St -> Sr.

The lower sandstone facies association differs from the upper one by being primarily composed of medium to coarse-grained sandstones rather than pebbly sandstones. The major facies include St, St(c), Sh and minor Sp. Cycles average 10.6m in thickness (n=5, s=4.78m), FU in the lower part (eg. cycle HI,HIII, see App.5) and CU in the upper part (eg. HIV).

3.3.2 Summary

The following chart (Table 2), summarizes the characteristics of the coarse member sandstone facies association.

Trends and Characteristics of the Sandstone Facies Association in Sections 01, 02, 03 (TABLE 2)

CHARACTERISTIC*	01	02	03
FU	40%	73.7%	75.0%
CU (in bottom 2m)	60%	18.2%	25%
CUFU	30%	18.2%	-
NON FU	40%	27.3%	0%
AMALGAMATED	10%	63.5%	37.5%
COARSE MEMBER THICKNESS (mean)	14.9m	13.9m	7.5m
TOTAL CYCLE THICKNESS (mean)	18.6m	15.8m	7.8m
SHEET-LIKE	YES	YES	YES
STEPPED CHANNEL BASES	MORE COMMON THAN 02	YES	NO
OVERHANGING CONTACTS	COMMON	COMMON	COMMON

*NOTE: Each category is out of 100% and accounts for only that specific property, eg. NON FU may include cycles that CU in the lower two metres.

3.4 Conglomeratic Facies Association

The conglomeratic facies association is almost exclusively found in section 03, except for cycles BII, BIII (see App.2). It comprises two thick conglomeratic facies sequences interlayered with sandstone units, both conglomeratic sequences showing an overall FU motif. The conglomeratic facies association consists of interbedded Gt(c), Gt(m), Gm, St(c) and minor Sp, Sh(u), Sh(l), and Sr.

Units of the conglomeratic facies association are sheet-like in geometry and resemble sandstone facies association units in many respects. They have concordant upper and lower contacts which commonly rest on the heterolithic facies assemblage. Cycles are erosively based and FU in all cases; with only 27.3% CU in the lower parts; and 36.4% being amalgamated cycles. Complete cycles average 14.7m (n=11, s=9.9m) in thickness, while the coarse member has a mean thickness of 13.4m (n=11, s=8.7m).

The lower sequence of conglomeratic facies association comprises three upwardly thickening/FU cycles (GI, GII, GIV, and lateral equivalent FI, see App.4). Each cycle is erosively based and fines upward in the upper 2m to 4m and is sharply and concordantly overlain by a thin (<1.5m) heterolithic fine member. Successive conglomeratic cycles coarsen-upwards with respect to the previous one, hence creating a series of FU cycles with an overall CU motif (Appendix 4). Cycles are internally stratified with complex interbedding of Gt, Gm and minor Gp, Sp, St(c). Cross-stratal sets are commonly thicker than 1.0m, often reaching 4m, and commonly arranged into type 1 and type 2 Gp complexes (Fig.10). U-shaped channels (Fig.25) with apparent widths of 40m and depths up to 6m (width/depth=6.7) are common in the lower conglomeratic facies and are internally concordantly stratified by Gm and thin lensic sandstone beds (Fig.26). Matrix- to clast-supported Gm also occurs within low angle cross-cutting scours and comprises between 30% to 70% of the cycles. Common facies associations displayed are Se -> thick sequence of interbedded Gm, Gt, St(c) and Gp -> St -> Sh.

The upper conglomeratic facies association can be traced laterally through subsections E, F, the upper part of G, and comprises an overall CU then FU sequence. Cycles from subsections E and F are erosively based, fine-upward and are amalgamated or overlain by a thin discontinuous mudstone bed; cycles from subsection G are thinner, and are capped by thicker laterally continuous heterolithic facies assemblages. Stratification and internal geometry is similar to the lower conglomeratic facies association differing only in the thinner cycle thickness of the upper conglomeratic assemblage.

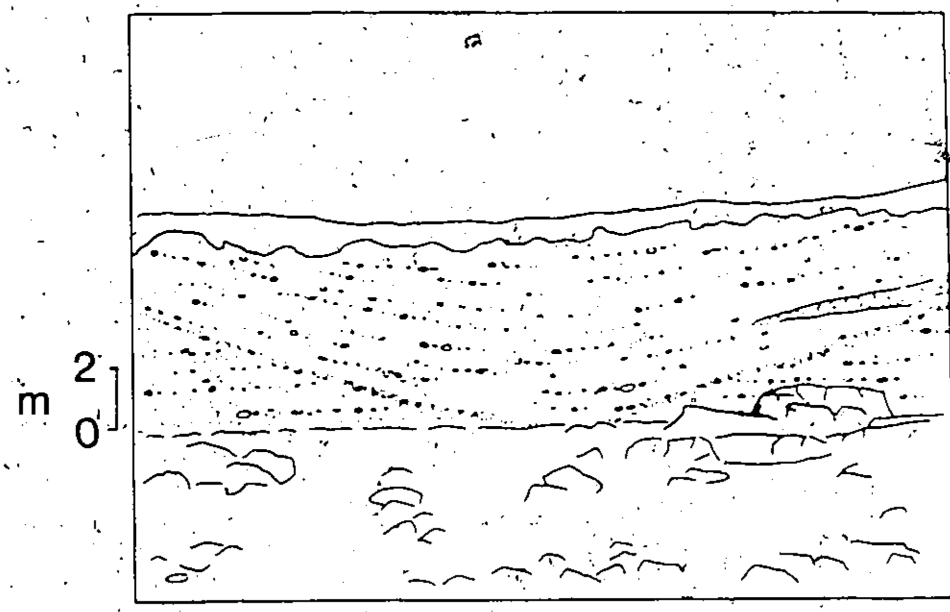

Fig. 25 Large U-shaped channel in cycle GI
at loc. 28

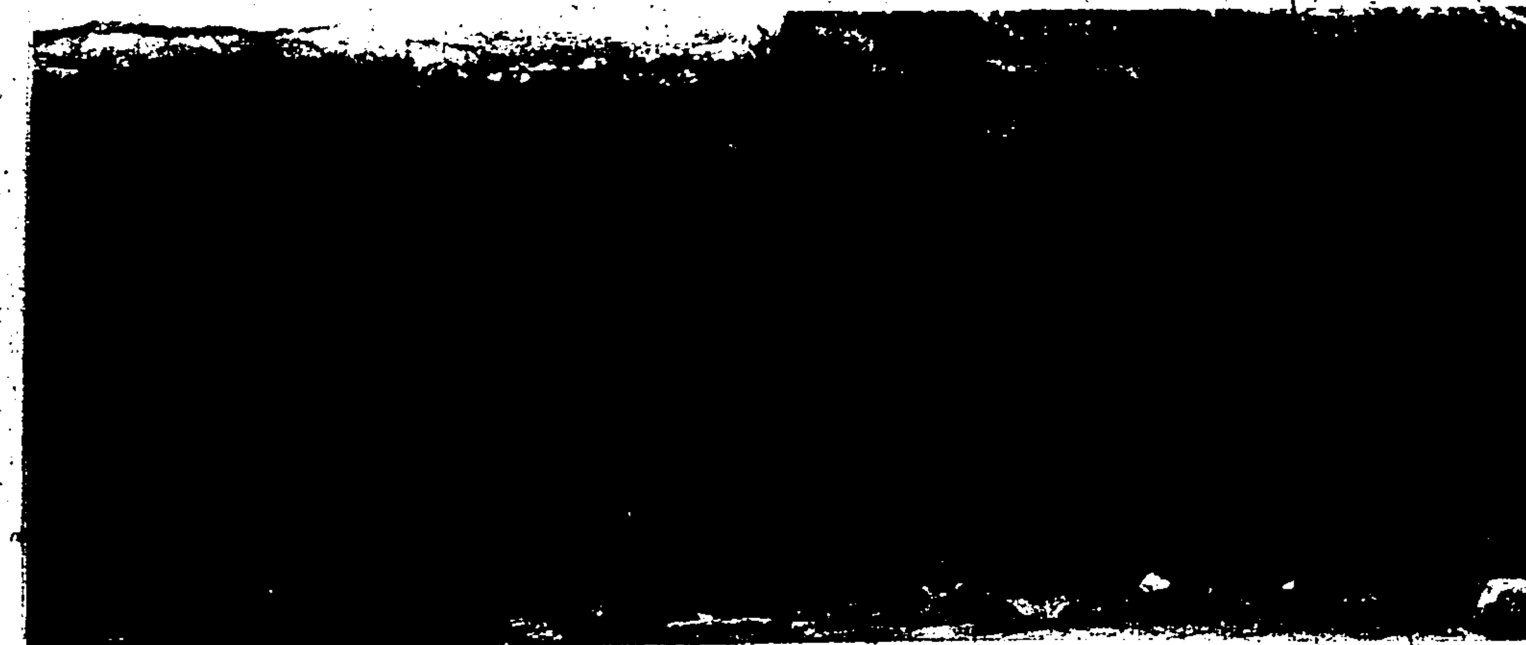

Fig. 26 Internal stratification of large channel in cycle FI (100m south of loc. 17). Scale is 1m.

Vertical trends in the conglomeratic facies association are plotted in Fig.27 as the moving average of the percentage of conglomeratic facies assemblage comprising a cycle. The plot shows three major peaks- the first a maximum; the second a minimum; the third another maximum. The minimum (above cycle GIV) in the moving G% is due to the sandstone facies assemblage which caps the upper units of the conglomeratic facies association, while the two maxima correspond to influxes of conglomeratic material from tectonic pulses (discussed in 6.2). Peaks 1 and 3 are laterally correlative to peaks 2 and 3 from the sandstone facies association of section 02.

Vertical trends for the major lithofacies (Gm, Gt) comprising the conglomeratic facies association are plotted in Fig.27 and show a predominance of Gm/Gt (i.e. complex interstratified Gm and Gt) and Gm in the lower conglomeratic facies sequence and predominance of Gm/Gt in the upper conglomeratic assemblage.

3.4.1 Summary

The following chart (Table 3) summarizes the characteristics of the conglomeratic facies association.

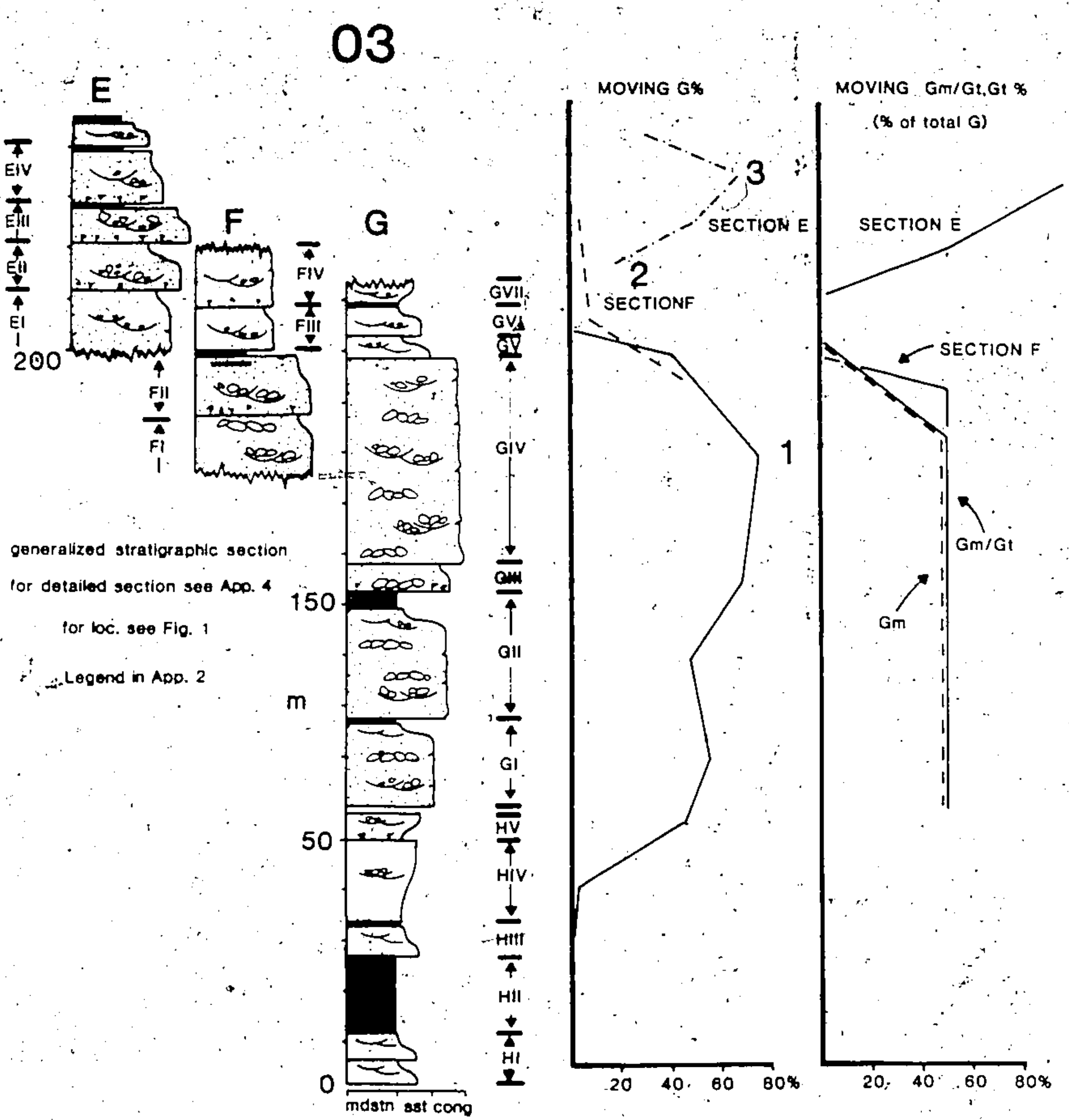
03
E
F
G
EIV
EIII
EII
EI
FIV
FIII
FII
FI
200
150
m
50
0
mdstn sst cong
GVII
GVI
GV
GIV
GIII
GII
GI
HV
HIV
HIII
HII
HI
generalized stratigraphic section
for detailed section see App. 4
for loc. see Fig. 1
Legend in App. 2
MOVING G%
3
SECTION E
2
SECTIONF
1
20 40 60 80%
MOVING Gm/Gt,Gt %
(% of total G)
SECTION E
SECTION F
Gm/Gt
Gm
20 40 60 80%

Fig. 27

Trends and Characteristics of the Conglomeratic Facies Association (Section 03), TABLE 3*

FU	100%
CU (in bottom 2m)	27.3%
CUFU	18.2%
NON FU	-
AMALGAMATED	36.4%
COARSE MEMBER THICKNESS	13.4m
TOTAL CYCLE THICKNESS	14.7M
SHEET-LIKE	YES
STEPPED CHANNEL BASES	-
OVERHANGING CONTACTS	-

* NOTE: each category is out of 100% and accounts for only that specific property.

4.0 BEDDING THICKNESS PATTERNS

4.1 Introduction

Bed thickness is a rarely measured property that can be quite useful in determining depositional patterns within basins. Mathematical analysis of bedding thickness was first endeavoured by Kolomogorov (1951). He found that bedding thicknesses were strongly skewed towards the thinner beds, (reflecting the rarity of major events that deposit thick strata) and proposed that they were lognormally distributed. Subsequently, many workers have shown that lognormal distribution of bedding thicknesses are found in many depositional environments ranging from volcanoclastic (Potter and Scheidegger, 1966), flysch deposits (Schwarzacher, 1953; Bokman, 1953; McBride, 1962) to fluvial (Way, 1968).

In all the aforementioned environments, except fluvial, deposition is characterized predominantly by episodic events, which in general are not erosive. Beds within these sequences are usually quite distinct and easily lend themselves to bed thickness analysis. Thus a bed thickness study on these environments would likely reveal characteristics about the mode of emplacement (i.e. their episodic nature). In fluvial sequence analysis interpretation of bed thickness is more difficult because of difficulty in measuring bed thickness, and because of the nature of deposition. Within fluvial deposits, especially braided systems, individual beds are difficult to discern and of variable thickness due to their complexly interstratified nature, hence the definition of "bed" becomes more nebulous. The problem in analysing bed thickness, *per se*, in a perennial fluvial system is that except for floods the primary mode of sedimentation is in most cases *not episodic* (as it is in flysch and volcanoclastic deposits), but rather takes place by continuous cutting-and-filling, so that laterally persistant beds are rare. Lateral persistance of beds is also restricted by channel and floodplain confinement. The term "bed" *sensu stricto*, within a fluvial system, hence becomes a poor choice for statistical bed thickness analysis and thus a more easily measured property must be found.

In a braided fluvial system rapid changes in discharge along with unstabilized channel margins allow unrestricted migration of channels to deposit various lithofacies units (eg. cosets of Gt, units of Sh et cetera). The type of lithofacies unit will depend on where in the system it was deposited (eg. transverse bar, longitudinal bar, low order channel et cetera). Overbank sandstones, although deposited by an episodic event can still be combined with in-channel deposits since each bed represents a "depositional event" in its own right. The continuity between overbank and in-channel sandstone sedimentation can be discerned by analysing the shape of the cumulative frequency curve (analogous to testing for different grain size populations). If the line can be dissected into two (or more) straight line segments then different populations would be suspected, reflecting overbank and in-channel deposition. Should the curve closely approximate a straight line (i.e. a high linear correlation coefficient) then a continuum between in-channel and overbank deposition is indicated.

In conclusion, to properly analyse bed thickness within a fluvial sequence, only deposits from distinctive depositional events should be measured. In most cases such events are represented by lithofacies units, which were measured for the present study, since laterally persistant beds were not available.

Apart from studies by Potter and Scheidegger (1966); Schwarzacher (1953); Bokman (1953); McBride (1962); and Way (1968) very little has been done to treat bedding thickness statistically. Statistical analysis of cyclically bedded sequences may be very important in determination of deposition-controlling mechanisms, especially in subsurface work.

4.2 Procedure

Cumulative percentages of bed thickness frequency for sandstones (including conglomerates) and mudstones were tabulated for sections 01/02 and 03. Sections 01 and 02 were combined since they are composed primarily of sandstone, whereas section 03 comprises mainly conglomerate. The following procedure was used to test whether the beds were lognormally distributed. First the data were plotted on probability-arithmetic paper, to show that the relationship was not linear. A logarithmic regression was then programmed into a Hewlett Packard-11C calculator and the data were processed. Results for the sandstone and mudstone beds of sections 01/02 and 03 show correlation coefficients for logarithmic plots of cumulative frequency and bed thickness: section 01/02, $r_s = 0.970$, $r_m = 0.973$, section 03, $r_s = 0.953$, $r_m = 0.986$). The best fit lines were then plotted back onto the log-probability paper and displayed sharply curving tails at the both ends of the lines, indicative of a poor fit at the extremities of the population - hence the relationship was not logarithmic near the tails of the curve.

In order to test for lognormality the raw data were then plotted on log-probabilty paper and transferred onto arithmetic paper. Each data point was recalculated as a point on the arithmetic grid, and a linear regression was carried out between the bed thickness frequency and the bed thickness. The linear regression showed in all cases a higher correlation coefficient than the logarithmic regression (eg. section 01/02, r_s =0.991, r_m =0.973; section 03, r_s =0.985, r_m =0.993). The best fit lines were plotted back onto the log probabilty paper (Fig.28,29).

In order to further quantify bedding properties a geometric theta scale (Bokman,1957), akin to the phi scale, was used in order to aid in statistical computations. The theta scale, as defined by Bokman (1957) is analogous to the phi scale:

$$\theta = -\log_2 t$$ where t is the bed thickness (mm)

A modification of Bokman's theta scale was used to calculate statistical parameters. In this study the thickness was measured in millimetres in order to make use of graphic statistical methods already in use. The original equation was also changed in order to make it dimensionless (after McManus,1963).

$$\theta = -\log_2 t/t_0$$

where t is the thickness in mm and t_0 is the "standard bed thickness" (i.e. 0.001m).

Fig. 28

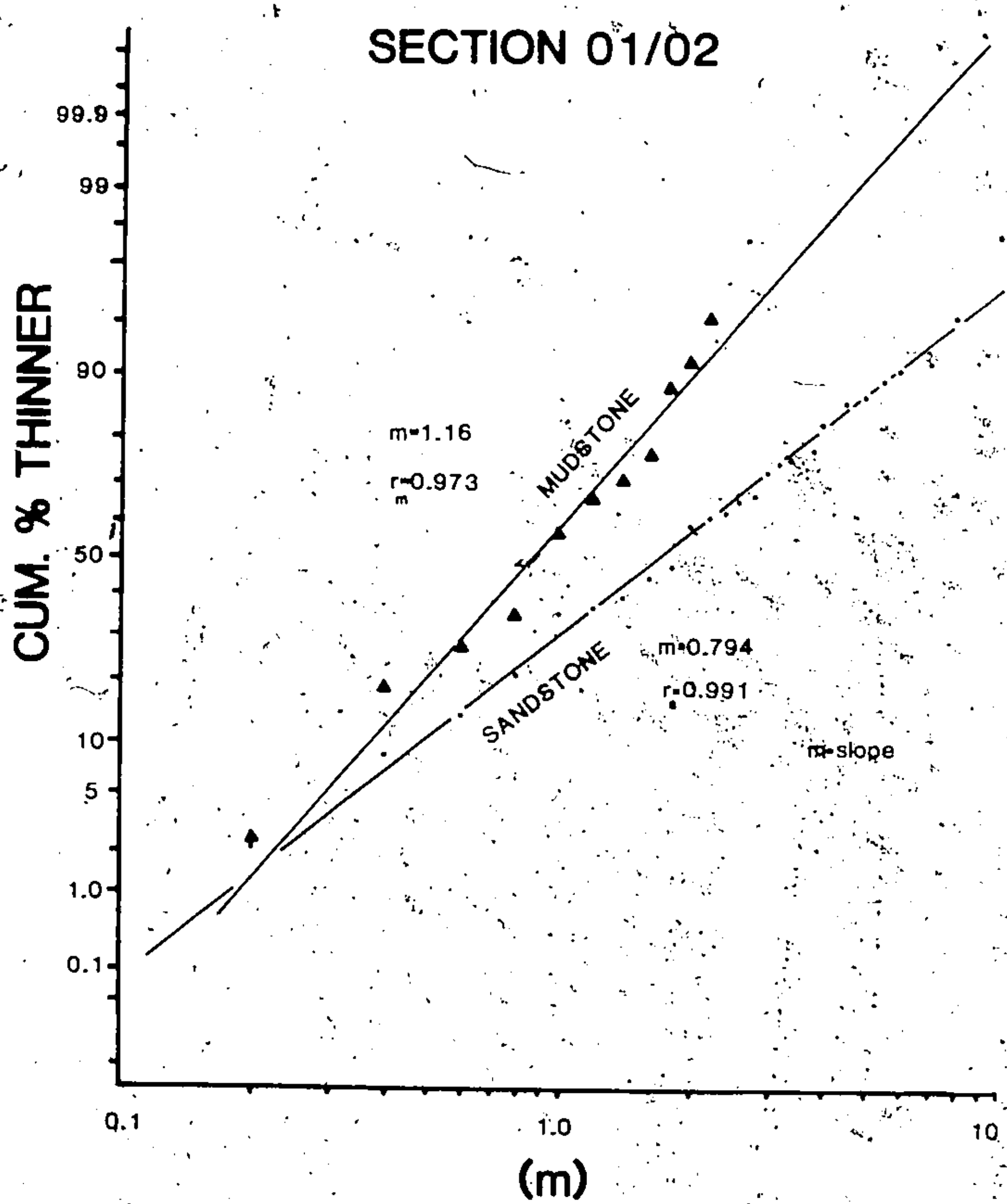
SECTION 01/02
CUM. % THINNER
99.9
99
90
50
10
5
1.0
0.1
0.1
1.0
10
(m)
MUDSTONE
SANDSTONE
m=1.16
r_m=0.973
m=0.794
r=0.991
m=slope

Fig. 29

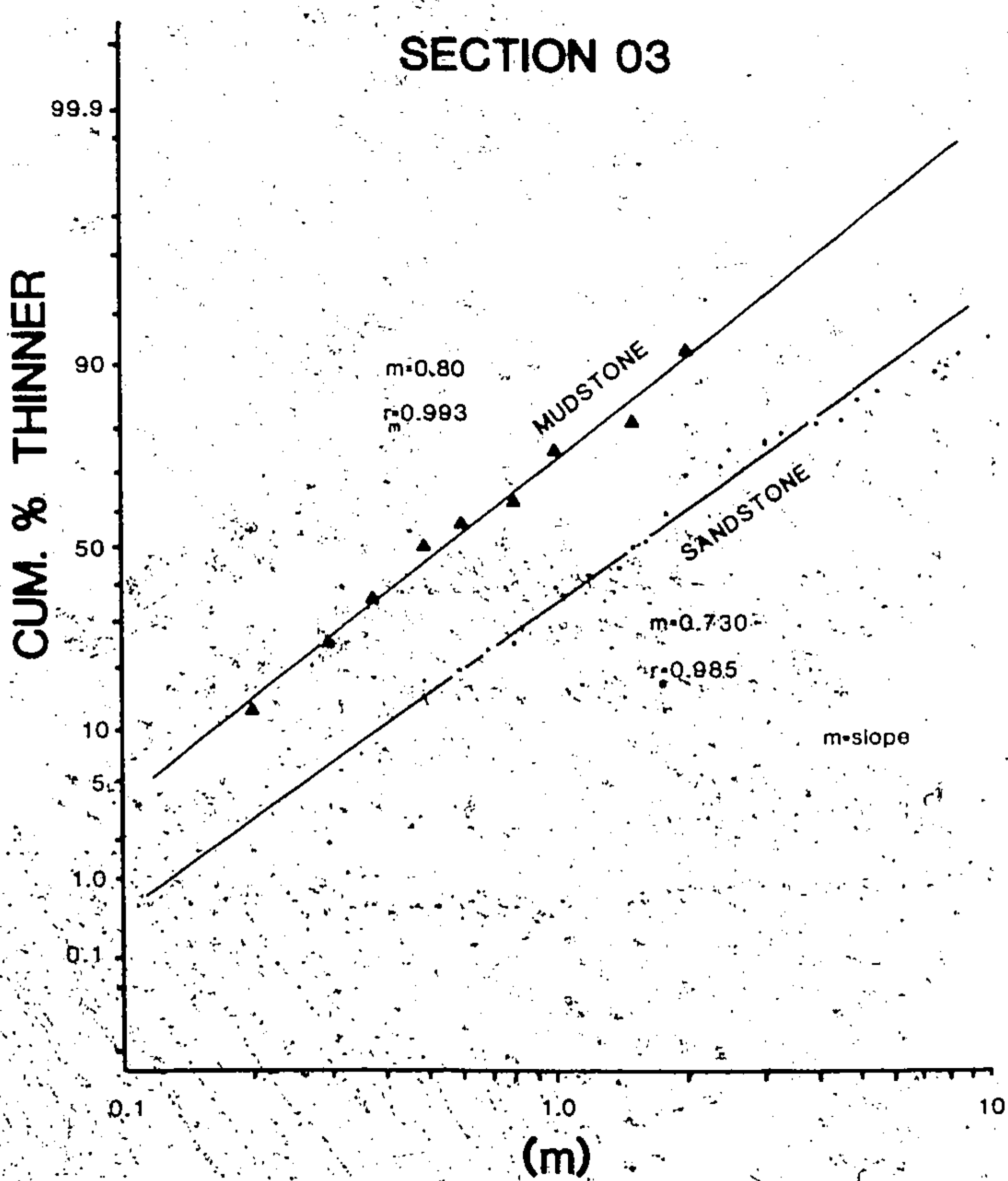
SECTION 03
CUM. % THINNER
99.9
90
50
10
5
1.0
0.1
0.1
1.0
10
(m)
m=0.80
r_m=0.993
MUDSTONE
SANDSTONE
m=0.730
r=0.985
m=slope

The use of a modified theta scale proves very useful because it: i) permits the use of arithmetic rather than logarithmic paper and; ii) it simplifies graphic and numerical calculations.

Statistical parameters were calculated for the cumulative bed thickness curves using graphic measures proposed by Folk and Ward (1957), herewith defined as:

Mean $M = (\emptyset_{16} + \emptyset_{50} + \emptyset_{84})/3$

Sorting $S_I = (\emptyset_{84} - \emptyset_{16})/4 + (\emptyset_{95} - \emptyset_{5})/6.6$

Skewness $S_K = (\emptyset_{84} + \emptyset_{16} - 2\emptyset_{50})/2(\emptyset_{84} - \emptyset_{16}) + \emptyset_{95} + \emptyset_{5} - 2\emptyset_{50})/2(\emptyset_{95} - \emptyset_{5})$

Kurtosis $K = (\emptyset_{95} - \emptyset_{5})/2.44(\emptyset_{75} - \emptyset_{5})$

Another parameter, the dispersive index (D%) was used to compare variation between sections. It is defined as:

$$D = 100\ (M/S_I)\ \text{or}\ 100\ (x/S_D)$$

where S_D is the standard deviation from the arithmetic measures

Arithmetic statistical calculations were also computed in order to compare results with graphic measures. Results from the graphic measures and arithmetic statistical calculations are tabulated in Table 4. Graphic and arithmetic calculations were also made for the Joggins section (Middle Coal-bearing Unit) using Way's (1968) data, which were compared with results from this study (see below).

TABLE 4: Bedding Characteristics

	WAY (1968)	SECTION 01/02	SECTION 03
Graphic Measures:			
SST $M(m)$:	1.65	1.66	1.51
$S_I(m)$:	0.002	0.002	0.003
$D(\%)$:	0.1	0.1	0.2
S_K:	-0.006	-0.103	0.147
K:	0.588	0.552	0.803
Arithmetic Measures:			
$X(m)$:		2.47	3.25
$S_D(m)$:		2.80	5.46
N:		85	51
$D(\%)$:		113.4	168.0
Graphic Measures:			
MDST $M(m)$:	3.81	0.83	0.55
$S_I(m)$:	0.003	0.002	0.002
$D(\%)$:	0.1	0.2	0.4
S_K:	0.193	-0.220	0.002
K:	0.839	0.488	0.592

Arithmetic Measures:

X(m):	1.35	0.994
S_D (m):	1.01	0.990
N:	48	16
D(%):	74.8	99.6

M(m)= mean in metres, S_I (m)= sorting (standard deviation) in metres, D(%)= dispersive index as a percentage (defined in 4.3), S_K= skewness, K= kurtosis
X= arithmetic mean, S_D= arithmetic standard deviation, N= number in sample

4.3 Discussion of Results

Examination of Figs.28,29 shows many similarities and differences between sections 01/02 and 03. Comparison of best fit lines for sandstone beds in sections 01/02 and 03 shows very high correlation coefficients between cumulative frequency of bed thickness and bed thickness with similar slopes (m=0.794 and 0.730 respectively) but differing y intercepts. Comparison between best fit mudstone lines in sections 01/02 and 03 show quite dissimilar slopes (m=1.16 and 0.80 respectively) suggestive of different controlling factors on deposition (discussed later). Contrasts between Fig.28,29 show sandstone and mudstone best fit lines to have similar slopes for section 03, whereas those from sections 01/02 differ markedly.

It is postulated that the slope and y intercept of a best fit line reveal important information about controls on sedimentation. The slope of the line is determined by the frequency and magnitude of deposition events (whether beds or units) and reflects the deviation from the mean ($S_D \propto 1/m$, F. Agterberg, pers. comm., 1986). A line with a gentle slope will have ~~a~~ larger deviation from the mean, marking large variation within a depositional system (eg. proximal braided systems). Steep slopes indicate a small deviation from the mean, suggestive of more consistent depositional patterns as would be expected in anastomosed and meandering rivers, compared to braided rivers. The above statements imply two corollaries: i) shallow slopes result from allocyclic controls, since the largest variations would be expected within the tectonically-controlled proximal alluvial reaches; ii) steep slopes are more likely to reflect autocyclic controls since more consistent depositional patterns would be expected in distal fluvial systems (eg. meandering and anastomosed). Parallelism (i.e. equal dispersive indices) between lines is postulated to indicate <u>similar</u> depositional styles (and controls) although magnitudes (i.e. mean bed thickness) may differ. In the case of section 03 similar slopes between sandstones (including conglomerates) and mudstones rule out autocylically controlled depositional mechanisms on the basis of their contrasting modes of emplacement. It is more likely, in this case, that similar slopes between mudstones and sandstone best fit lines are allocyclically controlled. Different slopes between mudstones and sandstones in section 01/02 imply that mudstone deposition was controlled by another factor, most likely autocylicity. Similar slopes between sandstone beds from sections 01/02 and 03 imply similar deposition controlling mechanisms, most likely allocyclicity, based on facies and facies associations (discussed further in section 6.2).

Analysis of statistical parameters shown in Table 4 reveals important sedimentological properties of proximal and distal deposits. Proximal deposits are represented by section 03 and display similar graphic means and larger arithmetic means than section 01/02 for the sandstone beds, and lower graphic and arithmetic means for the mudstone beds. Results show a downstream decrease in sandstone thickness (also borne out by a downstream decrease in set size, c.f. Table 1) and an increase in mudstone bed thickness. Analogous downstream decreases in thickness of sandstone bodies and set size have been annotated from the Wood Bay Formation, (Spitsbergen), the Vidal Supergroup (Greenland), and in the Mio-Oligocene Luna and Huesca systems of the Ebro Basin (Spain) by Friend (1978) and Friend et al. (1985). Downstream decreases in channel depth may be due to several factors (Friend,1978; Friend et al.,1985): 1) loss of water into permeable alluvium and/or; 2) evapo-transpiration. An alternative explanation for the downstream decrease in bed thickness may be the increased truncation of beds, which results in a smaller mean. Although possible, the latter suggestion is unlikely since the downstream decrease in cross-stratal set size is also marked by an increase in foreset curvature, thus confirming that the decrease is real and not caused by truncation of formerly large sets.

The skewness data also support a downstream decrease in channel depth. Sandstone and mudstone beds from sections 01/02 are negatively skewed implying a deficiency in thick beds, possibly caused by shallower channels which did not allow formation of thicker beds. Section 03 contrasts by being positively skewed (i.e. thin bed poor). Positive skewness may be due to several factors: i) preservation of only the thicker beds (flood-generated) or; ii) deeper channels only allowed deposition of larger bedforms. The ubiquitous presence of larger bedforms (Figs.25,26) in sections 03, along with a downstream decrease in set size (Table 1) suggests that the latter point may be the more important factor determining positive skewness.

Comparison of dispersive indices (arithmetic and graphic) between sections 01/02 and 03 show a downstream decrease for sandstone and mudstone beds. A decrease in dispersive indices implies less variation in bed thickness due to more stabilized channels (also implied from the vertical sandstone/mudstone contacts and the abundance of rooted mudstones).

Analysis of kurtosis displays platykurtic curves for mudstones and sandstones from sections 01/02 and 03, furthermore beds from section 01/02 have lower values than those from section 03. The platykurtic property displayed by bed thicknesses may indicate the following: i) preferential erosion of beds with thicknesses approximating the mean; ii) fluctuations in stage producing a wide range of bed thickness; iii) there was a wide range in channel depths, which caused the development of a broad statistical mode. The first explanation suggests that the truncation of beds around the original mode (i.e. the most common bed thickness) may create a distribution which lacks a distinctive mode as seen in the platykurtic properties of both sections. The second explanation is plausible due to the abundance of reactivation surfaces. However, the persistance of large scale crossbedding suggests that flows were sustained long enough to produce equilibrium bedforms (discussed in section 7.2), destroying smaller bedforms created during waning stage (Jones,1977). This would result in a positively skewed population in the proximal section. The third suggestion seems more reasonable since a braided system comprises a wide range of channel depths hence creating a normal distribution with a weak mode i.e. a platykurtic curve. Proximal to distal relationships in sandstones show a decrease in kurtosis with increasing distality. This may be on account of an even more poorly defined mode for channel depths in the distal reaches, possibly due to higher braiding indices, or increased truncation of original units (this is unlikely for the reasons previously given). Mudstones also show a decrease in kurtosis with increasing distality. This may be due to the increasing randomness of distal floodplain deposition caused by vegetation of channel margins.

Data processed from Way's (1968) study on the Lower Fine Unit of the Cumberland Group (Table 4, Fig,30) show that both sandstones and mudstones have platykurtic properties but differ in skewness, with the former showing negative skewness (thick bed poor) and the latter positive skewness (thin bed poor). Results concur with what is expected on floodplains within meandering fluvial reaches. i.e. deposition of thin sandstone due to episodic overbank flooding and thick mudstones due to pervasive suspension deposition. Interestingly, mudstones and sandstones from this study area also have platykurtic properties which may suggest that kurtosis is being controlled by the actual distribution of the beds rather than subsequent modification by erosion.

4.4 Summary:

1) Similar slopes in cumulative bed thickness curves indicate similar controls on bed forming processes.

2) Sandstone bed thickness decreases downstream while mudstone bed thickness increases. Along with decreases in set size this trend may indicate a downstream reduction in channel depth possibly due to percolation of water into the alluvium or evapo-transpiration.

3) Sandstone and mudstone beds are negatively skewed in section 01/02 and positively skewed in 03 suggesting a downstream decrease in channel depth.

4) Dispersive indices decrease downstream implying more stabilized channels in the distal reaches.

5) All sections show platykurtic properties. This may be on

Fig. 30

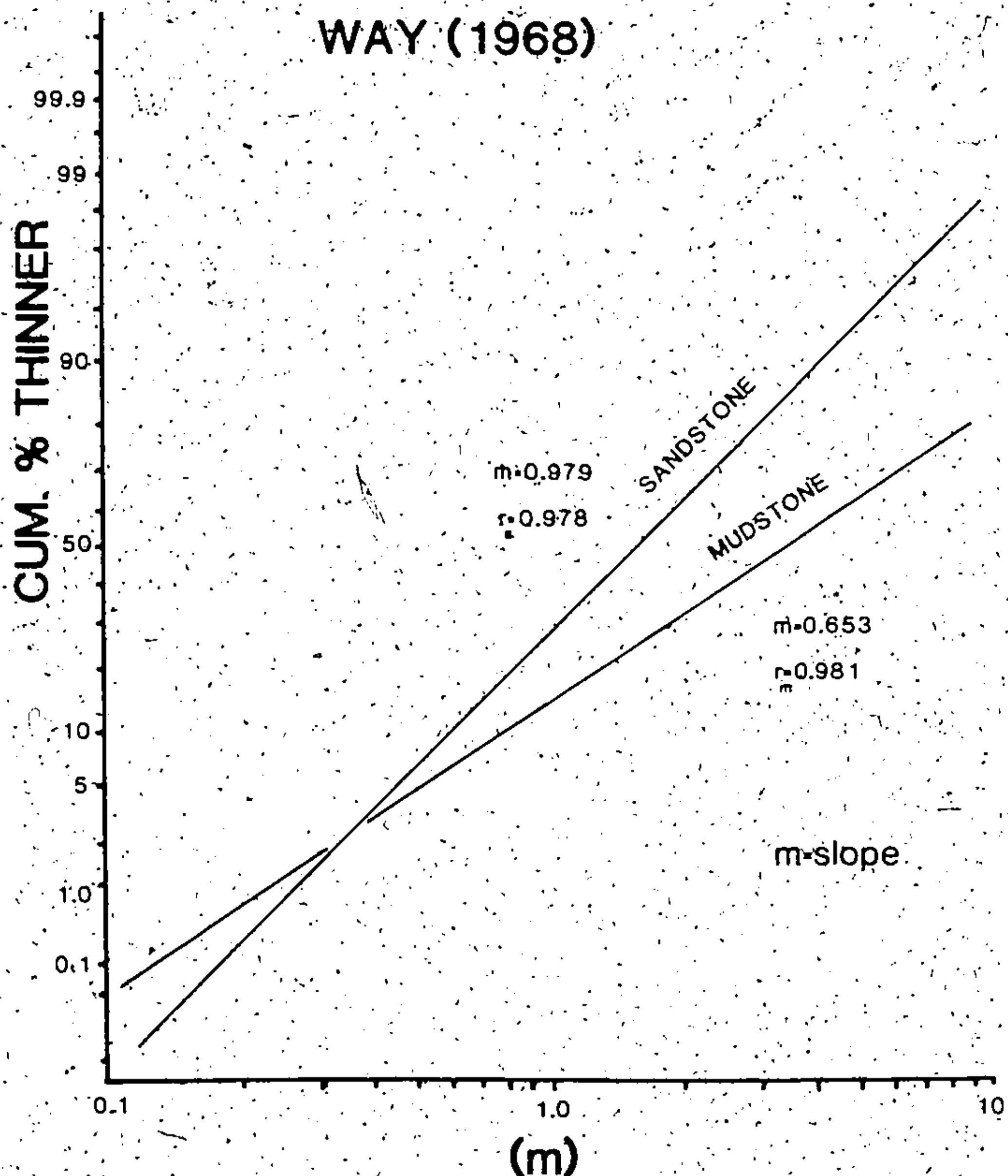

WAY (1968)
CUM. % THINNER
99.9
99
90
50
10
5
1.0
0.1
0.1
1.0
10
(m)
SANDSTONE
MUDSTONE
m=0.979
r=0.978
m=0.653
r=0.981
m=slope

account of actual distribution of beds rather than subsequent erosional modification.

6) Kurtosis decreases downstream but the cause is unknown.

5.0 PREFERRED FACIES TRANSITIONS

5.1 Introduction

Preferred facies transitions are commonly tested by Markovian analysis. A Markov process is a stochastic process which describes a sequence of states for which the occurrence of one state exhibits a dependence on the previous state (or states). First order, or embedded Markov chains analyse the probability of entering a certain state from the previous state occupied and exclude transitions between identical states (Kemeny and Snell, 1960).

Although Markovian analysis have been used commonly, (Gingerich, 1969; Selley, 1970; Miall, 1973; Cant and Walker, 1976) they suffer from theoretical and statistical inadequacies. Theoretical problems are especially common in the application of Markov processes to braided fluvial systems. Studies on these types of fluvial systems suffer from the attempt to categorize a laterally highly variable system into a one dimensional vertical sequence (Collinson, 1978), hence "evaporating" all the important data on lateral facies relationships. The statistical problems are quite numerous and are discussed by Carr (1982), Powers and

Easterling (1982), Walker (1984), and Harper (1984) and are herewith summarized:

i) By definition embedded matrices, cannot have transitions between two identical states, so that diagonal frequencies must be structural zeroes, thus invalidating the usual tests (chi-square, or G^2) for independence (Powers and Easterling, 1982). Independence is defined as $P_{ij} = P_{j}$ (for i=1,2,3,...n), where P_{ij} is the probability of a transition from i to j i.e. a transition to state j occurs with the same probability regardless of the present state.

ii) Application of a chi-square (X^2) test to the matrix only tests the whole matrix for non-randomness. That is, it does not evaluate the statistical probabilities for <u>individual</u> cells (Carr, 1982; Powers and Easterling, 1982).

In order to alleviate the first problem a quasi-independent model (Goodman, 1968) is used to accommodate structural zeroes. In this model expected cell transitions ($E(n_{ij})$) are calculated as follows:

$$E(n_{ij}) = a_i b_j \quad i \neq j$$
$$E(n_{ij}) = 0 \quad i = j \text{ where } i,j = 1,2,3,\ldots n$$

a_i and b_j are parameters calculated using iterative proportional fitting techniques. The iterative procedure is as follows (Powers and Easterling, 1982):

First Iteration: $a_i^{(1)} = n_{i+}/(n-1)$ $i = 1,2,\ldots n$
(where n_{i+} is the summation of the i^{th} row)

$b_j^{(1)} = n_{j+}/\sum_{i\neq j} a_i^{(1)}$ $j = 1,2,\ldots n$

(where n_{j+} is the summation of the jth row)

I^{th} Iteration: $a_i^{(I)} = n_{i+}/\sum_{i\neq j} b_j^{(I-1)}$ $i = 1,2,\ldots n$

$b_j(I) = n_{j+}/\sum_{i\neq j} a_i(I)$ $j = 1,2,\ldots n$

This procedure is continued until a preset convergence value is reached:

$$\left|a_i^{(i)} - a_i^{(I-1)}\right| < r(a_i^{(I)}) \quad i = 1,2,\ldots n$$

$$\left|b_j(I) - b_j(I-1)\right| < r(b_j)(I) \quad j=1,2,\ldots n$$

(r = preset conversion factor which varies between 0-1.0 i.e. between 0-100%)

Once a_i and b_j values are reached E_{ij} values may be tabulated, and an E_{ij} probability matrix may be constructed. From this, the observed probability matrix can be subtracted, as in the "old method" and a difference matrix is obtained.

In order to solve the second problem (testing the whole matrix for significance rather than individual cells) Harper (1984) advocates the use of the binomial probability theorem to test each individual cell for significance i.e. testing for at least n transitions in N trials. This can be calculated as follows:

$$P(n)=\sum_{n}^{n=N} C(N,k)\; p^{n} q^{N-n}$$

where $C(N,k)= N!/(N-n)!n!$

p= observed probability

q= 1-p i.e. probability of failure

N= total trials in i^{th} row

n= observations

To determine significance, the results of P(n) can be checked against the null hypothesis (that transitions are random) at a certain level of confidence. By using this method specific facies transitions can be deemed statistically significant and correct facies relationship diagrams may be drawn.

5.2 Procedure

In order for Markov chains to be statistically correct column and row totals should be equal, although discrepancies between two columns and rows are allowable (Powers and Easterling,1982). Discrepancies between column and row totals can be avoided, or at least dampened by counting facies transitions within sections rather than partitioning into facies assemblages as some workers have done.

Facies transitions were tabulated for sections 01, 02, and 03. Coarse and fine member assemblages were separated in order to test for non-randomness in each. The problem of column totals not equalling row totals was solved by having a separate transition state for the overlying coarse or fine member assemblage (depending on which facies assemblage was being tested). This eliminated unwanted "noise" from the facies assemblage which was not being tested, and still maintained equal row and column totals. Erosional surfaces were tabulated between coarse and fine members only when evidence for erosion existed (i.e. basal intraclasts, erosional relief) and not at the junction of every cycle.

Results were then analysed using a program developed by W.L. Duke, and transcribed by the this author for the PCjr, based on Powers and Easterling's (1982) quasi-independence model for Markov chain anlaysis and Harper's (1984) binomial probabilty method for testing individual cell significance. Individual cell significance was tested by setting confidence limits (α) at 0.10 and 0.20 and a null hypothesis of : H_0 : $p>0.10$ (or 0.20); H_a : $p<0.10$ (or 0.20) hence the null hypothesis would be rejected if $p<0.10$ (or 0.20) and the transition would be significant. In the event that several cells within the same row had similar binomial values higher than the highest preset confidence limits (i.e. $p=0.20$), the lower value would be taken as the most probable to occur. The whole matrix was then tested with a chi-square test (d.f.=$(N-1)^2-N$) using observed values and those expected values obtained through the iteration process. The use of the quasi-independence model for determining expected cell values validates the use of a chi-square test (Harper,1984; Powers and Easterling,1982).

Those values found to be significant using Harper's method (1984) were then plotted as a facies relationship diagram, from which preferred facies transition paths were calculated using the multiplicative law of probability (P_T). Average lithofacies thicknesses were then used along with the facies relationship diagram to construct a theoretical summary sequence (Walker and Cant,1984).

5.3 Results

The raw results for sections 01, 02, and 03 coarse members are tabulated in Appendix 10, while the facies relationships and local summary sequence diagrams representing idealized cycles based on statistically significant transitions are in Figs.31,32, and 33 respectively.

Section 01 (Fig.31) shows that the vertical succession was derived by a non-random process (X^2=94.2, d.f.=55), significant at the 0.995 level. Significant transitions using the calculated binomial probability cell values indicate three possible pathways. The most likely to occur (P_T=0.004) is: F -> Sr -> St(c) -> Sh -> F (see Fig.31). This concurs with field observations (cf. Table 2). Type cycles are seen

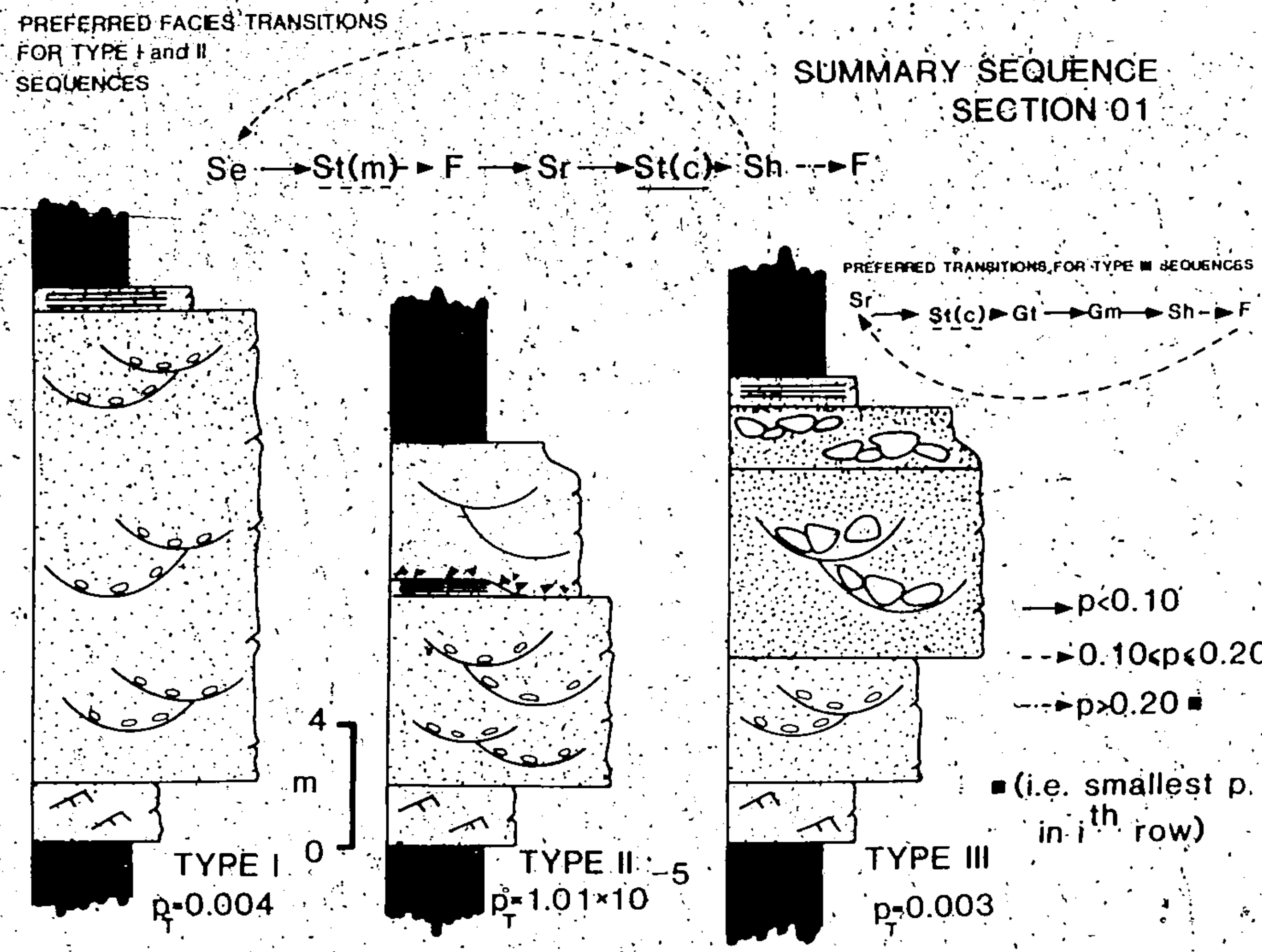
PREFERRED FACIES TRANSITIONS FOR TYPE I and II SEQUENCES
Se ⟶ St(m) ⇢ F ⟶ Sr ⟶ St(c) ⟶ Sh ⇢ F
SUMMARY SEQUENCE
SECTION 01
PREFERRED TRANSITIONS FOR TYPE III SEQUENCES
Sr ⟶ St(c) ⟶ Gt ⟶ Gm ⟶ Sh ⇢ F
4
m
0
TYPE I
$p_T = 0.004$
TYPE II
$p_T = 1.01 \times 10^{-5}$
TYPE III
$p_T = 0.003$
⟶ $p < 0.10$
⇢ $0.10 < p < 0.20$
⇢ $p > 0.20$ ■
■ (i.e. smallest p in i^{th} row)
LITHOFACIES LEGEND IN APP. 2

Fig. 31

in the middle reaches of section 01 (eg. BIV, AI, AII, see App.2) and are characterized by thick coarse members with CU bases, little if any FU nature, and sharp tops. Variants of this type could have a slight fining-up in the upper quarter of the cycle.

The second type of possible transition pathway has a much smaller probability of occurring ($P_T = 1.01*10^{-5}$) and has the following transitions: F -> Sr -> St(c) -> Sh -> Se -> St -> F. The sequence defines a CUFU cycle and differs from the first type by the amalgamation of a St unit. Field observations show that CUFU-type cycles are the least common (30% of the cycles in section 01, Table 2) and no exact replicas of type two cycles were found, although variants exist.

The third type of transition pathway has a higher probability ($P_T = 0.003$) and has the following transitions: F -> Sr -> St(c) -> Gt-> Gm -> Sh -> F. The preferred transition pathway defines a very well developed CUFU sequence, variants on this theme are cycles BII and BIII at the base of section 01 (see App.2).

Comparisons between preferred transition pathways (i.e. theoretical cycles) and observed cycles show the following trend: cycles at the base of section 01 are dominated by type III cycles (conglomeratic CUFU cycles); the middle parts have primarily type II cycles (thick CU amalgamated cycles) while the upper parts have type I cycles (sandstone CUFU). Depositional environments for these sequences will be discussed in section 6.2.

Chi-square tests on the observed/expected transition matrices from section 02 negate the null hypothesis (X^2=41.3, d.f.=30) at the 0.90 confidence level, a slightly lower level than section 01. Preferred transition pathways using calculated binomial probability cell values show two preferred pathways, although neither have very high confidence limits.

The first type has a 0.011 probability of occurring (law of multiplicative probabilities) and shows the following transitions: Se -> St(c) -> St -> Se (Fig.32). The preferred transition pathway denotes a FU amalgamated cycle and is represented in section 02 by cycles CII, DII (see App.3). The presence of FU amalgamated cycles was corroborated by field observations (cf. Table 2).

The second type of pathway has a much lower probability of occurring (P_T=4.23*10^{-6}) and is defined by the following pathway: Se -> St(c) -> St -> Sh -> Sr -> Fm -> Se. The pathway defines a cycle which differs from the first type by not being amalgamated, i.e. it is a complete cycle.

Chi-square tests on section 03 (Fig.33) also show non-randomness (X^2=88.0, d.f.=55) at the 0.995 confidence level.

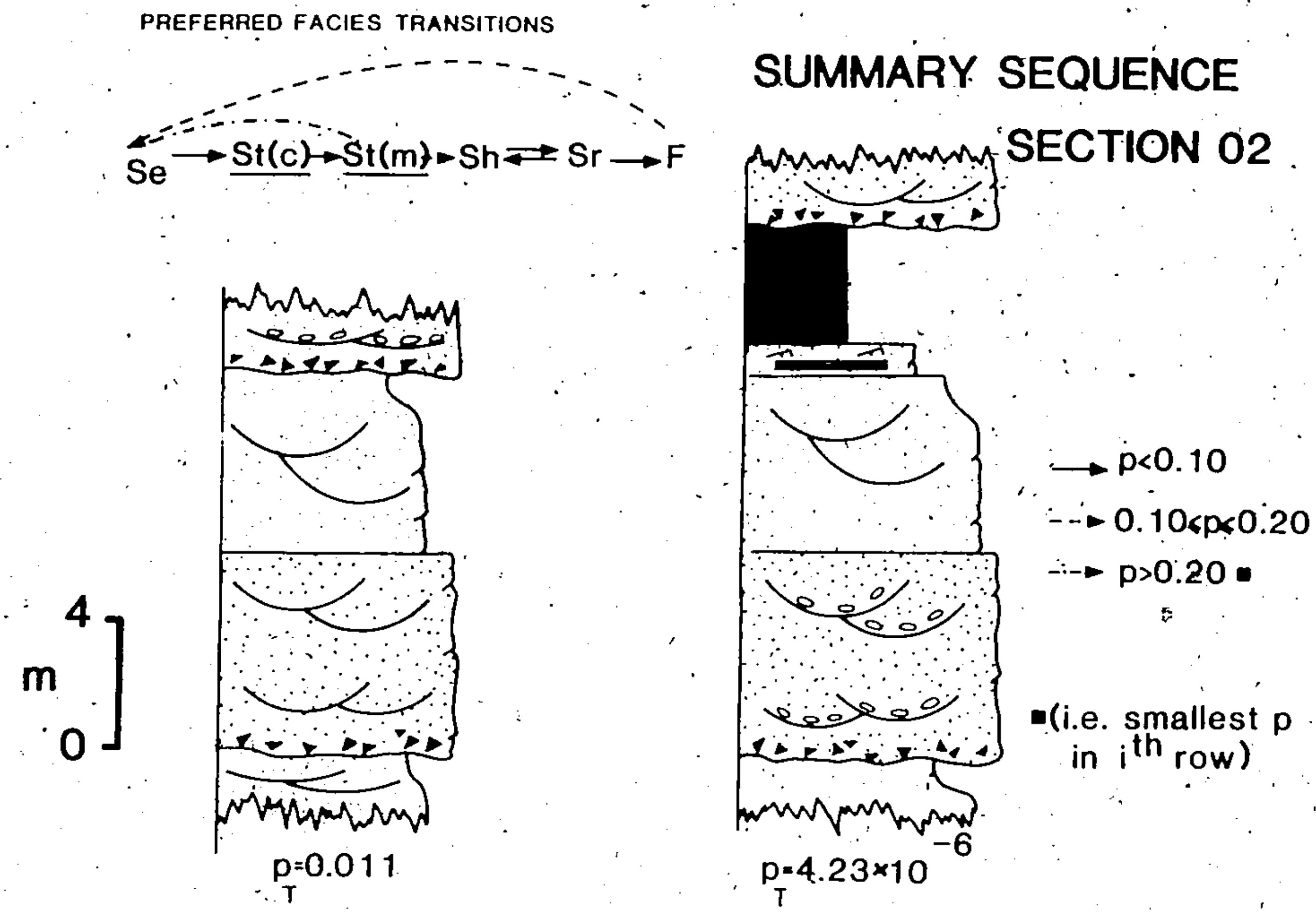

Fig. 32

LITHOFACIES LEGEND IN APP. 2

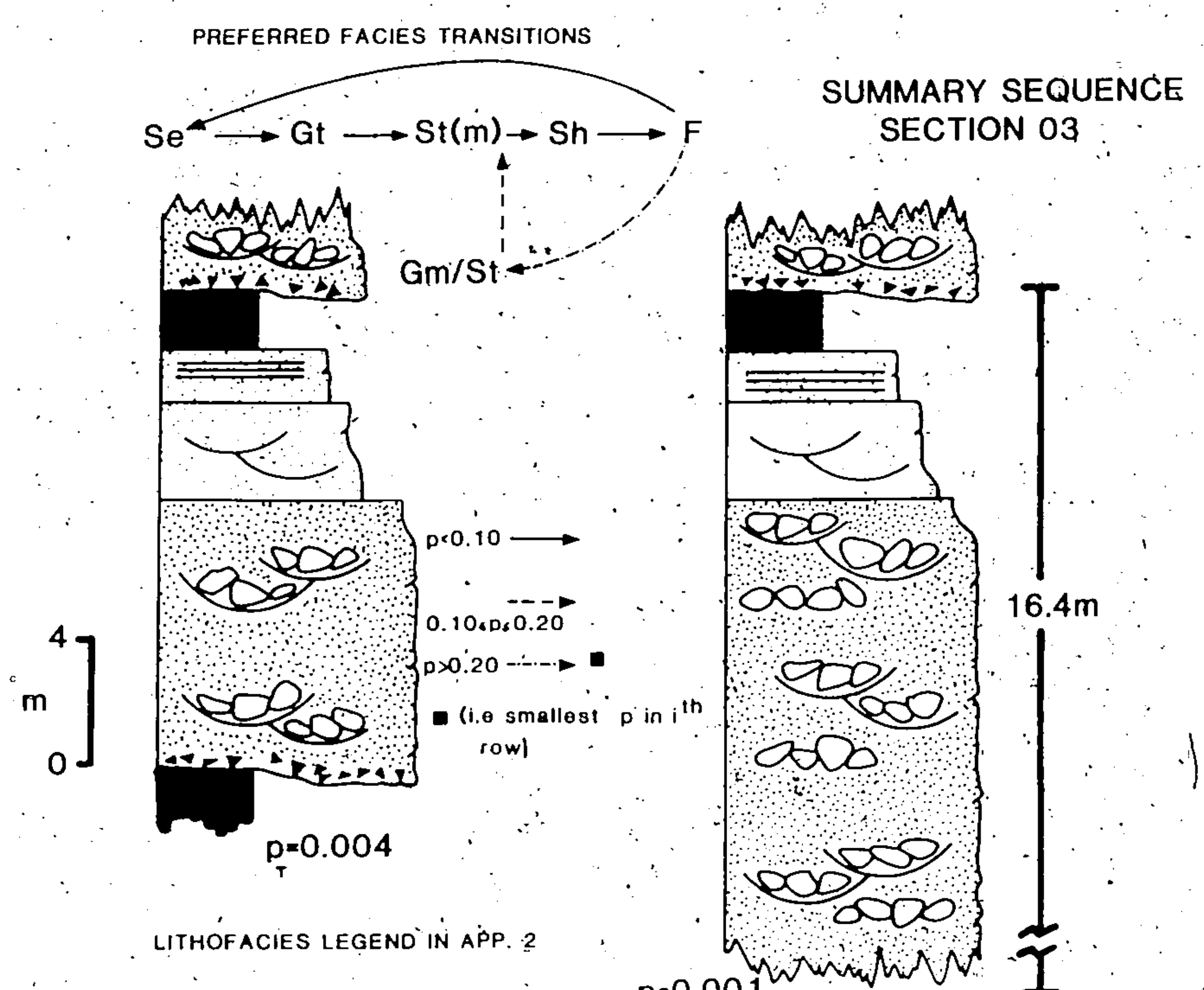
PREFERRED FACIES TRANSITIONS
Se → Gt → St(m) → Sh → F
Gm/St
SUMMARY SEQUENCE
SECTION 03
p<0.10
0.10<p<0.20
p>0.20
■ (i.e smallest p in i th row)
4
m
0
p_T=0.004
16.4m
p_T=0.001
LITHOFACIES LEGEND IN APP. 2

Fig. 33

Significant transitions imply two preferred pathways. The most likely pathway ($P_T = 0.004$) shows transitions: Se -> Gt -> St -> Sh -> Fm -> Se. The transition pathway outlines a well-developed, erosively-based, FU sequence. The less preferred pathway ($P_T = 0.001$) involves: Gm/Gt -> St -> Sh -> Fm -> Gm/Gt with variants found primarily in the lower part of section 03 (eg. GI, GII, GIII, see App.4). This less preferred sequence also fines-up but is thicker and has multiple internal erosion surfaces.

Results from the analysis of the fine members (heterolithic facies assemblages) of section 01/02 are tabulated in Appendix 10, while the preferred facies pathways and summary sequence diagram are in Fig.34. It should be noted that cycle BI was excluded from the analysis since it was of a different origin (i.e. thick floodplain succession) than the other fine members.

Chi-square tests show that the heterolithic facies assemblage from sections 01/02 was derived by a non-random process (X^2 = 70.6, d.f.= 41) significant at the 0.995 level. The most probable ($P_T = 0.0005$) facies transition pathway is (Fig.34) coarse member -> Fl -> Sr -> red Fm -> mottled Fm -> coarse member. A slightly less significant capping sequence is: ...Fm(m) -> Fm(g) -> coarse member.

SUMMARY SEQUENCE FOR THE HETEROLITHIC FACIES ASSOCIATION

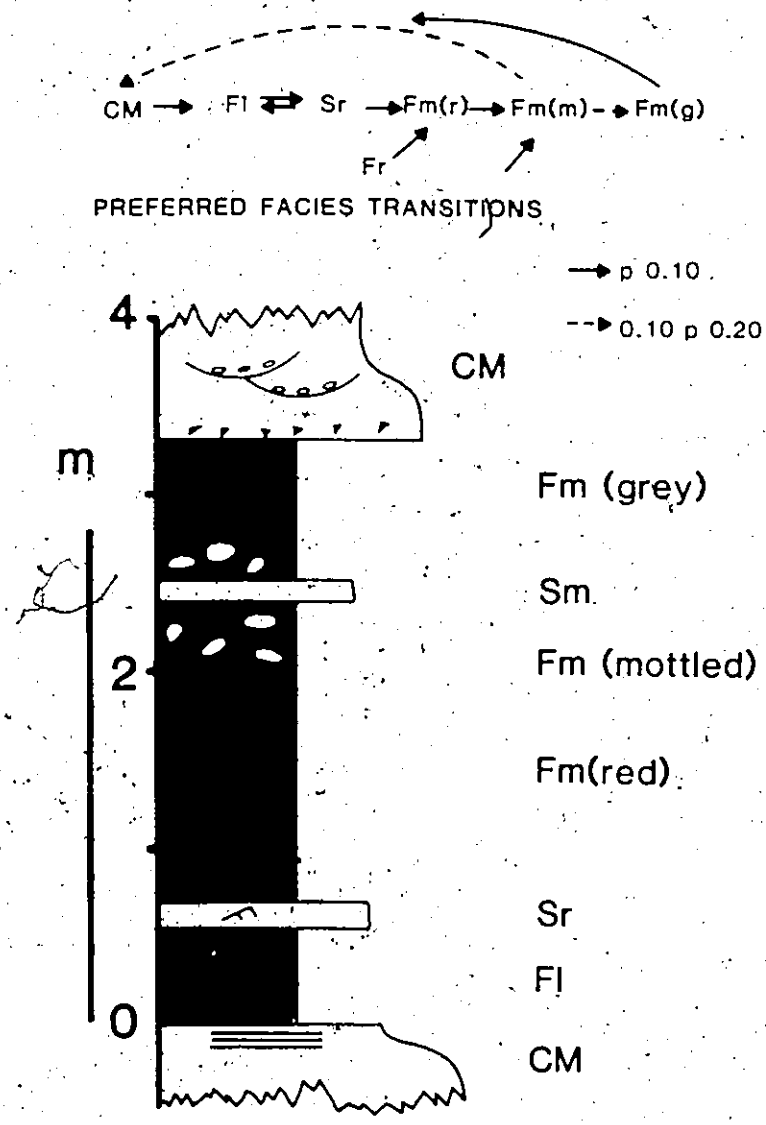

Fig. 34

6.0 DEPOSITIONAL ENVIRONMENT AND CYCLICITY

6.1 Introduction

Facies, facies associations and bedding characteristics suggest that sections 01, 02 and 03 were deposited on a low gradient braidplain. Channel morphology varies according to proximity to source: proximal reaches are characterized by wide, deep, gravelly channels while distal channels are sandy, shallower and laterally stabilized by cohesive vegetated mud banks. Areally extensive floodplains flank distal reaches and are marked by mudstone deposition and occasional overbank sheetsand deposits.

Vertical sequences show two orders of cyclicity - the first, controlled by intrinsic properties of the fluvial system (autocyclic controls), the second, regulated by extrinsic controls (allocyclic mechanisms) from outside the basin. Allocycles can be correlated throughout the three sections whereas autocycles vary in lateral extent.

6.2 Depositional Environment

Braided fluvial deposition can be recognized by four criteria (Steel and Thompson, 1983; Friend, 1983); i) sand/gravel body shape; ii) paleocurrent variance; iii) facies associations and fabric; iv) paleogeographic setting.

The first criterion for braiding is sand body shape and is marked by sheet-like laterally extensive sands, which are often multistoried and lenticular in nature. The lenticular and multistorey styles are distinctive characteristics described by many workers (Friend and Moody-Stuart,1972; Leeder,1973; Campbell,1976; Nami and Leeder,1978; Cotter,1978; Friend,1983; Allen,1983; Nemec and Steel,1984).

The second criterion requires unimodal low variance paleocurrents. Although low variance unimodal paleocurrents are the norm, bimodality and high paleocurrent dispersion can occur under ephemeral conditions (Mader and Teyssen,1985) and by the preservation of low and high order channel deposits (_sensu_ Rust, 1978a), thus making distinction between high and low sinuosity rivers difficult.

The third criterion, fabric and facies associations, are one of the most definitive aspects of braided fluvial deposition. Meandering rivers can be distinguished from braided systems on the basis of texture (Rust,1978b). Texture, _sensu lato_ is defined as the proportion of gravel to sand and is characterized in meandering "gravelly" rivers (Wabash, Amite, Endrick) by localized gravel lags at the base of the channel, in which gravel is predominantly sand matrix-supported. In contrast, a framework-supported fabric is typical of gravelly braided streams. However, an argument based on framework support may not by itself be sufficient to distinguish gravelly single channel rivers (the "wandering rivers" of Church, 1983; Ferguson and Werrity, 1983) or gravelly anastomosed rivers (Smith and Smith,1980). Facies associations in conjunction with the other criteria provide a powerful method for discerning the type of fluvial system. The absence of lateral accretion surfaces and recognition of certain types of bar deposits (eg. longitudinal, linguoid, transverse, diagonal) are often cited as characteristics of braided streams.

Lastly, the paleogeographic positioning of deposits may be very helpful in pinpointing, or at least bracketing the location of possible braided fluvial environments. Non-genetic fluvial classification schemes, like Rust's (1978b), are very useful for such purposes. In conclusion, no one criterion may be definitive in distinguishing braided fluvial deposits, but the use of all criteria will lead to unequivocal results in most cases.

Section 01, 02 and 03 all display the four aforementioned criteria for recognition of braided fluvial systems. The following points were used to discern a braided fluvial depositional environment for sections 01, 02, and 03:

Sandbody Shape: i) laterally extensive sheet-like geometry
ii) multistorey nature of cycles
iii) lenticular internal geometry

Paleocurrents: i) low variance, unimodal (discussed in section 7)

Facies Associations: i) no lateral accretion deposits

ii) predominance of high flow regime bedforms
iii) coarse-grained units not confined as lags
iv) facies associations do not conform with meandering fluvial models (cf. Jackson, 1976b)
v) abundance of large-scale Gt, Sp, St indicative of large linguoid and crossbedded simple bars

Fabric: i) preponderance of framework-supported conglomerates within the conglomeratic facies association

Paleogeographic Setting: i) within a non-marine basin
ii) paleocurrents and grain size distribution compared to basin geometry suggests braided fluvial environment

Within braided fluvial systems a continuum in grain size, lithofacies, and vertical profiles exists between proximal and distal reaches. The upper part of section 03 (subsections E,F,G) displays characteristics similar to (proximal to) distal gravelly braided deposits (type G_{III}; Rust,1978b). Preferred cycles (Fig.33) are marked by laterally extensive sheet-like gravels arranged into: Se -> Gt (or Gm/Gt) -> St -> Sh -> Fm -> Se. The cycles are interpreted as deposited within vertically aggrading low sinuosity braided gravelly channels. Common internal erosion surfaces and rapid lateral lithofacies changes indicate that channels were unconfined and that lateral channel switching must have been aided by fluctuations in stage. Fluctuating flow conditions are inferred from type 1 and 2 Gp-Sp type bar complexes and from common convex-up reactivation surfaces (Collinson,1970; Jones,1977). The presence of large scale cross-strata (>4m, eg. Figs.7,10,25,26) implies that flood stage conditions must have persisted long enough to allow the formation of large-scale equilibrium bedforms. Flood stage generated bedforms include longitudinal bars within shallow channels, depositing Gm, and linguoid bars in areas of flow divergence or deeper tracts (Hein and Walker, 1977), hence depositing Gm/Gt (Bluck,1979; Thompson and Steel, 1983). The predominance of Gm/Gt along with internal erosion surfaces of varying lateral extent (5-40m), in cycles GI-IV (App.4), suggest that these were flood generated deposits. Preservation of flood-stage bedforms necessitates a moderately paced decline in flood stage levels, since a rapid decay in flood stage would dissect the large bedforms, and subsequently destroy them during low stage (eg. Platte R.: Blodgett and Stanley,1980; Jones,1977). Hence it is imperative that the difference between flood and low stage be moderate (to low) in order to preserve flood-generated bedforms. Low stage modifications of the gravels include draping of lensic sandstone beds on the sides or fronts of bars (Williams and Rust,1969; Rust,1972; Rust and Koster,1984; Nemac and Steel,1984) which are ubiquitous in lower subsection G.

Individual cycles in subsection G (eg.GI,II,IV; see App.4) display a fining-upward nature in the upper fifth of the cycle. The cycles are sharp-based and complexly stratified with Gm/Gt, with lensic sandstones and internal erosion surfaces. The aforementioned characteristics, along with positive skewness of stratal thickness (which suggests top-truncation of units, see section 4.3), and thick crossbed sets (often >4m), indicate rapid, erosive channel switching of relatively deep channels (approximately 10m, B.R. Rust pers. comm., 1985). It is inferred that sediment input rates must have been greater than subsidence to allow for the accumulation of thick cycles and the abundance of internal erosion surfaces (McLean and Jerzykiewicz, 1978). Reduction of stage levels (i.e. gradual channel abandonment) and/or avulsion, possibly allocyclically induced (discussed later), created the FU sequence and sharp contacts between coarse and fine members. It is probable that the FU nature was tectonically induced since peaks in the moving fine member percentage (F%, Fig.16) can be correlated with those of section 01, a distance of 8.0km away. The well defined FU nature in the upper part of these cycles, compared to the sharp non-FU tops of cycles in section 01 (see Table 2 and Fig.83) denotes gradual channel abandonment terminated by in-channel deposition of mudstones.

Stacking of cycles in section 03 is shown by the fact that the lower megasequence of conglomeratic facies association (i.e. cycles GI, GII, GIV) coarsens-upward (see App.4), comprises three upwardly thickening/FU cycles and is capped by several FU sandstone cycles. The succession is interpreted as a series of sedimentary responses to reactivation of hinterland faults (or uplift), henceforth named the first tectonic pulse. This is in accordance with similar coarsening/thickening type cycles that have been documented by various workers (Steel et al.,1977; Heward,1978; Rust and Koster,1984; Mack and Rasmussen,1984) as allocyclic responses to rejuvenation of faults or basin subsidence. The capping thinning/fining sequence indicates the equilibration of the system as the influence of the first tectonic pulse waned.

Similar allocyclic controls are envisaged for the upper conglomeratic facies association (eg. cycles EII,III,IV; see App.4) although on a much smaller scale. The upper units of the conglomeratic facies association coarsen then fine upward and are bounded by a sandstone facies association. The smaller scale of the units, compared to those of the lower conglomeratic facies association, along with a finer grain size (discussed in section 8.4) suggest that this was an allocyclic response to a second, less severe tectonic pulse. This pulse is attributed to back-stepping of boundary faults or uplift in the surrounding borderlands (further discussed section 8.7; Heward,1978, Fig.6b; Rust and Koster,1984). Gm is not present in the upper conglomeratic assemblage, indicative of a lack of deeper channels allowing the formation of gravel dunes and hence Gt. The upward increase in the difference between Gt and St set thicknesses suggests that in the lower units of the conglomeratic succession abundant gravels were deposited during flood stage, thus creating large bedforms, whereas sandy bedforms deposited during falling or low stage were much smaller. In the upper conglomeratic succession the dearth of Gm suggests deeper channels, thus enabling sandy bedforms to be comparable in size to gravelly bedforms.

In reviewing the facies, facies associations and bedding characteristics of section 03, a transitional proximal to distal gravelly braidplain (in between G_{III} and G_{II}; Rust,1978b) interpretation is most consistent with the observations. A braidplain depositional environment rather than a valley-confined braided river is proposed due to its lateral extent and lateral variability (Rust,1984a). Ancient analogues might include the Upper Member of the Cannes de Roche Formation (Rust,1981a; 1984b; Rust and Koster,1984) but there are many differences namely: i) cycles in subsection G are much thicker, ranging from 16.5m to 40m compared with the average of approximately 8m in the Cannes de Roche; ii) cycles found in section 03 can be laterally correlated into sections 02 and 01, hence indicating overriding allocyclic controls on sedimentation, whereas cycles in the Cannes de Roche are interpreted as autocyclic; iii) the Cannes de Roche is interpreted as a valley-confined braided river. A more appropriate analogue, although glacially controlled, may be the distal Skeidarasandur (Iceland) at flood stage (Boothroyd and Nummedal,1978; Figs.11a,11c). The migration of linguoid and longitudinal bars under upper flow regime conditions would deposit vertical sequences akin to those of section 03. The addition of tectonic controls (or cycles of glacial advance/retreat) to a Skeidara-like system is envisioned to create the laterally extensive capping FU beds for each cycle.

Proximal braidplain deposits, although tectonically produced are not organized into smaller scale cycles which might represent individual tectonic pulses (Rust and Koster,1984) as seen in alluvial fan deposits (eg. Steel et al.,1977; Steel and Gloppen,1980; Muir and Rust,1982). Rust and Koster (1984) argue that the influence of individual tectonic pulses is lost due to fluvial transport, thus sedimentological properties are of autocyclic origin. The arrangement of the lower conglomeratic facies association into an overall CU sequence comprising three distinctive FU/thickening cycles implies that these individual cycles have been influenced by individual tectonic pulses - hence the allocyclic nature was not overprinted by autocyclic mechanisms. This may be due to the very rapid subsidence rates occurring within the Cumberland Basin (0.69km/Ma, after Bradley,1982). Therefore the downstream control may indeed be allocyclic if tectonic controls such as fault reactivation and/or subsidence are strong enough.

Section 02 is characteritic of distal pebbly braidplain deposits (between S_{II} and G_{III}; Rust,1978b). Preferred cycles (Fig.32) are characterized by: Se -> St(c) -> St -> Se. The preference for such FU amalgamated cycles and low probabilities for fully developed cycles (eg. Se -> St(c) -> St -> Sh -> Sr -> F -> Se) along with intraclast strewn internal erosion surfaces denote rapid channel switching within unconfined braided tracts. Channel avulsions, although common, were not as frequent as in section 03, as indicated by a greater percentage of mudstones, and thicker mean cycle thickness (Tables 2,3). A decrease in set size (Table 1), and smaller mean bed thickness (Table 4, see section 4.3) indicates shallower channels than section 03. The much lower percentages of gravel within these channels also allowed the formation of larger sandy bedforms within the higher order channels, which in the proximal reaches were dominated by gravelly bedforms. The presence of both gravelly and sandy bedforms in these higher order channels hence produced a decrease in the difference between set thickness.

Flood-generated bedforms within these channels commonly created sets greater than 4.0m (eg. cycle DII), as in section 03, indicating that flood stage persisted for long enough periods to allow the formation of such equilibrium bedforms. Falling and low stage modifications are noted from type 1 and 2 Sp-Gp type bar complexes, reactiviation surfaces and slump blocks. Fluctuating stage conditions, both waxing and waning, along with an excess of sediment input over subsidence rates produced the abundance of internal erosion surfaces and incomplete cycles.

The presence of common internal erosion surfaces along with the lateral extent and amalgamated FU nature implies that the cycles were allocyclically controlled. Completely developed cycles (eg. DI, DIV, see App.3) are commonly found only at horizons laterally equivalent to FU cycles within section 03 (cf. Figs. 15,16). Lateral tracing of one such unit (cycle DIV) shows a gradual FU nature in its most proximal exposure and a non-FU sharp upper coarse member contact in the most distal locality. This example shows the lateral transitions between the well develpoed FU capping beds of the proximal cycles and the sharp non-FU upper contact of the distal cycles (cf. Tables 2,3). These cycles, as with their lateral equivalents in section 03, are thought to be overprinted by allocyclic controls which triggered the avulsions, hence creating correlatable cycles between both sections.

Stacking of cycles in section 02 (subsection C) does not show the same distinct overall FU/thickening-upward trend as in section 03. Probable correlations with cycles from section 03 are shown in Fig.35. Sediments shed from the first tectonic pulse are seen in cycles CI-VI and DI (App.3) while those from the second pulse include DII-IV.

A transitional distal gravelly (G_{III}) to proximal sandy (S_{III}) braidplain environment is envisaged for section 02. Possible ancient analogues include the Devonian Battery Point Formation (Cant and Walker,1976) and the Jurassic Westwater Canyon Member (Campbell,1976). The former displays FU amalgamated cycles internally stratified by trough crossbeds and abundant planar cross-strata, formed during low stage by

CORRELATION OF CYCLES WITHIN SECTIONS 01,02,03

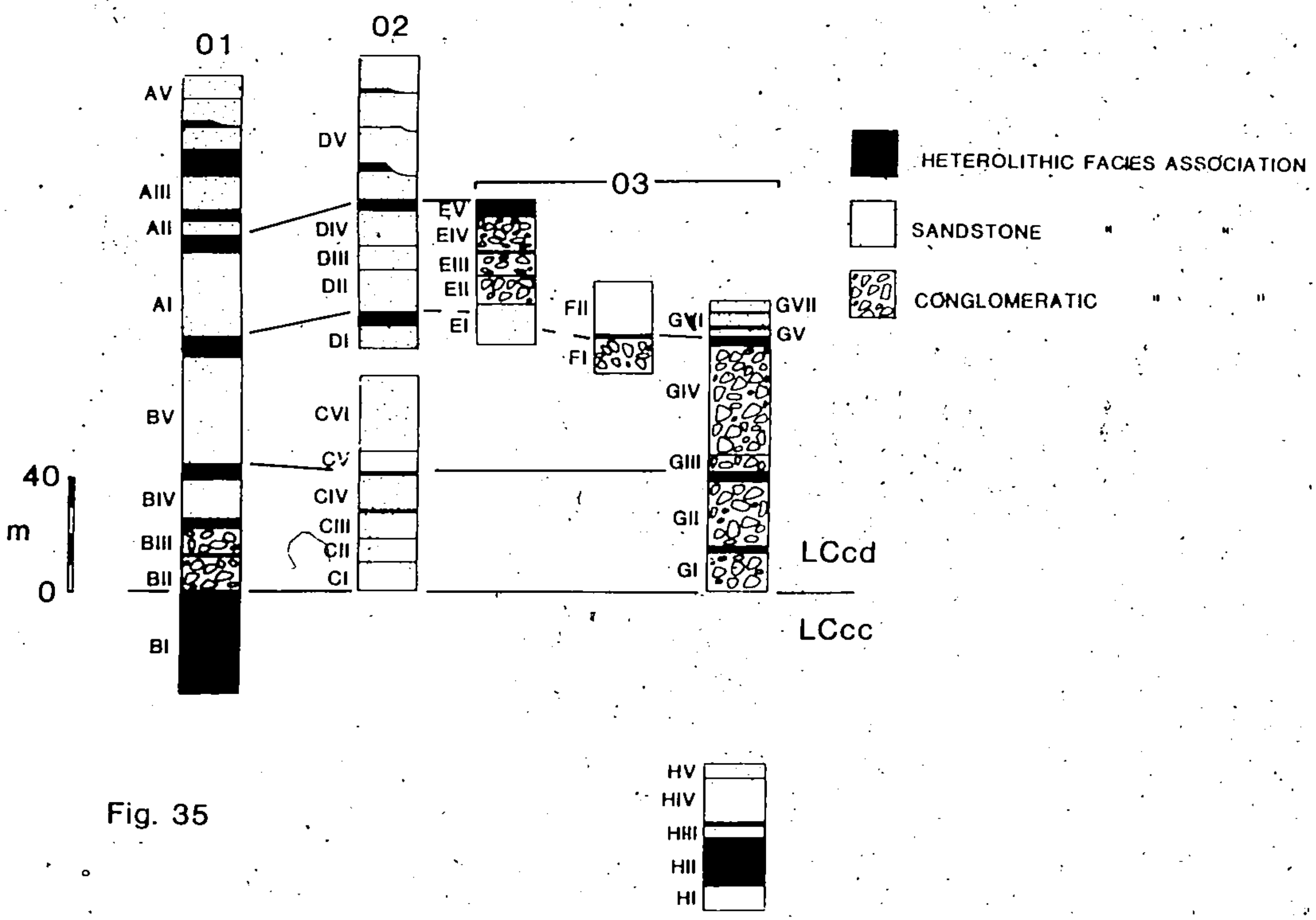

Fig. 35

laterally migrating transverse bars. Planar cross-strata are not as abundant in section 02 as in the Battery Point Formation, and do not show a large paleocurrent divergence. For these reasons they are thought to have formed during flood stage. The Westwater Canyon Member, although lacking planar cross-strata, may be a better analogue. It comprises amalgamated FU cycles arranged into 3m to 33m sequences capped by Sr and mudstones. Campbell (1976) interpreted this sequence as due to coelescing braided stream deposits terminated by floodplain deposition. The main difference between the Westwater Canyon Member and section 02 is in the dearth of planar cross-strata in the former. This may be on account of short duration flood stages, which did not allow the predominantly sinuous-crested bedforms to equilibrate with the flows. A modern analogue to section 02 may be found in the distal reaches of the Yana or Scott outwash plains, Alaska (Boothroyd and Nummedal, 1978). The distal reaches of the Yana R. are 30km from the Malaspina glacier and are characterized by 4m thick FU cycles comprising large scale cross-strata (St or Sp), which pass into Sr, Sh, or Fm. Lateral to the distal reaches are marshes and swamps which help stabilize channels and create leveed channel margins. During flood stage breaching of leveed margins may produce crevasse- or sheet-splays (Gersib and McCabe,1981; Fig.11; Boothroyd and Nummedal, 1978, Fig.13a).

Section 01 displays three preferred types of cycle (Fig.31) depending on their stratigraphic location. Type III cycles (conglomeratic CUFU) are seen near the lower part of the section, above BI, and comprises F -> Sr -> St(c) -> Gt -> Gm -> Sh -> F. Type I cycles (CU) are found in the middle parts of the section, laterally equivalent to cycles produced by the first and second tectonic pulses in section 03, and consists of F -> Sr -> St(c) -> Sh -> F. Type II cycles (sandstone CUFU) are found above the former and are made up of F -> Sr -> St(c) -> Sh -> Se -> St -> F.

Conglomeratic CUFU cycles are interpreted as formed by a combination of lateral encroachment of a braided tract upon its marginal sediments (i.e. deposition within low order channels) and vertical aggradation (discussed further in section 7.4), followed by deposition within high order channels and finally lateral migration away from the site (i.e. gradual channel abandonment). Sandstone CUFU cycles are formed in the same manner. CU cycles (eg. BIV, BV, see App. 2) are also formed by lateral encroachment and synchronous vertical aggradation upon marginal sediments, but differ by not fining-up and having a sharp upper contact with the fine member rather than a gradational contact. The difference between gradational and sharp tops of cycles reflects lateral migration (or gradual abandonment) and avulsion, respectively. Avulsions, as seen in cycles BIV, BV, CI (see Apps.2,3) are thought to be tectonically induced since they can be correlated between sections while lateral channel migrations are autocyclically controlled.

Fine member preferred sequences are as follows: coarse member -> Fl -> Sr -> red Fm -> mottled Fm -> grey Fm -> coarse member (Fig.34). The lateral extent and high ratio of Fr and Fm indicate deposition on floodplains (previously discussed in 3.2.2), created by overbank deposition into abandoned channels (Miall,1985). An upward increase in Fr (and decrease in Fm) and Sr (decrease in Sh) denotes increased channel stability and lower competence, which is reflected in an increase in vertically stepped channel margins, thinner coarse members and thicker fine members. These changes are incurred by allocyclic controls and create the upward increasingly distal nature.

Compilation of cycles demonstrates the same patterns seen in the proximal section (03). The lower sequence shows braided deposits (conglomeratic CUFU, eg. cycles BII,III) that prograded over marginal floodplain (meandering?) sediments indicative of initiation of the first tectonic pulse. Subsequent thick amalgamated non-FU cycles with CU bases (eg. BIV,BV,AI, see App.2) reflect distal braidplain sedimentation intercalated with episodic allocyclically-induced avulsions which created the sharp tops and thick fine members. Internal erosion surfaces within these thick cycles formed in response to sedimentation rates that exceeded subsidence rates (McLean and Jerzykiewicz,1978) as previously seen in laterally correlative cycles in section 03. Cycles above the second tectonic pulse (cycle AI) return to the CUFU motif but differ lithologically from the basal ones. The prevalence of sandstone CUFU cycles with thick fine members is attributed to diminution of sedimentation rates i.e. subsidence exceeding sediment input, thus creating more stabilized channels. The appearance of thick amalgamated sequences therefore appears to be controlled by sedimentation rate > subsidence rate. Assuming constant subsidence rates (as inferred from Fig.4, Bradley,1982), the tectonically controlled sediment input rate is the dominant force in determining cycle architecture.

A distal sandy braidplain (S_{II}) environment is most consistent with the observations discussed above. Ancient distal braided fluvial analogues displaying CUFU-type cycles are not known to the author, although they have been documented in alluvial fan environments (Muir and Rust,1982). Thicker amalgamated sequences (cycles BIV,BV,AI) are similar in character to those from the Westwater Canyon Member (Campbell,1976), previously discussed.

7.0 PALEOCURRENTS

7.1 Introduction

Paleocurrents are a very important diagnostic tool in interpreting many depositional environments. Fluvial systems are often described as having unimodal paleocurrents, the dispersion from the mean being used to classify low and high sinuosity rivers. Low sinuosity fluvial systems (eg. braided rivers) are often characterized as having a low variance while high sinuosity systems display a high variance (Selley, 1968; Walker and Cant, 1978). This common characteristic is somewhat idealistic since there is a general increase in directional variance with decrease in the size of the current indicator (Allen, 1967; Miall, 1974). Hence low sinuosity shallow braided streams may create moderately dispersed paleocurrents, because they form predominantly small-scale structures (Smith, 1972; Rust, 1972; Cant, 1978; Martini and Salas, 1983; Mader and Teyssen, 1985). Paleocurrents also diverge depending where in the channel they are measured (Williams and Rust 1969; Cant and Walker, 1978; Hein, 1984). The proper interpretation of paleocurrents must therefore rely on careful comparison between the scale of the current indicator and the vertical and lateral positioning within the outcrop, and not merely on a lumped aggregate of readings.

7.2 Procedure

Paleocurrent indicators of all types were measured wherever possible for each cycle (eg. trough crossbedding, sole marks, parting lineation *et cetera*). Each type was kept as a separate category, hence maintaining the sedimentary structure hierarchy (Allen, 1967; Miall, 1974). Most readings are from the coarse member, since there was a dearth of well exposed current indicators in the fine member heterolithic assemblage. The presence of large wave-cut platforms allowed greater confidence in paleocurrent determination from higher rank structures such as trough cross-strata and also permitted studies on in-channel variance. Abundant fossilized logs exposed along the cliff sections also provided important information about paleocurrents and flow regimes (McDonald and Jefferson, 1985). However log orientation is quite variable depending flow regimes and site of preservation.

Data collected were corrected for tectonic dip on a stereonet and the results can be seen in Appendix 11.

7.3 Directional Statistics

Two dimensional orientation data may be analysed using: circular distributions; spherical distribution statistics or eigenvalue and eigenvector analysis (Mader and Teyssen, 1985). The first method, being the most common, will be used in this study.

Circular distributions, especially from cross-strata can be approximated using a wrapped normal- (Gumbel et al., 1953; Curray, 1956) or a Von Mises distribution (Mardia, 1972). The latter is the most appropriate and is defined as:

$$f(\theta, \mu_0, k) = [1/2\pi I_0(k)]\, e^{k \cos(\theta-\mu_0)}$$

$$0 < \theta < 2\pi$$
$$k > 0$$
$$0 < \mu_0 < 2\pi$$

where $I_0(k)$ is the modified Bessel function of the first kind and order zero;

$I_0(k) = \sum_{r=0}^{\infty} 1/r!^2 \, (1/2k)^{2r}$ where μ_0 = mean direction, k= concentration parameter, Ø= a random variable which is Von Mises distributed.

The Von Mises distribution is unimodal, hence the need for a concentration parameter, and is symmetrical about $Ø = \mu_0$. The Von Mises distribution of cross-strata negates the use and validity of Gaussian test statistics (F. Agterberg pers. comm., 1984; cf. Miall, 1974, 1976).

Mean circular directions can be derived from the Von Mises distribution (Mardia, 1972) and calculated using vector summation (Gumbel et al., 1953; Curray, 1956), that is, summing the components parallel to the orthogonal axes:

$V = \sum_{i=1}^{n} u_i \cos Ø_i$ NS component n = unit vector with azimuth $Ø_i$

$W = \sum_{i=1}^{n} n_i \sin Ø_i$ EW component

$\bar{Ø} = \tan^{-1}(W/V)$ mean azimuth

Measures of dispersion can be calculated using:

$R = [V^2 + W^2]^{1/2}$ where R is the vector strength, which can also be expressed as a percentage:

$L = (R/N)\,100$

The circular standard deviation (Mardia,1972) can be calculated as:

$$s_D = [-2 \ln(1 - S_O)]^{1/2} \quad \text{where } S_O = 1 - R/N$$

Statistical significance was verified using a Rayleigh test, defined as:

$$P = 1 - e^{(-R^2/N)}$$

The null hypothesis (H_O) is defined as the probability less than 0.90 of a number being random:

$$H_O: p < 0.90 \; ; \; H_a: p > 0.90$$

An alternative Rayleigh test (Stephens,1969) is defined for a small sample (n<100) as:

$$\bar{R} = R/N$$

$\bar{R}$ can then be tested at a certain level of confidence using appropriate tables (Mardia,1972; Appendix 2.5). Sample larger than 100 are chi-square distributed and can be approximated to:

$$X^2 = 2n\bar{R}^2 \text{ with } n\text{-}2 \text{ degrees of freedom}$$

Testing of significant differences between means is accomplished using the following:

$$\text{if } \bar{R} > 0.95 \text{ then } F_{1,n-2} = (n-2)(R_1 + R_2 - R)/(n - R_1 - R_2)$$

with 1 and n-2 degrees of freedom

if $\bar{R} > 0.70$ then $F_{1,n-2} = (1 + 3/8k)\,[(n-2)\,(R_1 + R_2 - R)/$
$n-2)\,(n - R_1 - R_2)]$

k is from the Von Mises distribution and is obtained by knowing R (where $R = \vec{R}_1 + \vec{R}_2$] and cross referencing it with Appendix 2.3 of Mardia (1972) or Table 2 of Gumbel et al. (1953). The null hypothesis is rejected if the test value is greater than the F value at $\alpha = 0.05$.

Results for the mean, vector strength, and significance of results are contained in Appendix 11, while results from computations on statistical differences between cycles can be seen in Table 6.

7.4 Intrachannel Variability.

Intrachannel paleocurrent variability is defined as paleocurrent variations occurring within a given braided channel complex. The paleocurrent dispersion, created by migrating bedforms, and other paleocurrent indicators within these migrating braided channels can be seen in the coarse members of cycles. In general cycles are characterized by the following succession: basal sole marks indicating a large angular deflection from the cycle mean; low variance in-channnel paleocurrents; and high dispersion in fining upward beds at the top.

Basal sole marks within sections 01/02, and especially those from CUFU or CU cycles show a large divergence from the cycle mean (average variation is 81.3^{o}, $S_D = 48.3^{o}$). This contrasts with the low deviations from the cycle mean found within section 03 cycles (average=18.7^{o}). The presence of scours and fluting at the base of CU-type cycles, along with the divergent paleocurrents suggest that lateral migration was due to flood-induced breaching of leveed channel margins. Deeper, less stabilized (i.e. non-leveed) channels in section 03 allowed unrestricted migration of braided channels, hence there was less divergence between the sole marks and the in-channel deposits. Similar patterns are described by Peel (1972) and Smith (1983) in anastomosed reaches of the Saskatchewan and Columbia Rivers where new channels are created by avulsions which initially started as crevasse-splays. Thus breaching of leveed margins in anastomosed rivers is hypothesized to create a sequence showing basal sole marks at angles diverging from the original channel trend followed by Sr, also at diverging angles, and finally in-channel deposits (St, Sp) which diverge from the original channel trend but by a much lesser degree than the underlying crevasse-splay deposits (Cross and Smith,1985). A lower divergence within the newly created in-channel deposits (compared to the original channel trend) is expected since higher order structures (eg. channels) diverge less from the grand vector mean than smaller order structures (Miall,1974). Cycles displaying such sequences commonly are seen in section 01 (eg. BI-V, AI-III, see App.2). Although vertically the signature implies avulsions similar to anastomosed systems the lateral relationships are uncharacteristic of anastomosed deposits. Vertical and lateral sequences through anastomosed deposits are characterized by vertically aggrading sandbodies with limited lateral extent, high depth-to-width ratios, stepped channel bases and abundant floodplain (wetland) deposits (Smith and Smith,1980; Smith, 1983; Rust and Legun, 1983; Rust et al.,1984). CU and CUFU- type cycles from section 01 differ in that they are laterally extensive, implying unrestricted lateral channel shifting <u>within</u> braided tracts, confined laterally by areally extensive floodplains and subdued levee deposits (terracing is unlikely due to the rapidly aggrading nature). Breaching of these levees by floods, tectonic tilting of the plain or as a consequence of aggradation of active channels could then avulse the system into an area with a more favourable energy gradient (i.e. the axis of maximum subsidence) thus creating the observed CU and CUFU-type cycles and laterally extensive floodplain deposits (Fig.36). North-stepping vertical mudstone/sandstone contacts along with a progressive northerly shift in the paleocurrents (discussed in 7.5) suggest that the plain was adjusting to uplift in the south i.e. the Cobequid Highlands.

In-channel paleocurrents generally show a low dispersion about the cycle mean. Moving vector strengths (Figs.37-39) vary between 60.2% to 98.4% (i.e. standard deviation (s_D) varying from 50° to 9°) with lower values corresponding to thick cycles emplaced by the first and second tectonic

Fig.36. Formation of new braided tracts via crevasse-splays. The arrows show the diverted path of flow. The rectangle shows the typical sequence expected as the crevasse-splay advances into ponded waters and creates a new braided tract: F -> Sr -> St and eventually Gt if the main channel is diverted.

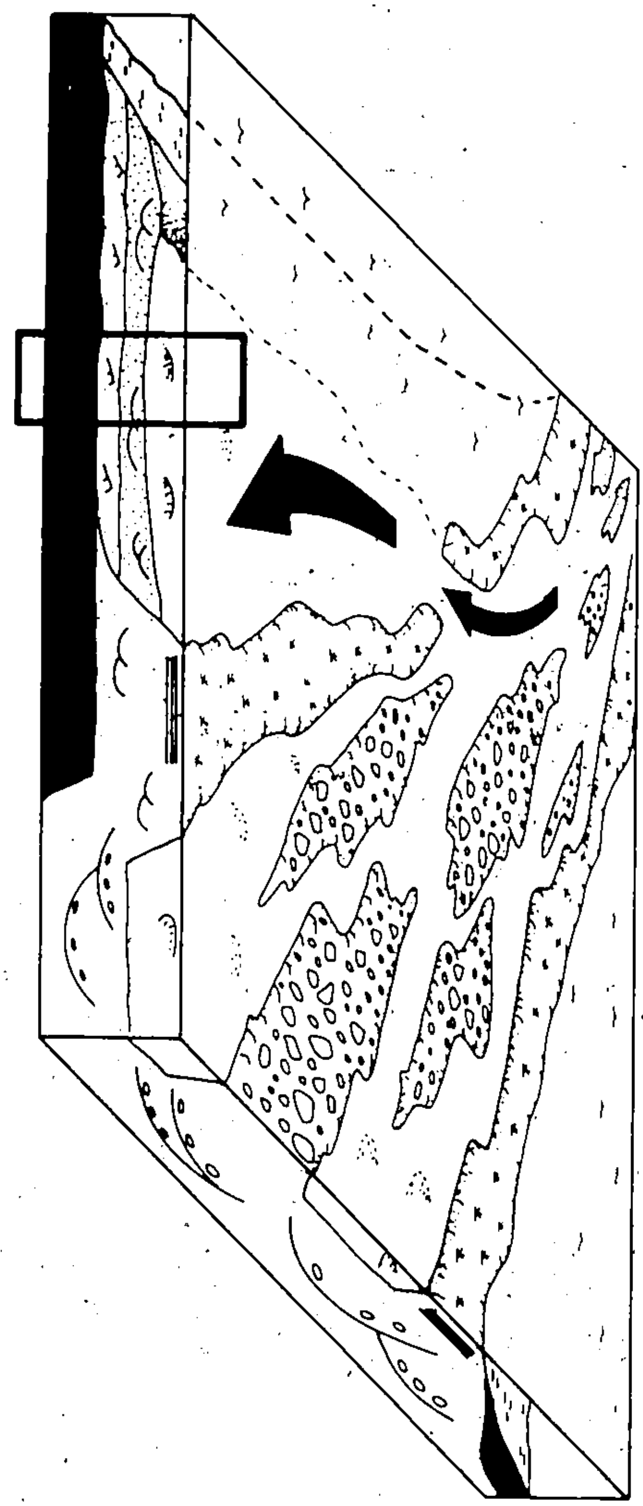

Fig.37

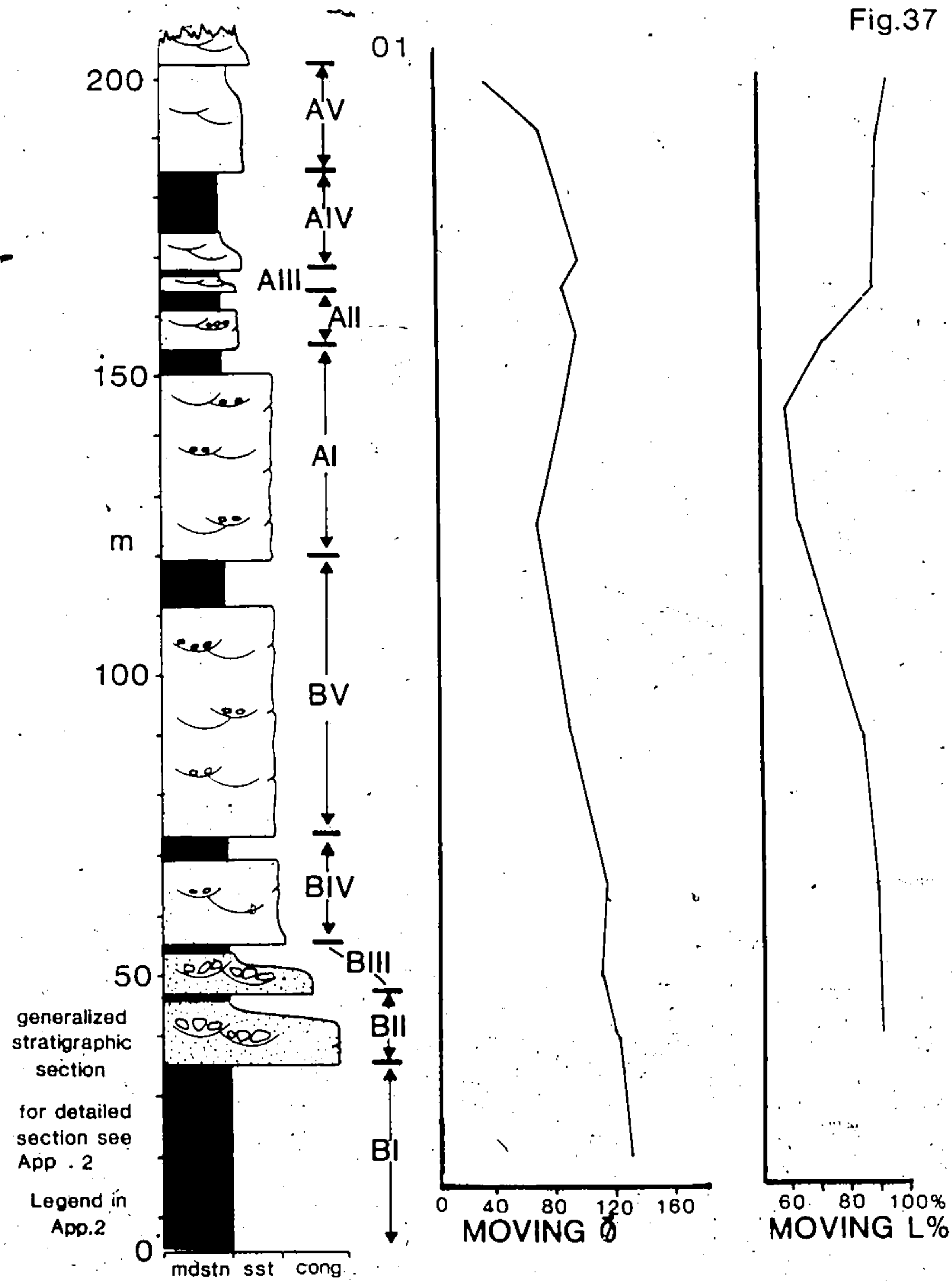

01
200
150
m
100
50
0
AV
AIV
AIII
AII
AI
BV
BIV
BIII
BII
BI
generalized stratigraphic section
for detailed section see App . 2
Legend in App.2
mdstn sst cong
0 40 80 120 160
MOVING Ø
60 80 100%
MOVING L%

Fig. 38

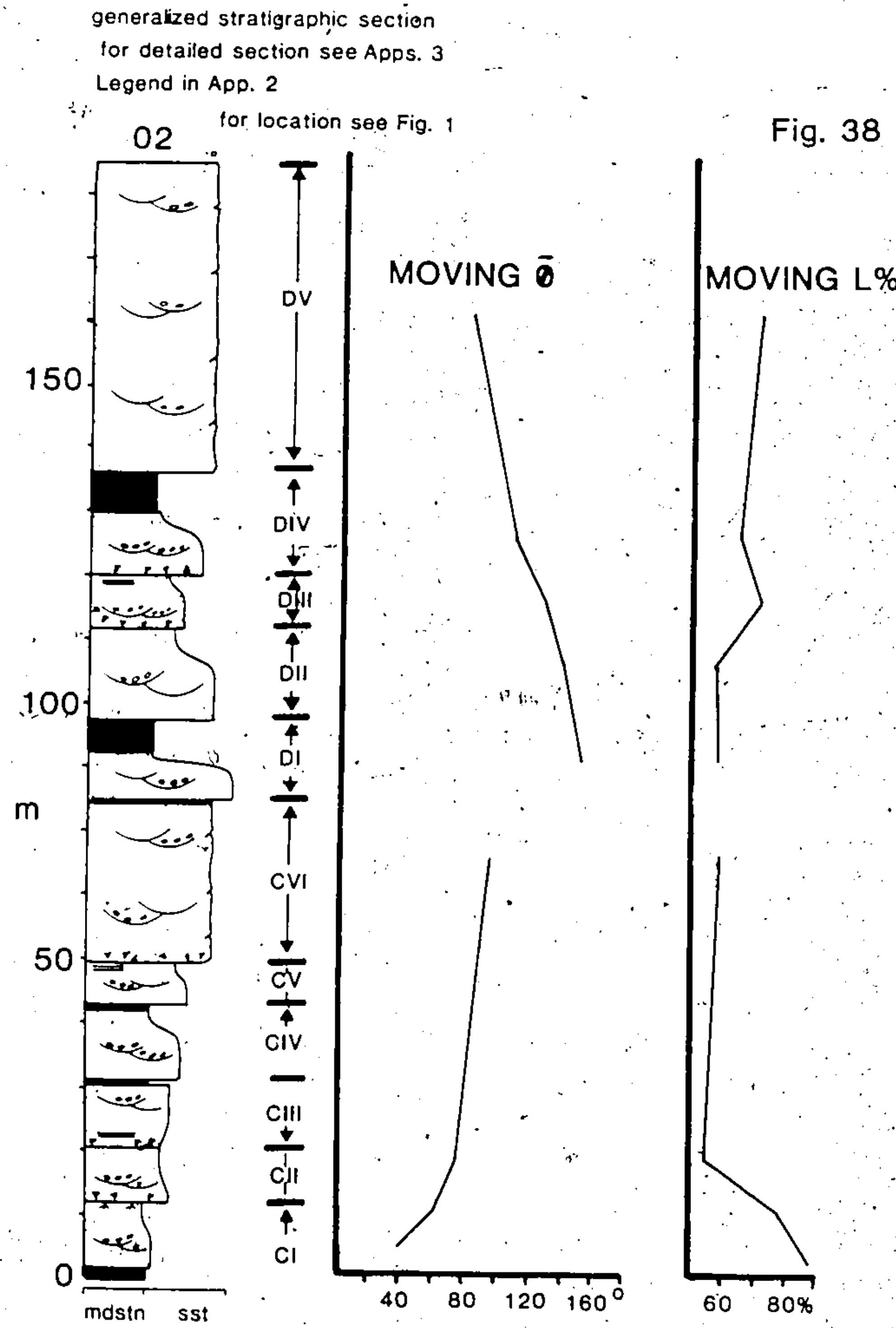
generalized stratigraphic section
for detailed section see Apps. 3
Legend in App. 2
for location see Fig. 1
02
150
100
m
50
0
mdstn
sst
DV
DIV
DIII
DII
DI
CVI
CV
CIV
CIII
CII
CI
MOVING $\bar{\emptyset}$
40
80
120
160°
MOVING L%
60
80%

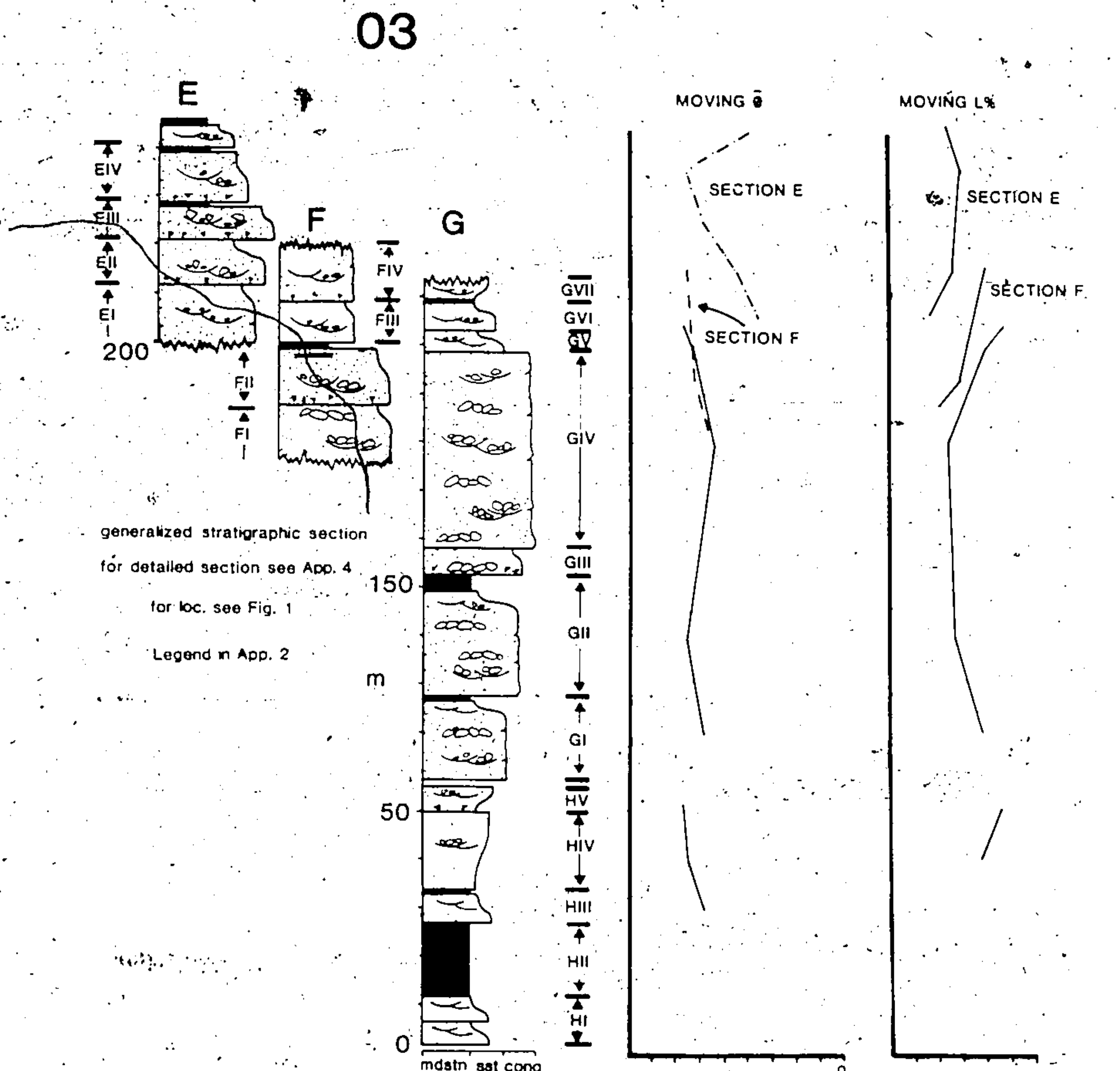
03
E
F
G
EIV
EIII
EII
EI
FIV
FIII
FII
FI
GVII
GVI
GV
GIV
GIII
GII
GI
HV
HIV
HIII
HII
HI
200
150
m
50
0
mdstn sst cong
generalized stratigraphic section
for detailed section see App. 4
for loc. see Fig. 1
Legend in App. 2
MOVING $\bar{\theta}$
SECTION E
SECTION F
60 100 140 180°
MOVING L%
SECTION E
SECTION F
50 70 90%

Fig. 39

pulses. In general cycles from sections 02/03 have lower vector strengths than 01. Lower intrachannel dispersion in section 01 is attributed to <u>stabilized</u> channels which did not allow rampant channel migration as in the deeper <u>non-stablized</u> channels of section 02/03, nor the formation of low stage-induced cross-channel bars (Cant and Walker, 1978; Walker and Cant, 1984).

Variations between constituent in-channel lithofacies show no consistent trends. Paleocurrents from Gt and St were measured at various localities within sections 02/03 (Table 5) and show significant differences at $\alpha=0.06$ in only three of the seven locations. Differences between the means range from 1.6° to 30.3°. Dispersion of paleocurrents for St and Gt show an average standard deviation of 26.4° and 30.2° respectively. Frequency of standard deviations for St and Gt at 19 sites is plotted in Fig.40 and shows modes at 25.6-30.5 for St and 20.6-25.5 for Gt. The lack of overall paleocurrent trends between in-channel facies suggests no detectable patterns were developed within the braided channels.

Fining- upward beds which cap cycles often show a wide deflection from the cycle mean. This is mostly seen in plane-laminated beds (Sh) where the deviation ranges from 2.6° to 94.2° from the in-channel mean (average deviation is 45.6°, $S_D = 38.1^\circ$). Ten to twenty degree variations in the average paleocurrent for small-scale St in the upper parts

TABLE 5: STATISTICAL COMPARISON BETWEEN PALEOCURRENTS FROM Gt AND St

UNIT	COMPARISON	LOC	S_{D1}	S_{D2}	N	F	SIG
D7	Gt-St	at 2	52.3	31.6	23	9.35	0.01
	Gt-St	at 3	23.2	29.7	18	2.44	-
	Gt-St	at 10	23.7	33.1	13	3.09	-
D9	Gt-St		30.3	37.3	22	4.15	0.06
Section E	St-Gt		54.1	18.1	13	4.14	0.06
G6	St-Gt		29.2	23.0	88	2.19	-
G8	St-Gt		26.1	17.4	16	1.03	-

LOC = location where sampling occurred

S_{D1} = standard deviation of the first listing

S_{D2} = standard deviation of the second listing

N = number of observations

F = F-test (Mardia,1972), see section 7.3

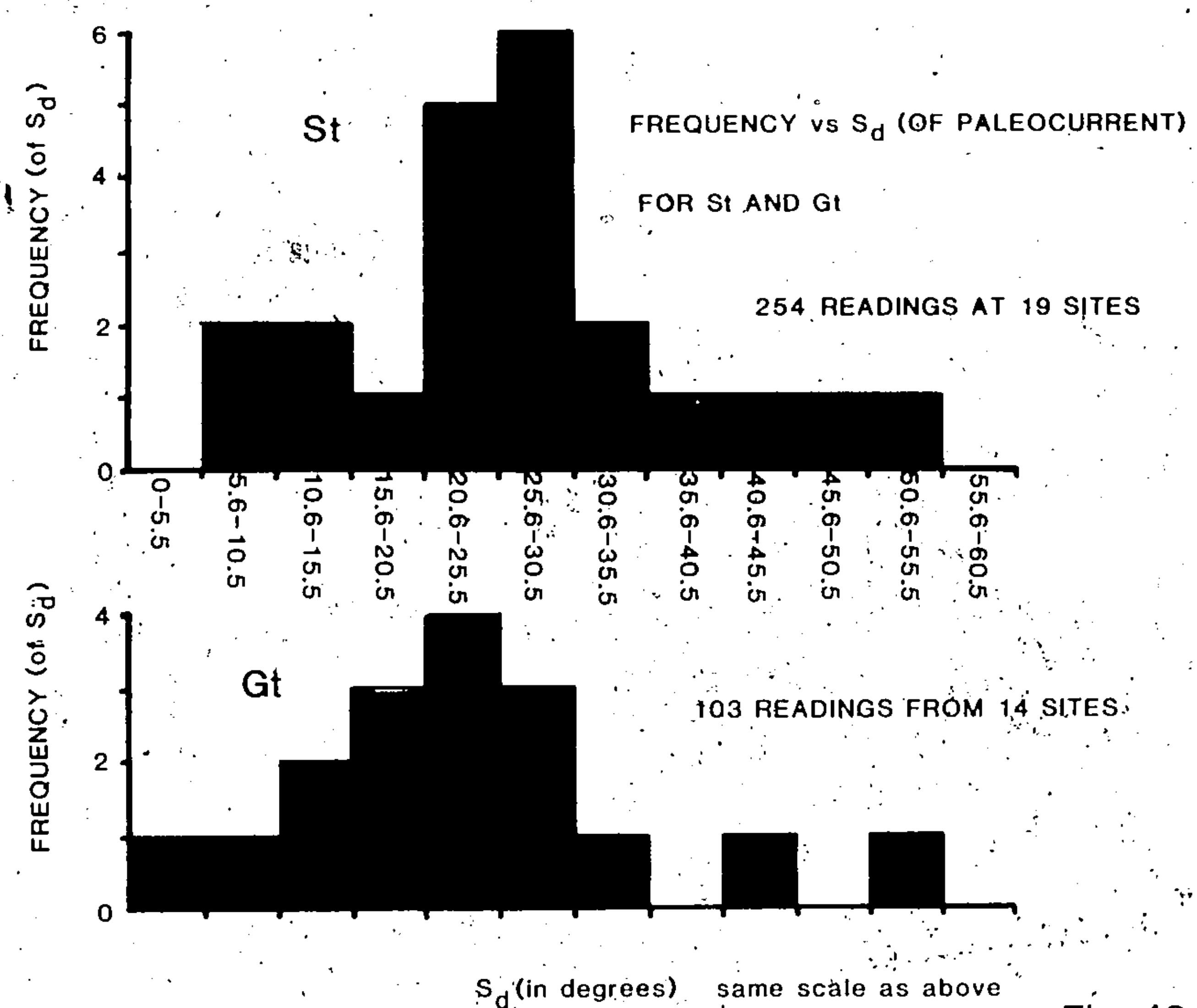
FREQUENCY vs S_d (OF PALEOCURRENT)
FOR St AND Gt
St
254 READINGS AT 19 SITES
FREQUENCY (of S_d)
6
4
2
0
0-5.5
5.6-10.5
10.6-15.5
15.6-20.5
20.6-25.5
25.6-30.5
30.6-35.5
35.6-40.5
40.6-45.5
45.6-50.5
50.6-55.5
55.6-60.5
Gt
103 READINGS FROM 14 SITES
FREQUENCY (of S_d)
4
2
0
S_d (in degrees)   same scale as above

Fig. 40

are common (eg. upper and middle parts of cycle DIV, App. 11). Fining-upward beds are interpreted as deposits of higher topographic levels, hence deflections are caused by oblique, sometimes orthogonal paleocurrents from gradually avulsing braid tracts onto the channel margin sediments.

Lateral paleocurrent variability throughout all sections can be studied using correlatable sequences comprising the first and second tectonic pulses (Fig.41,42). Uppermost cycles belonging to the first tectonic pulse were used (cycles BV, CVI, FII, GIV), while cycles belonging to the second tectonic pulse were divided into upper and lower, hence allowing studies of the overall vertical and lateral trends. In general lateral variability does not range higher than 21° between adjacent sample sites in the proximal sections (02/03) for the lower pulse, and 33° for the higher one. Much larger variations are seen in the distal section (01) where paleocurrent differences between adjacent sample sites are as large as 51°. Larger variations in the distal section are attributed to an increase in sinuosity, or lower paleoslopes.

7.5 Interchannel Variability

Interchannel variability is defined as paleocurrent variations between cycles. Each cycle represents deposits from a particular braid tract, whereas paleocurrent deflections between successive cycles reflect responses to

LATERAL VARIABILITY IN PALEOCURRENTS FOR CYCLE DIV AND EQUIVALENTS

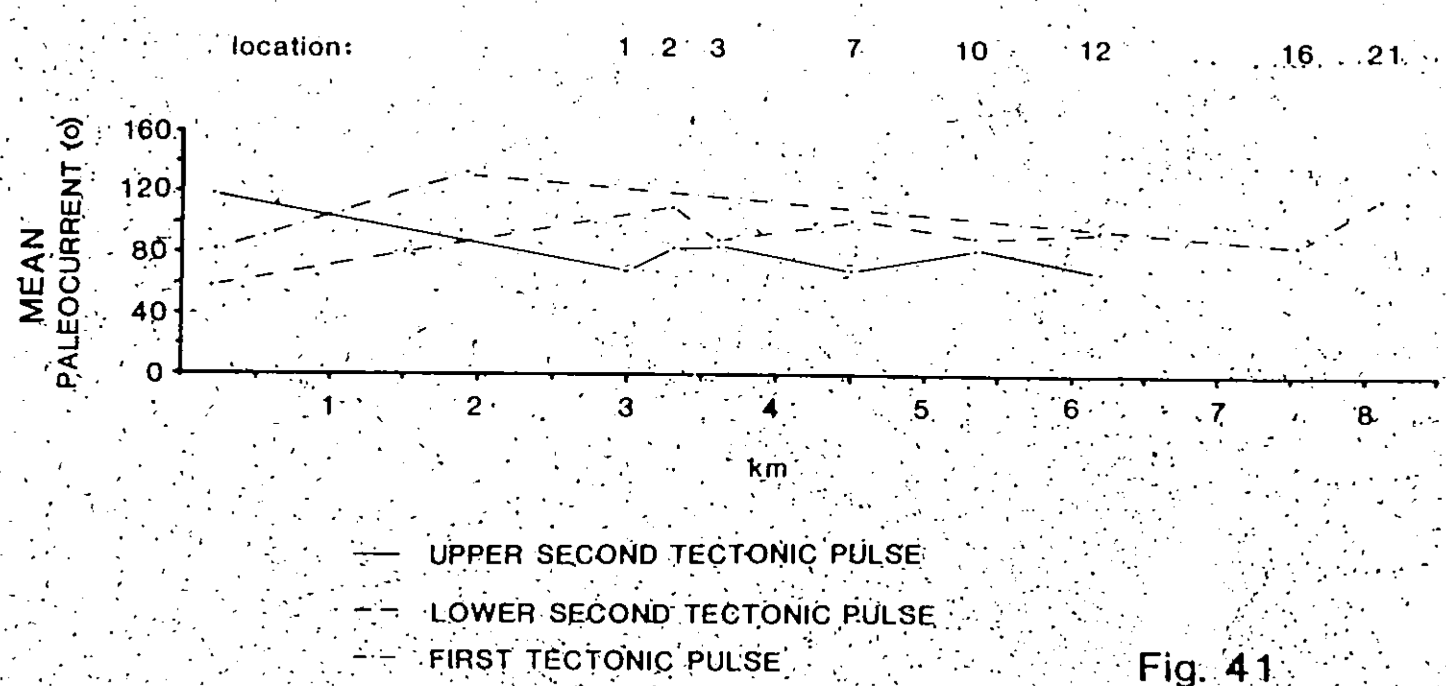

Fig. 41

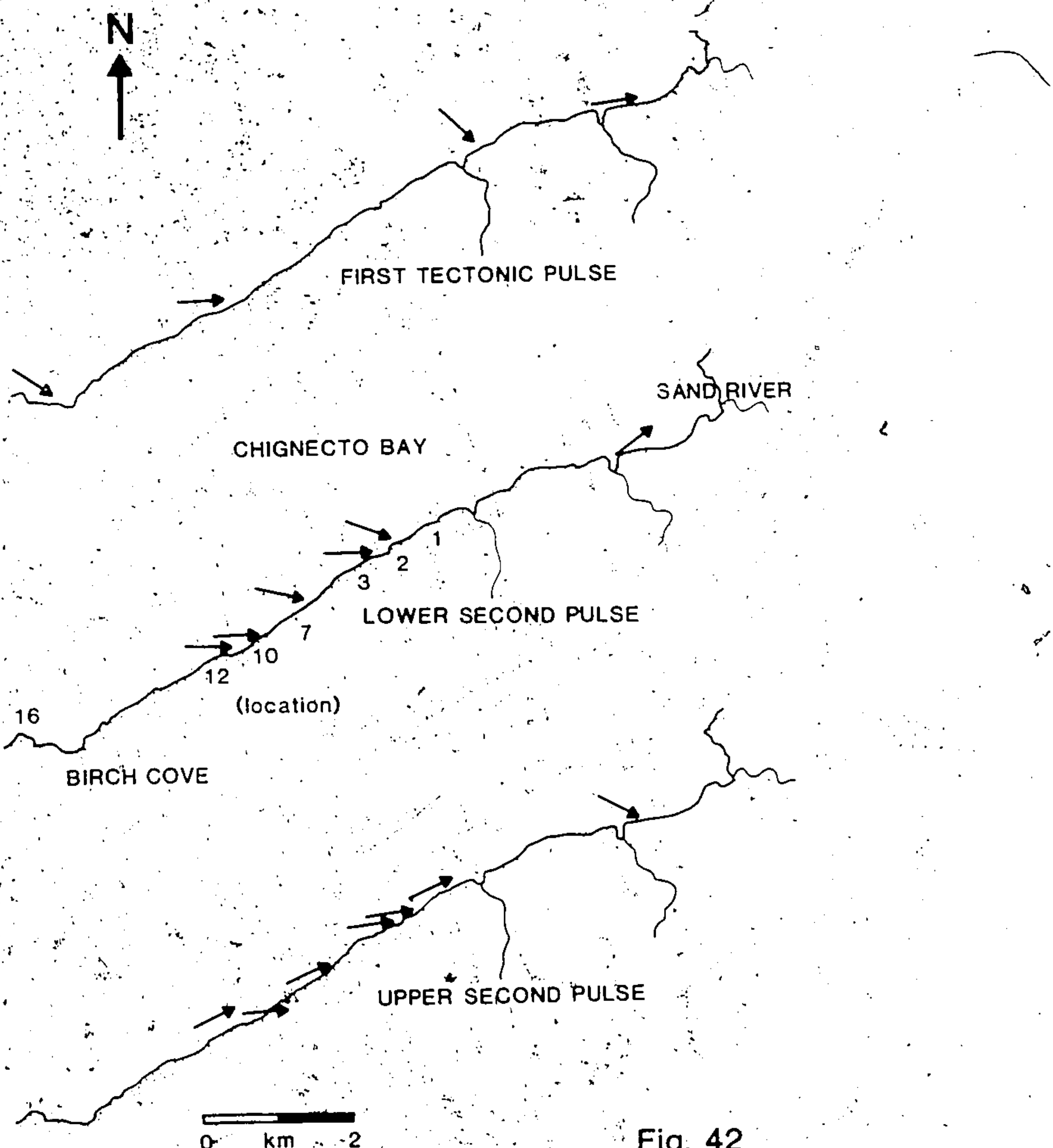

Fig. 42

MEAN PALEOCURRENTS

channel avulsion (autocyclic or allocyclic) and tectonic tilting of the alluvial plain (allocyclic controls).

Successive cycles from section 01 show that within nine transitions four were significant at the 0.06 level i.e. 44.4% of the avulsions had paleocurrents significantly different at the 0.06 level from the preceding cycle (Table 6). Of the four significant deflections, three were located in the upper parts of section 01 (subsection A) while only one was found in the lower part (subsection B). The average deflection in section 01 was 27°. Section 02 shows three out of six recorded transitions were significant at 0.01 (50% of the avulsions had significantly different paleocurrents at the 0.06 level from the underlying cycle) with two of the significant deflections occurring in subsection D (Table 6). The average deflection between adjacent cycles in section 02 is 32.3°. In section 03, of eight successive transitions seven were significant (87.5%) at the 0.05 level, with an average deviation from the preceding cycle of 41.0°.

Results from analysis of paleocurrent deviations between successive cycle transitions show conclusively that deviations are largest in the proximal reaches and decline with distance away from the source. This may be on account of two factors; i) stronger allocyclic imprinting in proximal areas and/or; ii) stabilization of channel switching by vegetation in the distal areas. The proximal location of deposits from section 03 suggests that switching on alluvial

TABLE 6: PALEOCURRENT DIFFERENCES BETWEEN CYCLES

COMPARISON	θ_1	θ_2	N	F	SIG
AIII-IV	103	34.6	31	97.8	0.01
AI-II	99.8	77.0	30	6.95	0.05
AII-III	77.0	103	22	5.27	0.06
AIV-V	34.6	51.8	19	3.60	-
BI-II	126.9	115.6	21	1.26	-
BIV-II	120.3	115.6	26	1.09	-
BIV-V	120.3	81.7	21	7.91	0.01
CI-II	37.4	66.4	22	1.95	-
CVI-II	130.1	66.4	28	11.8	0.01
DI-II	156.1	126.6	8	1.92	-
DIII-II	136.6	126.6	19	2.53	-
DIII-IV	136.6	89.8	123	23.2	0.01
DV-IV	75.0	89.8	130	4.04	0.01
GI-II	82.3	69.9	107	4.89	0.05
GIV-II	118.8	69.9	53	21.9	0.01
GIV-V	118.8	35.3	28	30.8	0.01
GVI-V	100.5	35.3	5	55.5	0.01
FI-II	85.0	70.4	31	1.06	-
EI-II	126.6	93.1	25	6.0	0.05
EIV-II	67.4	93.1	22	4.29	0.05
EIV-V	67.4	169.2	17	23.9	0.01
HI-IV	89.3	69.0	13	2.64	-
HV-IV	74.3	69.0	10	3.13	-

COMPARISON = comparison of paleocurrents between two cycles

θ_1 = paleocurrent for the first cycle

θ_1 = paleocurrent for the second cycle

N = total observations

F = F-test (Mardia, 1972)

SIG = statistical significance

fans, controlled by episodic tectonism and/or autocyclicity, may be responsible for larger variations in the proximal reaches than in the distal areas. Stabilization of distal braid tracts by abundant vegetation, levees and more uniform slopes also aided in the lower deflection in paleocurrent between successive cycles.

Vertical paleocurrent trends between cycles for sections 01, 02, 03 are plotted as moving averages in Fig. 37-39. Section 01 (Fig. 37) shows a sinusoidal-like curve with a general northeasterly to southeasterly trend and a gradual upward northerly shift in paleocurrent from 126.9° to 36.6° (a deviation of 90.3°). A linear correlation of stratigraphic height versus paleocurrents shows a slope of 0.49°/m (r=0.84). The moving average is marked by minor pertubations and a slight southerly deviation in cycles AI (upper), AII, AIII, which is correlative with the third peak in the moving average of F% in Fig.12. Section 02 (Fig.38) shows an upward southerly shift in subsection C and a marked northerly shift in subsection D (a deviation of 73.9° between both subsections). Stratigraphic height and paleocurrents were also correlated for subsection D and showed a rate of change of 1.46°/m (r=0.98). A gradual overall northerly shift (deviation 14.4°) is seen in section 03 (Fig.39), with the most rapid northerly deflection (maximum deviation of 56.9°) occurring within the distal upper conglomeratic facies assemblage (in subsection E) and the sandstone facies association overlying the lower conglomeratic facies assemblage. Correlations similar (i.e. stratigraphic height versus paleocurrent) to the previous two denoted: i) no significant trends in the lower conglomeratic assemblage (r=-0.24); ii) rates of 0.86°/m (r=0.97)) and 1.73°/m (r=0.96) for proximal and distal equivalents of the upper conglomeratic facies associations.

Rapid northerly shifts in paleocurrents are apparent in the upper parts of all three sections. This rapid shifting corresponds to cycles deposited during the second tectonic pulse and hence the trend is interpreted as a northerly tilting of the alluvial plain due to allocyclic mechanisms. This is corroborated by Fig. 4f, which shows the laterally correlative gradual northerly shift in paleocurrents between the first and second tectonic pulse (eg. units A13, B7, E1-5). The sectionwide correlative nature of paleocurrent deflections indicates overriding allocycllic controls must have been in effect.

The lack of any consistent paleocurrent trends in sediments shed from the first tectonic pulse i.e. lower conglomeratic facies association and subsecton C, may indicate that rapid sedimentation rates precluded any minor changes in the gradient of the alluvial plain caused by tectonism. Hence proximal braided reaches did not receive a strong paleocurrent signature indicative of progressive tilting. Even though the vast majority of avulsions in section 03 are statistically different from the preceding cycle (previously discussed), the deflections are not organized into a consistent overall pattern, implying a rapidly aggrading system whose drainage pattern was not controlled by subsidence rates i.e. sedimentation rate > subsidence rate. In contrast, distal reaches show an excellent correlation between paleocurrents and stratigraphic height throughout the section. This may be due to either subsidence rates (or "tilting" rates) exceeding sedimentation rates or a decrease in sedimentation rates. Thus any tectonic activity causing tilting or subsidence of the basin created a preferred migration of braided tracts towards the axis of maximum subsidence (Bluck,1976; Alexander and Leeder,1985).

Sediments from the second tectonic pulse (the upper conglomeratic facies association and lateral equivalents) contrast with the first pulse by being finer-grained, thinner and showing a very good linear correlation between paleocurrents and stratigraphic height. All these factors indicate more distal deposits which may have resulted from either back-stepping of boundary faults (Heward, 1978; Gloppen and Steel, 1980) or peneplanation of uplands. The progressively more distal nature allowed subsidence to overtake sedimentation rates (i.e. a decrease in sedimentation rates), thus creating the very good correlation between paleocurrents and stratigraphic height.

Maximum paleocurrent deviations have been used by Miall (1976) in conjunction with Langbein and Leopold's (1966) empirical equation to relate angular paleocurrent range to sinuosity in ancient sediments. The equation is converted to degrees rather than radians as in the original equation, and is of the form :

$$\text{sinuosity} = 1 / 1 - (\theta/252)^2 \quad \text{where } \theta \text{ is the maximum angular deflection}$$

Results for section 01, 02, 03 are tabulated in Table 7. Results show average sinuosities of 1.05, 1.08 and 1.01 for sections 01, 02, 03 respectivelly - all within Schumm's (1968) designation for a bedload river.

Although this method has been used by other workers (Miall,1976) to determine sinuosity in lithified sediments its validity in this study is suspect. The presence of high correlation coefficients between paleocurrents and stratigraphic height over large thicknesses of section is suggestive of allocyclic controls (previously discussed). This implies that successive braid tracts could preferentially accrete laterally in one direction (under unidirectional flow) with no ensuing change in sinuosity. The equation is also defective by not taking into account the thickness over which the deflection occurred and hence the test may be detecting allocyclic-incurred deflections rather than pure autocyclic variations. It seems imperative that proper testing of braided channel sinuosity should use only within-channel variations. Otherwise, testing successive cycles may only show allocyclically-induced variations

TABLE 7: SINUOSITY

SECTION	CYCLE	CHANGE(°)	THICKNESS(M)	SINUOSITY
01	BI-AI	59.0	140	1.06
	AI-II	67.7	35	1.02
	AII-V	63.1	30	1.07
	AVERAGE			1.05
02	CVI-I	60.9	75	1.06
	DI-V	73.9	60	1.09
	AVERAGE			1.08
03	HIII-HV	82.6	72	1.00
	HV-GVI	37.6	70	1.02
	GVI-EIII	10.3	80	1.00
	EI-IV	56.9	40	1.05
	AVERAGE			1.01
04	LII-V	17.3	45	1.00
	LV-I II	71.7	210	1.09
	I III-IV	27.0	15	1.01
	I IV-VI	36.0	25	1.02
	I VI-XI	39.4	45	1.03
	AVERAGE			1.03

CHANGE = paleocurrent change between compared cycles

THICKNESS = thickness over which the change occurs between braid tracts, in contrast with high sinuosity rivers for which proper sinuosity analysis would involve measurements made between cycles.

7.6 Paleocurrent Relationships

In order to get a better understanding of relationships between paleocurrent trends and other sedimentological parameters, a series of correlations were conducted.

Fig.43 shows relationships between the angular deflection of a cycle from the preceding one versus the thickness of the coarse member. Thick amalgamated cycles from sections 01/02 (eg. BV, AI, DV, see Apps.2,3) were not included since individual FU sequences could not be discerned, while sandstone facies associations were omitted in section 03 due to their large variations from the overall trend. The results for section 01/02 show a strong correlation (r=0.727 and 0.731 respectively) between paleocurrent deviation and coarse member thickness, and similar slopes ($m=2.08^{\circ}/m$ and $1.89^{\circ}/m$ respectively). Although these correlation values are large they are not significant at $\alpha = 0.05$. Section 03 shows a weak correlation (r=0.335) and a lesser slope ($m=0.712^{\circ}/m$). Although the small sample size did not allow statistically significant results, the trends imply that distal CU- and CUFU-type cycles have a larger deviation if the resulting avulsion involves a larger braid tract than a smaller one (an autocyclic control), which contrasts with proximal reaches

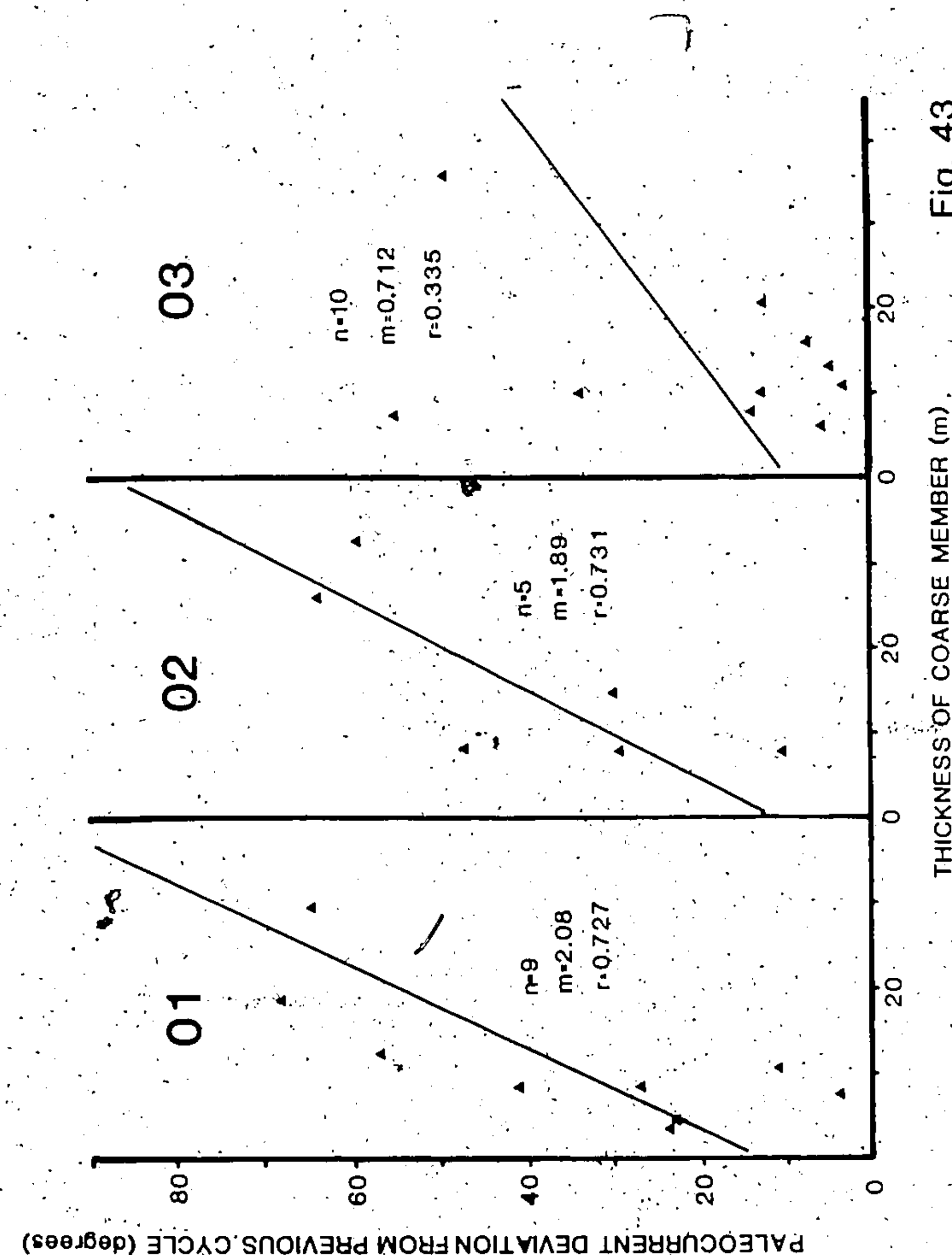
01
n=9
m=2.08
r=0.727
02
n=5
m=1.89
r=0.731
03
n=10
m=0.712
r=0.335
PALEOCURRENT DEVIATION FROM PREVIOUS CYCLE (degrees)
0
20
40
60
80
THICKNESS OF COARSE MEMBER (m)
0
20

Fig. 43

where deflections between cycles are only weakly related to the coarse member thickness, and hence the magnitude of the deflection does not vary with the size of the braid tract. The lack of consistent relationships in proximal reaches may be due to: i) insufficient data or ;ii) allocyclic overprinting of autocyclic mechanisms. The presence of allocyclic controls on sedimentation in the proximal reaches (previously discussed) suggests that the latter is probably more likely.

Fig.44 plots the angular deflection of a cycle from the preceding one versus the moving average grain size. Section 01 shows the strongest correlation (r=0.60) and displays an inverse relationship, section 02 displays a poor inverse relationship (r=-0.13) while 03 displays a weak positive correlation (r=0.34). Results from section 01, although statistically insignificant (at α =0.05), reflect the increasingly distal nature upward, i.e. as the grain size decreases upwardly the deflections between successive cycles also increase, perhaps due to increased sinuosity. With increasing proximality the inverse relationship becomes weaker and finally switches to a weak positive one in section 03 showing that coarser-grained proximal channels are more likely to have a larger deviation than finer grained ones. The CU nature of the majority of the section suggests once again that allocyclic controls must have played a vital role in the relationship between inter-cycle deflections and grain size.

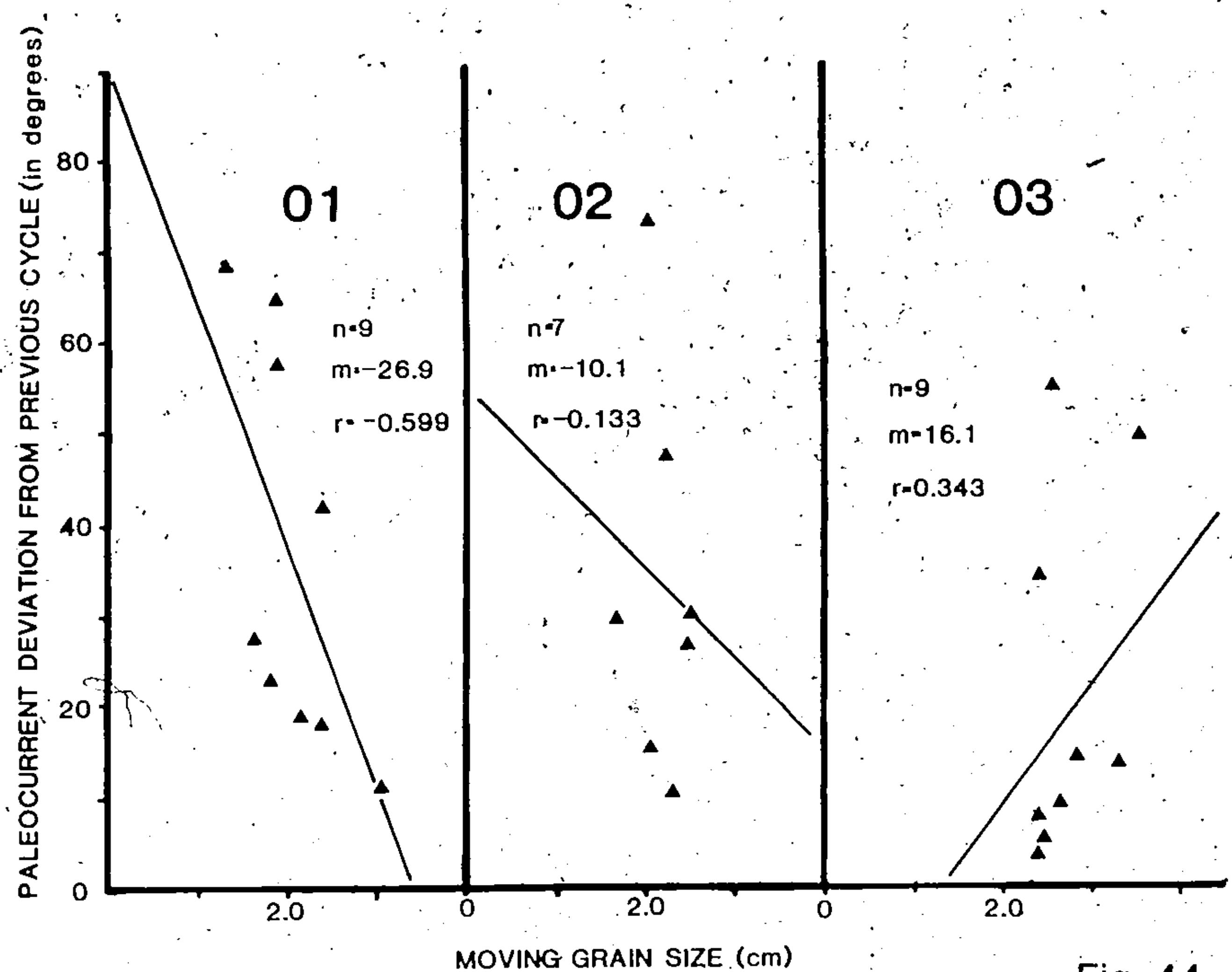

PALEOCURRENT DEVIATION FROM PREVIOUS CYCLE (in degrees)
80
60
40
20
0
01
n=9
m=−26.9
r=−0.599
02
n=7
m=−10.1
r=−0.133
03
n=9
m=16.1
r=0.343
2.0
0
2.0
0
2.0
MOVING GRAIN SIZE (cm)

Fig. 44

8.0 CLAST ANALYSIS

8.1 Introduction

A series of analyses on clasts were conducted to elucidate vertical and lateral trends in fluvial style, provenance, allocyclic controls, and transportation modes. These tests included petrographic analysis, grain size analysis, angularity studies, and clast provenance studies. Results reveal: gradual downstream diminution of grain size; rapid changes in angularity in proximal portions and no marked changes in the distal reaches; a predominant Caledonian Highlands source throughout the section with an upwardly increasing clast component from the Cobequid Highlands. These results also concur with findings from paleocurrent studies (discussed in section 10.3).

8.2 Grain Size

8.2.1 Procedure

Field procedure for clast analysis involved: measuring apparent "a" and "b" axis for clasts with "a" axis > 1.0cm (the degree of induration did not allow removal of clasts from matrix), angularity classification using an image comparator (Powers,1953; Fig.1), determination of lithology, and photographing the locality for subsequent calculation of matrix percentage. This method was done for the largest ten clasts (MPS of Bluck,1967) and the mean 100 clasts. The mean 100 clasts were selected by first locating the area having the largest clasts within a cycle (lags excluded), then randomly picking a spot within the area. Once the area was picked clasts > 1.0cm were systematically analysed by starting at a point and analysing each adjacent clast in a concentric fashion until 100 clasts were measured. This was done for every cycle, and if the cycle showed lateral continuity the procedure was repeated at various intervals.

8.3 Comparison between MPS and Mean 100

The MPS and mean 100 were both measured in order to compare the precision of the two methods. The MPS (mean particle size) is based on the largest ten clasts (Bluck, 1967) and has been shown to be very effective, in conjunction with bed thickness (BTh) in determining and classifying sediment gravity flows (Bluck,1967; Steel,1974; Gloppen and Steel,1981; Nemec and Steel,1984). Juxtaposed with fluvial environments, correlations between MPS and BTh have shown no significant relationships due to the contrasting modes of deposition. Unlike sediment gravity flows, fluvial deposits are characterized by "grain-by-grain" mode of emplacement rather than mass deposition. It therefore seems inappropriate to use grain size descriptors which are based on clasts larger than the 90th percentile (Andrews,1983). For this reason, the mean 100 should be a better measure of grain size.

In order to test the suitability of using the MPS for fluvial gravels the MPS for each sample location was plotted versus the mean 100. If the MPS varied on a one-to-one basis with the mean 100 a perfect correlation would result, but since sorting plays a factor, the correlation was expected to deviate from the ideal. Fig.45 shows the correlation from 55 sample sites and reveals a moderate correlation coefficient of $r = 0.65$. The lack of a strong correlation between the two demonstrates that the MPS is not a precise measure of grain size and hence could not be used with any certainty to detect minor changes in distal/proximal conglomerates.

8.4 Vertical and Lateral Trends in Grain Size

Vertical and lateral trends in the moving grain size average (mean 100) for the three sections are plotted in Fig.46-48, while the raw data are tabulated in Appendix 13. Beside the moving grain size, the moving normalized standard deviation for the "a" axis is also given. The normalized standard deviation (S_N) is normalized with respect to the mean "a" axis ($S_N = S/\text{mean}$) and is a relative measure of the sorting i.e. those with poor sorting have values approaching 1.0, or even exceeding it, while low values indicate good sorting (zero would be perfect sorting). The normalized standard deviation has been termed the coefficient of variation by Church (1972) in his studies of modern outwash plains.

Fig. 45

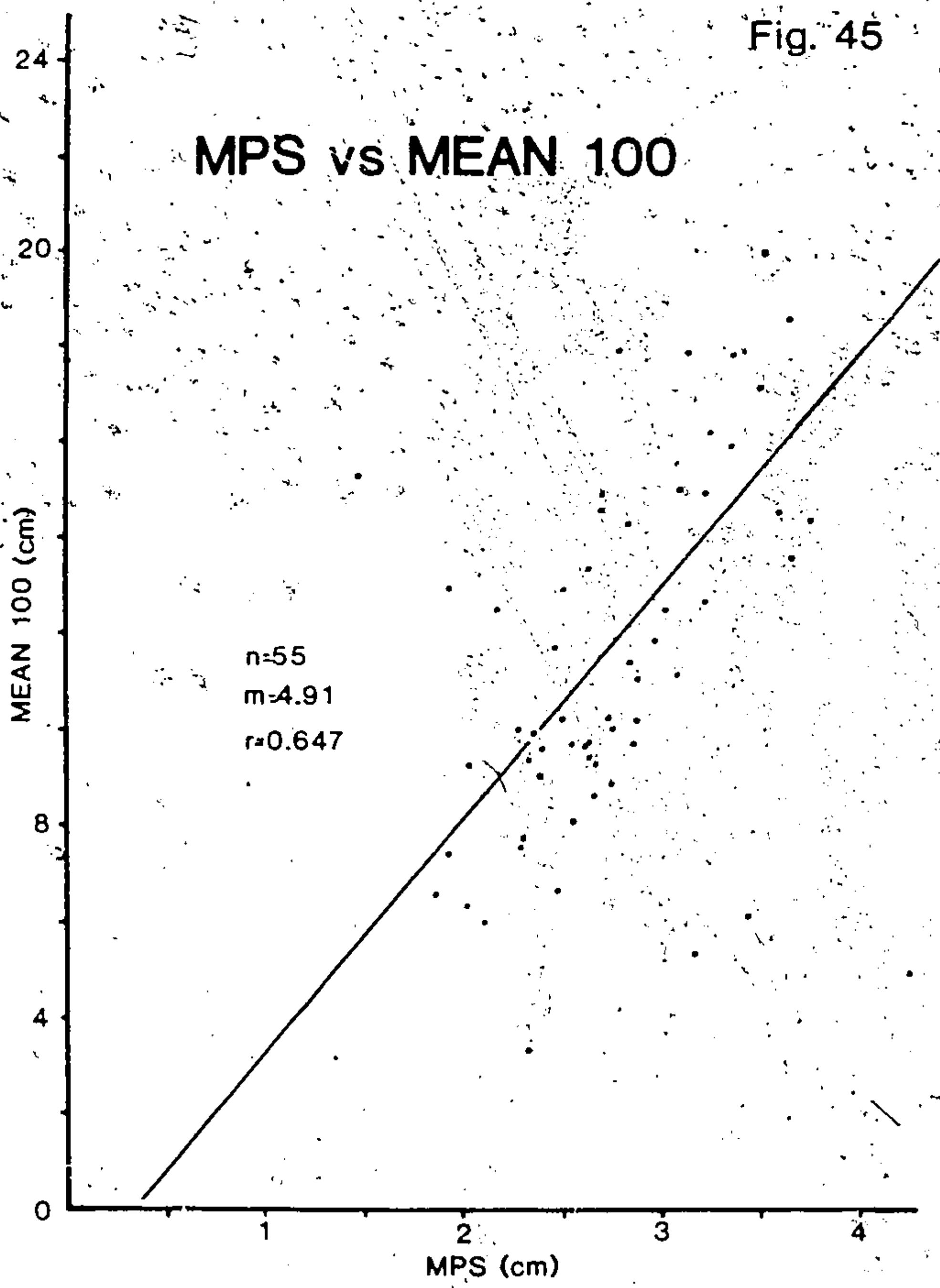

Fig. 46

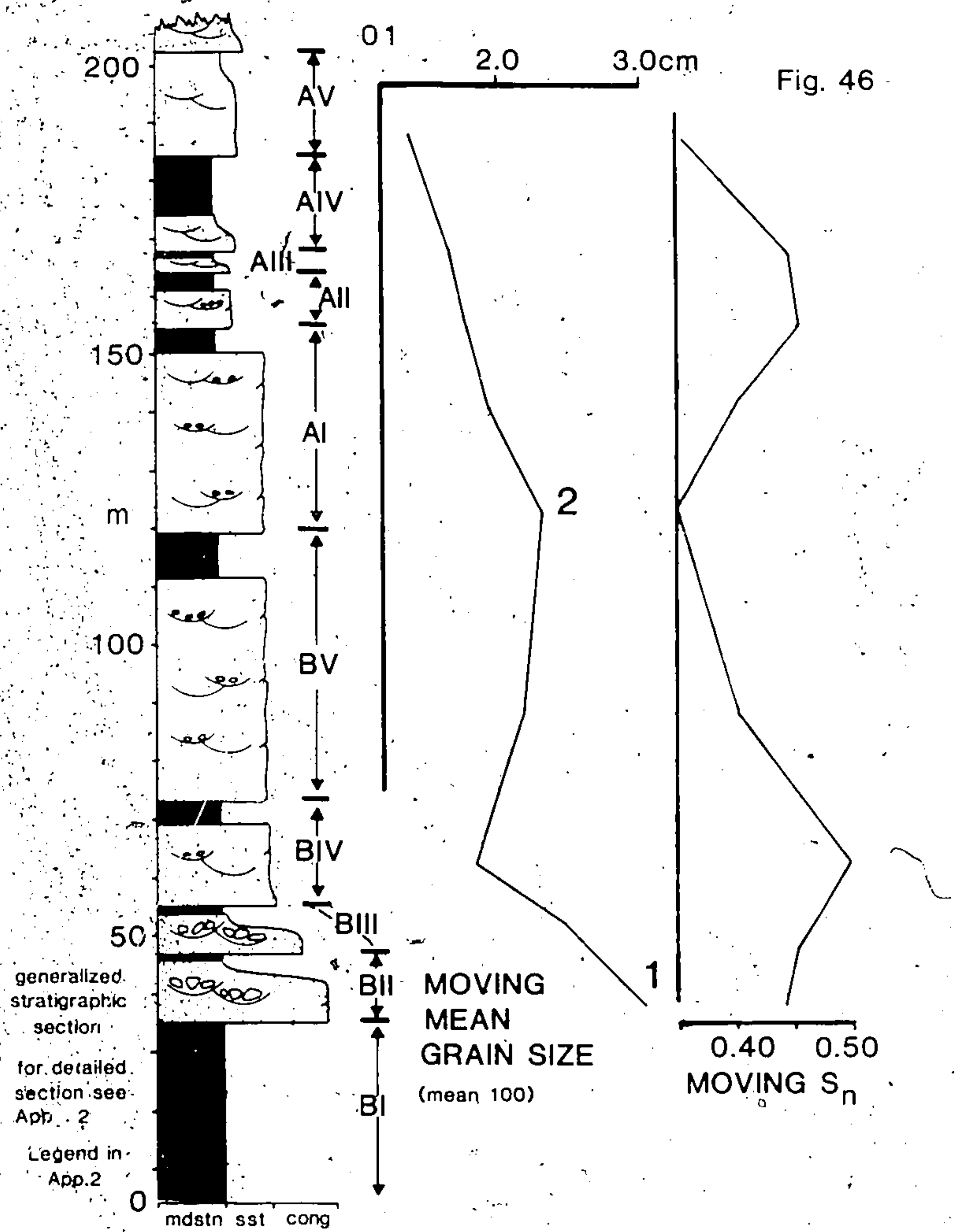
200
150
m
100
50
0
generalized stratigraphic section
for detailed section see App. 2
Legend in App.2
mdstn sst cong
AV
AIV
AIII
AII
AI
BV
BIV
BIII
BII
BI
01
2.0
3.0cm
2
1
MOVING MEAN GRAIN SIZE
(mean 100)
0.40
0.50
MOVING S_n

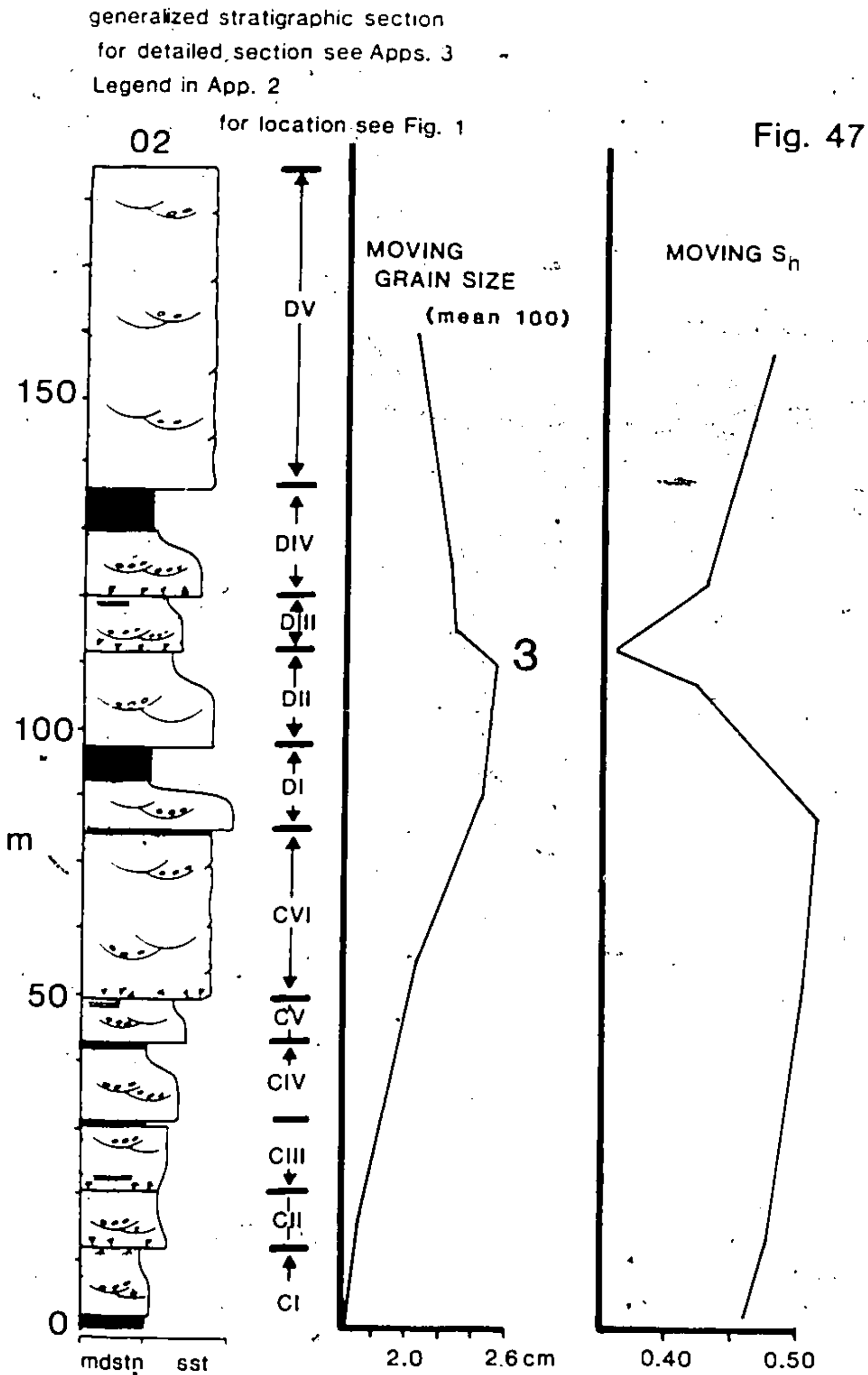
generalized stratigraphic section
for detailed section see Apps. 3
Legend in App. 2
for location see Fig. 1
02
150
100
m
50
0
mdstn
sst
DV
DIV
DIII
DII
DI
CVI
CV
CIV
CIII
CII
CI
MOVING
GRAIN SIZE
(mean 100)
3
2.0
2.6 cm
MOVING S_h
0.40
0.50

Fig. 47

Fig. 48

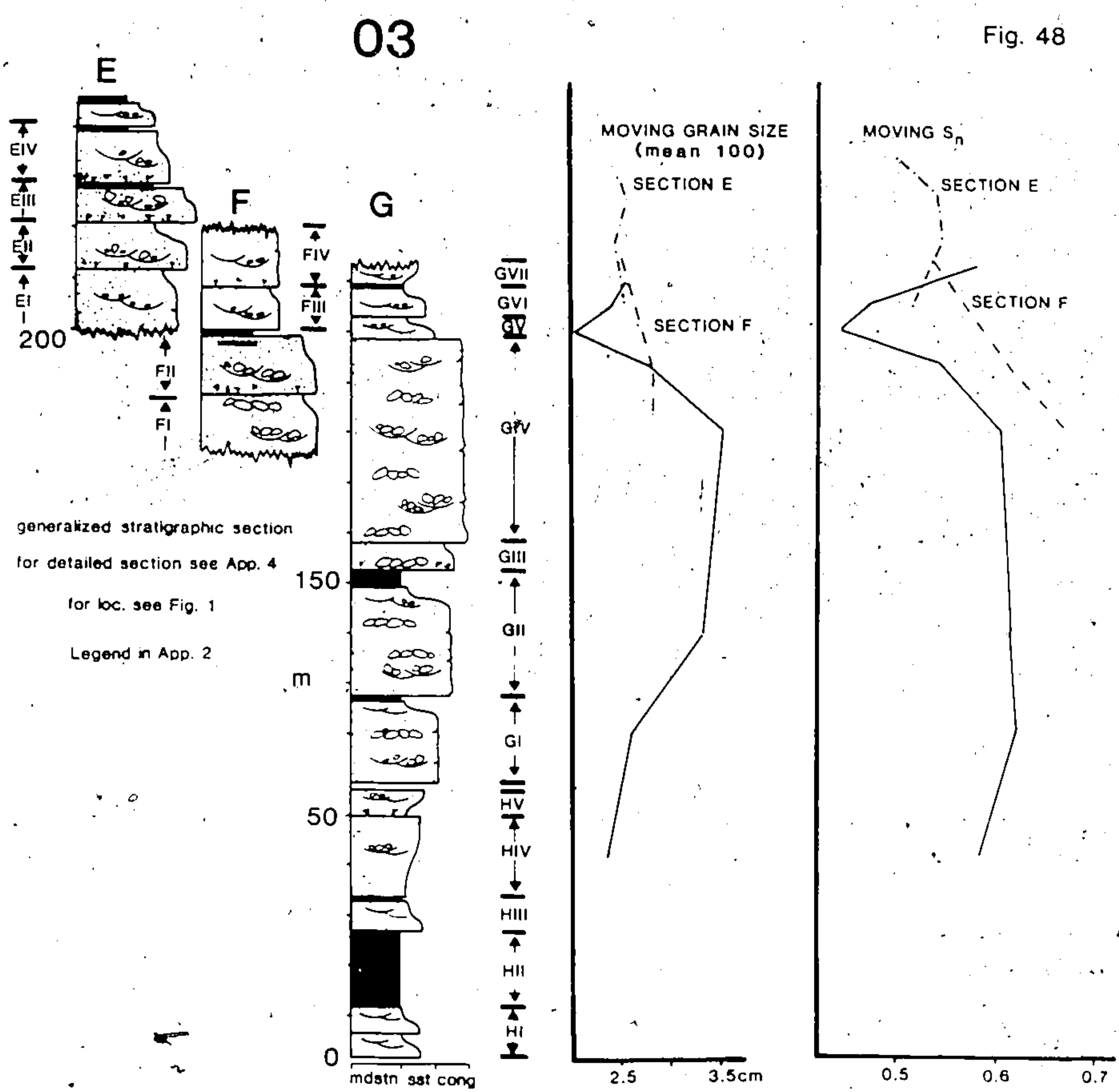

generalized stratigraphic section

for detailed section see App. 4

for loc. see Fig. 1

Legend in App. 2

Section 01 shows an overall FU trend with two high points labelled 1 and 2 in Fig. 46. The lower peak shows conglomerates sharply overlying floodplain sediments and fining-up to cycle BIV. This sequence is interpreted as an initial response to the first tectonic pulse. The second peak comprises a CU sequence ending at the lower part of cycle AI and is interpreted as a response to a combination of the first and second tectonic pulses. The remaining FU sequence is due to equilibration of the alluvial system to hinterland faulting.

Section 02 displays a CU then FU trend with one major peak labelled 3 in Fig.47. The CU sequence reflects progradation of sediments shed from the first and second tectonic pulse while the FU sequence implies relaxation of tectonism in the hinterlands (Heward,1978).

Section 03 displays an overall CU trend with one major peak (Fig.48) corresponding to the first tectonic pulse. A peak for the second tectonic pulse is not readily discernable from the moving average due to low values over- and underlying it. The capping sandstone facies associations show a rapid decrease in grain size reflecting a quiescent period in hinterland faulting.

Lateral trends between sections 03, 02, 01 show a gradual northward decrease in clast size from 2.73 cm to 1.99 cm respectively. Similar trends are seen in laterally extensive cycles such as DIV, FI, and GI (Fig.49). Linear regressions on lateral grain size variations show cycle DIV has a downstream diminution rate of 0.19cm/km (r=0.67) with minor fluctuations caused by deposition within various orders of channels. Much more rapid diminution rates are seen in sediments from the first tectonic pulse- 0.95cm/km (r=0.96) for cycle FI and 0.36cm/km (r=0.99) for GI, furthermore rates at the top of the CU sequence (0.95cm/km) are much faster than those at the base (0.38cm/km). Diminution rates at the top of the first tectonic pulse are slightly less than reported values from the midreaches of the Scott braided outwash of 1.25cm/km, (Boothroyd and Ashley,1975) the Ekalugad Sandur (1.50cm/km, Fig.37 of Church and Gilbert,1975) and greater than the midreaches of the Knik River (0.61cm/km, taken from kilometre 10 to 16, Fig.37 Church and Gilbert,1975). Assuming that Cumberland Basin clasts proximal to the source ranged between 20cm to 30cm, and diminution rates were 0.95cm/km, the source lay between 21km and 32km upstream, which is consistent with provenance from the Caledonian Highlands.

Apparent a/b ratios were calculated for all sample sites in order to see if clast shape was a function of transport (Table 8). Apparent a/b ratios for subsections D through to G are tabulated in Table 8 for the mean 100 and the MPS. Comparison of a/b ratios to Zingg shape diagrams (1935) indicates that clasts lie within the bladed-prolate field; field observation on "c" axes suggest that the clasts would

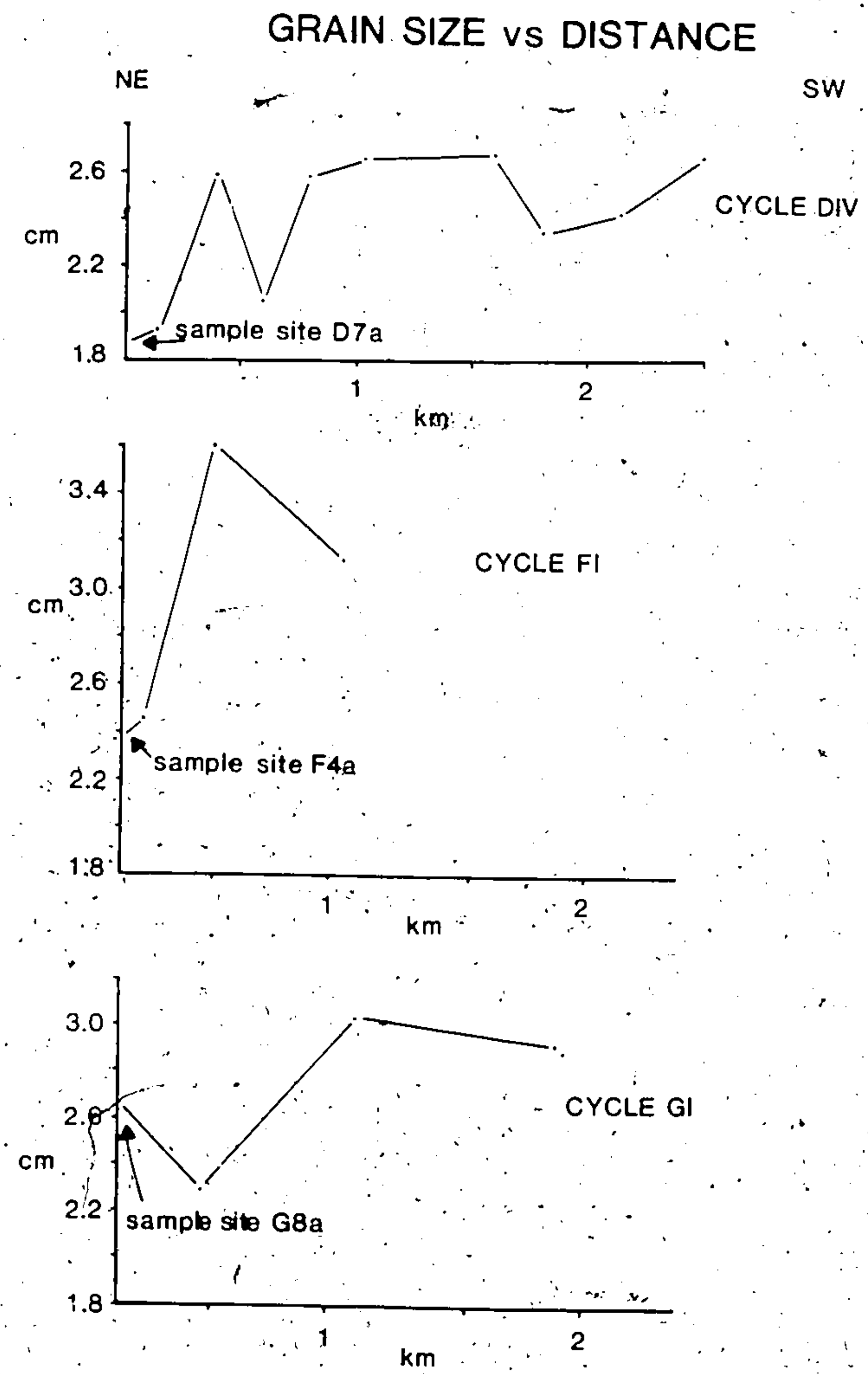
GRAIN SIZE vs DISTANCE
NE
SW
2.6
cm
2.2
1.8
sample site D7a
1
2
km
CYCLE DIV
3.4
3.0
cm
2.6
2.2
1.8
sample site F4a
1
2
km
CYCLE FI
3.0
2.6
cm
2.2
1.8
sample site G8a
1
2
km
CYCLE GI

Fig. 49

TABLE 8: a/b RATIOS FOR SUBSECTIONS A-G

SECTION	UNIT	MPS A/B	MPS S_D	MEAN 100 A/B	MEAN 100 S_D
02	D5b	1.8	4.93	1.50	0.97
	D7c	1.97	3.92	1.61	0.97
	D7d	1.51	4.2	1.63	0.99
	D7e	1.75	4.65	1.49	1.24
	D7f	1.86	7.14	1.75	1.41
	D7g	1.53	6.38	1.57	1.38
	D7h	1.79	5.33	1.56	1.18
	D7i	1.63	5.89	1.56	1.44
	D7j	1.60	5.34	1.56	1.38
AVERAGE		1.71	0.15	1.58	0.06
03	E7a	1.55	6.61	1.55	1.41
	E9	1.59	8.12	1.62	1.31
AVERAGE		1.57	0.03	1.58	0.05
	F4a	1.42	6.94	1.63	1.93
	F4b	1.49	8.39	1.63	1.37
	F4b(ii)	1.59	9.19	-	-
	F4c	1.61	8.99	1.59	2.68
	F4d	1.71	10.4	1.68	2.14
AVERAGE		1.56	0.11	1.63	0.04
	G2	1.41	6.9	1.66	1.47
	G4	1.78	8.91	1.60	1.97
	G6a	1.45	7.74	1.55	1.61
	G6b	1.49	9.28	1.61	2.71
	G8a	1.55	9.18	1.60	2.12
	G8b	1.61	7.22	1.63	1.69
	G8c	1.43	8.85	1.53	1.47
	G8d	1.75	8.58	1.53	1.70
AVERAGE		1.56	0.14	1.59	0.05

S_D = standard deviation of "a" axis

be closer to bladed than prolate. There are no apparent trends relating shape and the mean 100, but the MPS for subsection D shows significantly higher a/b ratios than the other sections analysed. Lateral trends in extensive cycles (Fig.50) show increasing a/b ratios in a distal direction. This may reflect either grain shape changes within an increasingly distal fluvial environment, where equant grains transported by traction would become more prolate with increasing transport distance or selective transport (heavier equant grains left behind, B.R. Rust, pers. comm., 1986).

8.5 Vertical and Lateral Trends in Sorting

Studies of modern gravelly braided outwash plains (sandurs) have shown various relationships between grain size and sorting (Church, 1972; Bradley et al., 1972; Church and Gilbert, 1975). Commonly, grain size decreases downstream as sorting increases and hence the converse is also expected to be true i.e. towards the upstream reaches the size increases while sorting decreases. Studies on proximal fluvial gravels demonstrate that as sorting increases the grain size decreases (Gustavson, 1974). Work by Church (1972), and Church and Gilbert (1975) on the Ekalugad sandur in Baffin Island essentially showed parallel trends between the mean grain size and the standard deviation (i.e. no downstream change in sorting even though grain size decreased). Furthermore, they noted that sorting depended on where the gravels were deposited - those in the channels were better

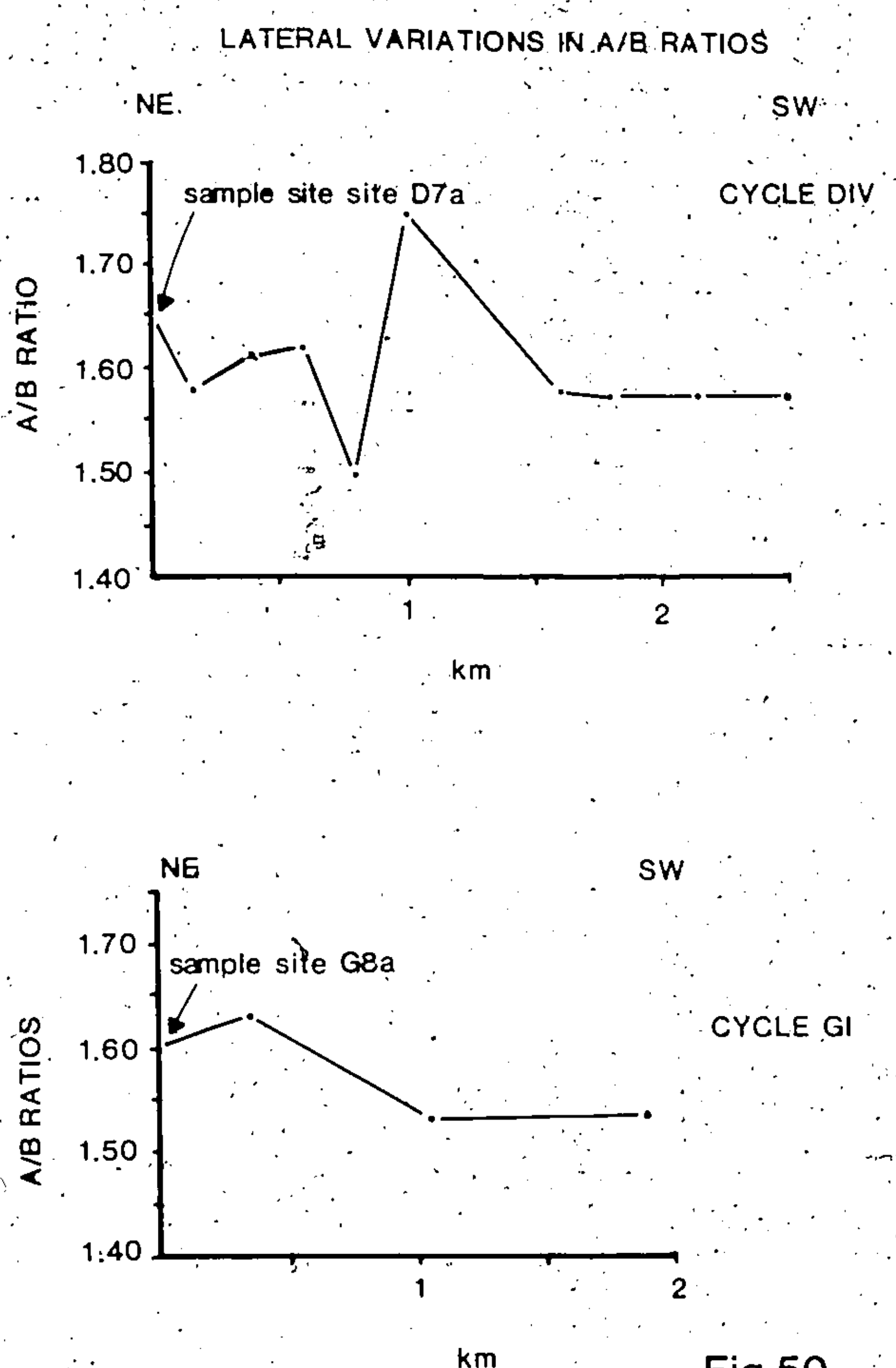
LATERAL VARIATIONS IN A/B RATIOS
NE.
SW
sample site site D7a
CYCLE DIV
A/B RATIO
1.80
1.70
1.60
1.50
1.40
1
2
km
NE
SW
sample site G8a
CYCLE GI
A/B RATIOS
1.70
1.60
1.50
1.40
1
2
km

Fig.50

better sorted than those on subaerially exposed bar surfaces.

Downstream changes in sediment sorting have been attributed to a myriad of causes. Russel (1939) first suggested that rapid aggradation and extreme variations in discharge promote good sorting. Russel's (1939) latter suggestion seems unlikely since flood stage will entrain the vast majority of clasts and low stage will only winnow granules, hence creating a poorly sorted deposit. Blissenblach (1954) concentrated on the relation between mechanics and grain size populations to state that sorting was a function of: i) range of particle size; ii) transportation and depositional mode; iii) distance of transport. Bradley et al. (1972) demonstrated that downstream increase in sorting was due to selective deposition rather than diminution of grain size. These results contrast with Church's (1972) work on Arctic sandurs in which sediment sorting was attributed to selective transport rather than selective deposition.

In order to better understand possible relationships between grain size, sorting (S_N), downstream transportation and allocyclic controls, vertical trends in grain size and sorting were plotted (Fig.51). Section 03 (Fig.51) shows a lower CU sequence (the first tectonic pulse) comprising a lower part showing a decrease in sorting and an upper part which increases in sorting. The lower part, showing an increase in grain size (from cycle HV to GI) along with a

LATERAL AND VERTICAL VARIATIONS IN SORTING

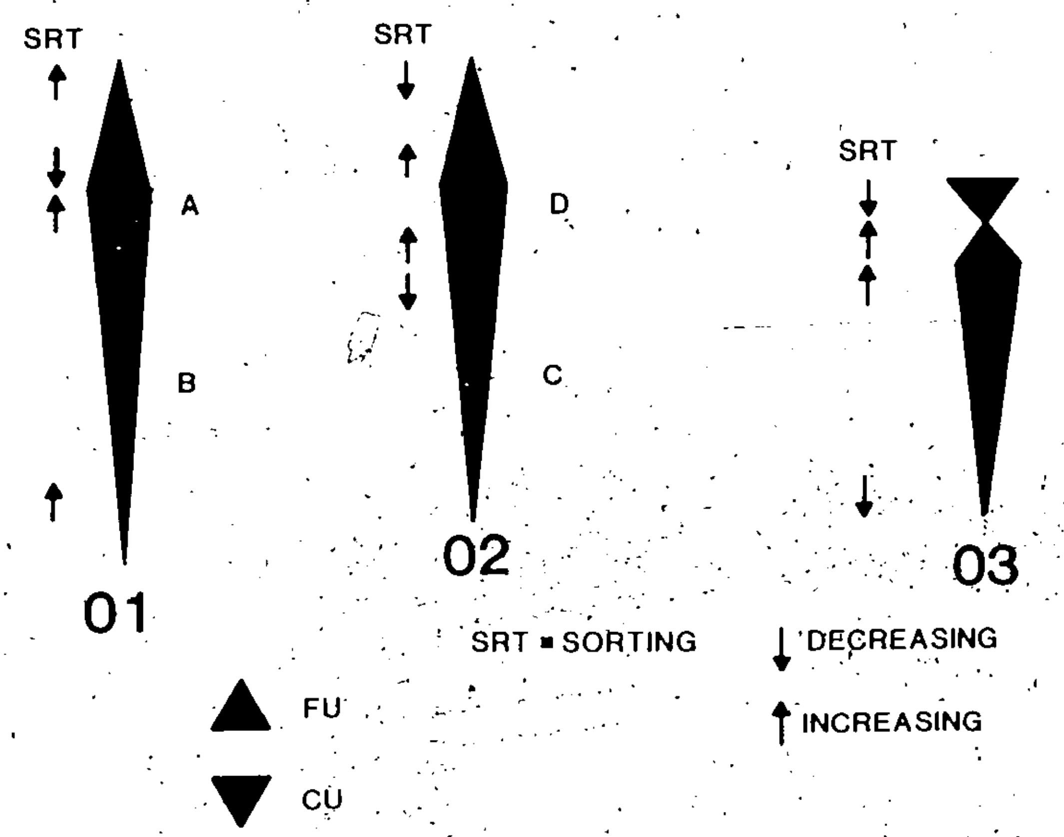

Fig. 51

decrease in sorting, displays what might typically be found in proximal reaches (Gustavson,1974). This can be explained by understanding firstly that small grains in a non-uniform bed will be hidden in the turbulent wake of larger particles and secondly that the shear stress needed to entrain a larger particle over smaller particles is much less than that needed to entrain a small particle over larger ones (Andrews, 1983; Allen,1983). Experimentally Andrews (1983) has shown that particles 0.3 to 4.2 times the mean diameter in naturally sorted river beds can be entrained at nearly the same discharge regardless of depth and hence clasts between 0.35cm to 4.9cm (for cycle GI) would be entrained and deposited at approximately the same discharge - thus creating poorly sorted deposits. This same relationship between sorting and grain size is seen in the CU sequence of section 02.

The upper part of the CU sequence in section 03 shows an increase in grain size and sorting (i.e. sorting and grain size increase upstream). These results differ from those of Bradley et al. (1972), Church (1972), Church and Gilbert (1975) and Gustavson (1974) who report either a downstream increase in sorting (i.e. grain size decreases and sorting increases) or constant sorting values. The exact cause of the sorting variation in section 03 may be a result of either selective deposition (Bradley et al.,1972) or selective transport (Church and Gilbert,1975). The rapid aggradation rates inferred for cycle GIV along with the increased grain size indicate possibly higher competence flows which might have been able to suspend a larger fraction of the fine population, thus allowing elutriation of the fines as suggested by Church and Gilbert (1975). Selective deposition may be a more difficult explanation to invoke since the entrainment/deposition of clasts ranging from 0.48cm to 6.7cm (from cycle GIV) could be achieved by the same approximate dimensionless critical shear stress. Similar trends in sorting and grain size are seen in the CU sequence of section 02 (i.e. sediments from the second tectonic pulse, see Fig.51).

The FU sandstone facies association capping the lower conglomeratic association in section 03 shows an upward increase in sorting typical of a progressively distal fluvial environment (Fig.51). The basal part of the FU sequence in section 02, and the FU conglomeratic facies associations at the base of section 01 all show the same trend.

The CU sequence corresponding to the second tectonic pulse in section 03 (Fig.51) shows a decrease in sorting similar to the beginning of the lower CU sequence in section 03. No similar patterns are seen in section 02.

Cycles dominated by sandstone lithofacies, such as those from section 01, mostly display antithetic relationships between grain size and S_N, i.e. clast size is proportional to sorting.

The CU sandstone sequence in section 01 shows an upward increase in sorting, similar to those seen in CU sequences from sections 02 and 03, and is interpreted as a response to increasing proximity to the source. The capping FU sequence shows a decrease followed by an increase in sorting (Fig.51).

Lateral changes in sorting show a progressive distal increase in the average sorting values (i.e. poorer sorting) from S_N =0.589 (n=22), to 0.459 (n=19) to 0.426 (n=10) in sections 03, 02, 01 respectively. Laterally extensive cycles such as DIV (section 02) also show a gradual distal increase in sorting values (Fig.52) over 6km.

8.6 Grain Size Analysis

Grain size analyses at various locations were calculated in order to determine the distribution of the coarse grained fraction and possible mechanisms of deposition. The well indurated matrix did not allow the common procedure of sieving and weighing various size fractions. Instead, apparent grain size diameters ("a" axis") were measured, since the true diameter could not be measured.

The procedure first involved photographing the sampled location in order to later calculate matrix percentages. An acetate sheet was then ruled with dots separated at 1cm photo-equivalent intervals (mean grain size calculated from clast count at locality) and placed over the photograph.

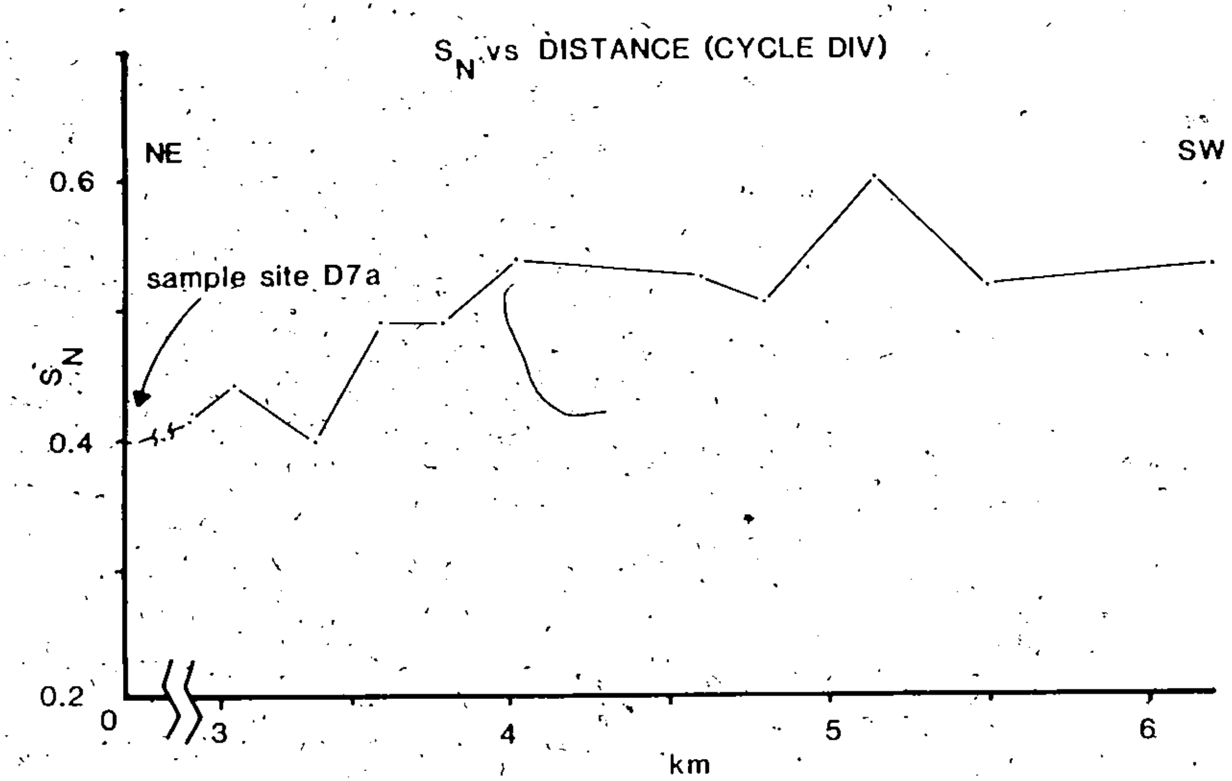
S_N vs DISTANCE (CYCLE DIV)
NE
SW
sample site D7a
S_N
0.6
0.4
0.2
0
3
4
5
6
km

Fig. 52.

Glagolev-type traverses were then conducted on the photograph by counting whether a clast or matrix (matrix defined as anything smaller than one spacing i.e. one centimetre) underlay the dot. Traverses were varied across the photograph until 200 points were completed. Percentages of matrix and clasts were then calculated (Appendix 14). The percentage of matrix varies between 27% and 75% with the percentage increasing towards the distal reaches. Frequency distributions (from field counts) at 1/2ϕ intervals for clasts ranging from -3.00ϕ to -8.00ϕ were tabulated for each locality. These were then converted into cumulative percentages and corrected for the percentage of matrix using the following equation:

$$P_{Ti} = [(P_{Ci} * C)/100] + M$$

where P_{Ti} = cumulative % of the i^{th} fraction

P_{Ci} = cumulative % of coarse grain i^{th} fraction

C = % clasts

M = % matrix

The data were then plotted on probability paper (Fig.53) halfway between each class interval i.e. if the class interval is -3.00ϕ to -3.50ϕ, then it is plotted at -3.25ϕ.

The results from laterally extensive cycle DIV are shown in Fig.53 and reveal an increase in the mean up to -3.85ϕ, along with an increase in the coarse size fraction (from 12% in D7a to 62% in D7g) in an upstream direction. Grain size analyses on several cycles from section 03 (FI, GI, GII) show the following vertical trends: an upward increase in the

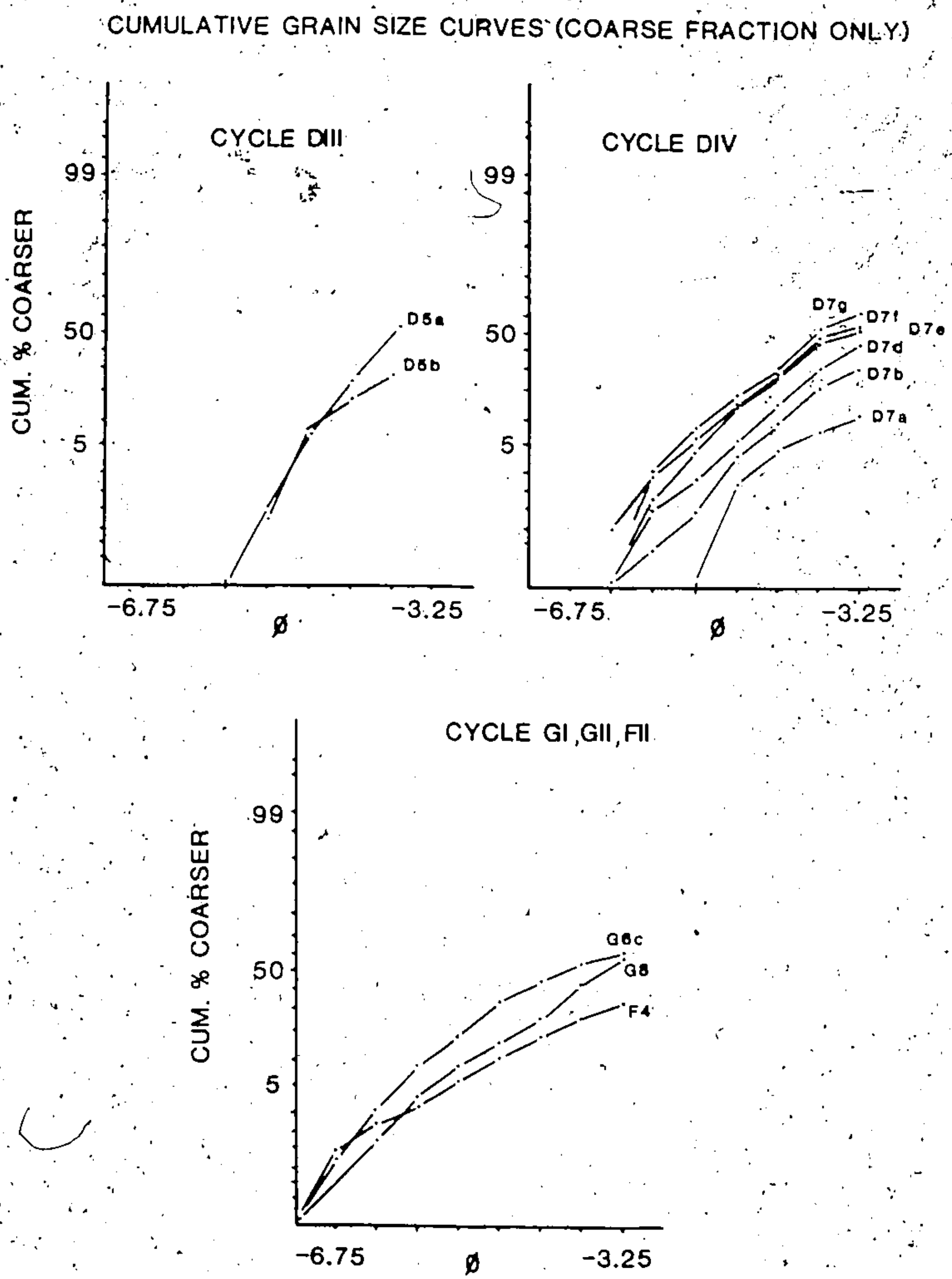
CUMULATIVE GRAIN SIZE CURVES (COARSE FRACTION ONLY)
CYCLE DIII
CUM. % COARSER
99
50
5
D5a
D5b
-6.75
ø
-3.25
CYCLE DIV
99
50
5
D7g
D7f
D7e
D7d
D7b
D7a
-6.75
ø
-3.25
CYCLE GI,GII,FII
CUM. % COARSER
99
50
5
G6c
G8
F4
-6.75
ø
-3.25

Fig. 53

coarse fraction from 32% to 62%, and an increase in the mean grain size up to -4.0ø (1.6cm).

The convex-up shape of the curves is typical of the traction population (Middleton, 1976); the lack of any slope break (except for sample D-7a and D-5b) suggests that the intermittent-suspension population was not sampled and hence it is hypothesized that sediments between -3.25 ø and -6.75ø were transported by predominantly tractive processes (Middleton and Southard,1984).

8.7 Clast Lithotype Analysis

Trends in size, abundance and angularity were analysed for individual clast lithotypes in order to learn more about allocyclicity and provenance. Clast lithologies were divided into four major classes: felsics, siliciclastics, metamorphics, and others.

The siliciclastics group is the most abundant and is made up of sandstones, mudstones and quartzites (classified under siliciclastics and not metamorphics). Sandstones comprise variously coloured fine to medium grained quartz arenites, red medium grained quartz arenites, and brown medium to coarse grained arkosic arenites. Mudstones are made up of grey, brown or black mudstones (and shales); and brown/grey siltstones. Quartzites (petrography discussed in 8.9) are usually fine to medium grained and range in colour from white through grey, and red to green with grey being the most common.

The felsic group comprises syenites (including quartz syenites and quartz-poor alkaline granites), trachytes/porphyritic rhyolites, granites and foliated granites (feldspathic gneisses) and constitutes the second most abundant group.

The metamorphics are a minor group comprising green phyllites and green schists, which are not represented at all sample sites. The "other" group constitutes multicouloured cherts and white vein quartz.

Percentages for the various clast lithotypes are found in Appendix 15 while tabulated averages for subsections A through G are seen in Table 9. General trends from Table 9 show an upward increase in the percentage of felsics and no marked patterns in the siliciclastics. A plot of the moving percentage for each clast lithotype for section 03 (Fig.54) shows an upward increase in felsics, and a decrease in siliciclastics. A similar plot for section 01 (Fig.55) shows a close resemblance to shapes seen in Fig.54, differing only in their magnitudes. The much larger percentage of sandstone clasts in the distal section (01) suggests either closer proximity to the sandstone source or a greater proportion of broken rounds. Comparison between Figs.54 and 55 reveals equivalent peaks in the siliciclastics/felsics (labelled 1

TABLE 9: CLAST LITHOTYPE PERCENTAGES

SECT		SYEN	GRAN	GNS	RHY	QTZT	SST	MDST	PHY	N
01	A	11.3	11.5	9.3	3.7	16.5	41.3	0.5	-	400
	B	7.6	3.4	1.6	0.6	19.5	60.9	2.4	-	300
02	D	11.6	16.3	3.4	0.4	34.5	27.6	1.68	0.2	1600
03	E	12.0	7.0	2.0	2.0	35.0	35.0	4.0	-	200
	F	8.3	4.5	2.2	-	41.4	33.8	4.6	-	500
	G	8.5	8.5	1.9	0.1	35.9	37.0	1.6	2.9	800

SYEN = syenite
GRAN = granite
GNS = gneiss
RHY = rhyolite
QTZT = quartzite
SST = sandstone
MDST = mudstone
PHY = phyllite
N = number of observations

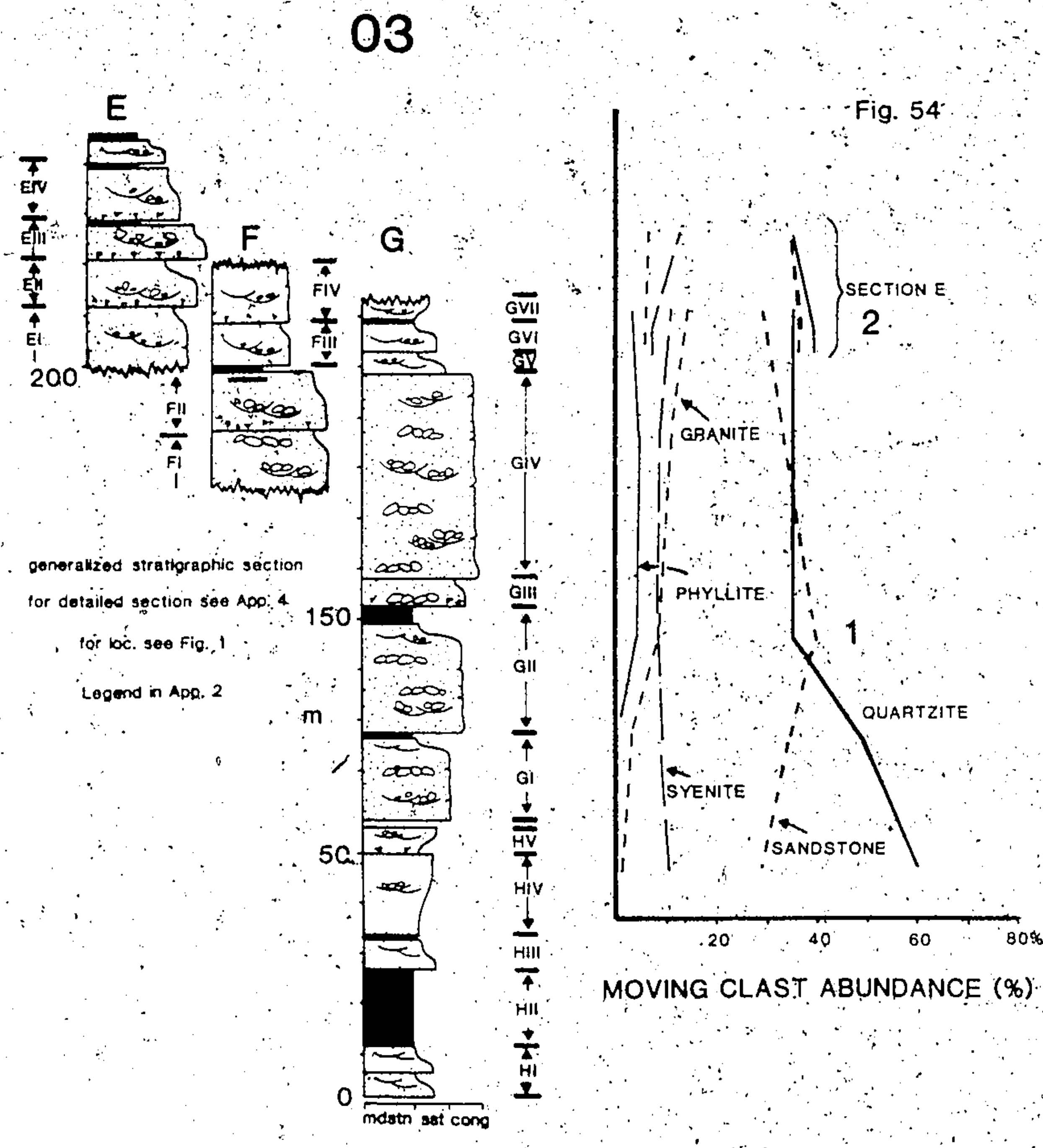
03
Fig. 54
E
F
G
EIV
EIII
EII
EI
200
FIV
FIII
FII
FI
GVII
GVI
GV
GIV
GIII
GII
GI
HV
HIV
HIII
HII
HI
150
m
50
0
mdstn sst cong
generalized stratigraphic section
for detailed section see App. 4
for loc. see Fig. 1
Legend in App. 2
SECTION E
2
1
GRANITE
PHYLLITE
QUARTZITE
SYENITE
SANDSTONE
20
40
60
80%
MOVING CLAST ABUNDANCE (%)

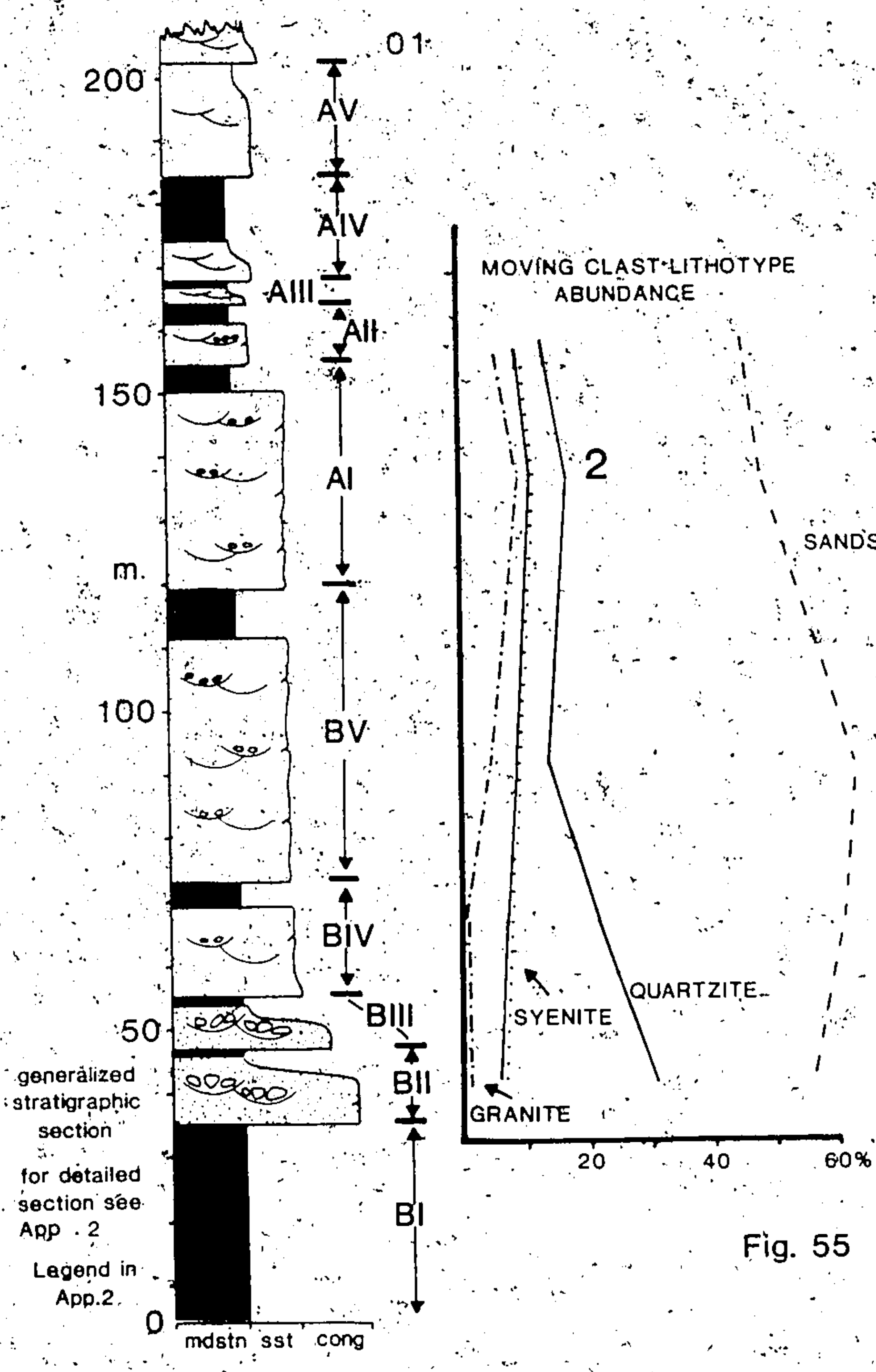

01
200
AV
AIV
AIII
AII
150
AI
m.
100
BV
BIV
BIII
50
BII
BI
0
mdstn sst cong
generalized stratigraphic section
for detailed section see App . 2
Legend in App.2
MOVING CLAST LITHOTYPE ABUNDANCE
2
1
SANDSTONE
QUARTZITE
SYENITE
GRANITE
20
40
60%

Fig. 55

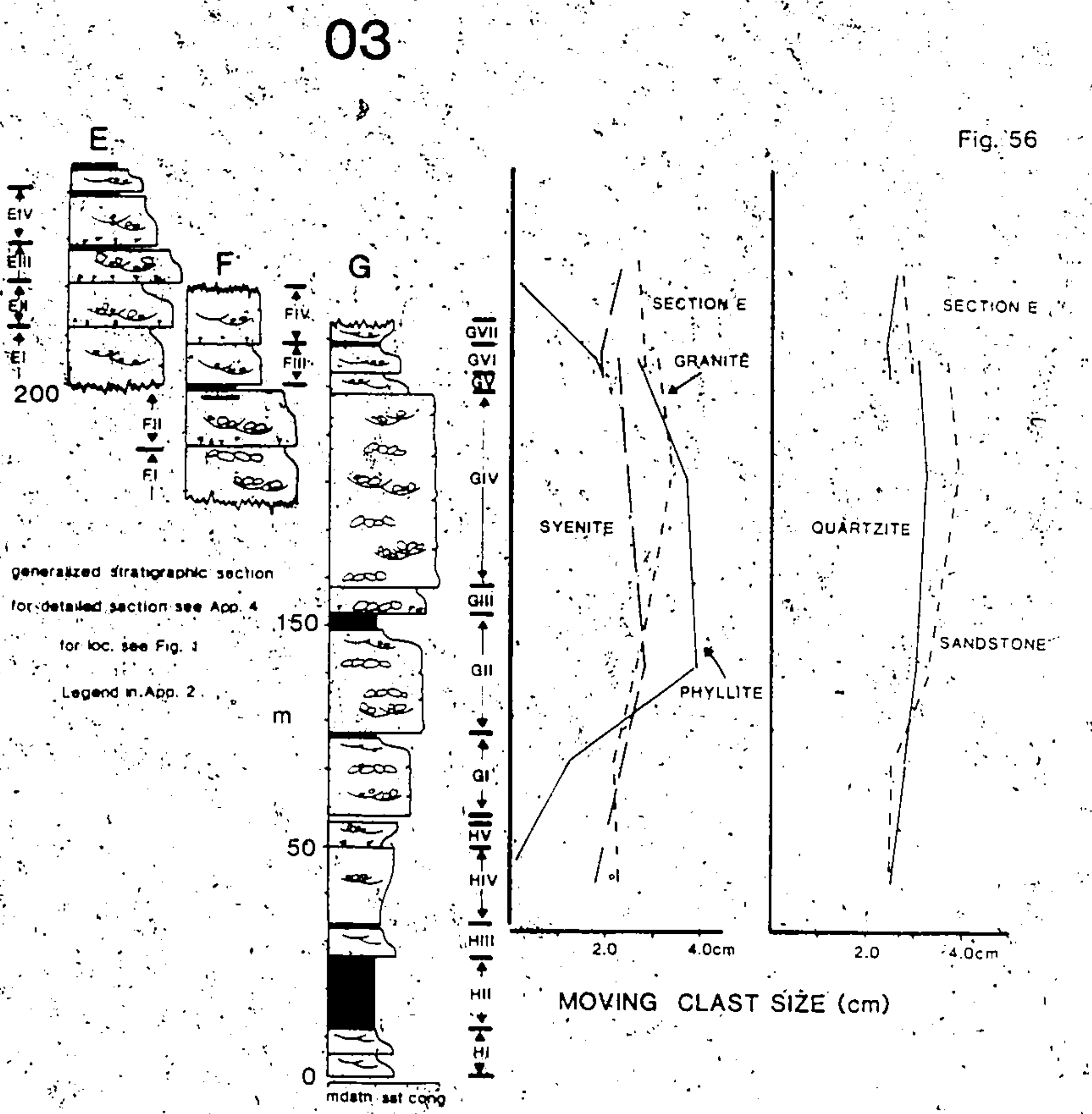
03
Fig. 56
E
F
G
EIV
EIII
EII
EI
FIV
FIII
FII
FI
200
generalized stratigraphic section
for detailed section see App. 4
for loc. see Fig. 1
Legend in App. 2
150
m
50
0
mdstn sst cong
GVII
GVI
GV
GIV
GIII
GII
GI
HV
HIV
HIII
HII
HI
SECTION E
GRANITE
SYENITE
PHYLLITE
QUARTZITE
SANDSTONE
2.0
4.0cm
MOVING CLAST SIZE (cm)

and 2 respectively) at much higher stratigraphic levels in section 01 than 03, typical of a progressively onlapping clastic wedge.

8.7.1 Progradational/Retrogradational Trends from Clast Analysis

Vertical trends in the grain size and abundance maxima are commonly used to delineate progradation/retrogradation of sediments shed from adjacent uplands. Results from this study show that dissection of the moving grain size into its constituent components can aid in the determination of the type and location of orogenic events. This can be done by understanding the relationship between: i) downstream morphological changes in individual clast lithotypes and ii) relationships between moving grain size and abundance maxima.

Clast morphology depends on: i) original shape from the parent rock; ii) mineralogical characteristics; iii) size; iv) transport distance; v) transporting agent; and vi) probability (i.e. chance) (Sneed and Folk, 1958). It is almost impossible to conduct a study incorporating all these factors, hence theories attempting to understand downstream changes in morphology are often speculative. Kuenen (1956), in an exhaustive study showed that downstream changes in morphology were controlled primarily by the nature of the bed and the kinetic energy of the colliding pebble - a pebbly floor will abrade more than a sandy one; while increased kinetic energy is more likely to abrade the pebble. Kuenen (1956) also showed in his flume experiments and from fluvial studies that fracturing (i.e. breaking into two or more pieces) was not a major abrasion process, rather "chipping" and "cracking" were the pervasive methods of morphological change. Pittman and Ovenshine (1968) studied pebble morphology in the Merced River (California), observing depletion of intermediate-sized granitic clasts and increases in broken rounds in proximal parts of the river. They suggested that these effects may be caused by attainment of kinetic energy exceeding the pebble's fracture strength. A cataract was envisaged to provide the needed kinetic energies for fracturing of the pebbles. Studies by Bradley (1970) in the Colorado River showed that granitic pebbles abraded primarily by fracturing and chipping, hence creating broken rounds. It was also noted that the abrasion process was dramatically accelerated if the granitic clast had undergone prior weathering (up to a 40% increase over fresh granitic clasts). These results were borne out in Vicary Creek (Alberta) by Pearce (1971) who documented downstream change of trachytic cobbles from angular to rounded within 3km and attributed it to rapid fracturing and chipping. Schumm and Stevens (1973) noted that abrasion in fluvial systems occurred much more quickly than in tumbling tanks. Theoretical and flume studies showed that clasts could attain sufficient kinetic energy by intermittant saltation to fracture upon impact with other clasts, a factor which was not discernable from tank experiments.

The dominant process in pebble abrasion can be ascertained by plotting hypothetical frequency versus size plots for coarse fluvial gravels. If clast fracturing is an important process one would expect a negative slope on a frequency versus size plot (Fig.57b) i.e. the fracturing of large, (or intermediate) clasts will deplete that size fraction and augment the smaller sizes. In the opposite case, should "chipping" be the predominant abrasive process, then a positive slope would be more likely (Fig.57a) since the original size distribution would tend to be preserved with only minor depletions in the coarse fraction and minor additions to the fine fraction.

Using these criteria, deposits from various cycles were analysed. Visual examination of felsic lithoclasts (granites and syenites) showed that six out of ten populations demonstrate a negative slope indicative of fracturing (Fig.58). This is also corroborated by noting that in cycles GI,II the felsic size fraction between -4.0ϕ and -5.0ϕ is depleted even though it constitutes a prominent portion of the total grain size distribution (cf. with the underlying histograms) thus reflecting the fracturing of clasts. Further evidence for breakage during transport is seen in the abundance of broken rounds (Fig.59) in the field. The results for felsic clasts show conclusively that fracturing was the dominant process creating morphological changes as opposed to gradual pebble diminution by chipping. If quartzite is examined in a similar manner no dominant slope trend can be

HYPOTHETICAL FREQUENCY VS GRAIN SIZE FOR PROXIMAL SEDIMENTS

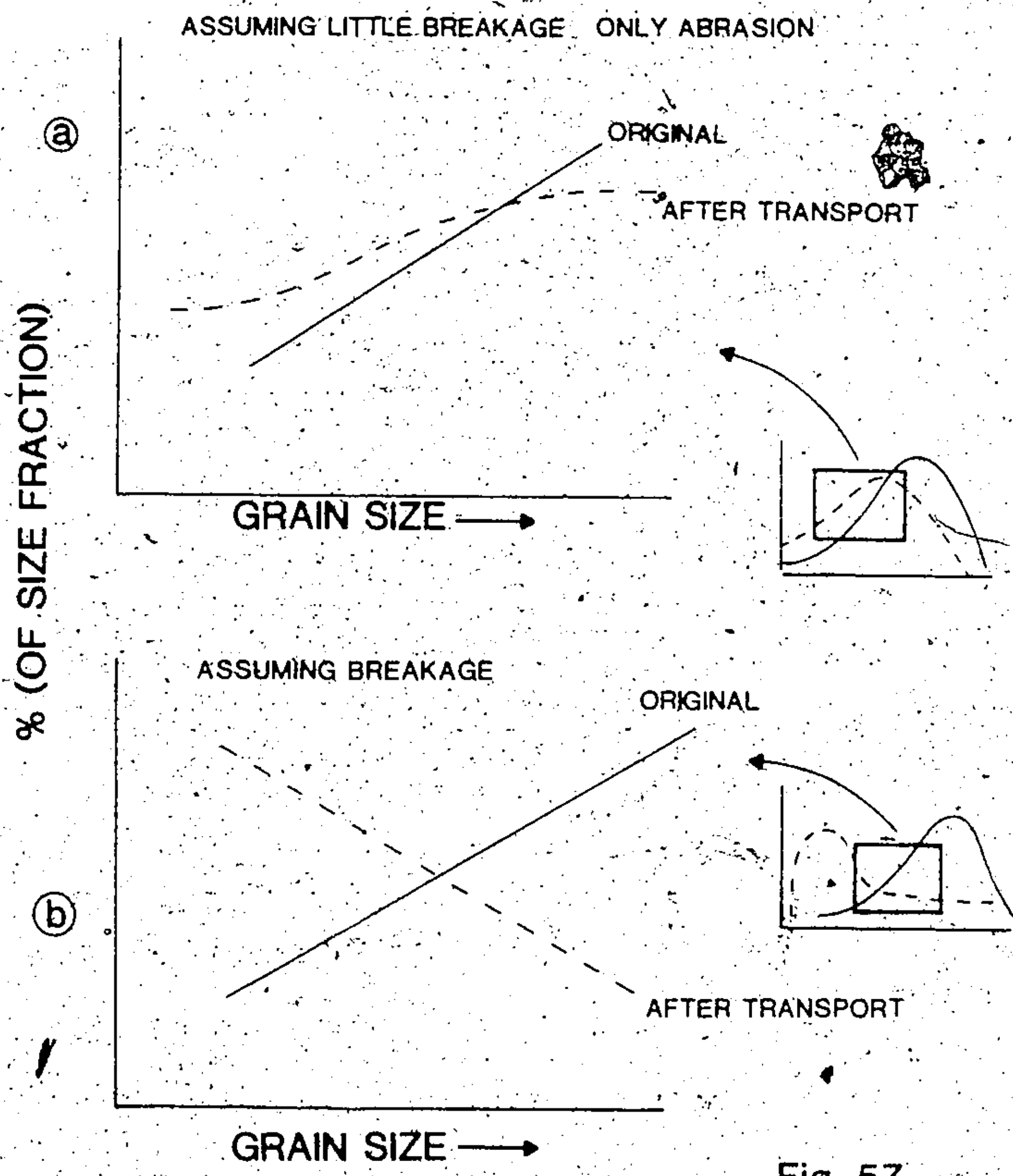

Fig. 57

GRAIN SIZE (Ø) VS FREQUENCY (%)
FOR LITHOTYPES WITHIN VARIOUS
CYCLES

Fig. 58

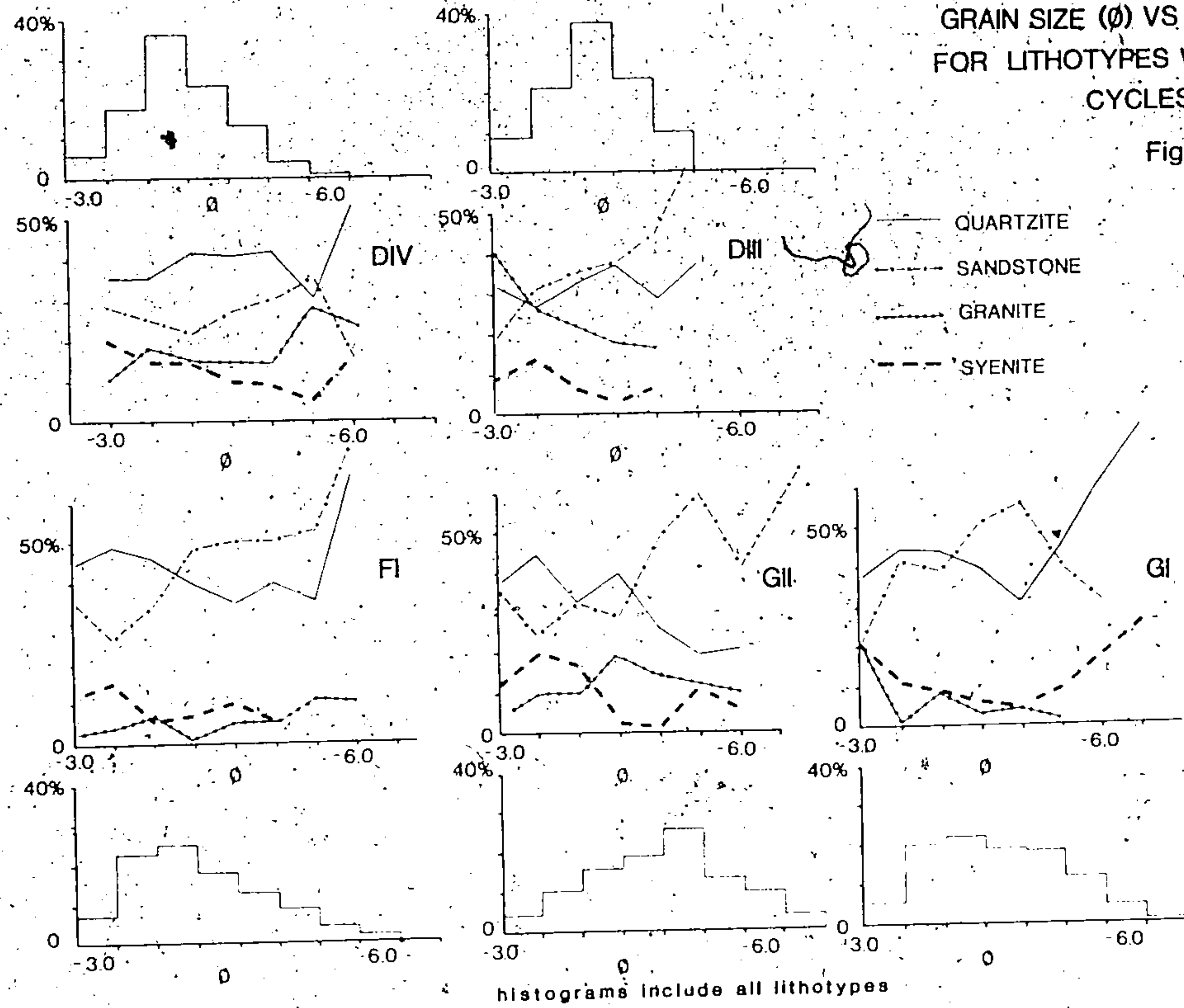

Fig. 59. Granitic broken rounds (unit E-9, cycle EI, at loc.14.).

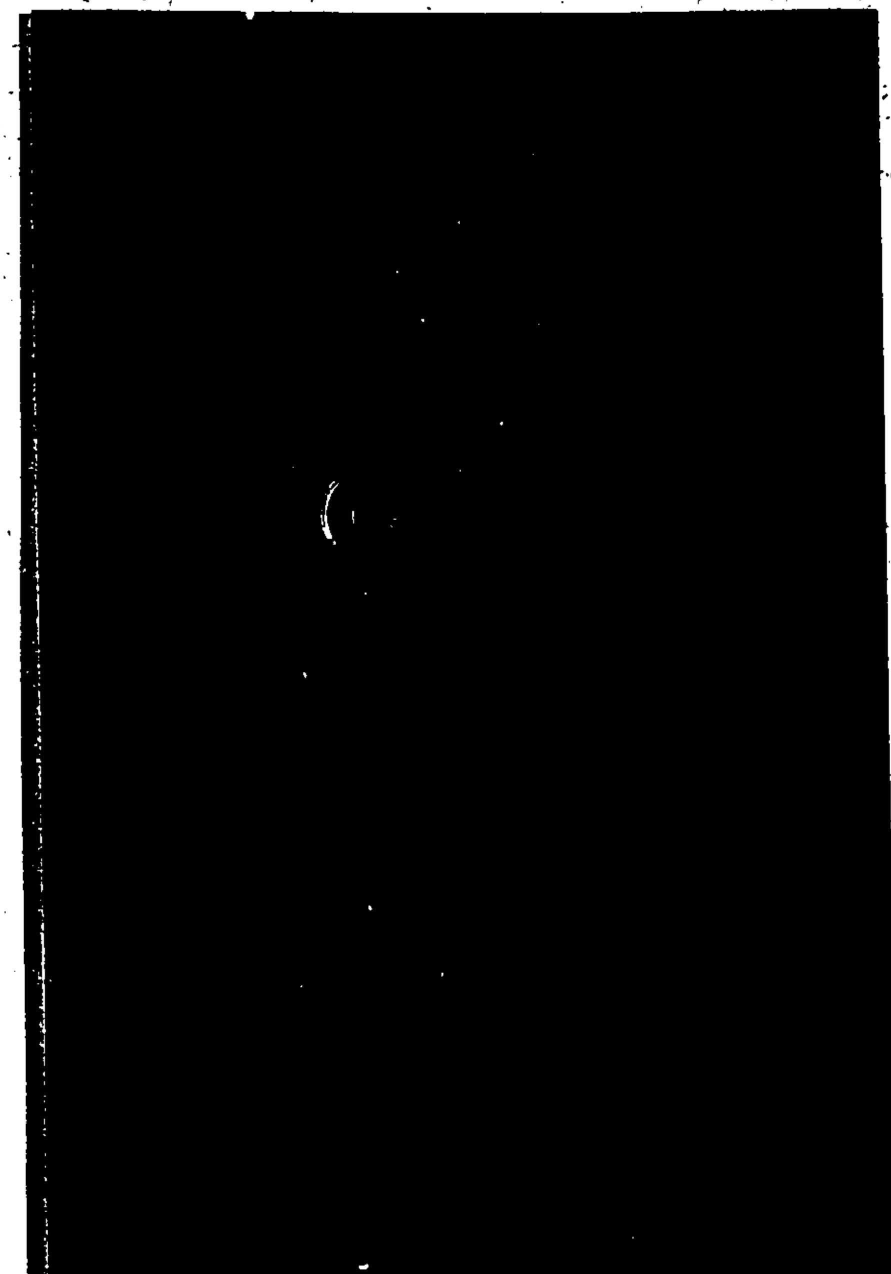

delineated but depletions can be seen in grain sizes between 5.0ϕ and 6.0ϕ (Fig.58). This depression, although not as well documented as the previous case, may be partly due to breakage and/or natural depletion of those grain sizes in the source rock. Sandstones in three out of five cases show a general positive slope indicative of gradual abrasion rather than fracturing, phyllites also show the same trend. This may be on account of the less brittle tendencies of the latter two lithotypes, which do not allow fracturing. These findings concur with studies by Bradley (1970), Pearce (1971), Thomas and Ovenshine (1968), and Schumm and Stevens (1973) which see fracturing as an important element in the determination of clast morphology. The vigour of currents needed to fracture the clasts is also in agreement with conclusions from section 7.2. Results from this study can be used to infer the following downstream changes in pebble size and abundance: i) felsic clasts abrade primarily by fracturing, hence with increasing transport there was a decrease in large pebbles and an increase in small ones. The net result was a downstream <u>increase</u> in the abundance of felsic clasts along with a decrease in size; ii) quartzite clasts are brittle and some fracturing is expected, but not to the degree of the felsic clasts. Downstream transport tended to slightly increase the abundance and decrease size; iii) sandstones and phyllites are relatively soft hence transport tended to gradually abrade rather than fracture them. Downstream trends would show no increase in their abundance, just the diminution of <u>all</u> size fractions.

To reiterate, in a fluvial system transporting various subequally abundant lithotypes, the following general relationships will be noted in proximal and distal reaches for fracture-prone clasts: i) in proximal reaches the clasts, although larger, will have a relatively low abundance: ii) subsequent fluvial transport into the distal reaches will cause a reduction in size and breakage of clasts, some more quickly than others, resulting in a greater relative abundance of some clasts due to the increase in broken rounds and the total destruction of more labile clasts. Hence downstream transport of a specific clast lithology under these conditions is expected to yield a higher abundance of smaller clasts in the distal reaches compared to larger, less numerous ones in the proximal reaches. Clasts with gradual abrasion tendencies will not show the same pattern i.e. downstream transport will not increase the abundance, only reduce the grain size.

The addition of allocyclic controls to the fluvial system can then cause the maximum grain size to overlie the maximum abundance of a fracture-prone lithotype in a prograding system and the opposite to occur in a retrograding system (Fig. 60). Hence fracture-prone clasts (eg. felsics) showing the maximum abundance overlying the maximum grain size suggest a retrograding (i.e. back-stepping or peneplaining) source while the opposite relation marks rejuvenation (i.e. uplift or subsidence). The application of this relationship to abrasion-prone clasts (eg.

RELATIONSHIP BETWEEN MAX. GRAIN SIZE AND MAX. ABUNDANCE

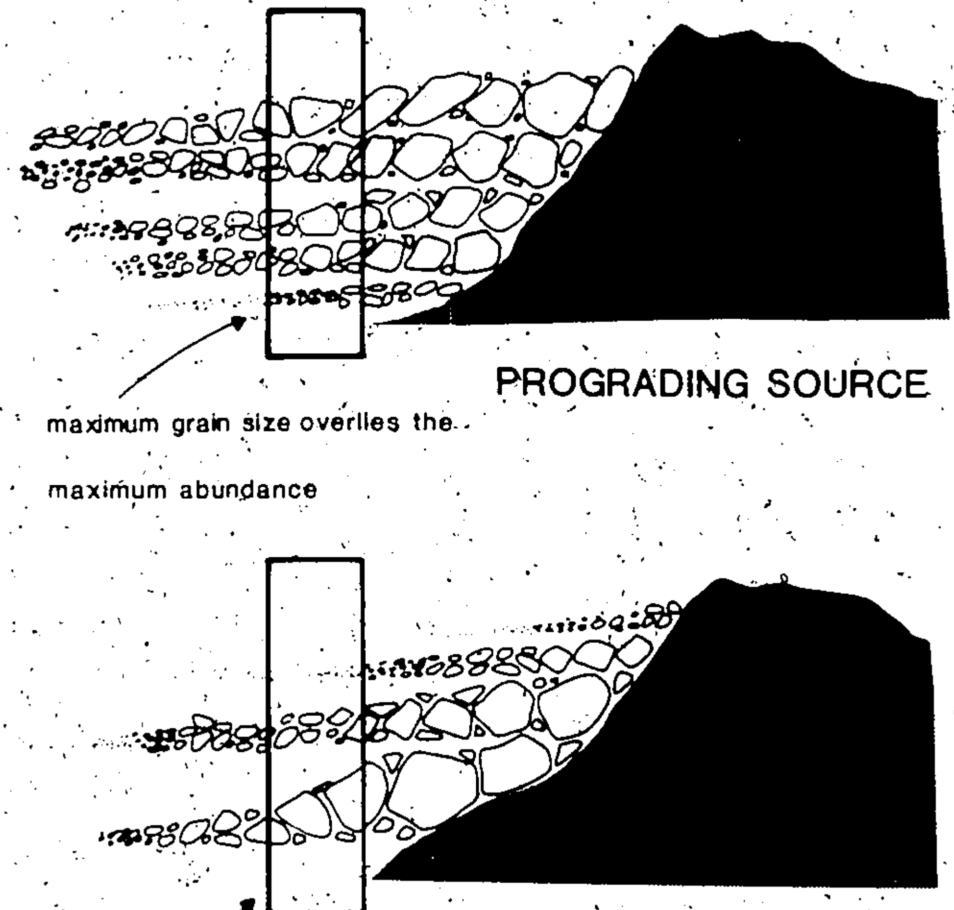

Fig.60

sandstones;phyllites) is more complicated. If abrasion were the only process effecting pebble morphology then there should be no downstream change in abundance. In fact, fracturing of some clasts along with the rapid disappearance of labile clasts tends to increase the downstream abundance resulting in a similar pattern to that seen in the fracture-prone clasts.

Application of these ideas to field examples shows consistent results. Fig.56 shows the moving grain size average for pebbles of the various lithotypes in section 03. Comparison between maximum (based on the mean 100) grain size and abundance peaks (Figs. 54,56) for similar siliciclastic lithotypes (i.e. quartzites and arenites) shows maximum peaks for the moving grain size stratigraphically overlying the maximum moving abundance peaks, indicative of a prograding sedimentary system. The same comparison for granitic lithotypes reveals the maximum moving abundance peaks stratigraphically overlying the maximum moving grain size peak, which reflects a retrograding system, possibly reflecting back-stepping of the granitic source. Syenitic and metamorphics lithotypes displayed no distinct relationships.

The predominance of siliciclastic rocks in the Caledonian Highlands along with the prograding nature of the siliciclastic lithotype component in section 03 implies that the first tectonic pulse was primarily effected by rejuvenation in the Caledonian Highlands. Granitic clasts imply a retrograding granitic source. The presence of granite plutons within the Caledonian and Cobequid Highlands along with no discernable difference in abundance between sections 01-03 and 04 did not allow the determination of provenance (discussed further in 9.6.1). In summary, the analysis of individual clast lithotypes in clastic wedges can not only provide useful information about overall tectonic trends, but in conjunction with knowledge of clast provenance, it can also reveal important information on the type and location of the tectonism.

8.8 Roundness

Most clasts from proximal and distal sections are rounded (Fig.61) with felsics being more angular than clastics (eg. 4.01 compared to 4.43). Overall vertical trends in roundness are not well marked, although lateral trends in the average roundness of specific clast lithotypes for each section can be discerned in laterally extensive cycles. Trends between sections 02 and 03 show distally increasing roundness (Fig.62) in all except syenitic clasts which have a minor decrease in section 02 (not shown). Lateral trends are most marked in proximal cycles (Fig.62, see cycle FII) where downstream increases in the subrounded subclasses are accompanied by decreases in the rounded and well rounded classes. The antithetic relationship between subrounded and well rounded subclasses are thought to be due to either

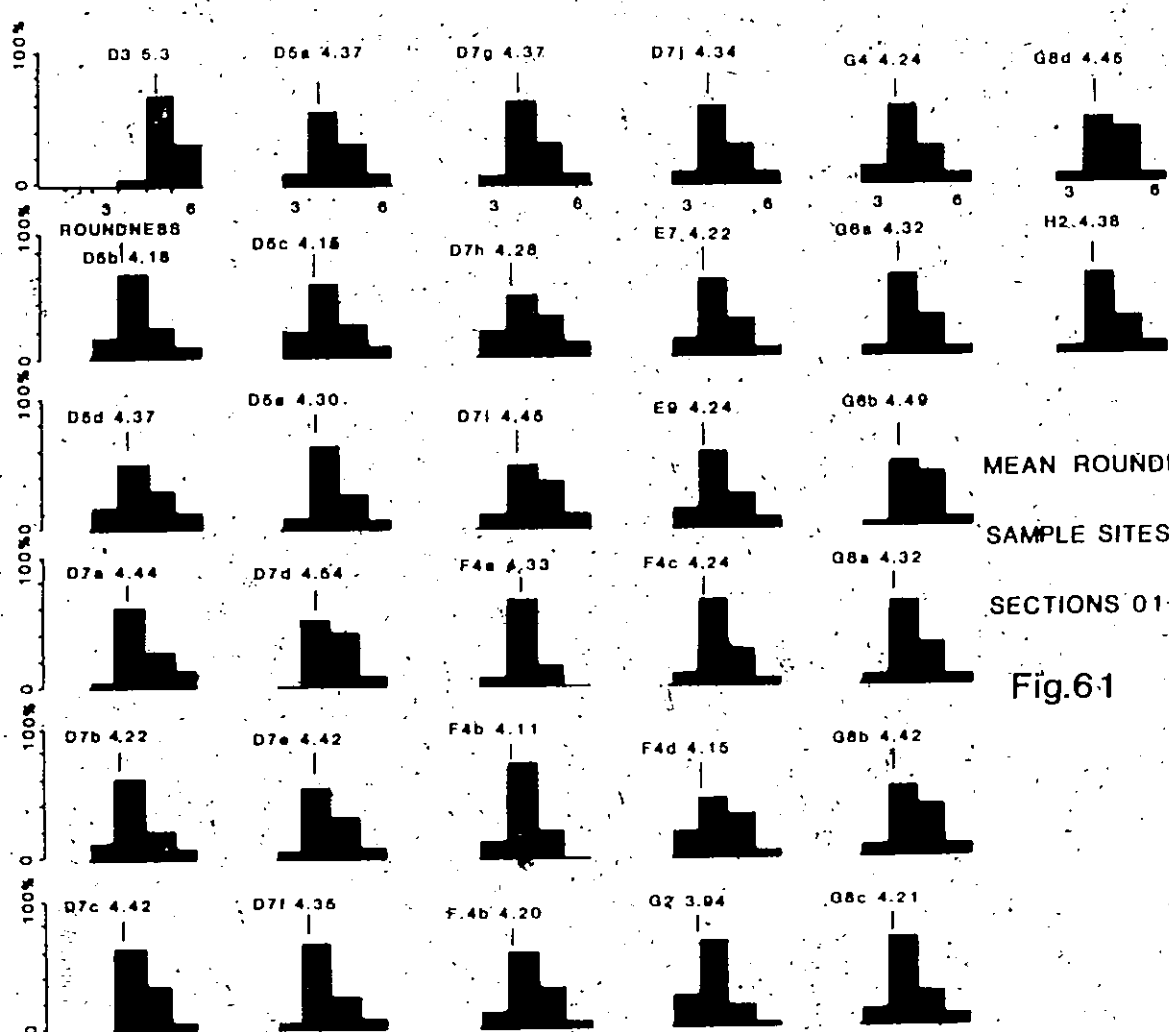

MEAN ROUNDNESS FOR SAMPLE SITES IN SECTIONS 01-03

Fig.61

Fig. 62

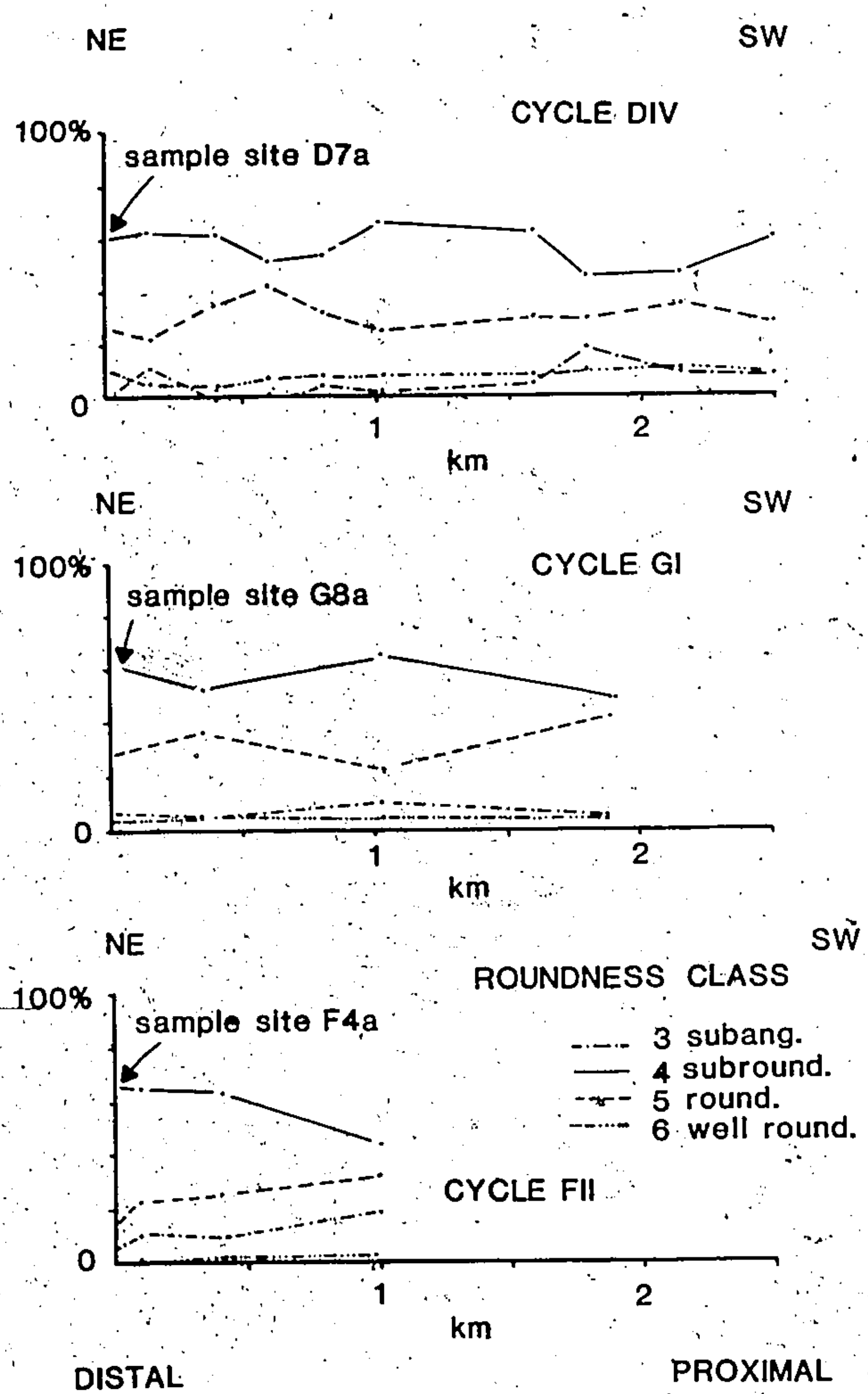
NE
SW
CYCLE DIV
100%
sample site D7a
0
1
2
km
NE
SW
CYCLE GI
100%
sample site G8a
0
1
2
km
NE
SW
ROUNDNESS CLASS
100%
sample site F4a
3 subang.
4 subround.
5 round.
6 well round.
CYCLE FII
0
1
2
km
DISTAL
PROXIMAL

operator inconsistencies in demarcating both class types, or a downsteam decrease in well rounded clasts lithotypes possibly due to fracturing. The latter is thought to be most probable since downstream decreases in sandstone clasts (the most rounded lithotypes) are noted in all three cycles shown in Fig.55.

Fig.63 plots roundness versus grain size for the various clast lithotypes. Results are typical of fluvial transport, and show that increased transport is marked by a diminution in size and increased rounding (Sneed and Folk, 1958). Examples from section 02 (DIII, DIV, Fig.63) show the same relationship except for the granite lithotype, which reveals a grain size decrease along with a roundness decrease. Pittman and Ovenshine (1968) described a similar situation with granitic clasts and attributed it to clasts attaining sufficient momentum by saltation during flood stage to permit fracturing upon collision, hence creating angular broken rounds. A similar mechanism is envisaged for the case reported here, and agrees with results found in section 8.7.1.

8.9 Petrography

Thirty eight stained thin sections of sandstones and conglomerate matrixes were examined to investigate provenance and lateral trends in mineralogy. The thin sections were stained for potassic and sodic feldspars using techniques

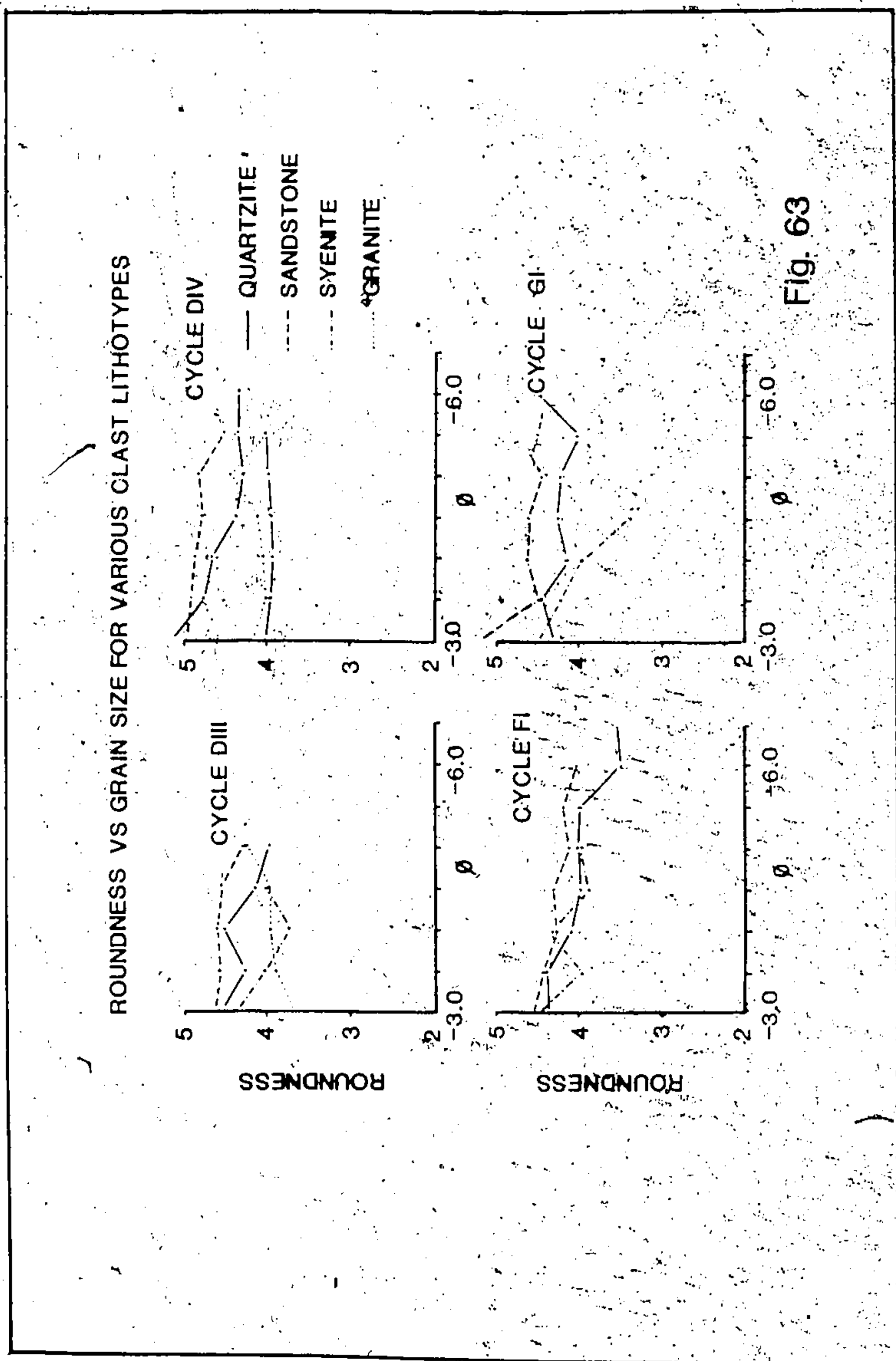
ROUNDNESS VS GRAIN SIZE FOR VARIOUS CLAST LITHOTYPES
CYCLE DIII
CYCLE DIV
CYCLE FI
CYCLE GI
QUARTZITE
SANDSTONE
SYENITE
GRANITE
ROUNDNESS
ROUNDNESS
ø
5
4
3
2
-3.0
-6.0

Fig. 63

described by Houghton (1980) and analysed using a Glagolev point count with a minimum of 300 counts per thin section. A total of thirteen categories were used to classify the samples: monocrystalline quartz (Q_{mcxl}); polycrystalline quartz (Q_{pcxl}); plagioclase (F_p); potassic feldspar (F_k); igneous rock fragments (IRF); type 1 sedimentary rock fragments (SRF 1); type 2 sedimentary rock fragments (SRF 2); type 1 metamorphic rock fragments (MRF 1); type 2 metamorphic rock fragments (MRF 2); heavy minerals (H); matrix (M); pore space (0) and carbonate cement (if any).

The various types of rock fragments were classified into the following categories based on the typical composition of an average thin section.

Igneous rock fragments can be subdivided into volcanic and plutonic types. Plutonic rock fragments are distinguished by common granophyric, micrographophyric, and perthitic textures. Composition of these IRF range from intermediate to silicic - quartz averaging 25%, sodic feldspars range from 10% to 60%, potassic feldspars from 10% to 30%, and 5% chlorite (i.e. altered mafics). Plutonics have rarely more than a few percent mafic minerals. Volcanic rock fragments are highly altered and are characterized by an almost isotropic felsic groundmass with acicular calcic plagioclase (based on staining) and possible acicular orthopyroxene phenocrysts. These are interpreted as intermediate volcanics.

Type 1 MRF are characterized by abundant micas (muscovite, biotite) which define a foliation and carbonaceous matter with minor aphanitic quartz and are interpreted as sericitic phyllites. Type 2 MRF are differentiated by the abundance of phaneritic foliated crenulate quartz with sutured contacts interspersed with crenulate potassic feldspars (up to 20%). Type 2 MRF are interpreted as quartzofeldspathic gneisses.

Type 1 SRF include quartz arenites, quartz wackes, intrabasinal clasts (determined from compacted outlines), siltstones, and laminated siltstones. Quartz arenites display very well sorted subrounded to subangular quartz and very minor (1% to 2%) SRF (which included sericitic siltstones and intraclasts). Other type 1 SRF fragments include quartz wackes which contain up to 10% matrix; mudstone rip-up clasts displaying poorly aligned clays, abundant organics (possible coal fragments), and muscovite flakes; siltstones with 20% authigenic clays displaying fair foliation and common organics; and laminated siltstones with intercalated very fine grain quartz and clay-rich laminae.

Type 2 SRF comprise various metasediments. Quartzites are the most common metasediment, typically having elongate crenulate quartz with minor sericite. Sericitic quartzites are also quite common, comprising almost entirely quartz framework components, with the percentage of authigenic clays varying from 5% to 30%. Sericitic siltstones/mudstones comprise 30% fine grain angular quartz and 70% foliated clay matrix, often displaying stylolites.

8.9.1 Results

The results of the point count studies can be seen in Appendix 16. The data were plotted according to McBride's (1963) classification where $Q = Q_{mcxl} + Q_{pcxl}$, $F = F_P + F_F$ and $URF = IRF + MRF + SRF$. If a sample plotted as a litharenite it was also plotted on a SRF-MRF-IRF diagram (Folk, 1968) in order to further classify the sample. Fine sand (<0.125mm), medium sand (0.5mm to 0.125mm) and coarse sand (>0.5mm) were plotted separately so as to avoid grain size effects (Ingersol, 1978; Korsch, 1984). Plots for sections 01-03 are shown in Fig.64 while the average for each section is found in Fig. 65.

Examination of the plots (Figs.64,65) reveals similar petrologies for sediments of the same grain size irrespective of the section. Coarse grained sediments are classified as litharenites (McBride, 1963), medium grained ones are litharenites bordering on feldspathic litharenites, while fine grained clastics are sublitharenties verging on lithic subarkoses. Plotting of litharenites on Folk's (1968) classification triangle shows all to fall in the sedarenite sector. Fig.65 shows a decreasing amount of unstable rock fragments (URF) with decreasing grain size - caused by a

Fig.64. Petrographic Classification.
Classification is as follows (see centre diagram):

1) litharenite
2) feldspathic litharenite
3) lithic arkose
4) arkose
5) lithic subarkose
6) sublitharenite
7) subarkose
8) quartzarenite

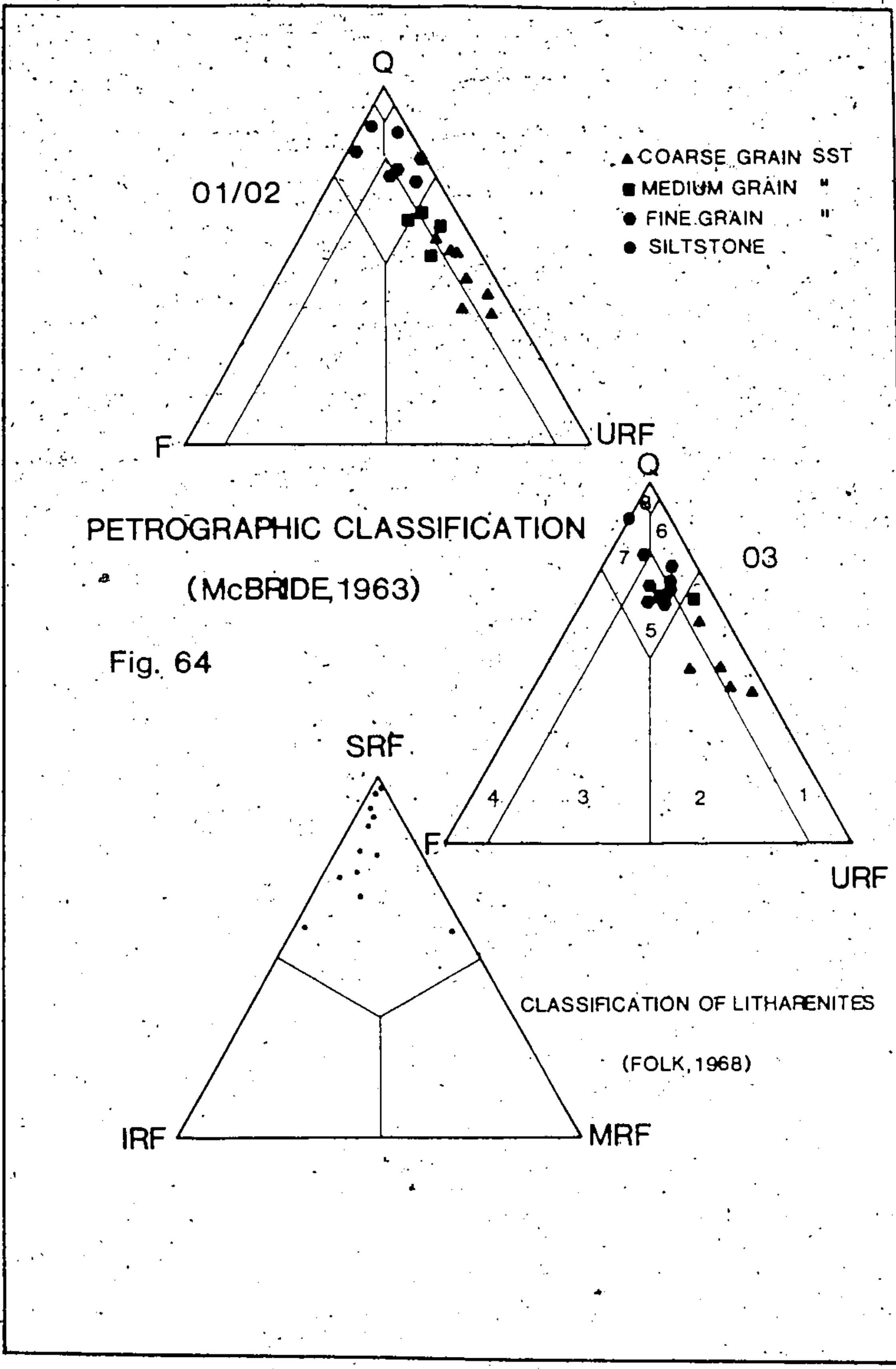

PETROGRAPHIC CLASSIFICATION

(McBRIDE, 1963)

Fig. 64

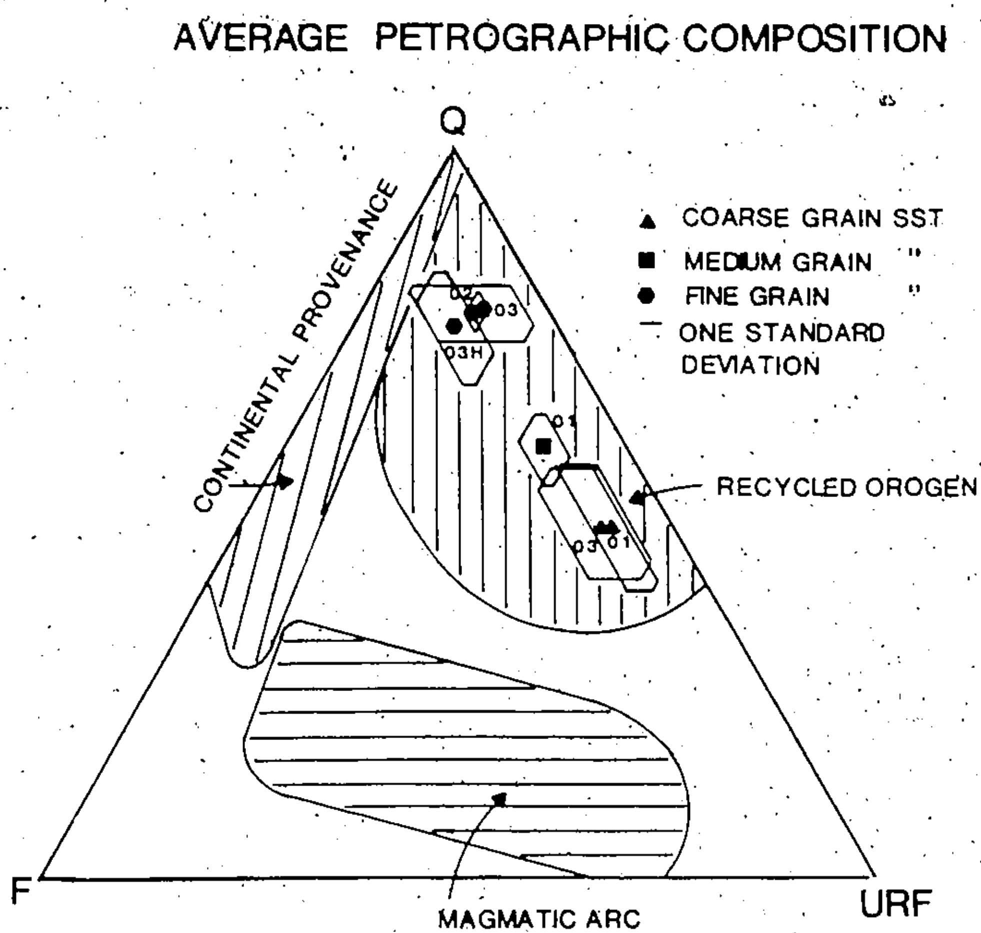

PROVENANCE FIELDS AFTER DICKENSON AND SUCZEK, 1979

Fig. 65

combination of lithic fragments (mostly arenites) fracturing into monocrystalline quartz (Q_{mcxl}) during transport and increased sorting in the finer grained units.

The predominance of sedarenites suggests provenance primarily from the Caledonian Highlands, whereas most of the felsics are thought to have originated from the Cobequid Highlands (discussed further in section 9.6.1). In many cases IRF can be specifically correlated with the uplifted Fountain Lake Group (discussed in 9.6.1).

Comparison of Fig.65 with Dickenson and Suscek's (1979) provenance fields (outlined in Fig.65) places the sediments within the recycled orogen field which is consistent with a foreland (or intermontane) basin interpretation for the Cumberland Group (Keppie, 1985; Bradley, 1982).

8.10 Summary of Clast Analysis

Clast analysis shows the following trends:

1) overall vertical grain size trends corroborate a two pulse origin for the sediments, which was previously envisaged from the facies associations.

2) lateral grain size trends show that clast diminution rates are typical of modern sandurs, presumably similar to non fluvio-glacial braidplain deposits. The trends indicate a source lying between 21km and 32km upstream.

3) vertical trends in sorting within proximal reaches are thought to be allocyclically controlled, while sorting in more distal gravelly deposits is regulated by downstream decreases in clast size and matrix proportions.

4) grain size analysis shows that coarse grained sediment (-3.25Ø to -6.75Ø) was transported primarily by traction.

5) downstream morphological changes in clasts are controlled by abrasion processes. Fracturing (due to collisions) is most common in felsic lithotypes, less common in quartzites, and rare in sandstones and phyllites.

6) Comparison of individual clast maxima for lithotype abundance and grain size shows provenance from prograding siliciclastic and retrograding felsic sources.

7) Roundness increases with increasing transport distance and with decreasing grain size - except with granites in the distal reaches, where roundness decreases with decreasing grain size due to fracturing of clasts.

8) the MPS is not a reliable trend indicator of detailed vertical and lateral changes in grain size within gravelly braidplain deposits.

Clast analysis shows a predominantly sedimentary and metasedimentary origin indicative of provenance from the Caledonian Highlands. Felsic clasts are less common than clastics and are thought to be primarily derived from the Cobequid Highlands.

Petrographic analysis of coarse grain sandstone and conglomerates (i.e. the sandy matrix) invariably classifies it as sedarenite. Decreases in grain size result in a decrease in unstable rock fragments and lead to a sublitharenite and lithic subarkose classification. Comparison of ternary QFL classification plots with Dickenson and Suscek's (1979) provenance fields suggests deposition in a recycled orogen, which is consistent with previous tectonic interpretations for the Cumberland Basin and findings in this study.

9.0 TRANSVERSE BRAIDPLAIN DEPOSITS (SECTION 04):

Section 04 is approximately 660m thick and is divided into six subsections I through to N. Subsections I and J (total 270m thick) are laterally equivalent to section 03 but differ markedly by comprising thin (<10m) distinct conglomeratic cycles capped by a unit of heterolithic facies assemblage - unlike the thick amalgamated allocycles seen in section 03. Paleocurrents suggest a northeasterly flow which also differs from the southeasterly paleocurrents from section 03. Clast analysis implies a predominant Cobequid Highland source, unlike the Caledonian source seen in section 03. Subsections I,J are interpreted as deposits of a tributary to a major trunk river in which the strata of sections 01-03 accumulated. Subsections K,L (total thickness 229m) underlie sections I,J, decrease downward in average grain size and have thicker fine members. Subsection N (140m thick) is characterized by poorly sorted horizontally stratified conglomerates, minor matrix-supported conglomerates and is interpreted as alluvial fan deposits. The overlying mudstones belonging to subsection M (20m thick) are interpreted as deposits of adjacent wetlands (lacustrine?).

9.1 Facies Associations: Introduction

Lithofacies from section 04 are the same as those found in the previous three sections and hence will not be redescribed, rather, percentages and average thicknesses for subsections IJ, KL, NM are tabulated in Table 10.

9.1.1 Heterolithic Facies Association (Subsections I-M)

The heterolithic facies association comprises intercalated mudstone (Fm, Fl, Fr) and sandstone lithofacies (Sm, Sr, Sh). Units of the heterolithic association most often overlie fining-up coarse members and range in thickness from 0.4m to 10.7m. Average thickness for each subsection is tabulated in Table 11. The percentage of fine members constituting complete cycles increases stratigraphically downward from 25.1% in subsection I to 50% in subsection K (see Table 11). The percentage of mudstone lithofacies in the heterolithic facies association also increases stratigraphically downward from 56.2% in subsection I to 82.2% in subsection L (Table 11). The moving average percentage of the fine member is plotted in Fig.66.

Mudstones are the major component of the heterolithic facies association with Fm being the most common (see the moving average of Fm, Fig.66). The percentage of Fm increases from 10.3% (subsection I) to 31% (subsection M not shown in Fig.66), with red Fm being most common (13.7%) in subsections K,L. Subsection M has exclusively grey Fm while subsections I,J contain almost three times the amount of grey Fm compared to red Fm. The predominance of grey Fm in subsections I,J,M suggests that higher water tables did not allow oxidation of

TABLE 10: AVERAGE THICKNESS AND ABUNDANCE OF LITHOFACIES IN SECTION 04

MUDSTONES:	PERCENTAGE			MEAN THICKNESS(m)		
	IJ	KL	M	IJ	KL	M
Fm(total)	10.3	20.8	31.0	0.42	0.95	-
Fm(m)	-	3.0	-	-	2.05	-
Fm(g)	7.5	4.1	31.0	0.42	0.48	0,69
Fm(r)	2.8	13.7	-	0.41	1.16	-
Fl	5.0	1.4	2.4	0.60	1.53	0.60
Fr	3.3	4.5	43.0	1.14	1.32	1.23

SANDSTONES:	IJ	KL	N	IJ	KL	N
Sm	9.0	6.3	7.5	0.55	0.63	-
Sr	9.8	5.4	1.5	0.75	0.68	-
Sh(l)	1.5	2.0	-	0.63	0.62	-
Sh(u)	1.5	7.8	1.5	0.82	1.41	-
St	6.9	34.8	36.7	1.25	3.15	-
St/St(c)	6.8	4.2	-	1,63	1,67	-

CONGLOMERATES:	IJ	KL	N	IJ	KL	N
Gt	20.3	5.3	-	2.79	3.6	-
Gm	12.7	7.3	88.4	1.59	-	10.2
Gms	-	-	1.9	-	-	1.3
Gt/Gm	9.3	6.6	-	3.04	2.2	-

Fm(m) = mottled Fm
Fm(g) = grey Fm
Fm(r) = red Fm

TABLE 11: AVERAGE THICKNESS AND ABUNDANCE FOR THE FINE AND COARSE MEMBERS OF SECTION 04

SECTION I

	CM	FM	TOTAL	HFA	
				MDSTN%	SST%
THICKNESS(m):	6.89	2.31	9.20		
PERCENTAGE:	74.9	25.1		56.2	43.8

SECTION J

THICKNESS(m):	3.79	1.82	5.26		
PERCENTAGE:	65.4	34.6		74.7	25.3

SECTION K

THICKNESS(m):	3.60	3.60	7.30		
PERCENTAGE:	50.7	49.3		74.3	25.7

SECTION L

THICKNESS(m):	8.1	3.6	11.3		
PERCENTAGE:	68.1	31.9		82.2	17.9

CM = coarse member
FM = fine member
HFA = heterolithic facies assemblage

generalized stratigraphic section
for detailed section see App 6 7

Legend in App 2

for location see Fig 1

SECTION 04

Fig. 66

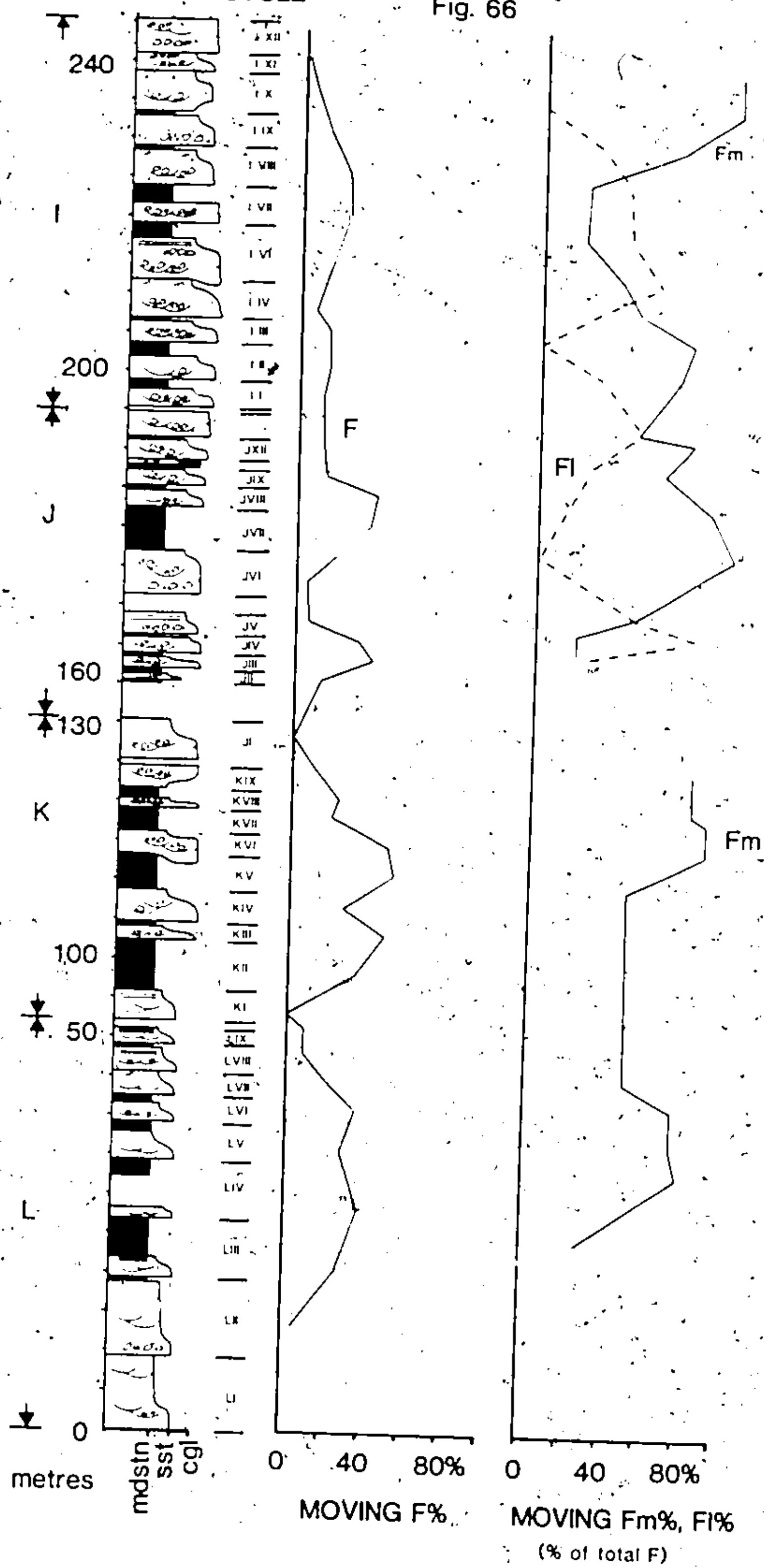

the mudstones. This is also corroborated by the thin coal seam (4.0cm) present in cycle JII and the three coal seams in subsection M, indicative of reducing conditions.

Rooted mudstones (Fr) become increasingly common downsection from 3.3% to 43.0%. Downsection increases in: total percentage of mudstones (F%), Fm, Fr, thickness and percentage of fine member, demonstrate an upsection decrease in floodplain deposition due to increasing proximality to the source and/or more rapid braid tract migration. The marked increase in Fl within subsections I,J also concurs with the proposal that mudstone deposition (tractive) often occurred within abandoned channels (or low order channels) rather than from suspension on adjacent floodplains (eg. Fm). The moving percentage Fm and Fl is plotted in Fig.66 and shows an antithetic relationship throughout subsections I,J (i.e. antithesis between suspension and traction influenced deposition).

Fine members mostly have sharp bases and scoured tops, although gradational bases are much more common than in sections 01-03, especially in subsections I,J. Heterolithic assemblage units are laterally persistent like those from sections 01-03 and in most cases fine-upward.

Lateral facies relationships between mudstone and sandstone beds are commonly gradational within subsections I,J, unlike sections 01-03. The gradational nature is most

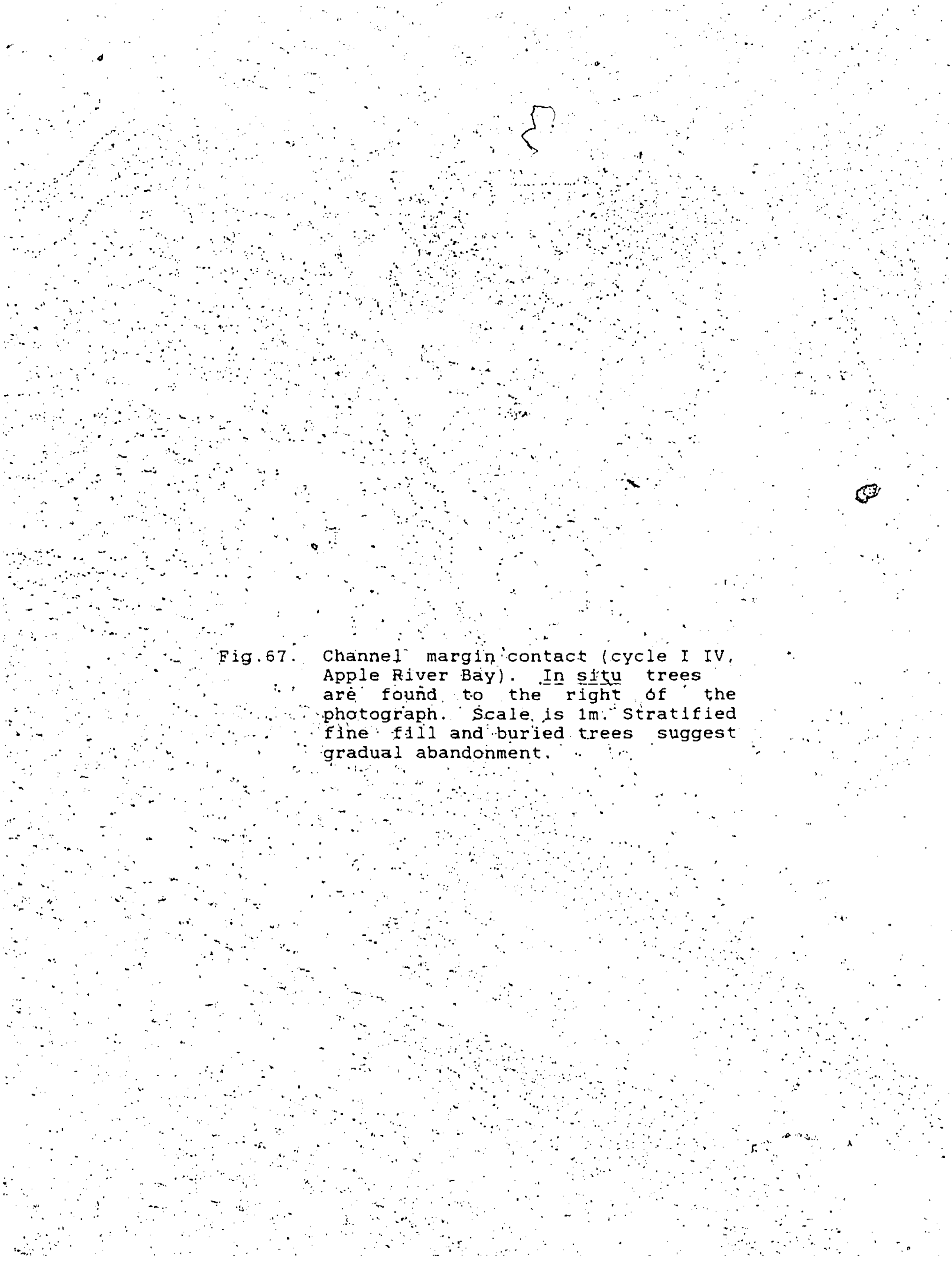

Fig.67. Channel margin contact (cycle I IV, Apple River Bay). *In situ* trees are found to the right of the photograph. Scale is 1m. Stratified fine fill and buried trees suggest gradual abandonment.

marked at the channel margins (Fig.67) where laminated (and rippled) Fl grades into rooted mudstones (Fr) which frequently display in situ trees (Calamites, Sigillaria) up to 1.5m tall. Channel margin heterolithic units thin towards the abandoned channel (possibly enhanced by differential compaction, Fig.67) and are interpreted as subdued levees. Vertical and lateral gradational contacts between fine and coarse members are not displayed by subsections K,L and closely resemble those from section 01.

9.1.2 Summary:

1) Units of the heterolithic facies association in section 04 commonly display gradational vertical and lateral contacts with the coarse member, unlike the sharp contacts seen in sections 01-03.

2) Fine member abundance and thickness increases downsection.

3) Predominance of grey Fm in subsections I,J,M suggests higher water tables and is corroborated by the presence of thin coal seams.

4) Upsection decrease in Fr and increase in Fl implies a decrease in floodplain deposition and a change in channel-switching style from avulsion into gradual channel abandonment.

9.1.3 Sandstone and Conglomerate Facies Associations (Subsections I - L)

Coarse members comprise sandstone and conglomeratic lithofacies, the latter becoming more prevalent upsection (from 13.3% to 42.3%). The average thickness of coarse member units (and coarse member percentage of each cycle) for each subsection shows a steady downward decrease from I to K

(6.89m to 3.60m, Table 11) and a marked increase in L (8.1m). The moving average for G and S type lithofacies is plotted in Fig.68 and shows four major peaks (labelled one through four). Peaks 1 and 3 are thought to be equivalent to the first and second tectonic pulses seen in sections 01-03. These peaks can also be detected in moving grain size curves (discussed in 9.5).

Coarse members in subsections I,J are composed primarily of conglomeratic lithofacies with Gt, Gm and Gt/Gm being the most common (Table 10). Gm is found predominantly in subsection J and decreases upwards into subsection I, as Gt increases concurrently upwards with its maximum lying in subsection J, and therefrom decreases upwards into subsection I (Fig.68). The change in lithofacies from Gm to Gt is attributed to deposition within deeper channels which allowed the formation of gravelly dunes (Hein and Walker,1977). Sandstone lithofacies are a minor constituent, with St being the most common, comprising 13.7% of the measured subsections (Table 10), and commonly capping coarse members. Sr makes up 9.8% of measured subsections and is commonly found at the base and tops of coarse members. Sr units at the top of coarse members have sharp upper and lower surfaces, although upper gradational contacts into Fl are quite common. Sr units at the base have sharp lower contacts and sharp, often scoured upper contacts.

Coarse members from subsections K,L differ from the

Generalized stratigraphic section
for detailed section see App. 6.2
Legend in App. 2
for location see Fig. 1

SECTION 04

Fig. 68

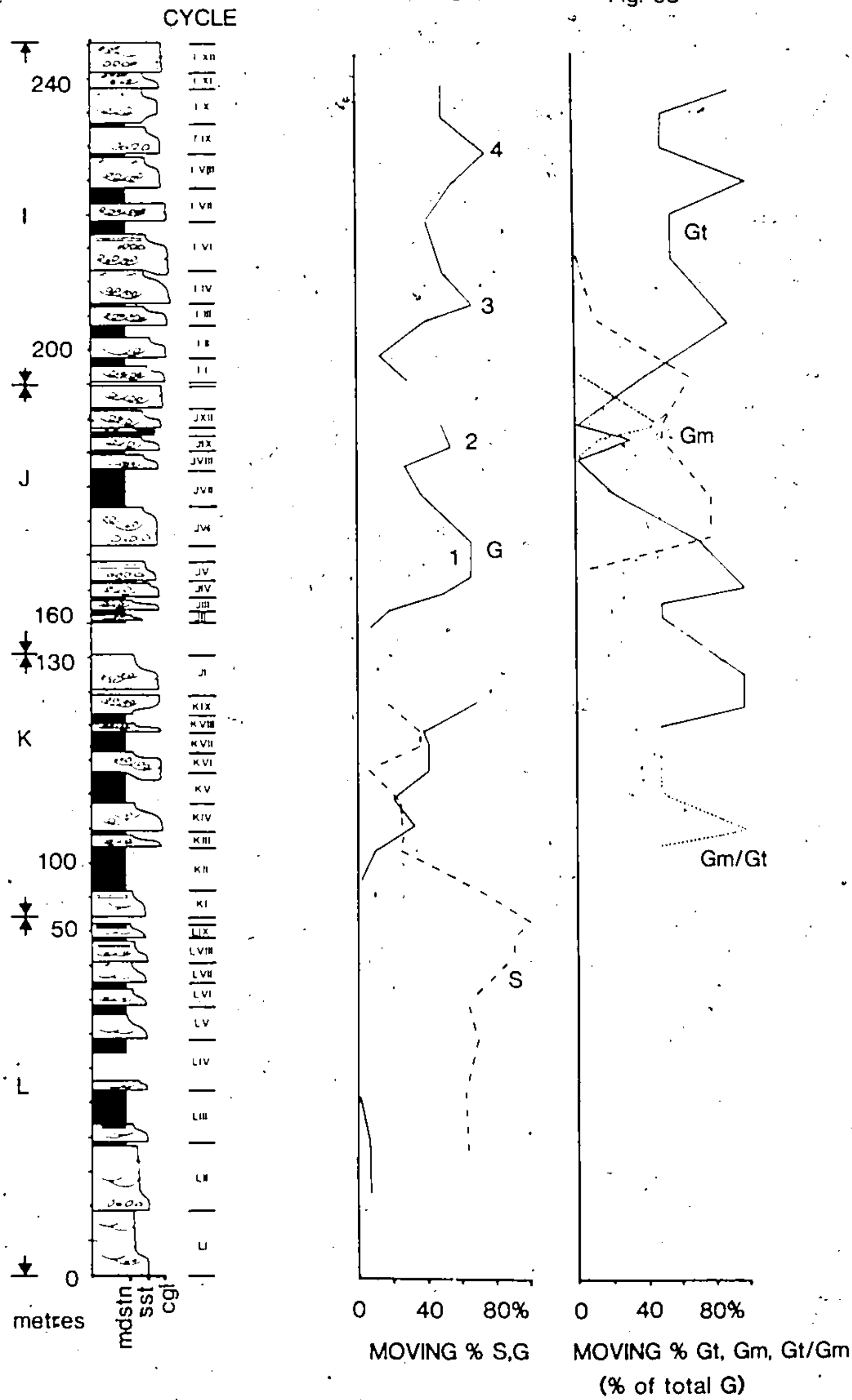

overlying subsections by mainly comprising sandstone lithofacies, with conglomeratic lithofacies becoming more abundant upsection. St is the most common facies making up 39.0% of the measured sections. Coarse members are commonly capped by an Sh(u) unit (58.3% of cases, averaging 0.63m thick) and rarely by Sr.

Units of sandstone and conglomeratic facies associations from subsections I - L, although not laterally traceable for any great distances, show similar characteristics. Coarse members are sheet-like, sharp- or erosively-based and FU in most cases (50% to 77.8% of cycles display FU). CUFU-type cycles such as those previously seen from section 01 are quite prevalent in section 04, with 40% of cycles in subsection I displaying this property. The abundance of identifiable leveed channel margins (with in situ trees) in subsection I, along with the highest percentage of CUFU-type cycles within section 04 supports an origin as either a crevasse-splay (or sheet-splay , Galloway,1981); or by vertical accretion of channel sands onto channel margins during channel abandonment for the formation of the CU part of the sequence. The sharp lower contact of some units implies a sudden event which lends support to a crevasse/sheet-splay origin (Cross and Smith,1985) whereas examples with in situ trees, gradational bases and laminated mudstones connote a vertically accreting origin. In summary, both processes may be responsible for CUFU-type cycles since flood stage could conceivably break a levee (or overflow its banks) and create a new braid tract (discussed in 7.4); while rapid subsidence rates could induce quick vertical aggradation and onlapping of channel sands onto channel margins. Cycles from subsection L differ from I,J,K not only in lithotype but also by the presence of amalgamated cycles (25% displaying this property), something not seen in the overlying cycles. The lack of amalgamated cycles in the upper subsections may be due to: i) subsidence rates exceeding sedimentation rates and/or; ii) lateral braid belt migration which allowed sufficient residence time before the returning braid tract occupied the original position, thus creating a multistorey geometry.

9.1.4 Conglomeratic Facies Association (Subsection N)

Subsection N lies with angular unconformity (a discrepancy of 11^{o}) on the underlying Fountain Lake Group (undifferentiated volcanics). The section is approximately 100-140m thick but the presence of several faults did not allow precise determination of thickness. Work on this section was further hampered by constantly falling blocks, hence detailed work was not carried out on the cliff section.

Subsection N coarsens-upward and comprises poorly sorted (angular) matrix-supported pebbly conglomerates (Gms) at the contact, passing upward into poorly sorted (angular) pebbly matrix-supported Gm (Fig.69). Cycles are sheet-like with sharp non-erosional bases, commonly FU in the lower part of

Fig.69. Poorly sorted pebbly matrix-supported Gm, 300m north of Squally Point.

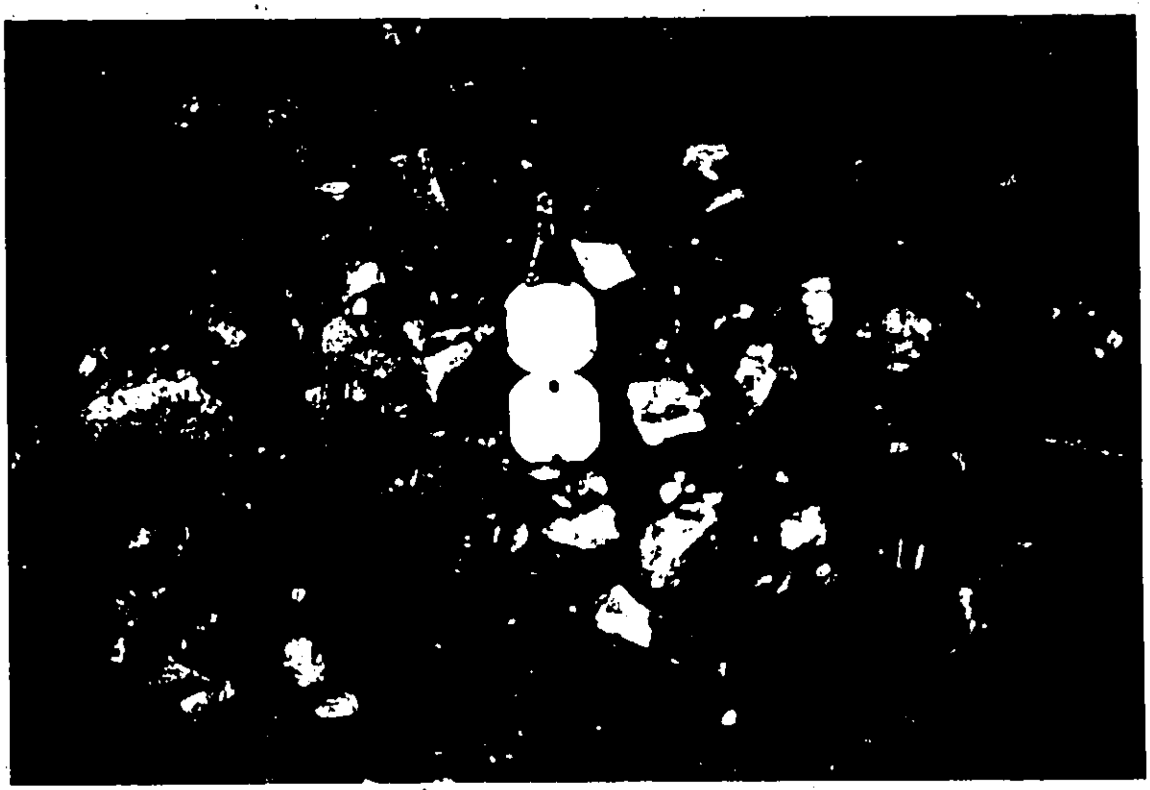

the section and CU (or CUFU) towards the top. Cycles range in thickness between 3m to 10m at the base and thicken upwards to a maximum of 25m (Fig.70). Most cycles comprise only one lithofacies (Gm) and FU only in the upper decimetres where they are sharply overlain by an unit of red Fm ranging in size between 0.10m to 6.0m. Beds within cycles average 0.56m in thickness (n=26, s=0.24m) and commonly do not show any grading (50% of cases); less commonly normal to inverse (19.2%) and inverse grading (15.4%); and rarely show normal (7.7%) and inverse to normal grading (3.8%). Many cycles near the top of the sequence are interspersed with thin (<1m thick) discontinuous lensoid sandstone beds.

Although not intensely studied, the moderately developed imbrication (discussed in section 9.4), commonly ungraded beds, overall poorly defined FU nature of cycles and high proportion of pebbly matrix suggest either deposition by ephemeral tractive currents or emplacement by surging fluidal sediment flows (Nemec and Steel, 1984). However, further detailed studies are needed to distinguish the exact mode of emplacement. The change in architecture from FU to CU cycles, and upward thickening of cycles is attributed to progradation of alluvial fans from the uplifted Cobequid Highlands (Heward,1978; Rust and Koster,1984). Deposits from this subsection are interpreted as distal alluvial deposits.

9.1.5 Summary:

1) Conglomeratic lithofacies increase upsection (from

Fig.70. Thickening and coarsening-upward cycles in subsection N (500m north of Squally Point). Foliation surfaces dip to the right while bedding dips to the left. Foliation is caused by late stage Maritime Disturbance folding. Contact with Fountain Lake Group is 500m to the right.

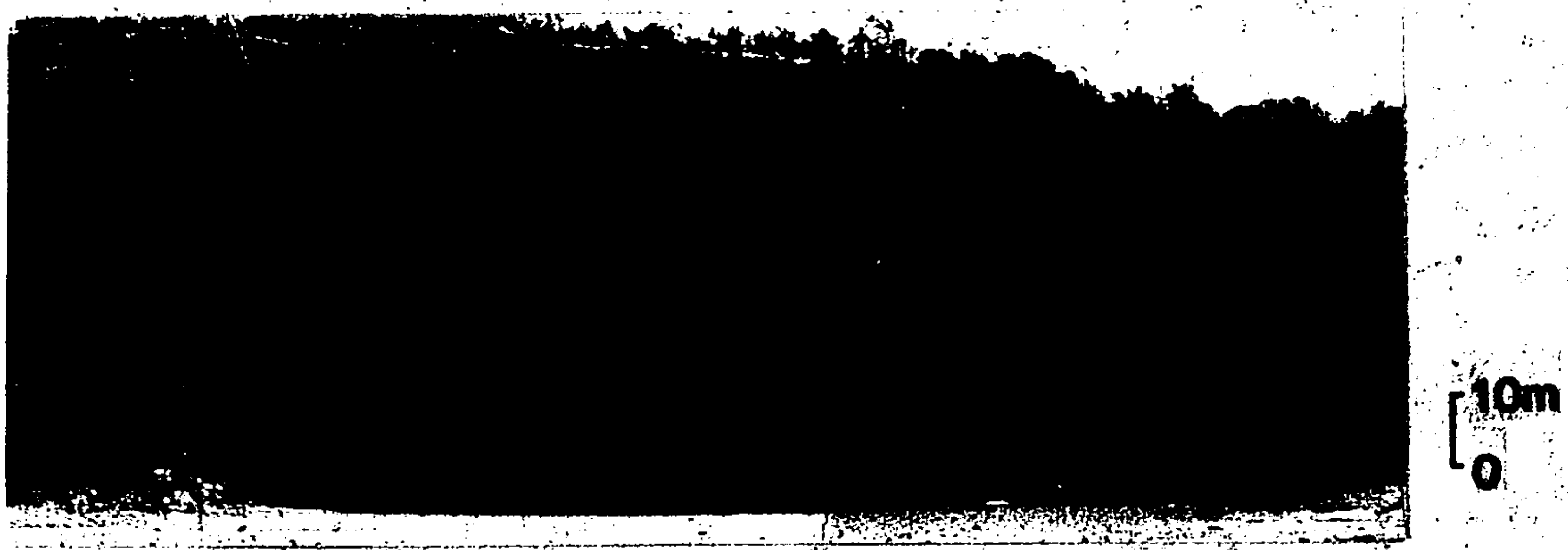

Fig. 70 Thickening and CU cycles in subsection N (500m south of Squally Point).

subsection L).

2) Coarse member thickness increases upsection (from subsection K).

3) Four major peaks in the abundance of the conglomeratic facies can be discerned, two of which can be correlated with the first and second tectonic pulse,

4) Compared to sections 01-03, coarse members are thin sharp-based and FU in most cases, although CUFU cycles become increasingly common upsection.

5) CUFU cycles are attributed to either avulsion into adjacent wetlands followed by channel migration and abandonment, or vertical accretion within an abandoned channel followed by channel migration and abandonment.

6) Subdued leveed margins are common in subsection I.

7) Subsection N was deposited by prograding alluvial fans.

9.2 Bedding Thickness Patterns (Section 04)

Bedding thicknesses for section 04 were analysed using the same procedure outlined in section 4.2. Results are tabulated in Table 12 and shown in Fig 71.

Comparison of sandstone cumulative bedding thickness plots between section 03 and 04 (Figs.29 and 71) show them to have almost identical slopes (m=0.730 and m=0.721), differing only in y intercepts. Parallelism between best fit lines was attributed, in section 4.3, to similar mechanisms controlling deposition. Similar best fit slopes found between all three study areas (i.e. sections 01/02, 03, and 04) imply that the same control was in existence throughout this part of the

TABLE 12: BEDDING CHARACTERISTICS (SECTION 04, SUBSECTIONS I,J,K)

Graphic Measures:

SST	M(m):	0.77	MDSTN M(m):	0.43
	SI(m):	0.003	SI:	0.002
	D%:	0.4%	D%:	0.5%
	S_K:	0.109	S_K:	0.258
	K:	0.590	K:	0.615

Arithmetic Measures:

X(m):	1.21	X(m):	1.52
S_D (m):	1.27	S_D (m):	1.18
N:	165	N:	48
D%:	105.0	D%:	77.6

Abbreviations shown in Table 4

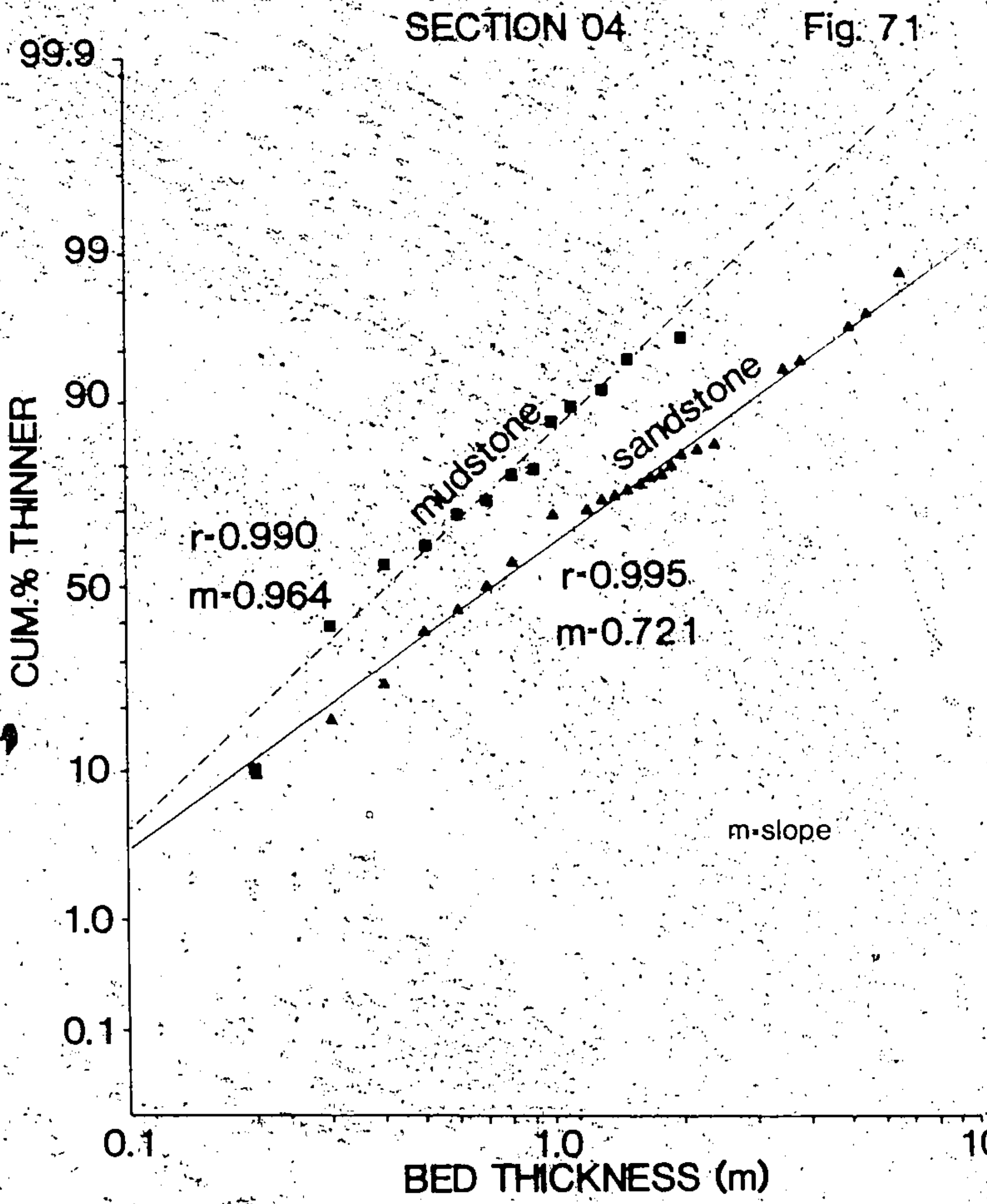

SECTION 04
Fig. 71
99.9
99
90
50
10
1.0
0.1
CUM.% THINNER
mudstone
sandstone
r-0.990
m-0.964
r-0.995
m-0.721
m-slope
0.1
1.0
10
BED THICKNESS (m)

basin. The relatively small distance between these sections also suggests that differential subsidence was unlikely.The difference in fluvial architectural style between cycles from sections 01-03 and 04 denotes predominance of either autocyclic or allocyclic controls. By arguments put forward in sections 6.2, 4.3, and 9.1.3 allocyclicity is envisioned as the dominating influence throughout the study area. Allocyclicity may be of climatic or tectonic origin (Beerbower,1964). The latter can be in response to subsidence- or sedimentation rates, and is thought to be the major factor delineating fluvial style in this study, for the following reasons: i) similar slopes for sandstone cumulative bed thickness plots suggests a similar dominating control (see section 4.3), most likely subsidence rates; ii) since studied sections have similar subsidence rates, the difference in architectural style between cycles in section 03 and 04 must be be due to differing sedimentation rates.

Statistical parameters from Table 12 show that section 04 has thinner mean graphic and arithmetic bedding thicknesses than section 01-03. The positively skewed bed thickness relationship of the sandstones (i.e. conglomeratic and sandstone beds) is attributed to a lack of thin beds, possibly due to preservation of only flood-generated deposits. The thickness of the mudstone beds also display a moderate positive skewness, indicating an excess of thick beds, which (compared to mudstones from sections 01-03) signifies that the interval between avulsion and relocation of the floodplain upon the previous site was the longest (Bridge, 1984) of the four sections. The dispersive index and kurtosis do not permit differences to be distinguished between sections 01-03 and 04.

9.3 Preferred Facies Transitions (Section 04)

Preferred facies transitions for the coarse and fine members were calculated using techniques described in section 5.2. Subsections I,J,K were included in the calculations, subsection L was excluded due to major lithological and architectural differences (see App.7).

Results for the coarse member (Fig.72) show that the vertical succession was derived by a non-random process (X^2=94.6, d.f.=71) significant at the 0.95 level. Significant transitions using the calculated binomial cell values show one preferred facies transition: F -> Se -> Gt -> Gm -> St(m) -> Sh -> F (P_T=2.96*10^{-4}). This concurs with field observations from subsections I,J,K, (App.7) and indicates gradual channel abandonment and vertical accretion rather than avulsion for the following reasons: i) well-developed FU sequences; ii) gradational contacts rather than sharp ones between coarse and fine members; iii) an upward decrease in channel depth as shown by the facies sequence, is more likely from vertical accretion and channel abandonment than avulsion.

Units of the heterolithic facies associations in section

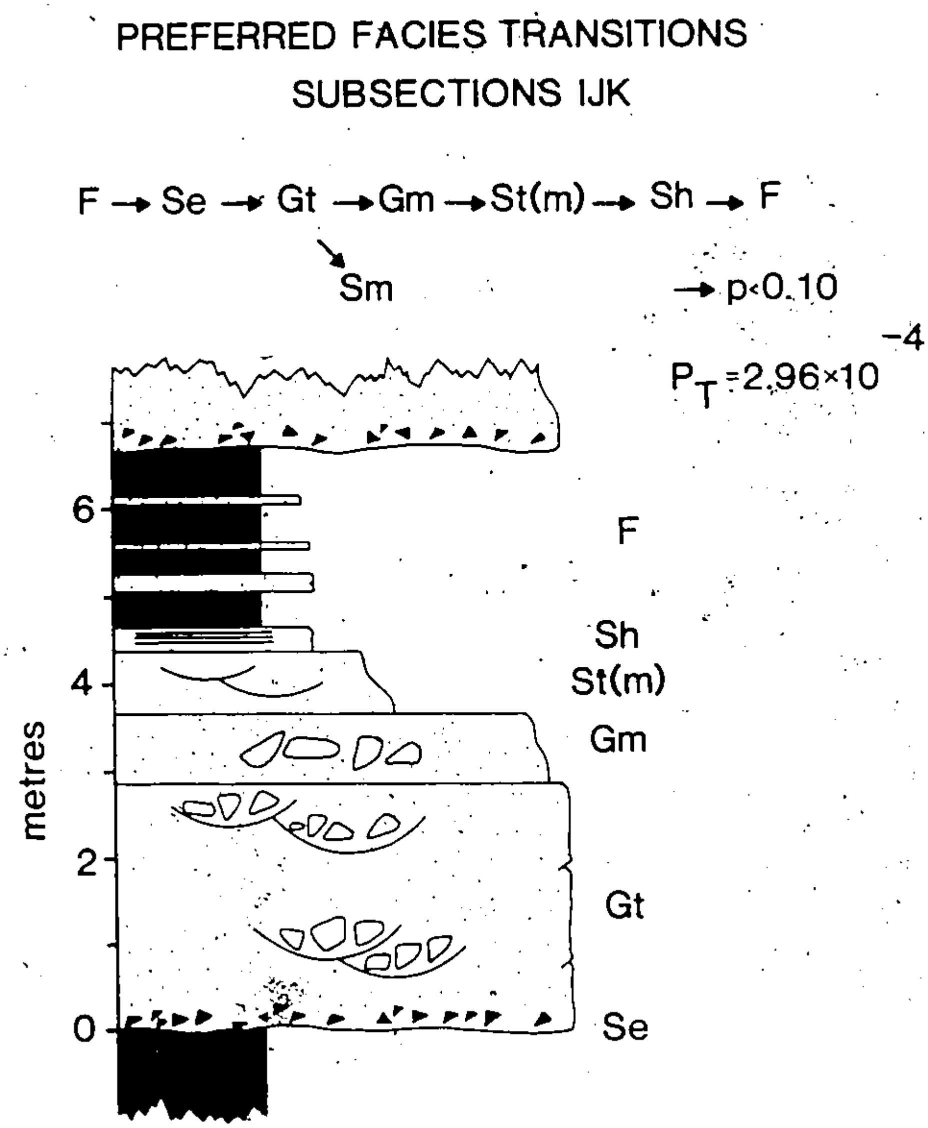
PREFERRED FACIES TRANSITIONS
SUBSECTIONS IJK
F → Se → Gt → Gm → St(m) → Sh → F
Sm
→ p<0.10
$P_T = 2.96 \times 10^{-4}$
metres
0
2
4
6
F
Sh
St(m)
Gm
Gt
Se

Fig. 72

04 show a more complex suite of preferred sequences than in sections 01-03 (Fig.73). Chi-square testing proved the matrix to be non-random (X^2=115.3, d.f.=55) and significant at the 0.995 level. Six statistically significant (at α <0.20) preferred sequences were established and are herewith listed:

1) coarse member (CM) -> grey Fm -> Sm -> grey Fm -> CM
2) CM -> grey Fm -> Sm -> Fr -> mottled Fm -> CM
3) CM -> Fr -> mottled Fm -> CM
4) CM -> grey Fm -> Sm -> red Fm -> Sr -> Fl -> CM
5) CM -> grey Fm -> Sm -> red Fm -> Sr or Sh -> red Fm -> CM
6) CM -> grey Fm -> Sm -> red Fm -> CM

The presence of numerous preferred sequences can be explained by understanding lateral relationships within the heterolithic facies association. Each preferred sequence represents a vertical profile through a section of the fine member, and hence compilation of enough preferred sequences would ideally give a good cross sectional generalization of subenvironments within the fine member. In this case (Fig.73) sequence 1 represents primarily mudstone deposition within an abandoned channel, with occasional deposition of overbank sandstones (Sm), now root turbated . The lack of red mudstones in this part of the channel is attributed to high water tables, along with proximity to the braid belt (towards the left of Fig.73), which did not allow oxidation of mudstones (Rust et al., 1984). Preferred sequence 2 is envisioned to lie closer to the old abandoned channel margin,

PREFERRED FACIES TRANSITIONS THROUGH AN ABANDONED CHANNEL

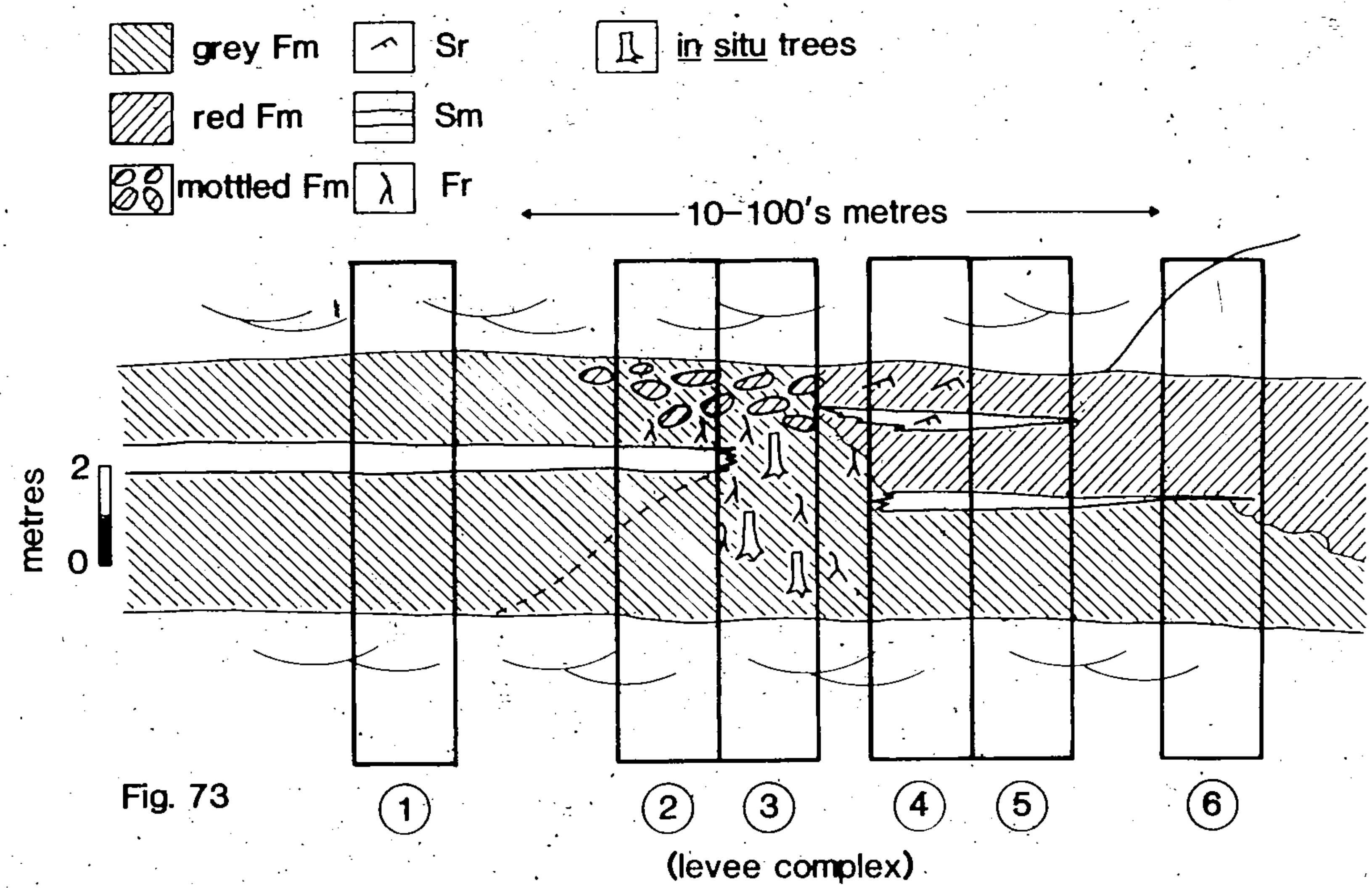

Fig. 73

and differs from the previous one by having a capping sequence of Fr and mottled Fm. Sequence 3 is interpreted as the channel margin, possibly a subdued levee complex (eg. Boothroyd and Nummedal,1978; Fig.13a). In situ trees along with abundant rooting and overlying mottled mudstones suggests better drained soils, possibly due to elevation above the water table. As the preferred sequences progress away from the old channel margin red mudstones begin to dominate the upper sequence, due to lower water tables, distance from the braid belt; and/or a tilted water table (B.R. Rust pers. comm.,1985). Sequences closer to the active channel margin (eg. 4,5) commonly have thin sheet-splay sandstones which thin away from the channel margin (i.e. 6). Further refinement of this model, with the aid of drill core could be used in exploring for possible economic coal seams within this succession.

9.4 Paleocurrents (Section 04):

Paleocurrent data were processed in the same manner outlined in section 7.3. Unfortunately, the lack of lateral exposure of cycles did not allow as many readings as in the previous sections, hence detailed comparisons of intrachannel trends were not possible. Raw data are tabulated in Appendix 11 and calculations are shown in Appendix 12.

Intrachannel dispersion can be analysed by examining the vector strength (L%) in Appendix 12 or Fig.74, and shows a

generalized stratigraphic section
for detailed section see App. 6.7
Legend in App. 2
for location see Fig. 1

SECTION 04

Fig. 74

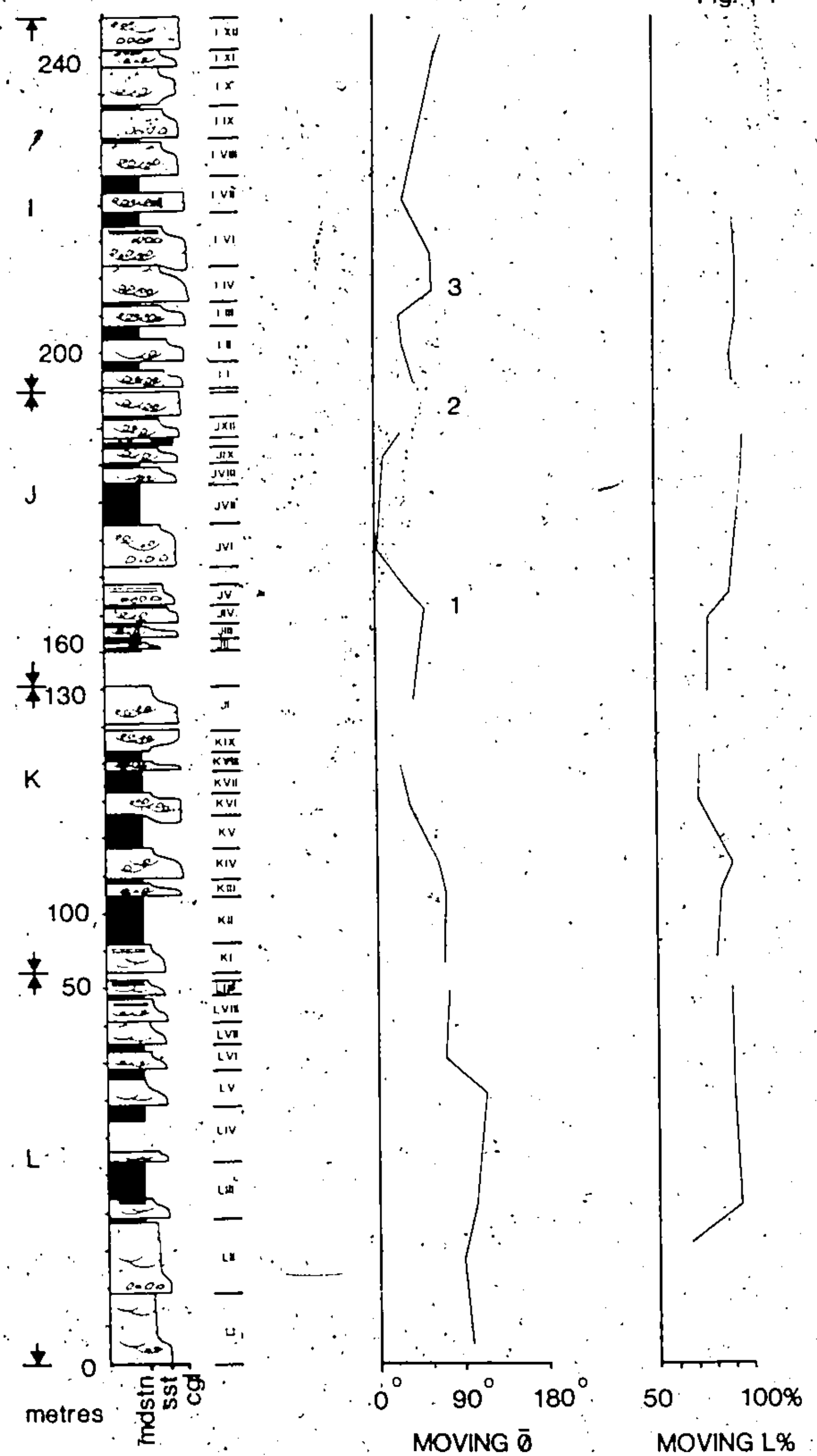

minor upward increase (i.e. a decrease in dispersion) from subsection K to I which may be due to a small sample or an increase in paleoslope. Dispersion between St, Gm and Gt lithofacies was compared (using Mardia's F-test,1972) in subsection I and showed a significant difference at α =0.05 between Gt-St (n=11) and Gt-Gm (n=10). Paleocurrent differences between lithofacies are attributed to deposition within various energy level subenvironments; large rivers with high discharge rates, such as those inferred from sections 01-03, would tend to suppress dispersion between lithofacies whereas smaller rivers with lower discharges would induce dispersion (unless valley confined).

There are insufficient data to allow statistical testing of interchannel variations as in section 7.5 but some trends are apparent. The moving paleocurrent average (Fig.74) reveals a general northerly deflection (with minor sinusoidal deflections) from subsection L to cycle JVI, then becoming increasingly easterly upsection. A linear regression analysis on the stratigraphic height versus the moving paleocurrent for the lower half of section 04 (up to cycle JVI) shows a rate of change of 0.369°/m (r=0.848), with a maximum deflection of 112.5°. Similar analysis on the upper half (above cycle JVI) shows a southerly increase in paleocurrents at the rate of 0.452°/m (r=0.856), maximum deviation being 71.2°. Such large correlatable paleocurrent change implies allocyclic controls, in this case probably due to tectonic tilting of the alluvial plain and lower sedimentation rates than section 03 (see discussion in section 7.5). It should also be noted that correlatable northerly shifts in paleocurrents were also found in all three sections discussed in section 7.5 and were attributed to the second tectonic pulse. Northerly shifts in paleocurrents seen in sections 01-03 lie stratigraphically higher than in section 04. This may be due to: i) the lag time between equilibration of the alluvial plain proximal and distal to the orogenic source and/or; ii) larger braided systems (as in sections 01-03) taking longer to re-equilibrate to alluvial plain tilting than smaller systems (eg. section 04).

Examination of the paleocurrent moving average (Fig.74) shows minor sinusoidal deflections of autocyclic origin upon the overall trends. Three such pertubations are seen in subsections IJ and are labelled 1-3 in Fig.74. These peaks are correlatable with peaks 1-3 from the moving G% (Fig.68) which comprise 35-40m CUFU sequences (sensu Heward,1978; see App.6). Each sequence shows a gradual upward southerly to northerly shift in paleocurrents. The southerly (or easterly) shift in direction corresponds to a thickening (and coarsening) of cycles, with the thickest one commonly having the most southerly (or easterly) deflection. The northerly shift in paleocurrent is concurrent with a thinning (and fining) of the cycles. This pattern of cyclicity could be caused by either autocyclic or allocyclic controls. An autocyclic explanation would involve the migration of slightly sinuous braid tracts across the alluvial plain. As the braid belt shifts towards and passes a certain locus, the following would be seen: low-, high-, and finally low order channel deposits (terminology after Rust, 1986 pers. comm.), thus creating the thickening/coarsening and thinning/fining nature of the sequences. Paleocurrent variations could then be caused by intrinsic fluvial controls, but this factor does not by itself satisfactorily explain the close relationship between the coarsest grain size and the most southerly (or easterly) deflection within the sequences. Allocyclically-induced avulsions better explain these sequences in which case the sequence would begin with gradual lateral shifting of the braid belt, hence depositing a CU sequence as previously explained. A tectonically-induced avulsion (due to southeasterly tilting of the alluvial plain) would divert the coarser high order channels into adjacent floodplains creating the southerly paleocurrent. Further autocyclically-controlled migration of the braid belt away from the locus of sedimentation would create the capping thinner, finer-grained cycles, and the northerly deflection (due to re-equilibration). A purely allocyclical explanation would involve three minor tectonic pulses tilting the alluvial plain, causing the southerly deflection and the progradation of coarser grained deposits. Relaxation within the highlands would allow the plain to equilibrate back to its original state (i.e. a northerly deflection) and a decrease in grain size. Although this could be possible, a purely allocyclic explanation is unlikely due to the thin overall sequence, thin cycles, facies associations and paleocurrent patterns -

all of which can be explained more simply by lateral shifting of the braidplain with intermittent tectonically-induced avulsions.

Paleocurrents in subsection N were analysed by measuring the strike of a/b planes for clasts with a:b axial ratios >2.0 and "a" axis >1.0cm. Data were processed using methods described in section 7.3 and are shown in Fig.75 and Appendix 11.

Imbrication studies showed no significant difference between results using a/b >2.0 and "a" axis >1.0cm (maximum difference was 1.0%). Strikes of A/B planes are plotted in Fig.75 and show a distinct unimodal imbrication. Mean paleocurrent averages display a northwesterly trend, ranging between 329° to 345°, which agrees with a Cobequid Highland provenance. Vector strengths range between 59.4% to 90.5%, averaging 73.2%. These relatively high vector strength values suggest that these are poorly sorted waterlain deposits rather than debris flow deposits (Mills,1984).

9.4.1 Paleocurrent Relationships:

Angular deviation from the preceding cycle was plotted versus the coarse member thickness and the moving grain size. Results showed no correlation existed between the parameters (i.e. r=-0.175 and r=0.032 respectively). The lack of

STRIKE OF A/B PLANES FOR CLASTS

IN SUBSECTION N

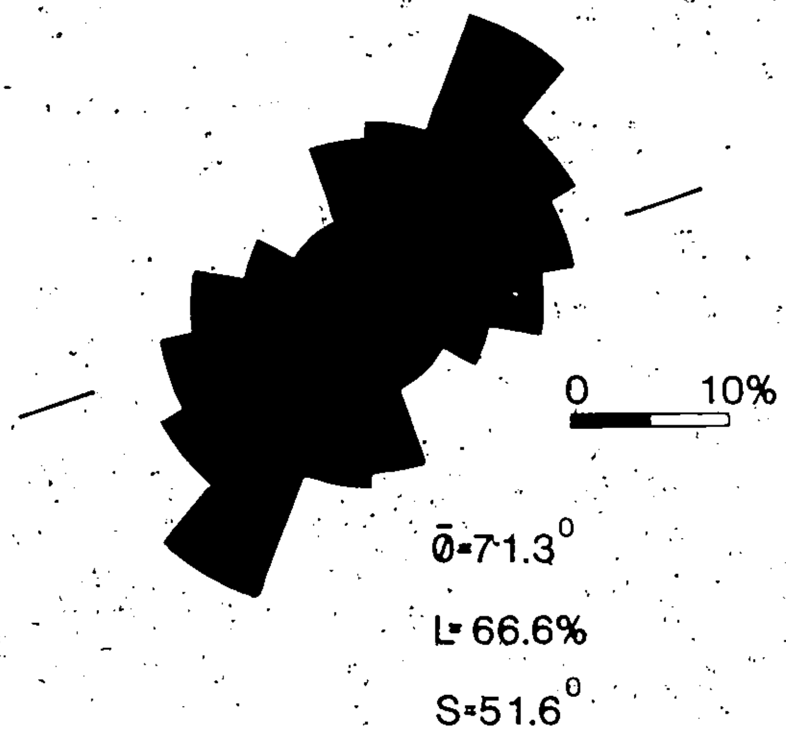

Fig. 75

correlation contrasts with moderate to good correlations found in sections 01-03 (discussed in 7.6, cf Figs.43,44) and is attributed to contrasting fluvial styles. Sections 01-03 were dominated by large trunk braidplain deposits which allowed sedimentation rates to exceed subsidence rates, thus creating thicker often amalgamated cycles with low fine-/coarse member ratios. In this system avulsions were quite common and probably the main mode for creation of new braid tracts. Section 04 contrasts by being a much smaller braidplain on which sedimentation rates could not keep up with subsidence rates, hence the cycles are well-developed with high fine-/coarse member ratios. In this system vertical aggradation and lateral migration of braid belts across the alluvial plain, were common methods of deposition. Rapid subsidence rates along with the lateral migration of braid belts would preserve both low and higher order channel deposits. Hence succeeding cycles would have paleocurrents independant of the underlying cycle, unlike in avulsion-related cycles, where paleocurrents in the overlying cycle would be expected to diverge significantly.

9.5 Vertical Trends in Grain Size and Related Parameters

Procedure for the sampling of clasts is outlined in section 8.2.1. The moving grain size and normalized standard deviation (S_N) are plotted in Fig.76. The moving grain size shows a CU megasequence up to cycle I IV where it begins to

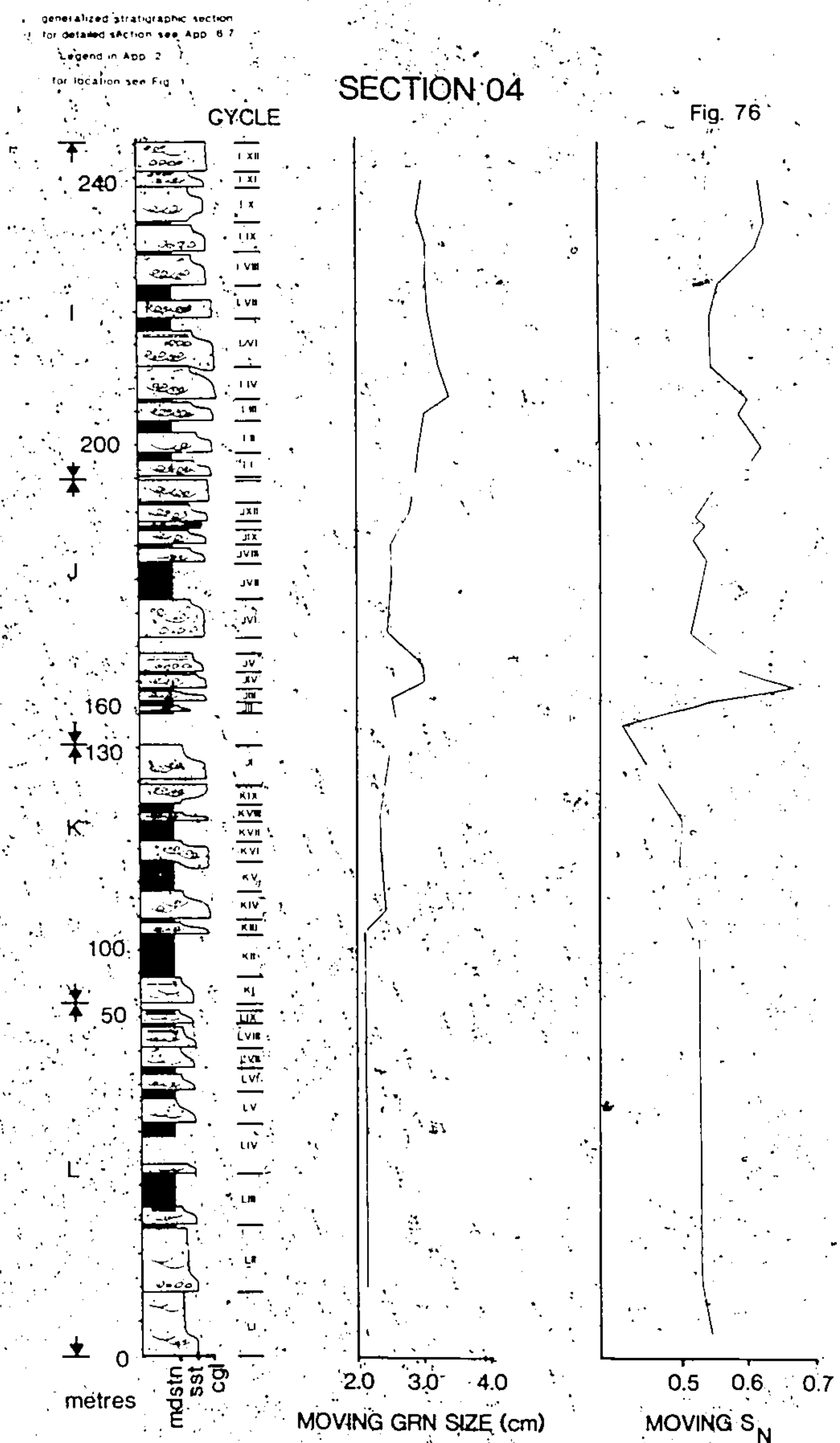
generalized stratigraphic section
for detailed section see App. 6.7
Legend in App. 2
for location see Fig. 1
SECTION 04
Fig. 76
CYCLE
240
200
160
130
100
50
0
I
J
K
L
metres
mdstn
sst
cgl
2.0
3.0
4.0
MOVING GRN SIZE (cm)
0.5
0.6
0.7
MOVING S_N

FU. The maximum grain size in section 04 is found stratigraphically higher than sections 01-03 and is attributed to progradation of a clastic wedge from the Cobequid orogenic belt, discussed further in section 9.6.1. a/b ratios are tabulated in Table 13 and show a small upsection decrease from 1.59 (n=300) in subsection K to 1.55 (n=1050) in subsection I, reflecting the progradation of coarser, more equant clasts (i.e. increasing proximality). Similar trends, reflecting progradation, are seen in the sorting values (Fig.76,77). Fig.77 plots the moving normalized standard deviation versus the moving grain size for cycles in the lower and upper half of section 04 (i.e. above and below cycle JI) and shows that increases in grain size are correlatable with increases in sorting in the lower section (r=-0.779) and decreases in sorting values in the upper section (r=0.606). Trends in the lower section are due to low clast/matrix ratios which allowed winnowing of the finer pebbles (i.e. selective transportation, Church and Gilbert, 1975) hence creating the well sorted deposits. The upper part of section 04 (Fig.77) typifies grain size and sorting trends expected within a proximal prograding fluvial system: increased grain size, increased clast/matrix ratio and decreased sorting (Gustavson, 1974).

9.6.1 Clast Analysis and Provenance

Vertical trends in clast size and abundance were analysed using techniques described in section 8.7; the

TABLE 13: A/B RATIOS FOR SECTION 04

SECTION	UNIT	MPS A/B	MPS S_D	MEAN 100 A/B	MEAN 100 S_D
I	I-3	1.54	11.1	1.50	1.75
	I-10	1.74	10.2	1.59	1.82
	I-12	1.49	7.65	1.58	1.50
	I-14	1.52	13.1	1.52	1.97
	I-16	1.52	9.78	1.47	1.92
	I-18	1.83	5.49	1.53	1.48
	I-21	1.64	7.24	1.63	2.13
AVERAGE		1.60	-	1.55	-
J	J-1	1.68	8.80	1.60	1.34
	J-3	1.73	6.40	1.50	1.71
	J-11	1.60	5.83	1.57	1.47
	J-16	1.67	11.1	1.60	2.55
AVERAGE		1.67	-	1.57	-
K	K-2	1.58	6.11	1.64	1.41
	K-6	1.71	5.45	1.70	1.37
AVERAGE		1.65	-	1.67	-
L	L-12	1.50	3.98	1.67	1.14
	L-13	1.69	5.74	1.52	1.36
	L-15	1.82	4.75	1.58	1.12
AVERAGE		1.67	-	1.59	-
N	N-1	1.46	9.83	1.76	2.20
	N-2a	1.69	9.55	1.76	2.53
	N-2b	1.44	7.06	1.65	1.23
	N-4	1.44	7.65	1.46	1.27
	N-8a	1.46	9.27	1.51	2.27
	N-8b	1.56	16.0	1.52	1.97
	N-8c	1.48	12.1	1.53	1.76
AVERAGE		1.50	-	1.60	-

S_D = standard deviation of "a" axis

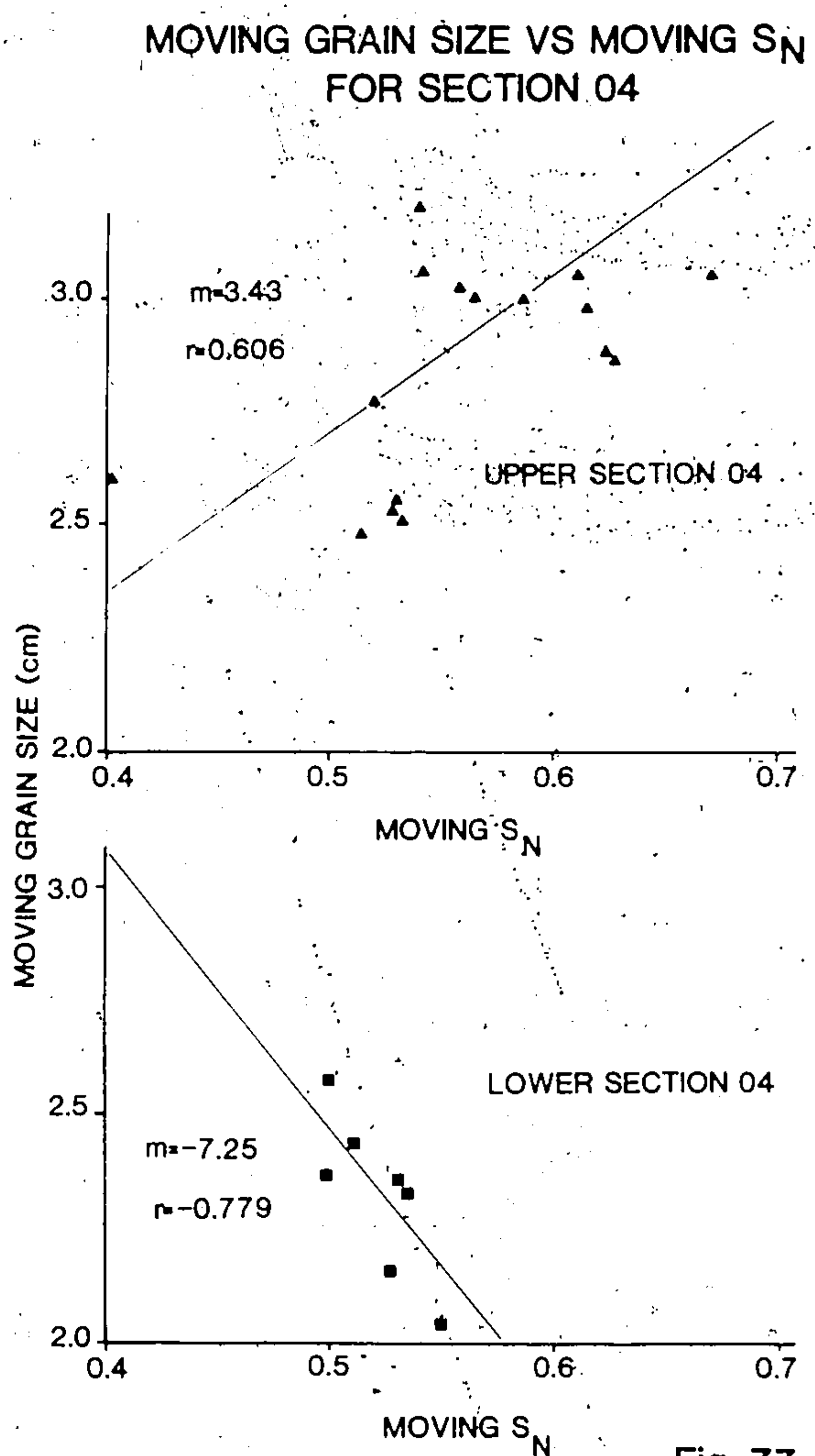
MOVING GRAIN SIZE VS MOVING S_N
FOR SECTION 04
MOVING GRAIN SIZE (cm)
m=3.43
r=0.606
UPPER SECTION 04
3.0
2.5
2.0
0.4
0.5
0.6
0.7
MOVING S_N
LOWER SECTION 04
m=-7.25
r=-0.779
3.0
2.5
2.0
0.4
0.5
0.6
0.7
MOVING S_N

Fig. 77

results support progradation of Cobequid Highland sediments.

Analysis of clast size for individual lithotypes displayed properties similar to the overall grain size curve (Fig.76).The moving clast size for the various lithotypes shows (Fig.78) a general upward increase in grain size with a slight FU of some constituents in the upper parts. Two major peaks correlatable with those seen in the moving grain size (Fig.76), are shown by syenitic and quartzitic lithotypes, but other lithotypes do not show such pronounced peaks. These peaks are attributed to high order channel deposits from laterally migrating braid belts (discussed in section 9.7).

Comparison of clast abundance between subsections IJK (section 04) and those from sections 01/02,03 distinctly show two different signatures (Fig.79) indicative of provenance from two sources. Subsections IJK are slightly enriched in felsics, significantly enriched in phyllites and depleted in sandstones compared to the adjacent section 03. Subsection IJK is also marked by other lithologies not present in sections 01-03, termed "others" in Figs.78,79 which include basalts, metabasalts, altered basic melanocratic volcanics, highly chloritized granites and feldspathic gneisses, and are most abundant in cycle I IV. The marked difference in lithotypes between these sections suggests provenance from two different sources.

Petrographic analyses were carried out on matrix samples

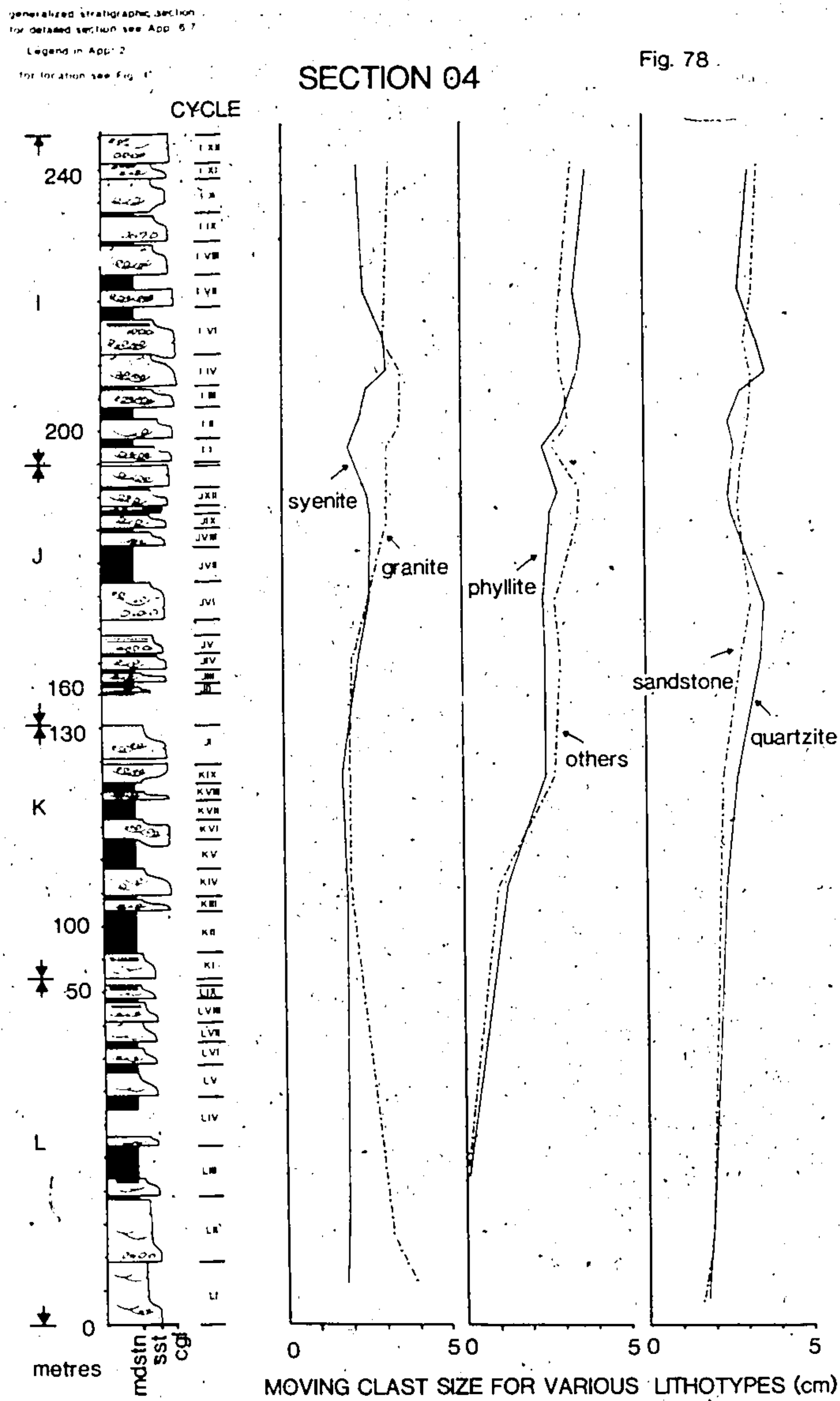
generalized stratigraphic section
Legend in App. 2
Fig. 78
SECTION 04
CYCLE
240
I
200
J
160
130
K
100
50
L
0
metres
mdstn
sst
cgl
syenite
granite
phyllite
others
sandstone
quartzite
0
5
MOVING CLAST SIZE FOR VARIOUS LITHOTYPES (cm)

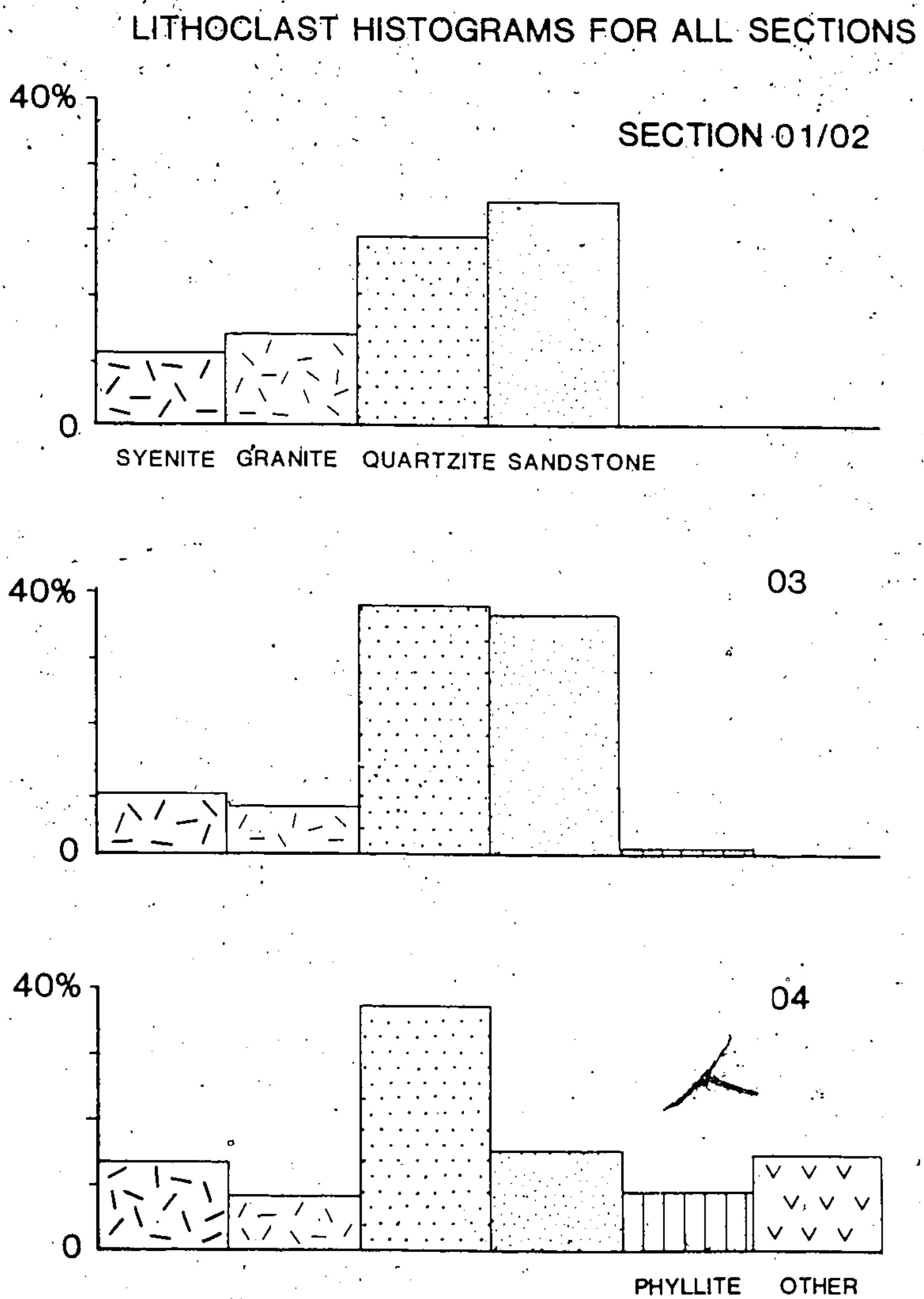
LITHOCLAST HISTOGRAMS FOR ALL SECTIONS
40%
SECTION 01/02
0
SYENITE
GRANITE
QUARTZITE
SANDSTONE
40%
03
0
40%
04
0
PHYLLITE
OTHER

Fig. 79

from section 04 in order to determine their provenance. Procedures described in section 8.9 were followed, with results as tabulated in Appendix 16 and shown in Fig.80. Samples from subsection N plotted as feldspathic litharenites due to the abundance of feldspar-rich groundmass and feldspar phenocrysts from the underlying rhyolites of the Fountain Lake Group. Segregation of samples from subsections IJK into coarse-, medium-, and fine-grain types (see section 8.9, 8.9.1) showed a decrease in labile fragments and an increase in quartz with decreasing grain size. This pattern is similar to samples from section 03 (see Fig.64). Comparison of similar grain sizes from section 03 (Fig.64) and subsections IJK (Fig.80) shows: i) coarse grain sizes from subsections IJK have a much greater abundance of unstable rock fragments (URF); ii) medium and fine grains from subsections IJK are enriched in feldspars and depleted in quartz. The enrichment of labile rock fragments and feldspars from matrix samples of subsections IJK compared to section 03 implies either a more immature sand (i.e. increased proximality) than section 03 and/or a different source. Facies associations and paleocurrent patterns previously discussed in section 9 suggest that a combination of both hypotheses may be most appropriate.

Although careful work was carried out on lithotype and petrographic classification of samples, determination of exact provenance proved difficult for various reasons. Petrographic studies, although more exacting, may not have

Fig. 80

MATRIX PETROGRAPHY –

PETROGRAPHIC CLASSIFICATION

(after McBride, 1963)

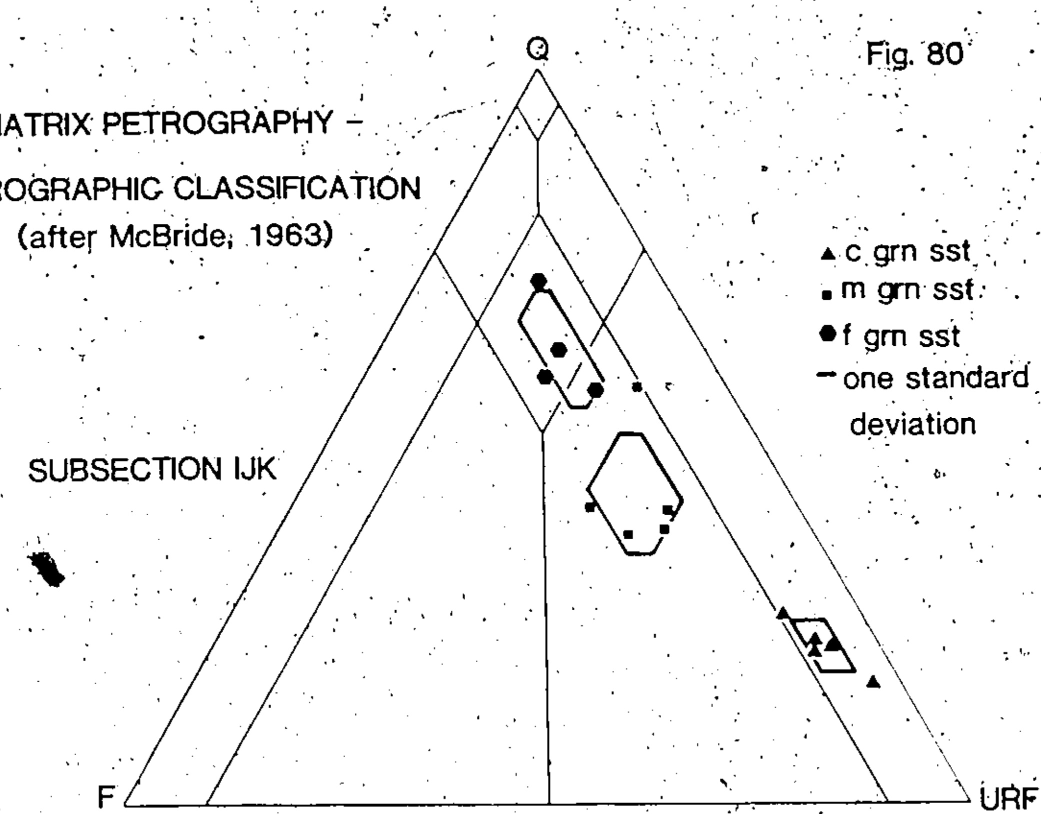

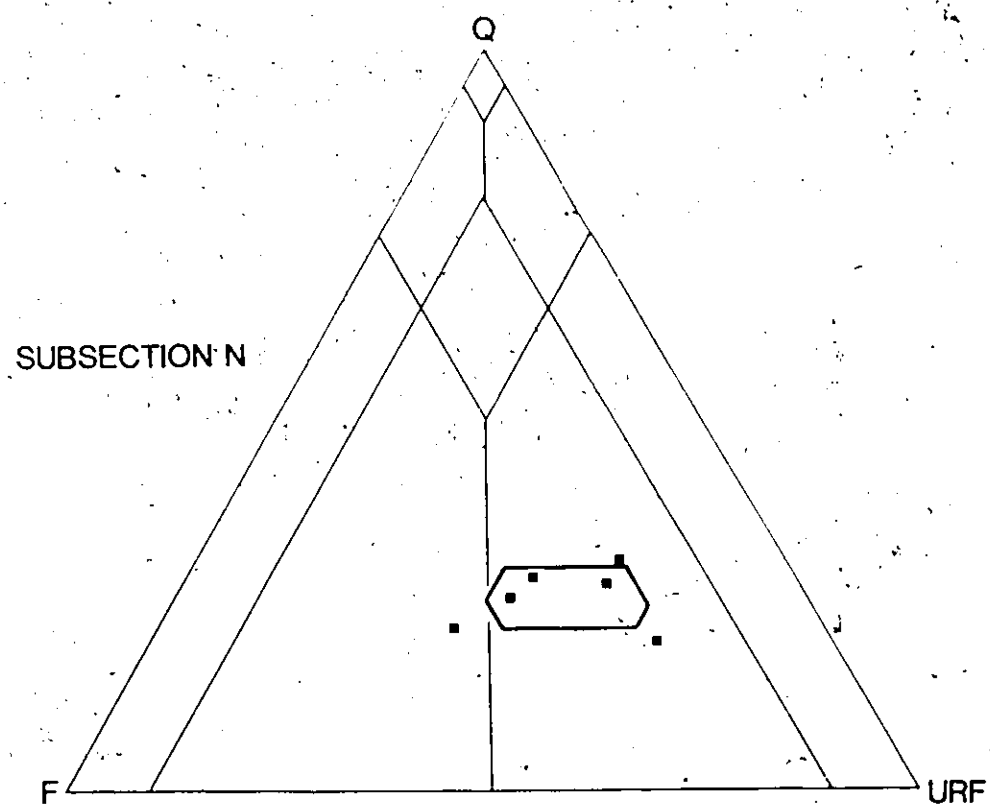

properly identified some IRF's due to staining of felsic-rich groundmasses from alkaline rhyolites (eg. Fountain Lake Group), hence misinterpreting the highly aphanitic groundmass as potassium feldspars. Highly vacuolized and altered acidic volcanic rock fragments may have also been misconstrued in thin section for other rock fragments, while silicified volcanics may have been misinterpreted as fine grained quartzites in handsample. The end result is that possibly distinctive lithologies may have been missed. Other more important factors are related to the basin and the lithologies found therein. First and foremost it should be noted that the lithological differences between the Caledonian and Cobequid Highlands are subtle i.e. there are no lithologies which are diagnostic of one highland. Possible source rocks from the Caledonian Highland include the Precambrian Coldbrook Group comprising predominantly siliciclastics with well developed schistosity in places, less common felsic and intermediate volcanics and minor chloritic/sericitic schists (Kindle, 1962). Interspersed within the Highlands are Precambrian (?) and Devonian felsic plutons. Possible Cobequid Highland source rocks include Devonian siliciclastics, Devono-Carboniferous felsic plutons and volcanics, and possible offshore (several kilometres south of Squally Point) metavolcanics and phyllites. The main difference may lie in the greater degree of metamorphism in the Caledonian rocks.

Certain characteristics were noted in some felsics which may be useful in detailed provenance studies. Many felsics were depleted in mafic minerals and quartz, possibly diagnostic of the source area. Another characteristic noted in many felsic samples (in hand sample and in thin section) was the dearth of plagioclase, denoting alkali granite affinities. Alkali granites are common in the Cobequid Highlands and are of Devono-Carboniferous age. The largest and closest example to the study area is the Cape Chignecto Pluton (Fig.81) which was probably exposed during the Westphalian.

Although exact provenances cannot be ascertained, the following generalities may be made:

i) Syenites (quartz syenites and alkali granites inclusive) may be from the Carboniferous Cape Chignecto Pluton (see Fig.81) or a Devonian pluton coeval with the New Yarmouth Pluton. The extent of the latter pluton cannot be delineated due to its coverage by the Bay of Fundy, and hence it may have been a major source.

ii) Granites are inconclusive as to provenance because they are found in both highlands.

iii) Rhyolites found in section 04 are most probably derived from the Fountain Lake Group.

iv) Quartzites in section 01-03 could have come from the Precambrian Coldbrook Group (Fig.82) while quartzites in section 04 could come from the Devonian Rapid Brook Formation and sources now covered by the sea.

v) Sandstones are more prominent in sections 01-03 and may be derived from Mississippian or Precambrian (Coldbrook Group) sediments (Fig.82). Sandstones from section 04 are less prominent and may be derived from the Rapid Brook Formation with minor amounts from the Fountain Lake Group.

vi) Phyllites/schists within section 04 are of uncertain provenance. The foliation textures seen in samples may be due to large intruding plutons capable of metamorphosing the adjacent sediments. This is seen in the strong cataclastic deformation in the Soldier

Fig. 81. Geology of the Cobequid Highlands. After Donohoe and Wallace (1982).

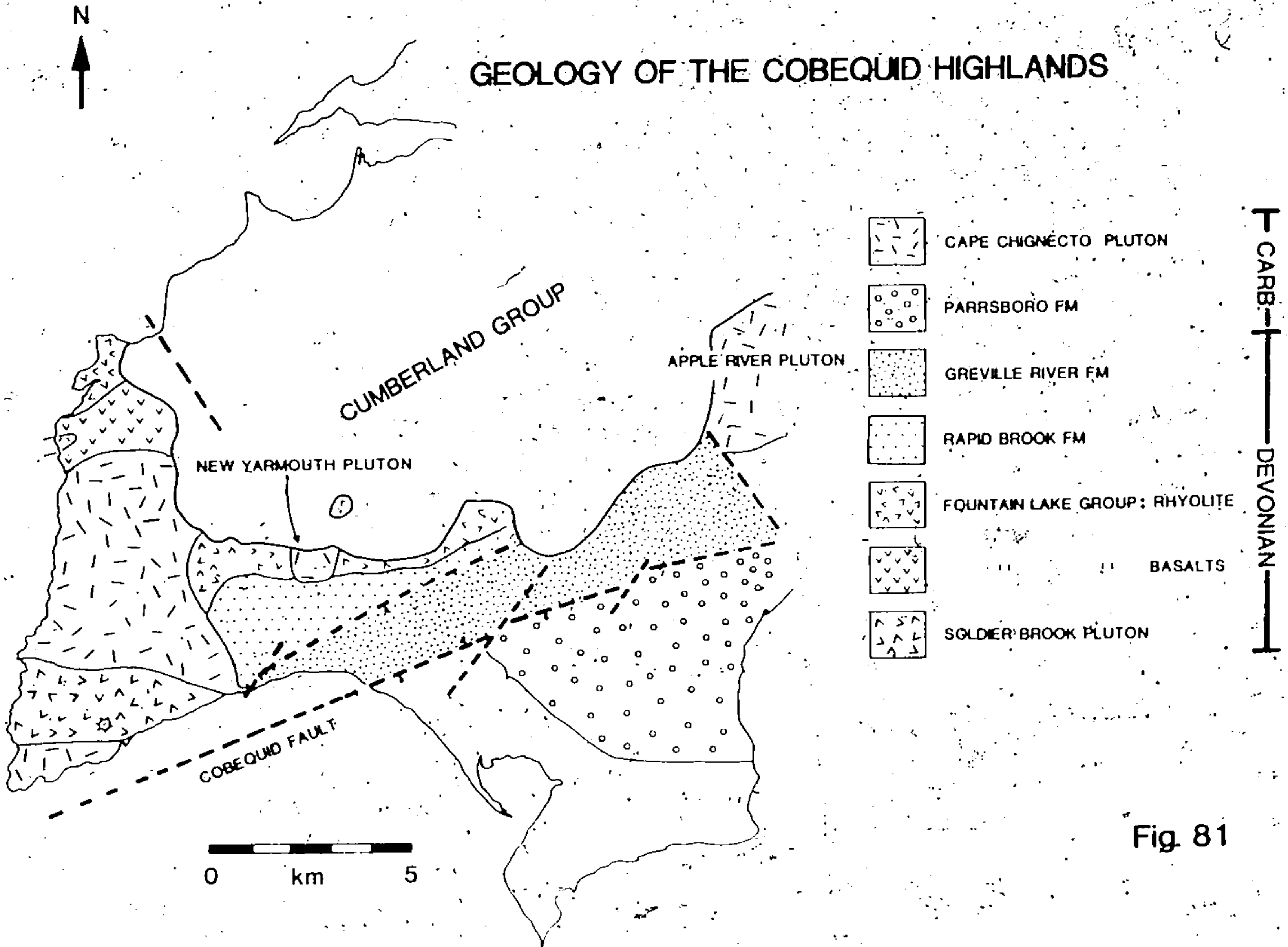
GEOLOGY OF THE COBEQUID HIGHLANDS
N
CUMBERLAND GROUP
NEW YARMOUTH PLUTON
APPLE RIVER PLUTON
COBEQUID FAULT
0
km
5
CAPE CHIGNECTO PLUTON
PARRSBORO FM
GREVILLE RIVER FM
RAPID BROOK FM
FOUNTAIN LAKE GROUP: RHYOLITE
BASALTS
SOLDIER BROOK PLUTON
CARB.
DEVONIAN

Fig. 81

Fig.82. General Geology of the Caledonian Highlands (after Giles and Ruitenberg, 1977).

GENERAL GEOLOGY OF THE CALEDONIAN HIGHLANDS

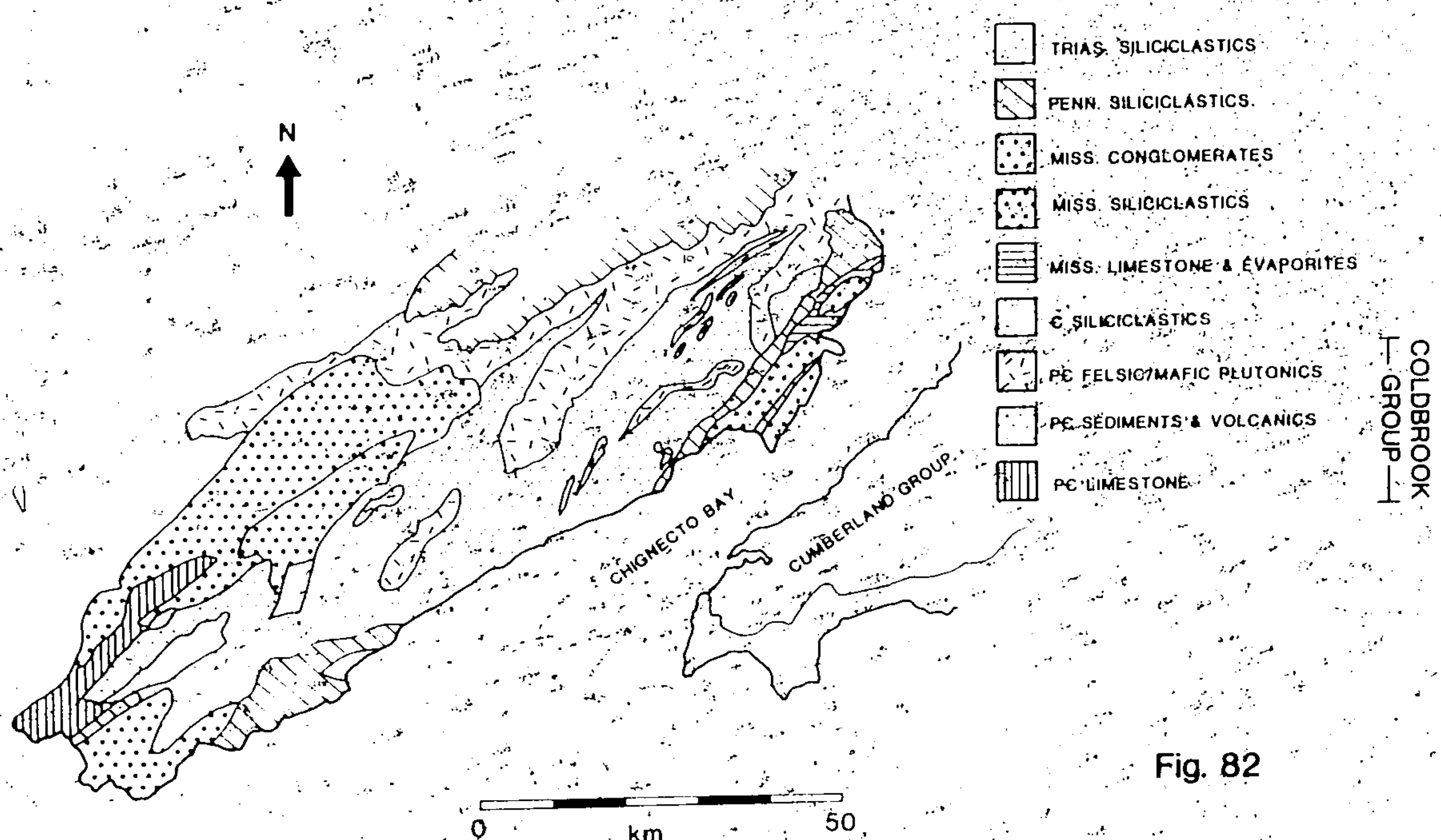

Fig. 82

Brook Pluton due to the emplacement of the Cape Chignecto Pluton (Donohoe and Wallace,1982). An alternate explanation is that the phyllites are coming from an unmapped source.

vii) Mafic lithologies (basalts and altered volcanics) found in section 04 are probably from the Devonian Fountain Lake Group.

Comparisons between the stratigraphic positioning of maxima for the abundance of certain lithotypes (Fig.83) and grain size (Fig.78) show results similar to those seen in section 8.7. Maximum grain size for a given clast overlies its maximum abundance in syenitic-, phyllitic, and siliciclastic lithotypes implying progradation as argued in section 8.9. The opposite relationship was seen with granitic lithotypes, denoting retrogradation of the system supplied from granitic source areas. Relating these events to provenance fields reveals no major discrepancies: prograding detritus shed from the Cobequid front could have been produced from the aforementioned areas; while retrogradation from a granitic source may indicate the peneplaining of granitic plutons. Comparison of patterns seen in sections 01-03 and 04 show similarities between siliciclastics (progradational) and granites (retrogradational). The ubiquity of siliciclastics in both Highlands may imply that progradation was achieved by basin subsidence and not localized uplifts (<u>sensu stricto</u>), hence shedding of sediments would be increased near basin margins creating a prograding clastic wedge from both adjacent highlands. Proximality of section 04 to the Cobequid basin margin means

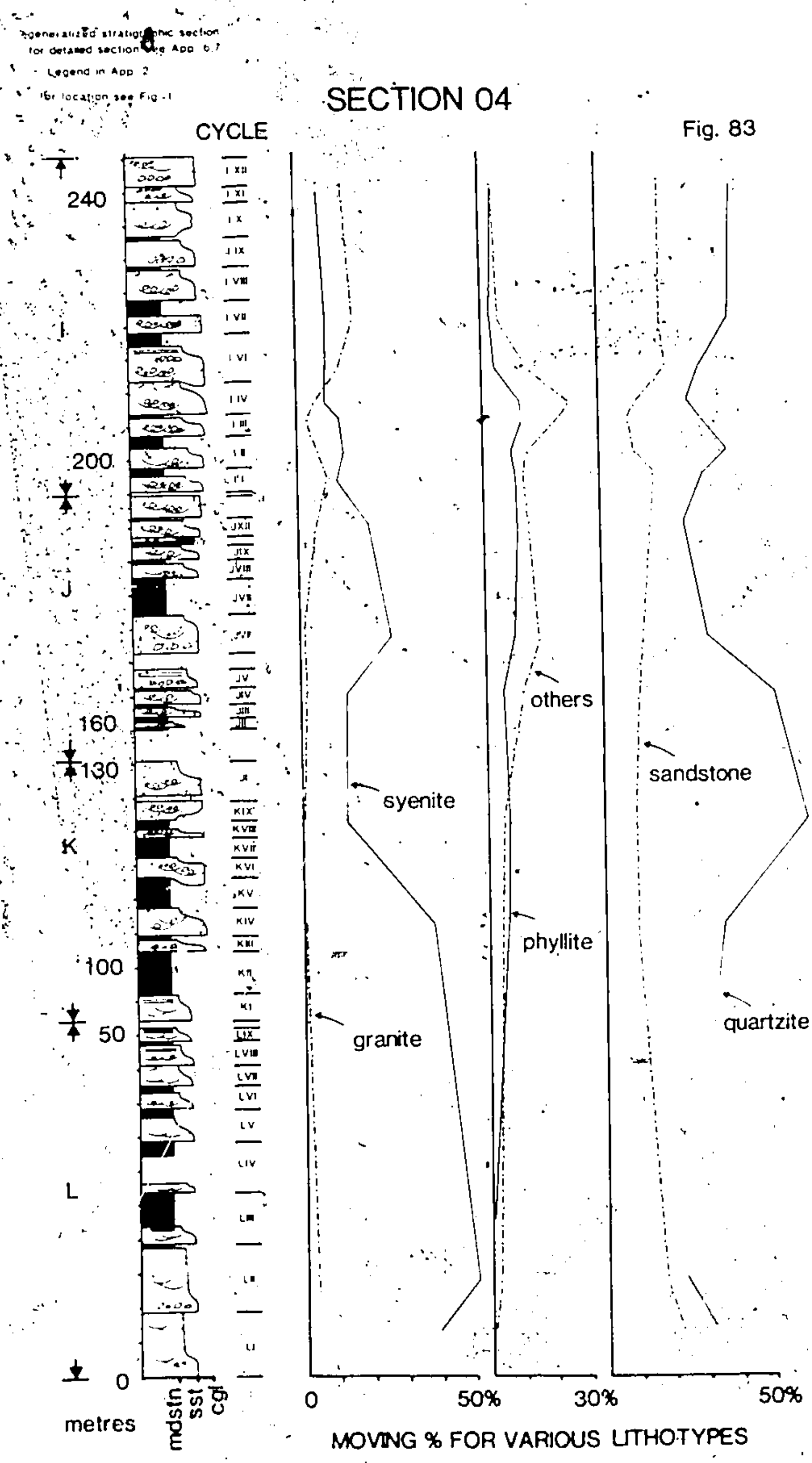
generalized stratigraphic section
for detailed section see App. 6.7
Legend in App. 2
for location see Fig. 1
SECTION 04
Fig. 83
CYCLE
240
200
J
160
130
K
100
50
L
0
metres
mdstn
sst
cgl
0
50%
30%
50%
syenite
granite
others
phyllite
sandstone
quartzite
MOVING % FOR VARIOUS LITHOTYPES

that sediments deposited during progradation from those Highlands. It is postulated that a similar study proximal to the Caledonian basin margin (if it were possible) would show similar patterns. Granites are also common in both Highlands but unlike the siliciclastics they display a retrogradational pattern. The presence of both similar prograding and retrograding lithologies from two different uplands requires an explanation. Feldspars are known to weather most rapidly in humid tropical regions (Press and Seiver, 1978). A similar environment in this region during the Carboniferous (D'Orsay and van de Poll,1985) would have greatly increased the weathering rates of Precambrian and Devonian felsic plutons (Bradley,1970). Given a substantial increase in relief, due to subsidence or tectonic uplift, felsic plutons would be expected to weather much more quickly than chemically resistive siliciclastics - the controlling factors on sedimentation patterns being the rates of weathering (chemical and physical) and subsidence (or uplift). For example (see Fig.84), if the weathering rate were much less than subsidence one might expect a continuum between equilibrium (i.e. no pro- or retrogradation) and progradation; if weathering rates were quite high and even approached subsidence rates the result would be peneplanation of the pluton, creating a retreating scarp and depositing a retrograding sequence. Therefore the differential weathering of felsic plutons and siliciclastics under humid/tropical conditions may have been an important factor in the differing sedimentation patterns.

Fig.84. Effect of weathering and subsidence on progradation/retrogradation patterns (see text for explanation).

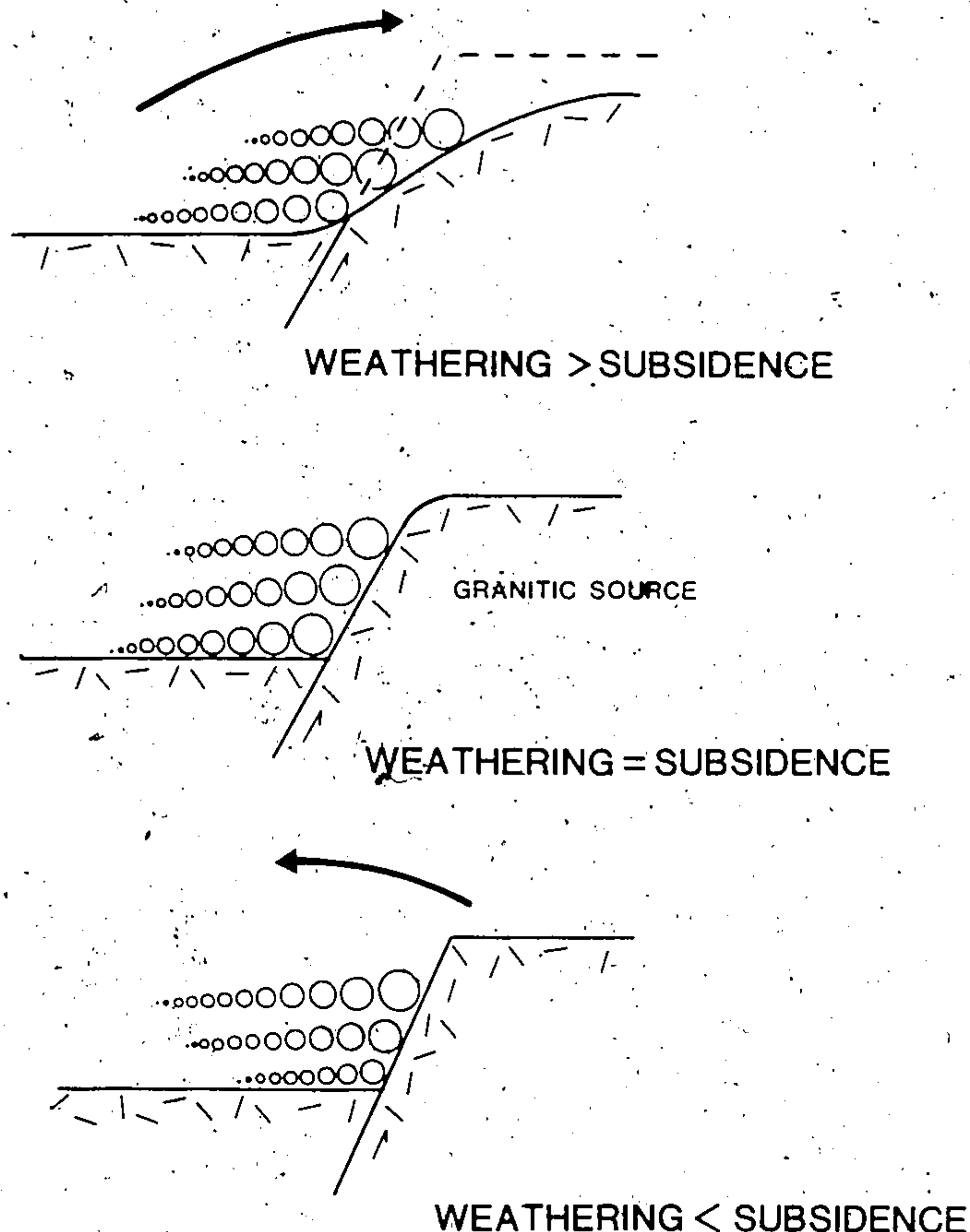
WEATHERING > SUBSIDENCE
GRANITIC SOURCE
WEATHERING = SUBSIDENCE
WEATHERING < SUBSIDENCE

Fig. 84

9.7 DEPOSITIONAL ENVIRONMENT (SECTION 04)

Deposits from subsections I-L are interpreted as braided fluvial for the same reasons proposed for sections 01-03 (see 6.2). Although both are attributed to braided fluvial origin, their architectural styles contrast significantly, implying different environments of deposition.

Cycles within section 04 are characterized by sharp concordant lower contacts overlain by conglomeratic (or sandstone) facies assemblages which grade up into sandstone and finally heterolithic facies assemblages (see Apps.6,7). Contacts between the coarse and fine members are commonly gradational. The presence of such well-developed FU cycles is often cited as a common characteristic of meandering fluvial deposits (Allen,1964,1965,1970; Bernard et al.,1970; Jackson,1976,1978) but is not applicable in this case for the following reasons:

- i) lack of lateral accretion surfaces
- ii) laterally extensive (up to 7km) sheet-like geometry
- iii) low variance unimodal paleocurrents
- iv) coarse grained units not confined as lags
- v) facies associations do not conform with Jackson's (1976,1978) meandering fluvial models
- vii) preponderance of framework-supported conglomerates within conglomeratic facies associations

Cyclicity within meandering systems is attributed to the preservation of both lateral- and vertical accretion deposits, the former being formed by erosion of the cut bank and deposition on the point bar due to spiralling flows (Allen,1970; Walker and Cant,1984), the latter by overbank sedimentation. The thickness of the fine member (or amalgamation of laterally accreted channel deposits) is controlled by rates of aggradation and avulsion, "since a channel belt will inevitably return to a given location on its floodplain, but at a different elevation" due to aggradation (Bridge,1984; Bridge and Leeder,1979; Allen,1978). If the system is avulsing at a rapid rate (<1000 years) overbank deposits will be thin. The rate of avulsion will be controlled by allocyclic mechanisms, most often subsidence/sedimentation rates.

Whereas well-developed FU cycles with relatively low coarse/fine member ratios are the norm in meandering fluvial systems, they are the exception in braided systems. Coarse/fine member ratios are quite low compared to most studied braided deposits ranging from 1:1 in subsection K and increasing upward stratigraphically to 3:1 in subsection I. Most braided systems are characterized by the dearth of overbank mudstones (eg. Battery Point Formation, Westwater Canyon Member, Cannes de Roche Formation, Malbaie Formation, et cetera) which is attributed to rapid channel switching not allowing the preservation of abundant overbank fines. Although cycles from section 04 fit the above characteristics, they are not of meandering origin for the reasons cited at the beginning of the section, hence the well-developed FU nature is not due to spiralling flows rather, aggradation and lateral braid belt migration (see sections 9.1.3, 9.3, 9.4, 9.4.1).

Such well-developed FU cycles with relatively low coarse/fine member ratios are only known to the author from the Miocene Kasaba Formation (Hayward,1983); the Cretaceous-Tertiary Brazeau-Paskapoo Sequence (McLean and Jerzykiewicz,1978) and the Cretaceous-Tertiary Saunders Group (Jerzykiewicz and Sweet,1985; T. Jerzykiewicz pers. com.,1985). The Brazeau-Paskapoo Formations and the Saunders Group are similar, comprising erosively-based thin coarse members internally stratified by thin lag deposits, Sh/Sl interspered with minor Sp; and overlain by a thick fine member. McLean and Jerzykiewicz (1978) gave no exact interpretation for the Brazeau-Paskapoo sequence, although a braided fluvial interpretation seems most appropriate. The Saunders Group has been interpreted as an anastomosed deposit (Jerzykiewicz pers. com.,1985) although it does not resemble modern or ancient analogues. The differences between coarse member lithofacies in the Brazeau-Paskapoo Sequence, Saunders Group and section 04 do not make them perfect analogues, although tectonic settings may be similar. The Miocene Kasaba Formation is a much better analogue, characterized by well-developed decametre scale cycles comprising an erosional base (Se) -> Gm -> minor St -> Sm -> thick fine member. These cycles, were deposited in a rapidly subsiding basin and are interpreted as autocyclic in origin, the thick fine member created by "low lateral confinement of the fluvial channel" allowing wide dispersal of suspended material even under moderate floods (Hayward,1983). The abundance of well-developed FU cycles (c.f. Fig.2 Hayward,1983), and lack of CUFU-type cycles is suggestive of avulsive channel migration akin to what is seen in lower section 04. The presence of primarily sharp contacts between coarse and fine members also suggests that avulsion was the dominant depositional style (discussed later in this section).

Well-developed cycles in section 04 can be subdivided into two major types, reflecting different depositional environments. Cycles from subsections IJK make up the first major group comprising well-developed FU and CUFU cycles. The coarse member is composed of primarily conglomeratic facies and has a gradational contact into the overlying heterolithic facies. The coarse member displays the following preferred transitions: F -> Se -> Gt -> Gm -> St(m) -> F. The fine member comprises grey mudstones with Fm and Fl being the most common. Preferred facies transitions shown by the heterolithic facies assemblage (see section 9.3) suggests deposition within an abandoned channel rather than overbank areas.

The aforementioned characteristics of cycles from subsections IJK infer that vertical accretion/gradual abandonment, rather than avulsion, was the dominant influence on depositional style. This hypothesis is substantiated by: the CUFU nature of many cycles (see section 9.1.3); the gradational contact with the heterolithic facies and the nature of coarse member preferred facies transitions (Bridge,1984; Rust and Jones, pers. comm.,1985). The lack of correlation between coarse member thickness and angular deviation between successive cycles also suggests that avulsion was not important in the formation of new braid tracts. The fine member shows characteristics consistent with deposition within gradually abandoned channels. These are: grey mudstones indicative of high water tables which did not allow oxidation; predominance of Fl (over Fr) suggesting that mudstone deposition occurred via tractive currents during channel abandonment, and not suspension deposition on the floodplain; preferred facies transitions displayed by the heterolithic facies assemblage (section 9.3) which are consistent with deposition within various parts of an abandoned channel rather than overbank deposition.

Stacking of cycles along with paleocurrent patterns infer deposition by a vertically accreting/laterally migrating braid belt (discussed in section 9.4). The presence of CUFU sequences (sensu Heward,1978; see examples in Apps.6,7) along with cyclic paleocurrent patterns are interpreted as the result of rapid aggradation rates which would allow the preservation of low-, high-, and low order channel deposits as the braid belt swept across the alluvial plain (Fig.85).

The second major cycle type is seen in section L and is markedly different from subsection IJK. Cycles from subsection L display a well-developed FU nature (see App.8), rarely are amalgamated, and never CUFU unlike those from subsections IJK (see Apps.6,7). Coarse members are composed of sandstone facies and have sharp contacts with the overlying heterolithic facies assemblage. The heterolithic facies assemblage is made up of predominantly red mudstone, with Fm and Fr being the most common.

Characteristics displayed by cycles in subsections L are indicative of gradual channel abandonment followed by avulsion, rather than vertical accretion/gradual channel abandonment as seen in cycles from subsections IJK. The lack of CUFU cycles and presence of sharp contacts with the overlying heterolithic facies assemblage and well developed FU cycles suggest that gradual channel abandonment was commonly preceded by avulsion. The abundance of red mudstones (Fm, Fr) and dearth of Fl indicates that fine members were deposited on floodplains rather than abandoned channels. The presence of lower water tables allowed the colonization of plants, hence creating Fr and the oxidation of the mudstones.

The evolution of section 04 shows that deposition occurred in several environments. Firstly, deposition occurred in alluvial fans (subsection N) prograding towards

Fig.85. Formation of CUFU cycles by a laterally migrating braid tract (see text for further explanation).

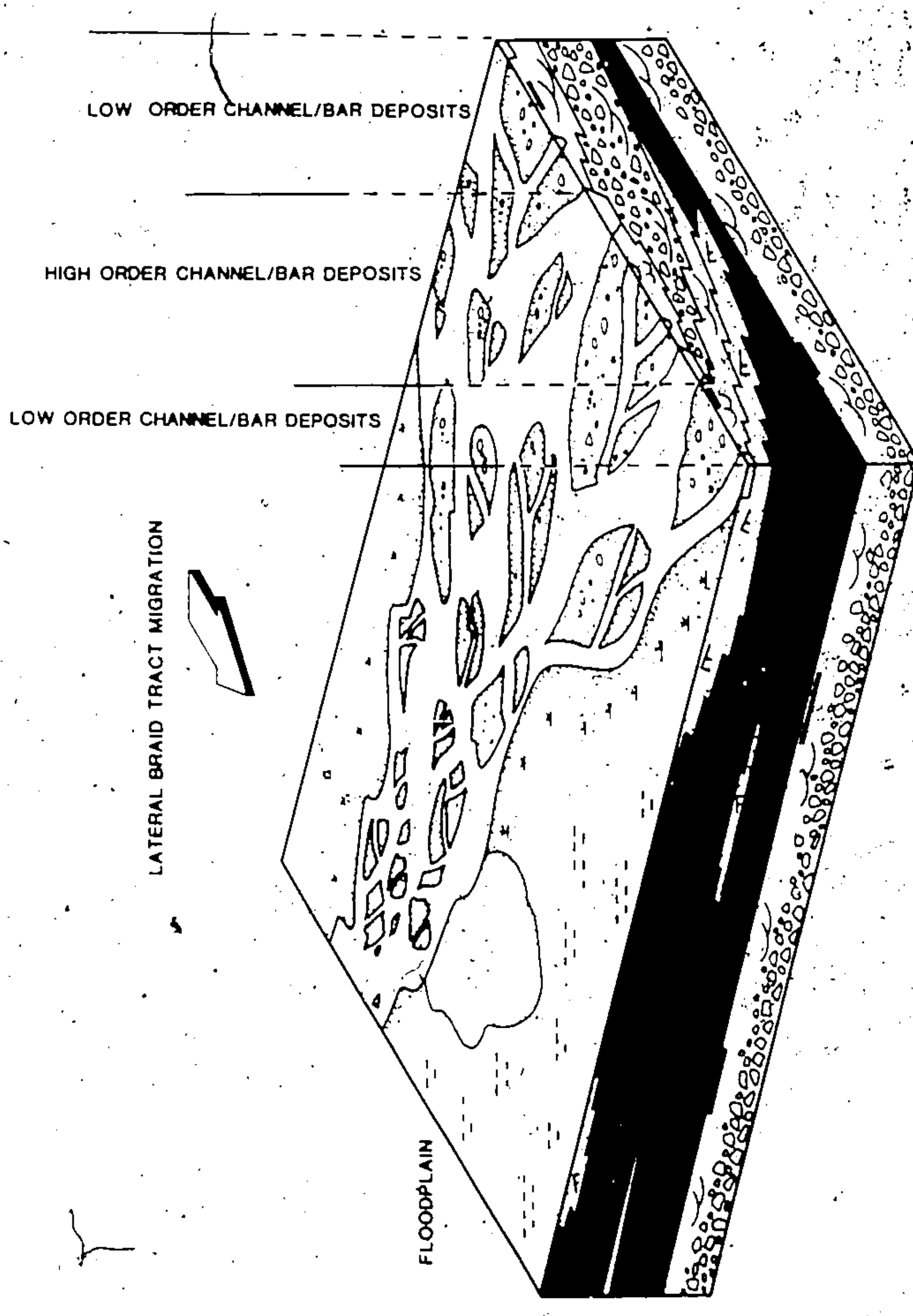
LOW ORDER CHANNEL/BAR DEPOSITS
HIGH ORDER CHANNEL/BAR DEPOSITS
LOW ORDER CHANNEL/BAR DEPOSITS
LATERAL BRAID TRACT MIGRATION
FLOODPLAIN

Fig. 85

the northwest from the Cobequid Highlands. Marginal to these fans were shallow ponded areas of possibly lacustrine or swamp affinities. These shallow lakes allowed the preservation of flora creating the thin coals seen in subsection N (i.e. Spicer's Cove, Hacquebard and Donaldson,1964). Similar scenarios are envisaged by Calder (1984) for the northeast part of the basin. Subsection L shows a CU megasequence with easterly paleocurrents implying basin margin onlapping braidplain deposits analogous to Permian deposits within the Sydney Basin (Australia) which show coals adjacent to alluvial fans (Hunt and Hodday,1985). This braidplain was probably marginal to a larger trunk braidplain which flowed longitudinally (northeasterly) down the basin (Fig.87). Subsection K continues the CU trend displaying increasingly northerly paleocurrents thicker fine members and distinctly different clast lithologies. As previously shown in section 9.4 the northerly shift in paleocurrent is attributed to uplift in these Cobequid Highlands, hence subsection K marks the initial progradation of detritus shed by tranversely flowing braided streams from the Highlands. Uplift is also borne out by the input of exotic clast lithotypes. The presence of two different fluvial systems is also corroborated by the change in depositional style between subsections L and IJK (previously discussed), and the predominance of grey mudstones in the upper subsections indicative of higher water tables. Subsections IJ also display properties demonstrative of progradation: CU megasequence (except for the the upper 30m), upward thickening of coarse members and a decrease in fine member percentage.

Comparison of subsections IJ to the laterally equivalent section 03 shows many differences not explicable by simple proximal/distal facies changes:

i) subsections IJ have thinner cycles, thinner coarse members and smaller mean bed thickness, but cycles in subsections IJ have larger grain size.

ii) subsections IJ have a predominance of grey mudstones, as opposed to red in sections 01-03.

iii) bases of heterolithic units are commonly gradational in subsections IJ, unlike the sharp contacts of 01-03.

iv) there are well-developed FU and CUFU cycles in subsections IJ.

vi) heterolithic facies associations in subsections IJK show preferred facies transitions related to deposition within abandoned channels.

vii) paleocurrents in subsections IJ are northerly, as opposed to easterly in section 03.

viii) there is a lack of correlation between coarse member thickness and angular deviation of suceeding cycles in subsections IJ - the opposite is seen in section 03.

ix) clast lithotypes and percentages differ between section 03 and subsections IJ.

The southwestward distal to proximal trend seen in sections 01 to 03 suggests section 04 should have a more proximal character if it were part of the same system. These distinct differences shown by section 03 and subsections IJ cannot be explained by simple proximal/distal facies changes. Two possibilities could explain the dichotomy: i) subsections IJ are the result of deposition by anabranching (i.e.

parallel) braided streams marginal to a much larger trunk braidplain (i.e. deposits from sections 01-03) or; ii) subsections IJ are deposits of small braidplains tributary (i.e. transverse) to the trunk braidplain. In light of the diverging paleocurrents, different clast lithotypes, and larger grain size of subsections IJ the latter hypothesis seems most appropriate.

10.0 TECTONISM AND SEDIMENTATION IN THE CUMBERLAND BASIN

10.1 Introduction

There are numerous tectonic models for the origin of the Appalachians. Full documentation of these models is beyond the scope of this thesis and hence only a brief overview will be presented.

Two general views exist on the tectonic interpretation of Appalachia. The first viewpoint is based on a "two-sided symmetrical model" (sensu Williams,1964; 1976; 1978; Rast et al.,1976; Schenk,1978; Bird and Dewey,1970). In this model the deformed belt is divided into five tectonic zones, each extending the entire length of the orogen. Accretion of these zones occurred via Wilson-type Cycles during the Late Precambrian and into the Late Paleozoic. An alternate explanation invokes a terrane model (Keppie,1985). A terrane is defined as an area underlain by continental crust and characterized by internal continuity which is distinct from that of neighbouring terranes. Modern analogues to these terranes include microcontinents, submarine plateaus, ridges, seamounts, volcanic arc complexes and small ocean basins. Some of these continental fragments are large enough to resist subduction and hence become accreted onto the continental margins. Keppie (1985) suggested that the previous model is far too simplistic; the orogen cannot be subdivided into zones extending along its entire length. In addition, the previous model fails to accomodate sinistral transcurrent movement of the Avalon terrane as detected from paleomagnetic studies (Morris,1976; Kent and Opdyke,1978; 1979; Van der Voo et al.,1979; Van der Voo and Scotese,1981). Recent paleomagnetic work by Irving and Strong (1984) on the early Carboniferous Deer Lake Group (Newfoundland) has found no evidence to support any large sinistral displacement of Acadia. They suggest that evidence for sinistral faulting found by other workers are the result of post Carboniferous imprinting. Further paleomagnetic work must be done in this field to clarify the position of Acadia during the Carboniferous.

The development of Appalachia can be related to four major orogenies: i) the Late Precambrian Avalonian Orogeny; ii) the Ordovician Taconic Orogeny; iii) the Devonian Acadian orogeny; and iv) the Maritime Disturbance which is correlatable with the American Alleghanian- and the European Hercynian Orogeny (Poole,1967, Schenk,1978; Williams,1979). Only the latter two tectonic events are of concern in this study.

The Acadian Orogeny has been attributed to the closure of the Iapetus Ocean with subsequent continental collision of Laurentia, Baltica, and Caledonia (Scotese et al.,1979; Schenk,1978; Bird and Dewey, 197[illegible] Howie and Barss,1975). This intepretation has been criticized (Williams,1979; Rust,1981a; Keppie,1985) due to the lack of thrusts (only upright folds); inconsistency with paleomagnetic data; dearth of ophiolites and wide zone of volcanism - together suggesting that subduction was not operating at this time. Rust (1981a) has suggested that most of these inconsistencies may be reconciled by the continental margin overriding a low dip subduction zone and parallel transforms with differing sense of slip. Although this latter suggestion does eliminate many problems it still does not address the alledged 1000-2000 km sinistral displacement of Avalonia (Kent and Opdyke,1978; Morris,1976; Van der Voo et al.,1979). It is clear that present tectonic models for the Appalachian Orogeny are inadequate and that future models should incorporate paleomagnetic findings.

The Maritime Disturbance, a late phase of the Acadian Orogeny (Howie and Barss,1975), was marked predominantly by strike-slip and oblique-slip faulting (Webb,1963,1969; Belt,1968; Bradley,1982) which ended by the late Westphalian (Belt,1968; Bradley,1982; Keppie,1985) as indicated by the over-stepping of faults by the Pictou Group. The Maritime

Disturbance culminated with the collision of Gondwana and Laurentia which is best recorded in the Alleghanian/Hercynian Orogeny of the Central Appalachians.

10.2 Tectonic Models for the Cumberland Basin

There is a dearth of studies on the tectonic origin of the Cumberland Basin. The Cumberland Basin lies within the much larger Fundy Basin which is interpreted by Belt (1963,1968) as a complex rift valley (termed an aulacogen by Schenk,1975 and Keppie,1977). It is bounded on both sides by high angle faults (Belt,1965) with coarse facies proximal to the faults and finer facies in the axial parts of the basin. Belt (1968) suggested that similar facies and tectonic patterns in the Fundy Basin and the Midland Valley of the Caledonide region (present day Scotland and Ireland) place them as part of the same rift valley system. This side-by-side interpretation is also borne out by paleomagnetic studies by Morris (1976).

East-west compression during the Late Devonian produced localized areas of tension (due to anastomosing faults) which created a graben system (Belt,1968) and associated volcanics. During the Early Carboniferous, compression changed to NW-SE and initiated a period of predominantly strike-slip tectonism (Belt,1968; Fralick and Schenk,1980; Bradley,1982) during which the Cumberland Basin (Westphalian A) and smaller coeval pull-apart basins were formed (eg.

Stellarton, Minas, Narragansett, Deer Lake et cetera). Basin architecture is not well known at present, although preliminary seismic studies between Springhill and the bordering Cobequid Highlands profiled a tilted half-graben configuration (A-B in Fig.86; Calder, pers. comm.,1985). Bradley (1982) noted that Late Paleozoic basins subsided episodically in two stages: i) an initial phase of stretching, thinning and rapid fault-controlled subsidence often associated with volcanism; and ii) a secondary phase of gradual subsidence. Bradley's curve for the Cumberland Group shows very rapid subsidence, which is also supported by the preservation of in situ trees (Logan,1845; Dawson,1854; Duff and Walton, 1973). Mississippian plutonism (eg. the Cape Chignecto Pluton) is problematic because it implies late Acadian crustal shortening.

Bradley (1982) suggested that the Cumberland Basin originated in response to extension between the sinistral Harvey-Hopewell Fault and the dextral Cobequid-Chedabucto Fault due to transpression in southern New Brunswick (Rast and Grant,1973; Ruitenberg et al.,1973). Bradley (1982) proposed that a possible modern analogue might be the East Anatolian intracontinental triple junction of sinistral and dextral transforms with a convergent plate. The junction is marked by the rapidly subsiding Neogene Karliova Basin (Sengor,1979; Hempton and Dunne,1983). Dewey and Sengor (1979) have shown that oblique continental collisions involving irregular margins can easily create strike-slip

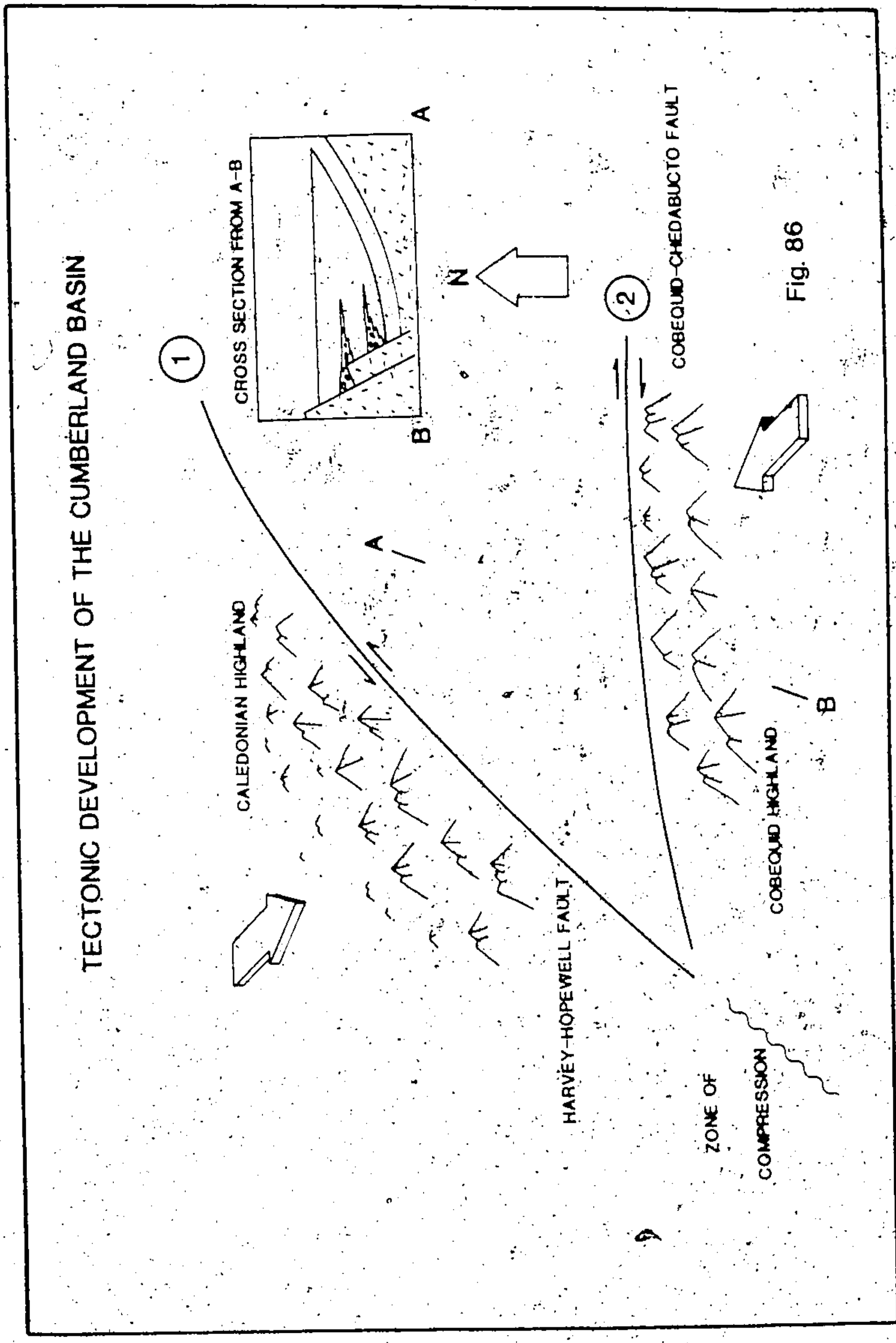
TECTONIC DEVELOPMENT OF THE CUMBERLAND BASIN
1
CROSS SECTION FROM A-B
A
B
N
2
COBEQUID-CHEDABUCTO FAULT
CALEDONIAN HIGHLAND
A
B
COBEQUID HIGHLAND
HARVEY-HOPEWELL FAULT
ZONE OF
COMPRESSION

Fig. 86

faulting with opposing senses (eg. the East Anatolian and North Anatolian Faults). Fig.86 shows a possible tectonic scenario for the creation of the Cumberland Basin. During the Late Acadian orogeny NW-SE transpression occurred in southern New Brunswick (Rast and Grant,1973; Ruitenberg et al.,1973; Bradley,1982) due to continental collision between Laurentia, Avalonia and Caledonia. Stress fields during this time created a sinistral megashear (transcurrent fault, Keppie,1985) and smaller sinistral side-stepping faults such as the synthetic Harvey-Hopewell Fault. The dextral Cobequid-Chedabucto Fault is seen as an antithetic fault which postdates the Harvey-Hopewell Fault (Fig.86) and resulted in the extensional nature of the basin (Bradley,1982).

10.3 Tectonics and Sedimentation: This Study

Sedimentation patterns in the study area can be related to the interaction of subsidence rates with the following elements: i) an easterly flowing axial braidplain; ii) transverse (to oblique) braidplains and iii) alluvial fans (Fig.87). During the early Westphalian A faulting along the Cobequid-Chedabucto fault created north-northeasterly prograding alluvial fans (eg. subsection N) which debouched into marginal elongate lacustrine (or swamp) areas (eg. subsection M, see Fig. 87a). These lacustrine areas are potential sites for coal exploration. Marginal to the swamps was an east-southeasterly flowing axial trunk braidplain (eg. section L). Rapid subsidence within the basin during the

Fig.87. Circled letters A,B, and C refer to different stages of deposition. The first stage (A) shows the deposition of the Lower Coarse and Middle Fine Units. The second stage (B) shows the deposition of the Upper Coarse Unit, which was initiated by rapid subsidence down the basin axis and subsequent progradation from the adjacent highlands (detailed discussion in text). The final stage (C) shows a northerly tilting of the alluvial plain. Capital letters refer to subsections from this study.

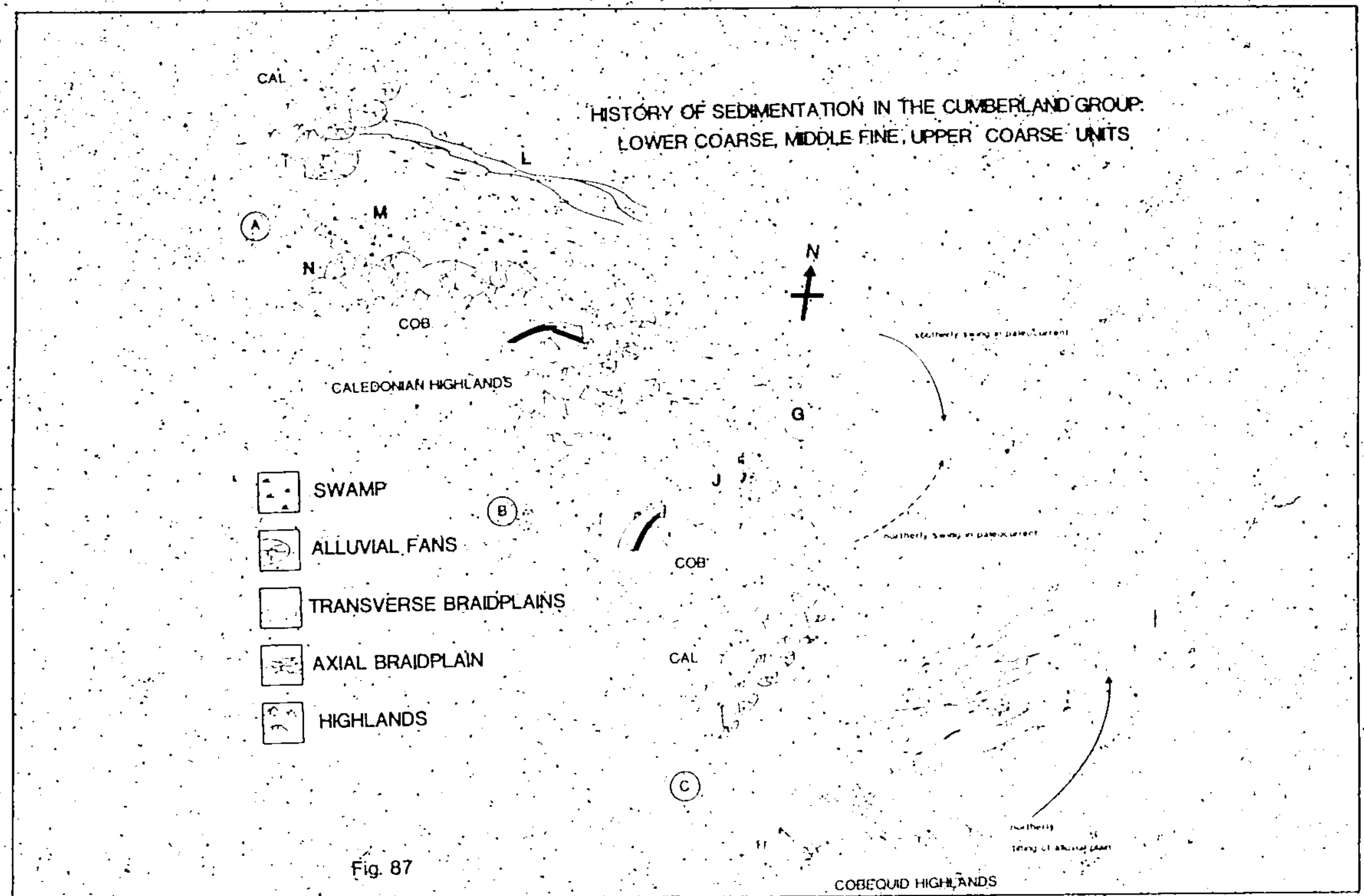
HISTORY OF SEDIMENTATION IN THE CUMBERLAND GROUP:
LOWER COARSE, MIDDLE FINE, UPPER COARSE UNITS
CAL
L
A
M
N
COB
CALEDONIAN HIGHLANDS
N
G
J
B
COB
CAL
C
COBEQUID HIGHLANDS
SWAMP
ALLUVIAL FANS
TRANSVERSE BRAIDPLAINS
AXIAL BRAIDPLAIN
HIGHLANDS

Fig. 87

STRATIGRAPHIC CROSS SECTION FROM SAND RIVER TO SQUALLY POINT

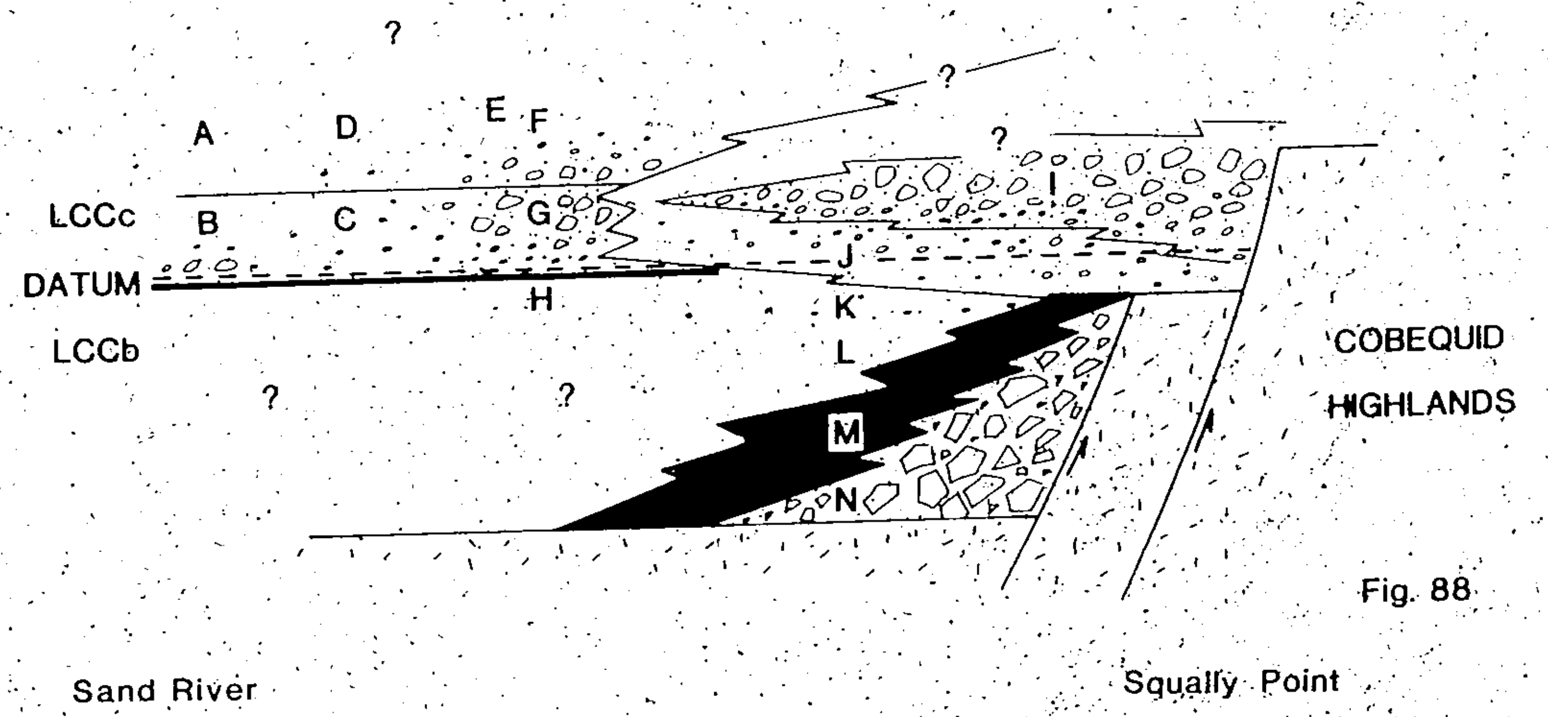

Fig. 88

Westphalian B stage created the progressive onlapping of the fans by the trunk braidplain (Fig.88, eg. subsection L). Southerly paleocurrent deflections at the base of sections 01 and 03, juxtaposed with northerly swings in the laterally equivalent subsection J indicate increased subsidence down the basin axis (Fig.87b), possibly due to sediment loading. The increased subsidence rates, down the basin axis, initiated upwarp along the basin margin (Beaumont,1981; Hayward,1984) hence resulting in progradation of transversely flowing braidplains (i.e. deposits from subsection J) from the Cobequid Highlands into the axial braidplain (Fig.87b, Fig.88). This was followed by a period of northerly tilting of the alluvial plain either due to differential subsidence to the north or uplift to the south (Fig.87c). The diachronous nature of the deposits should be noted.

Results of this study are in general agreement with Calder (1984) and Rust et al. (1984). Calder envisioned a similar scenario in the Springhill area with coal swamps bordering alluvial fans and marginal to an axial trunk system. Although models are similar, differing opinions exist on the integration of sedimentation and tectonics. Most workers on the Cumberland Basin (Hacquebard and Donaldson,1964; Calder 1984; Donohoe and Wallace,1982; Calder pers. comm.,1985) suggest a continuous onlapping of the basement by sediments. However, the evidence from this study is that increased sedimentation rates (or uplift) caused progradation of transverse fluvial systems from the adjacent borderlands (Fig.88). It is possible that differential subsidence could result in progradation of sediments in the western side of the the highlands and not in the eastern margin. Results from this study show conclusively, based on paleocurrents, provenance studies, and fluvial architecture that progradation did occur from the western Cobequid Highlands. Concern has also been expressed over a Caledonian Highland source (Calder, pers. comm.,1985) although the paleocurrent data also delineate an axial trunk system (Calder,1984; Salas and Rust,1985; Rust et al.,1984). However, many of the previous studies (Way,1968; Calder,1984; Duff and Walton,1973) assumed a Cobequid Highland source without paying attention to paleocurrent trends. Way (1968) showed southerly flow from his directional data at Joggins, ($\bar{\theta}$=186°, after Way,1968) and yet interpreted this as evidence for provenance from the Cobequid Highlands. The presence of abundant plagioclase (ranging between 7.7% and 18.3%) in Way's rocks contrasts with the dearth in Cobequid-derived sediments in this study, which implies that Way (1968) indentified a Caledonian rather than Cobequid source. This conclusion is also borne out by Rust et al. (1984), who demonstrated southeasterly mean paleoflow for channels around McCarren Creek, thus connoting a Caledonian source.

A problematic aspect of the axial drainage system is the absence of marine deposits to the northeast. Paleontological and sedimentological work by Duff and Walton (1973) on the Lower Fine Unit (LCCb) at Joggins showed no conclusive evidence for marine inundation. The presence of ostracodal and pelecypodal limestones within the dominantly mudstone sequence at Joggins was intepreted as brackish-to-freshwater conditions unlike their saline-to-brackish European counterparts. Duff and Walton (1973) interpreted the sequence to represent deposition within a delta plain, with the implication that the sea was a short distance to the northeast. Calder (1984), has suggested that an axial lacustrine system was present during the Westphalian B in the Springhill area. Detailed work on the northeast end of the basin by Calder (pers. comm., 1985) has found no evidence of marine conditions. It is postulated by this author that the Cumberland Basin may be of intermontane origin, thus the axial trunk system debouched into a lake. This claim is further substantiated by structural and sedimentological evidence. The presence of an unconformity between the Cumberland Group and the Riversdale Group in the northeast end of the basin implies a syndepositional structural high (Copeland, 1958, Garland, 1953). Copeland suggested that a northwesterly trending structural arch, possibly due to an extension of the Black River Diapir (Visean Windsor Group), was responsible for the structural high. A thickening of the Lower Coarse Unit (LCCa) in the Springhill area was interpreted by Bell (1944) as a direct result of this structural high, which presumably acted as a northeastern basin margin. Thus an intermontane origin (but <u>not</u> necessarily internally drained) for the Cumberland Basin is based on the lack of marine deposits, basin containment by fan deposits rimming the basin.

Depositional characteristics within the basin indicate that the trunk system passed from a distributary terminal fan (sensu Friend,1978) into an axial lacustrine system (Calder,1984). The downstream decrease in bed thickness along with the lack of readily identifiable deltaic deposits suggests that the axial fluvial system may have become distributary in nature towards its distal reaches. Similar conditions have been suggested by Friend (1978) and Friend et al. (1985) for the Wood Bay Formation (Spitsbergen), Viddal Supergroup (Greenland), Ebro Basin (Spain) and implied by Middleton et al. (1983,1985) for the Whirlpool Formation (southern Ontario). Friend (1978) suggested that downstream decreases in bed thickness, lack of incision, and lobate geometry are due to a distributary terminal fan formed where the river debouches into a lake, sea or dissipates due to soak-in (or evapo-transpiration). The lack of deltaic deposits may be due to: i) erosion of deltaic deposits in the northeast part of the basin or; ii) high density contrasts between inflow and the standing body of water hence not allowing the formation of conventional Gilbert-type deltas (i.e. only low angle clinoform structures). Although tenuous, the lack of well-defined marine and deltaic deposits, downstream decrease in bed thickness (from this study), and lack of incision (Way,1968; Salas and Rust,1985) implies a similar type of system may have been operational in the Cumberland Basin. The presence of an axial lacustrine system would also allow the accumulation of carbonate deposits, as in the deposits of ancient Lake Gosuite of the Green River Basin (Eugster and Surdam,1973; Surdam and Wolfbauer,1975; Eugster and Hardie, 1975). Hence the carbonate units descri~~bed by Duff~~ and Walton (1973) could be explained without invoking brackish or marine conditions.

Although an intermontane origin is in better agreement with depositional characteristics, a problematic aspect with this interpretation is the presence of higher sulphur coals at Joggins (average 6.0%) than Springhill (1.7%) (Copeland,1958; Hacquebard and Donaldson,1964). Horne et al. (1978) and others have shown from studies in the Carboniferous of the central Appalachians that high values of sulphur (>2.0%) most likely indicate marine-to-brackish conditions. In this case high sulphur values may indicate that: i) internal (or restricted) drainage of the basin allowed salinity levels capable of sustaining sulphur-reducing bacteria; ii) Joggins may have been closer to a sulphate source rock (Windsor Group?); iii) the lake had an outlet to the sea (eg. Lake Maracaibo, Hyne et al., 1979).

Basin evolution due to strike-slip faulting is common in the Carboniferous of the Maritimes (Fralick and Schenk,1981; Zaitlin and Rust,1983) but no definitive evidence was found in this study to support strike-slip sedimentation in the Cumberland Basin. Strike-slip basins are commonly identified by: basin asymmetry, great sediment thickness, longitudinal mode of sediment dispersal, elongate basin geometry, mis-match of pebble lithology with adjacent sources, rapid sedimentation rate and sparse volcanic activity (Reading,1980; Steel and Gloppen,1980). Only sparse igneous activity, rapid rate of sedimentation, elongate basin geometry and axial drainage are readily applicable to this basin. The other features cannot be ascribed to strike-slip origin. Basin asymmetry is due to the homoclinal nature of the basin, the sedimentary pile is thin (2km) compared to most strike slip basins (eg. the Hornelen Basin, 25km), and pebble mis-match is not discernable in the Cumberland Basin. This may be due to formations outcropping parallel to the Cobequid-Chedabucto Fault or lack of strike-slip movement. Although variations on the strike-slip theme exist (Bluck,1980; Heward and Reading,1980; Ballance,1980) the applicable characteristics could easily indicate sedimentation within intermontane, foreland, forearc or predrift graben basins (Miall,1981). Hence it is concluded from this and other studies that the Cumberland Basin is not of strike-slip origin and that the sediments were deposited within an intermontane basin (although the two are not mutually exclusive).

10.4 Tectonics and Cyclicity in the Cumberland Basin: An Overview

Detailed accounts and interpretation based on various aspects of cyclicity for the axial and transverse fluvial systems have been presented in sections 4.3, 5.5, 6.3, 7.4 and 9.1-9.1.4, 9.2-9.4, 9.7 respectively. A brief generalized overview of controls on cyclicity will be presented.

Cycles within the axial braidplain sequence display a continuum of architectural styles depending on their proximality. Cycles in the proximal reaches are amalgamated (i.e. multistorey) and are attributed to allocyclic origin. Most cycles have sharp contacts between coarse and fine members indicative of avulsion. Two of these (due to the first and second tectonic pulse) can be correlated proximally to distally and are interpreted as allocyclically-induced avulsions. With increasing distality bedding thickness decreases, cycles FU and become better developed. Distal reaches contain cycles displaying fluvial styles indicative of both avulsion and gradual channel abandonment. The increase in well developed autocycles with decreased paleocurrent dispersion in the distal sections suggest a decrease in sedimentation rates (section 7.5) and/or stabilization by vegetation.

The predominance of amalgamated cycles in the proximal reaches and well developed cycles in the distal parts has been attributed to the interaction between sedimentation and subsidence rates. Amalgamated cycles are thought to be indicative of sedimentation rates exceeding subsidence rates (McLean and Jerzykiewicz, 1978) whereas the opposite condition leads to better developed, separated FU cycles. On a basin-wide scale these authors noted that maximum deposition would occur in the proximal reaches if the sedimentation rate was less than subsidence, and in the distal regions if sedimentation exceeded the subsidence rates. Results from bedding thickness studies suggest that differential subsidence between proximal and distal localities was not a controlling factor in fluvial architecture - rather sedimentation rates determined the fluvial style. Moreover, the downstream decrease in bed thickness implies greater sedimentation rates in the upstream reaches.

These results contrast with McLean and Jerzykiewicz's (1978) findings since maximum sedimentation is occurring in the proximal reaches even though sedimentation rates exceed subsidence. This discrepancy may be due to very rapid subsidence rates in the Cumberland Basin (0.69km/Ma, after Bradley,1982) compared to those within the Rocky Mountain foredeep (0.10km/Ma, after McLean and Jerzykiewicz,1978) which did not allow sufficient time for the sediment to be transported to the distal reaches. The end result may have been that sediment was amassed in the proximal reaches (i.e. sedimentation rates> subsidence) and depleted in the distal regions. This had a marked effect on the fluvial architectural style as seen in the proximal deposits of section 03 and the distal deposits of 01. These results are also contradictory to those of Visser and Johnson (1978) on the Neogene Siwalik (Himalayan) molasse, who suggested that fluvial architecture and sedimentation rates were "only loosely related". Unfortunately the work (Visser and Johnson, 1978) suffers from conceptual problems in the delineation of multistorey units which make conclusions suspect. The study by Visser and Johnson (1978) also fails to address fluvial architecture as a dynamic system regulated by sedimentation and subsidence rates.

Cycles from the transverse braidplain (section 04) show characteristics quite different from the axial system (sections 01-03). The transverse braidplain cycles are well-developed, FU and have gradational contacts between coarse and fine members indicative of gradual channel abandonment, rather than avulsion as in the proximal axial deposits. Allocyclic avulsions induced by the first and second tectonic pulse are less distinct in the transverse system, possibly due to contrasting fluvial styles and/or different location on the alluvial plain. Fluvial architecture in the transverse system shows cycles arranged into CUFU megasequences which are attributed to lateral migration of the transverse braidplain - something not seen in the axial braidplain deposits. The close proximity between the proximal axial deposits and the transverse system (only 1 km separating the two) along with similar slopes of the best fit bedding thickness line (see sections 4.3 and 9.2) imply that subsidence rates must have been similar since differential subsidence could not have taken place over such a short distance - thus sedimentation rates must have been the dominant control on fluvial architecture. The fluvial style seen in the tranverse system was controlled by sedimentation rates being less than subsidence rates, the opposite of the axial system. It is concluded that although subsidence rates are equal for the two fluvial systems the depositional style was dictated by the difference in magnitude between the two systems.

The well-marked cyclicity within both axial and transverse braidplain sequences is becoming readily apparent from studies of other rapidly subsiding foreland/intermontane basins eg. the Himalayan Siwalik Super Group (Visser and Johnson, 1978; Kumar and Tandon, 1985; Tandon et al., 1985); the Canadian Rockies Foredeep - the Brazeau-Paskapoo Sequence and others (McLean and Jerykiewicz, 1978; Smith and Putnam, 1980; Jerzykiewicz and Sweet, 1985); and the Miocene Kasaba Basin (Hayward, 1983, 1984). Cyclicity within these tectonic settings is usually attributed to deposition by either braided and/or anastomosed fluvial systems - indicative of rapid aggradation. Anastomosed deposits are usually favoured by either i) rapid differential subsidence near the mountain front and slower subsidence rates in the distal reaches (i.e. a "backwater" effect), or ii) a "damming" effect due to prograding transverse fans (Smith and Smith, 1980; Smith and Putnum, 1980). Braided deposits on the other hand are favoured by high stream gradients (Schumm, 1968) and no marked differential subsidence. Fluvial style displayed by the distal axial system in this study, although braided, shows some characteristics of anastomosed deposits (see section 7.4) such as: thick overbank deposits, similar avulsive styles, and poor CU or FU development. Anastomosed deposits sensu stricto have been documented in the Lower Fine Unit at McCarren Creek by Rust et al. (1984). The presence of anastomosed-like properties (i.e. thick overbank deposits, similar avulsive styles and poor CU and FU development) in proximal and distal parts of the basin suggest that similar dominating controls must have been operative throughout the basin. Differential subsidence on a basin-wide scale due to sediment loading along the basin axis and proximal reaches, may have been responsible for the development of anastomosed-like qualities. Thus differential subsidence may have caused a "backwater effect" which led to deposits of the "anastomosed channels" seen in the distal axial section of this study and in the McCarren Creek section (Rust et al.,1984). Although differential subsidence may have been operative on a basin-wide scale (Rust et al.,1984), as seen in the large displacement of correlative coal seams between Joggins and Maccan (Copeland,1958), it is less likely to have caused the change in fluvial style between the proximal and distal axial sections in this study, as previously argued. It is suggested here that anastomosis (and anastomosed-like qualities) may be imparted not only by basin-wide differential subsidence but also by rapid subsidence and sedimentation rates. Rust (1981b) and Nanson and Rust (1985) have shown in the intracratonic Lake Eyre Basin that anastomosis is not related to differential subsidence but rather to many complex factors, notably basin-wide aggradation, stage levels and climate.

Vegetation is an important determinant in fluvial architecture, especially in the post Paleozoic (Cotter,1978). It has been noted that Lower Paleozoic and earlier fluvial systems were dominated by braided streams due to the lack of vegetative cover allowing unrestricted migration of channels (Schumm,1968; Cotter,1978). It is difficult to ascertain the exact effect vegetation had on the rocks of the study area, since downstream decreases in sedimentation rate were accompanied by increases in vegetation. In effect longer residence times of channels, due to lower sedimentation rates would allow colonization of plants on the floodplains and as such it is difficult to discern the exact relationship between these two factors. It appears that the cause/effect relationship between sedimentation rates and vegetative cover is difficult to separate.

10.5 Paleoclimate

A humid tropical environment is envisaged for the study area for the following reasons:

i) abundance of coalified trees indicative of abundant rainfall

ii) thin coals suggestive of peat swamps, typically found in humid climates

iii) lack of desiccation cracks

iv) raindrop imprints

v) abundance of grey mudstones suggestive of high water tables

vi) absence of calcretes and evaporites

vii) paleolatitude was 8-10^0 S (Irving and Strong, 1984)

viii) based on scanning electron microscopy of quartz grains D'Orsay and van de Poll (1985) suggest that the mid Pennsylvanian Fowler Head Formation (which lies on the south side of the Cobequid Highlands) was deposited in a humid tropical environment

11.0 CONCLUSIONS:

The Upper Coarse, Middle Fine and Lower Coarse Units of the Cumberland Group were deposited within a rapidly subsiding intermontane basin by a series of transverse alluvial fans, transverse braidplains and a trunk braidplain system.

The Lower Coarse Unit rests with angular unconformity on the Fountain Lake Group and comprises poorly sorted matrix-supported and pebbly matrix-supported conglomerates. The CU megasequence displayed by the succession, along with north-northwesterly paleocurrents indicate progradation of alluvial fans from the adjacent Cobequid Highlands. The fans were probably marginal to wetlands (the Middle Fine Unit) which allowed the growth of plants and preservation of thin coal deposits.

The Upper Coarse Unit was deposited by a dominant axial trunk braidplain that drained northeastward and a smaller transverse braidplain. After an initial fanglomerate phase, the axial trunk braidplain started to progressively onlap the alluvial fans and wetland deposits. Sedimentation on the braidplain was initially marked by sheet-like, well-developed FU cycles. The cycles are sharp-based and have a sharp contacts with the overlying red mudstones. This sort of fluvial style is attributed to vertical aggradation within a sandy braidplain followed by a moderate period of gradual abandonment, terminated by avulsion and finally suspension deposition on the floodplain.

Sediment loading along the basin axis and concurrent flexural upwarp on the basin-margin (the cause and effect could also be reversed) allowed progradation of sediments from the bordering highlands. During this phase fluvial architecture within the proximal axial braidplain was marked by much thicker (up to 40m) amalgamated FU conglomeratic cycles arranged into an overall CU/thickening upward megasequence. Cycles within this megasequence have sharp bases and contacts with the under- and overlying fine members. Facies associations indicate rapid vertical aggradation rates followed by a short period of gradual abandonment and finally allocyclically-induced avulsions and in-channel deposition of mudstones.

Megacyclicity is attributed to allocyclic controls. In the distal reaches of the axial system the fluvial architecture is quite different. Here three types of cycles are found: CUFU sandstone, CUFU conglomeratic and CU sandstone cycles. The CUFU cycles are interpreted to have been formed by the following series of events: lateral encroachment of a braided tract upon its marginal sediments (or avulsion into an adjacent floodplain) with simultaneous vertical aggradation, followed by in-channel deposition, gradual abandonment, and finally avulsion. The CU cycles differ only by the absence of deposits from gradual channel abandonment, hence coarse member development was terminated by a sudden avulsion. The fine members within the distal axial system are usually dominated by red mudstones, abundant root turbation and a negatively skewed bedding thickness distribution, indicative of deposition on distal floodplains with low water tables, and sufficient residence times to allow colonization by plants and oxidation of mudstones.

As differential axial subsidence continued, sediment was shed from the Cobequid Highlands, onto prograding transverse braidplains. Paleocurrents, fluvial style and clast provenance studies imply that this braidplain was marginal to the axial system and hence the Upper Coarse Unit did <u>not</u> onlap progressively onto the basin margin - on the contrary, offlap occurred. Paleocurrents show that the transverse fluvial system flowed obliquely into the much larger trunk braidplain. The fluvial architecture of the transverse braidplain is markedly different from the trunk braidplain, with much thinner, very well-developed CUFU and FU conglomeratic cycles. Fluvial style indicates predominantly vertical accretion and gradual channel abandonment rather than avulsion. The fine members also show characteristics consistent with deposition within gradually abandoned channels: grey mudstones; predominance of laminated over rooted mudstones and preferred facies transitions. Petrographic studies show the presence of exotic clasts not found in the axial braidplain deposits and differing percentages between many lithotypes.

The compilation of results from various fields of study shows that fluvial architecture is controlled by allocyclic and autocyclic factors. Within the rapidly subsiding Cumberland Basin allocyclic controls are a dominating force on fluvial architecture, of which the two most important allocyclic factors are sedimentation and subsidence rates. Analyses of bedding thickness along with the relatively close proximity between all four measured sections suggest that differential subsidence was not a controlling factor in fluvial architecture. It is conjectured from the presence of thick amalgamated cycles within the proximal axial section that sedimentation exceeded subsidence rates. This conclusion differs from that of McLean and Jerzykiewicz (1978) for the Rocky Mountain Foredeep who suggested that under the same conditions maximum sedimentation should occur in distal regions. It is suggested that this discrepancy may be due to subsidence rates within the Cumberland Basin that are seven times faster than those from the Rocky Mountain foredeep. Thus sediment deposited in the proximal reaches would not have sufficient time to be transported to the distal areas.

Several alternative methods were used to study the interaction between sedimentation and tectonics. The statistical analysis of bedding thickness provided results consistent with field observations, The dearth of previous work on this subject makes some of the conclusions tenuous, but with further study it could prove to be very beneficial in subsurface work where the third dimension is lacking. Detailed clast analysis also showed that vertical and lateral trends of various parameters could theoretically be used to discern separate tectonic events from different uplands - assuming that clast provenance is known.

12.0 BIBLIOGRAPHY

Alexander, J. and Leeder, M.R., 1985. Tectonic controls on alluvial architecture: Third Int. Fluvial Sedim. Conf., (abs.), p.7.

Allen, J.R.L., 1964. Studies in fluviatile sedimentation: six cyclothems from the Lower Old Red Sandstone, Anglo-Welsh Basin: Sedimen., v.3, p.163-198.

_______, 1965. A review of the origin and characteristics of Recent alluvial sediments: Sedimen., v.5, p.89-191.

_______, 1967. Notes on some fundamental paleocurrent analyses, with reference to preservation potential and sources of variance: Sedimen., v.9, p.75-88.

_______, 1968. Current Ripples: North Holland Pub. Co., Amsterdam. p.433.

_______, 1969. Some advances in the physics of sedimentology: Geol. Ass. Proc. G. Brit., v.80, p.1-42.

_______, 1970. Studies in fluviatile sedimentation: a comparison of fining-upwards cyclothems, with special reference to coarse-member composition and interpretation: J. Sedim. Geol., v.40, p.298-323.

_______, 1974. Studies in fluviatile sedimentation: implications of pedogenic carbonate units, Lower Old Red Sandstone, Anglo Welsh outcrop: Geol. J., v.9, p.181-208.

_______, 1978. Studies in fluviatile sedimentation: an exploratory quantitative model of the architecture of avulsion controlled alluvial suites: Sedim. Geol., v.21, p.129-147.

_______, 1982. Sedimentary Structures, v.1: Elsevier, Amsterdam, p.593.

_______, 1983. Studies in fluviatile sedimentation: bars, bar-complexes and sandstone sheets (low sinuosity braided streams) in the Brownstones (L.Devonian), Welsh Borders: Sedim. Geol., v.33, p.237-293.

_______, 1984a. Parallel lamination developed from upper-stage plane beds: a model based on the larger coherent structures of the turbulent boundary layer: Sedimen. Geol., v.39, p.227-242.

_______, 1984b. Gravel overpassing on humpback bars supplied with mixed sediment: examples from the lower Old Red

Sandstone, southern Britain: Sedimen., v.30, p.285-294.

Andrews, E.D., 1983. Entrainment of gravel from naturally sorted riverbed material: Geol. Soc. Am. Bull., v.94, p.1225-1231

Baker, V.R., 1973. Paleohydrology and sedimentology of Lake Missoula flooding in eastern Washington: Spec. Pap. Geol. Soc. Am., v.144, p.79.

Ballance, P.E., 1980. Models of sedimentation in non-marine and shallow marine environments in oblique-slip fault zones: in Sedimentation in Oblique-slip Mobile Zones, eds. P.F. Ballance and H.G. Reading, Spec. Pub. Int. Ass. Sedim. 4, p.229-236.

Bankitz, P. von, 1965. Uber kluffe I. beobachtungen in Thuringshen Schiefergebige geologie: Zeits. Gesam. Mineral., v.14, p.241-253.

Beaumont, C., 1981. Foreland Basins: Geophys. J.R. Astron. Soc., v.65, p.291-329.

Beerbower, J.R., 1964. Cyclothems and cyclic depositional mechanisms in alluvial plain sedimentation: in Symposium on Cyclic Sedimentation, ed. D.F. Merriam, State Geol. Surv. Kansas Bull. 169, p.31-42.

Bell, W.A., 1914. Joggins Carboniferous section of Nova Scotia: Geol. Surv. Canada Sum. Rept. 1912, p.360-371.

, 1944. Carboniferous rocks and fossil floras of northern Nova Scotia: Mem. Geol. Surv. Canada 238., 277p.

, 1958. Possibilities for the occurrence of petroleum resevoirs in Nova Scotia: Nova Scotia Dept. Mines, p.175.

Belt, E.S., 1964, Revision of Nova Scotia middle Carboniferous units: Am. J. Sci., v.262, p.653-673.

, 1965. Stratigraphy and paleogeography of Mabou Group and related middle Carboniferous facies, Nova Scotia, Canada: Geol. Soc. Am. Bull., v.76, p.777-802.

, 1968. Post-Acadian rifts and related facies, eastern Canada: in Studies in Appalachain Geology, Northern and Maritime, ed. E-An Zen, W.S. White, and J.B. Hadley, p.95-113, Interscience, New York.

Bernard, H.A., Major, C.F., Parrot, B.S., and LeBlanc, R.J., 1970. Recent sediments of southeast Texas: Texas Bur. Econ. Geol. Guidebook 11.

Bird, J.M., and Dewey, J.F., 1970. Lithosphere plate-continental margin tectonics and evolution of the Appalachian Orogen: Geol. Soc. Am. Bull., v.81, p.1031-1060.

Blissenbach, E., 1954. Geology of alluvial fans in semi-arid regions: Geol. Soc. Am. Bull., v.65, p.175-190.

Blodgett, R.H., and Stanley, K.O., 1980. Stratification, bedforms and discharge relations of the Platte braided river system, Nebraska: J. Sedim. Petrol., v.50, p.139-148.

Bluck, B.J., 1967. Deposition of some Upper Old Red Sandstone conglomerates in the Clyde area: a study in the significance of bedding: Scot. J. Geol., v.3, p.139-167.

_____, 1976. Sedimentation in some non-sinuous Scottish rivers: Trans. R. Soc. Edinburgh, v.69, p.425-456.

_____, 1979. Structure of coarse grained braided stream alluvium: Trans. Roy. Soc. Edin., v.70, p.181-221.

_____, 1980. Evolution of a strike-slip fault-controlled basin, Upper Old Red Sandstone, Scotland: in Sedimentation in Oblique-slip Mobile Zones, eds. P.F. Ballance and H.G. Reading, Spec. Pub. Int. Ass. Sedim. 4, p.63-78.

Bokman, J.W., 1953. Lithology and petrology of the Stanley and Jackfork Formations: J. Geol., v.61, p.152-170.

_____, 1957. Suggested use of bed thickness measurements in stratigraphic descriptions: J. Sedim. Petrol., v.27, p.333-335.

Boothroyd, J.C., and Ashley, G.M., 1975. Process, bar morphology, and sedimentary structures on braided outwash fans, northeastern Gulf of Alaska: in Glaciofluvial, Glaciolacustrine Sedimentation, eds. A.V. Jopling and B.C. McDonald, Soc. Econ. Paleon. Mineral. Spec. Pub.23, p.193-222.

_____, and Nummedal, D. 1978. Proglacial braided outwash: a model for humid alluvial fan deposits: in Fluvial Sedimentolgy, ed. A.D. Miall, Can.Soc. Petrol. Geol. Mem 5, p.641-668.

Bown T.M., and Kraus M.J., 1981. Lower Eocene paleosols (Willwood Formation, Northwest Wyoming, USA) and their significance for paleoecology, paleoclimatology, and basin analysis: Paleog. Paleoclim. Paleoeco., v.34, p.1-30.

Bradley, D.C., 1982. Subsidence in late Paleozoic basins in the Northern Appalachians: Tectonics, v. 1, p. 107-123.

Bradley, W.C., 1970. Effect on abrasion of granitic gravel, Colorado River (Texas): Geol. Soc. Am. Bull., v.81, p.61-80.

_____, Fahnestock, R.K., and Rowekamp, E.T., 1972. Coarse sediment transport by flood flows on Knik River, Alaska: Geol. Ass. Am. Bull., v.83, p.1261-1284.

Bridge, J.S., and Leeder, M.R., 1979. A simulation model of alluvial stratigraphy: Sedimen., v.26, p.617-644.

_____, 1984. Large-scale facies sequences in alluvial overbank environments: J. Sedim. Petrol., v.54, p.583-588.

Calder, J.H., 1982. Preliminary Geological Map of the Cumberland Coal Basin: Nova Scotia Dept. Mines Open File Map 84-1.

_____, 1984. Depositional environment of the Westphalian B Cumberland Basin coals of Springhill, Nova Scotia: Maritime Sedim. Atlan. Geosci., v.20, p.92.

Campbell, C.V., 1976. Resevoir geometry of a fluvial sheet sandstone: Am. Ass. Petrol. Geol. Bull., v.60, p.1009-1020.

Cant, D.J., 1978. Development of a facies model for sandy braided sedimentation: comparison of the South Saskatchewan River and the Battery Point Formation: in Fluvial Sedimentology, ed. A.D. Miall, Can. Soc. Petrol. Geol. Mem.5, p.627-640.

_____, and Walker, R.G., 1976. Development of a braided fluvial facies model for the Devonian Battery Point Sandstone, Quebec: Can. J. Earth Sci., v.13, p.102-119.

_____, and _____, 1978. Fluvial processes and facies sequences in the sandy braided South Saskatchewan River, Canada: Sedimen., v.25, p.625-648.

Carr, T.R., 1982. Log-linear models, Markov chains and cyclic sedimentation: J. Sedim. Geol., v.52, p.905-912.

Church, M., 1972. Baffin Island sandurs: Geol. Surv. Can. Bull. 216, p.208.

_____, 1983. Pattern of instability in a wandering gravel bed channel: in Modern and Ancient Fluvial Systems, eds. J.D. Collinson and J. Lewin, Spec. Pub. Int. Ass. Petrol. Geol. 6, p.169-180.

, and Gilbert, R., 1975. Proglacial fluvial and lacustrine environments: in Glaciofluvial and Glaciolacustrine Sedimentation, eds. A.V. Jopling and B.C. McDonald, Soc. Econ. Paleon. Mineral.23, p.193-222.

Coleman, J.M., 1969. Brahmaputra river: channel processes and sedimentation: Sedim. Geol., v.3, p.129-239.

Collinson, J.D., 1970. Bedforms of the Tana River, Norway: Geogr. Annlr., v.52a, p.31-56.

, 1978. Vertical sequence and sandbody shape in alluvial sequences: in Fluvial Sedimentology, ed. A.D. Miall, Can. Soc. Petrol. Geol. Mem. 5., p.577-586.

Copeland, M.J., 1958. Coalfields, West half Cumberland County, Nova Scotia: Mem. Geol. Surv. Canada 298., 89p.

Cotter, E., 1978. The evolution of fluvial style, with special reference to the central Appalachian Paleozoic: in Fluvial Sedimentology, ed. A.D. Miall: Can. Soc. Petrol. Geol. Mem.5, p.361-383.

Cross, T.A., and Smith, N.D., 1985. Comparative anatomy of contemporary and ancient crevasse splay and anastomosed crevasse channel complexes: Third Int. Fluvial Sedim. Conference, (abs.) p.14.

Crowell, J.C., 1959. Directional current structures from the Alpine Flysch, Switzerland: Geol. Soc. Am. Bull., v.66, p.1351-1384.

Curray, J.R., 1956. The analysis of two-dimensional orientation data: J. Geol., v.41, p.117-131.

Dawson, J.W., 1854. On the coal-measures of the south Joggins, Nova Scotia: Quart. J. Geol. Soc. London, v.10, p.1-41.

Dewey, J.F., and Sengor, A.M.C., 1979. Aegean and surrounding regions: complex multiplate and continuum tectonics in a convergent zone: Geol. Soc. Am. Bull., v.80, p.84-92.

Dickenson, W.R., and Suscek, C.A., 1979. Plate tectonics and sandstone composition: Am. Ass. Petrol. Geol., v.63, p.2164-2182.

Donohoe, H.V., and Wallace, P.I., 1982. Geological Map of the Cobequid Highlands, Colchester, Cumberland, Pictou Counties, Nova Scotia: Nova Scotia Dept. Mines Map 82-6.

D'Orsay, A.M., and van de Poll, H.W., 1985. Quartz-grain surface textures: evidence for a tropical climate during the Middle Pennsylvanian in eastern Canada: Can. J. Earth Sci., v.22, p.786-790.

Duff, P.McL.D., and Walton,E.K., 1973. Carboniferous sediments at Joggins, Nova Scotia: 7th Int. Cong, Carb. Strat. Geol., v.2 p,365-379.

Englelund, F., and Fredsøe, J., 1974. Transition from dunes to plane beds in alluvial channels: Tech. Univ. Denmark, Lynby, Inst. Hydrodyn. and Hydraul. Eng. Series Paper 4, p.56.

Eugster, H.P., and, Surdam, R.C., 1973. Depositional environment of the Green River Formation of Wyoming: A preliminary report: Geol. Soc. Am. Bull., v.84, p.1115-1120.

, and Hardie L.A., 1975. Sedimentation in an ancient playa-lake complex: the Wilkins Peak Member of the Green River Formation: Geol. Soc. Am. Bull., v.86, p.319-334.

Ferguson, R.I., and Werrity, A., 1983. Bar development and channel changes in the gravelly River Endrick, Scotland: in Modern and Ancient Fluvial Systems, eds. J.D. Collinson and J. Lewin, Spec. Pub. Int. Ass. Sedim. 6, p.181-193.

Folk, R.L., 1957. Brazos river: A study in the significance of grain size parameters: J. Sed. Petrol., v.27, p.3-27.

, 1968. Petrology of Sedimentary Rocks: Hemphill's Book Store, Austin, p.236.

Fletcher, H., 1908. A section of Carboniferous rocks of Cumberland County Nova Scotia, 2) from Shulie to Spicer Cove by Hugh Fletcher B.A. of the Geol. Surv. Can. Proc. Trans. Nova Scotian Inst. Sci., v.11, p.417-550.

Fralick, P.W., and Schenk, P.E., 1980. Tectonic control of Late Paleozoic sedimentation along the southeastern flank of the Merigomish structural sub-basin, northeastern Nova Scotia: Geol. Ass. Can. Prog. Abs., v.5, p.54.

, and , 1981. Molasse deposition and basin evolution in a wrench tectonic setting: the Late Paleozoic, eastern Cumberland Basin, Maritime Canada: in Sedimentation and Tectonics in Alluvial Basins, ed. A.D. Miall, Geol. Ass. Can. Spec, Paper 23, p.77-97.

Friend, P.F. 1978. Distinctive features of some ancient river systems: in Fluvial Sedimentology, ed. A.D. Miall, Can. Soc. Petrol. Geol. Mem.5, p.531-542.

, 1983. Towards the field classification of alluvial architecture or sequence: in Modern and Ancient Fluvial Systems, eds. J.D. Collinson and J. Lewin, Spec. Pub. Int. Ass. Sedim. 6, p.345-354.

, Hirst, J.P.P., Nichols, G.J., Van Gelder, A., 1985. General aspects of radial river distributary systems in the Ebro Basin (Oligocene and Miocene), Spain: Third Int. Fluvial Sedim. Conf. (abs.).

, and Moody-Stuart, M., 1972. Sedimentation of the Wood Bay Formation (Devonian) of Spitsbergen: regional analysis of a late orogenic basin: Norsk Polar. Skrifter, v.157, p.1-77.

Galloway, W.E., 1981. Depositional architecture of Cenozoic Gulf coastal plain fluvial systems: in Recent and Ancient Nonmarine Depositional Environments: Models for Exploration, eds, F.G. Ethridge and R.M. Flores, Soc. Econ. Paleon. Mineral. Spec. Pub. 31, p.127-155.

Garland, G.D., 1953. Gravity measurements in the Maritime Provinces: Dept. Mines Tech. Surv. Can. Dominion Observatory, v.16.

Gersib, G.A., and McCabe, P.J., 1981. Continental coal-bearing sediments of the Port Hood Formation (Carboniferous), Cape Linzee, Nova Scotia, Canada: in Recent and Ancient Nonmarine Depositional Environments: Models for Exploration, eds. F.G. Ethridge and R.M. Flores, Soc. Econ. Paleon. Mineral. Spec. Pub.31, p.95-108.

Gibling, M., 1978. Sedimentation in the Siluro-Devonian clastic wedge of Somerset Island, Arctic Canada: Unpub. Ph.D., Univ. Ottawa, p.334.

, and Rust, B.R., 1984. Channel margins in a Pennsylvanian braided fluvial deposit: the Morien Group near Sydney, Nova Scotia, Canada: J. Sedim. Petrol., v.54, p.773-782.

Giles, P.S., and Ruitenberg, A.A., 1977. Stratigraphy, paleogeography and tectonic setting of the Coldbrook Group in the Caledonian Highlands of southern New Brunswick: Can. J. Earth Sci., v.14, p.1263-1275.

Gingerich, P.D., 1969. Markov analysis of cyclic alluvial sediments: J. Sedimen. Petrol., v.39, p.330-332.

Gloppen, T.G., and Steel, R., 1981. The deposits, internal structure and geometry in six alluvial -fan-fan delta bodies (Devonian, Norway) - a study in the significance of bedding sequences in conglomerates: in Recent and Ancient Nonmarine Depositional Environments: Models for Exploration, eds. F.G. Ethridge and R.M. Flores, Soc. Econ. Paleon. Mineral. Spec. Pub.31, p.49-69.

Goodman, L.A., 1968. The analysis of cross-classified data: interdependence, and interactions in contingency tables with or without missing entries: J. Am. Statis. Ass., v.63, p.1091-1131.

Gumbel, E.J., Greenwood, J.A., Durand, D., 1953. The circular normal distribution: theory and tables: Am. Stat. Ass. J., v.48, p.131-152.

Gustavson, T.C., 1974. Sedimentation on gravel outwash, Malaspina Glacier Foreland, Alaska: J. Sedim. Petrol., v.44, p.374-389.

Hacquebard, P.A., 1960. A summary of Carboniferous stratigraphy and palaeontology of the Maritime Provinces of Canada (contribution to the stratigraphic colloquium): 4th Int. Cong. Carb. Strat. Geol., p.233-235, Table 3.

_____, and Donaldson, J.R., 1964. Stratigraphy and palynology of the Upper Carboniferous coal measures in the Cumberland Basin of Nova Scotia, Canada: 5th Int. Cong. Carb. Strat. Geol., p.1157-1169.

_____, 1972. The Carboniferous of Eastern Canada: 7th Int. Cong. Carb. Strat. Geol. v.1, p.69-90.

Haliburton, T.C., 1829. An historical and statistical account of Nova Scotia, in two volumes. Illustrated by a map of the province, and several engravings, Halifax.

Harper, C.W., 1984. Improved methods of facies sequence analysis: in Facies Models, ed. R.G. Walker, Geoscience Canada Reprint Series 1, p.11-13.

Harvey, L.D.D., 1980. Shearing and kolking phenomena in fluvial sediments, Old Crow, Yukon Territory, Canada: J. Sedim. Petrol., v.50, p.787-792.

Hayward, A.B., 1983. Coastal alluvial fans and associated marine facies in the Miocene of S.W. Turkey: in Modern and Ancient Fluvial Systems, eds., J.D. Collinson and J. Lewin, Spec. Pub. Int. Ass. Sedim. 6, p.323-336.

_____, 1984. Sedimentation and basin formation related to ophiolite nappe emplacement, Miocene, S.W., Turkey: Sedim. Geol., v.40, p.105-129.

Hazeldine, R.S., 1983. Descending tabular cross-bed sets and bounding surfaces from a fluvial channel in the Upper Carboniferous coalfield of north-east England: in Modern and Ancient Fluvial Systems, eds. J.D. Collinson and J. Lewin, Spec. Pub. Int. Ass. Sedim., v.6, p.449-456.

Hein, F.J., 1984. Deep-sea and fluvial braided channel conglomerates: a comparison of two case studies: in Sedimentology of Gravel and Conglomerates, eds. E.H. Koster and R.J. Steel, Can. Soc. Petrol. Geol. Mem.10, p.33-49.

, and Walker, R.G., 1977. Bar evolution and development of stratification in the gravelly, braided Kicking Horse River, British Columbia: Can. J. Earth Sci., v.14, p.562-570.

Hempton, M.R., and Dunne, L.A., 1983. Sedimentation in pull-apart basins: active examples in eastern Turkey: J. Geol., v.92, p.513-530.

Heward, A.L., 1978. Alluvial fan sequence and megasequence models: with examples from Westphalian D - Stephanian B coalfields, Northern Spain: in Fluvial Sedimentology, ed. A.D. Miall, Can. Soc. Petrol. Geol. Mem.5, p.669-702.

A.L., and Reading, H.G., 1980. Deposits associated with Hercynian to late Hercynian continental strike-slip system, Cantabrian Mountains, Northern Spain: in Sedimentation in Oblique-Slip Mobile Zones, eds. P.F. Ballance and H.G. Reading, Spec. Pub. Int. Ass. Sedim. 4, p.105-125.

Horne, J.C., Ferm, J.C., Caruccio, F.T., and Baganz, B.P., 1978. Depositional models in coal exploration and mine planning in Appalachian region: Am. Ass. Petrol Geol. Bull., v.62, p.2379-2411.

Houghton, H.F., 1980. Refined techniques for staining plagioclase and alkali feldspars in thin section: J. Sedim. Petrol., v.50, p.629-630.

Howie, R.D., and Barss, M.S., 1975. Paleogeography and sedimentation in the Upper Paleozoic, eastern Canada: Mem. Can. Soc. Petrol. Geol., v.4, p.45-57.

Hunt, J.W., and Hodday, D.K., 1984. Petrographic composition and sulphur content of coals associated with alluvial fans in the Permian Sydney and Gunnedah Basins, eastern Australia: in: Sedimentology of Coal and Coal-Bearing Sequences, eds. R.A. Rahmani and R.M. Flores, Spec. Pub. Int. Ass. Sedim. 7, p.43-60.

Hyne, N.J., Cooper, W.A., and Dickey, P.A., 1979. Stratigraphy of intermontane, lacustrine delta, Catumbo River, Lake Maracaibo, Venezuela: Am. Ass. Petrol. Geol., v.63, p.2012-2057.

Ingersol, R.V., 1978. Petrofacies and petrologic evolution of the Late Cretaceous fore-arc basin, northern and central California: J. Geol., v.86, p.335-352.

Irving, E., and Strong, D.F., 1984. Paleogeography of the early Carboniferous Deer Lake Group western Newfoundland: no evidence for mid-Carboniferous displacement of "Acadia": Earth Plan. Sci. Letters, v.69, p.379-390.

Jackson, R.G. II, 1976a. Largescale ripples of the lower Wabash River: Sedimen., v.23, p.593-623.

1976b. Depositional model of point bars in the lower Wabash River: J. Sedim. Petrol., v.46, p.579-594.

, 1978. Preliminary evaluation of lithofacies models for meandering alluvial streams: in Fluvial Sedimentology, ed. A.D. Miall, Can. Soc. Petrol. Geol. Mem.5, p.543-576.

Jerzykiewicz, T., and Sweet, A.R., 1985. Stratigraphy and sedimentology of coal-bearing Upper Cretaceous-Paleocene Saunders Group, Central Alberta Foothills between Athabaska and Blackstone Rivers: Geol. Surv. Can. Paper 85-8, p.8.

Jopling, A.V., 1965. Hydraulic factors controlling the shape of laminae in laboratory deltas: J. Sedim. Petrol., v.35, p.777-791.

, and Walker, R.G., 1968. Morphology and origin of ripple-drift cross-lamination, with examples from the Pleistocene of Massachusetts: J. Sed. Petrol., v.38, p.971-984.

Jones, C.M., 1977. Effects of varying discharge regimes on bed-form sedimentary structures in modern rivers: Geol., v.5, p.567-570.

Kaplan, S.S., and Donahue, J., 1980. Sedimentologic description of part of coal-bearing Carboniferous sequence exposed near Joggins, Nova Scotia: Am. Ass. Petrol. Geol. Bull., v.64, p.730-731.

Kemeny, J.C., and Snell, J.L., 1960. Finite Markov Chains: Princeton, Van Nostrand, p.210.

Kent, D.V., and Opdyke, N.D., 1978. Paleomagnetism of the Devonian Catskill red beds: Evidence for motion of the coastal New England-Canadian Maritime region relative to cratonic North America: J. Geophys. Res., v.83, p.4412-4450.

_, and, _ _ _, 1979. The early Carboniferous paleomagnetic field of North America and its bearing on tectonics of the northern Appalachians: Earth Planet. Sci. Lett., v.44, p.356-372.

Keppie, J.D., 1977. Plate tectonic interpretation of Paleozoic world maps (with emphasis on circum-Atlantic Orogens and southern Nova Scotia): Nova Scotia Dept. Mines Paper 77-3, p.1-45.

_, 1985. The Appalachian collage: in The Caledonide Orogen Scandanavia and Related Areas, eds. D.G. Gee and B.A. Sturt, Wiley Pub., Chichester, p.1267.

Kindle, E.D., 1962. Geology Point Wolfe, New Brunswick: Geol. Surv. Map 1109A.

Kolomogorov, A.N., 1951. Solution of a math problem in probability theory connected with the problem of the mechanism of stratification: Am. Math. Soc. Trans., v.53, p.8.

Korsch, R.J., 1984. Sandstone compositions from the New England Orogen, eastern Australia: implications for tectonic setting: J. Sedim. Petrol., v.54, p.192-211.

Kuenen, P.H., 1956. Experimental abrasion of pebbles: 2. rolling by current: J. Geol. v.64, p.336-368.

Kumar, P., and Tandon, S.K., 1985. Sedimentology of Plio-Pleistocene late orogenic deposits associated with intraplate subduction - the Upper Siwalik Subgroup of a part of Panjab Sub-Himalaya, India: Sedim. Geol., v.42, p.105-158.

Langbein, W.B., and Leopold, L.B., 1966. River meanders - theory of minimum variance: Prof. Pap. U.S. Geol. Surv., 422-H.

Leeder, M.R., 1973. Fluviatile fining-upward cycles and the magnitude of paleochannels: Geol. Mag., v.110, p.265-276.

_, 1975. Pedogenic carbonates and flood sediment accretion rates: a quantitative model for alluvial arid-zone lithofacies: Geol. Mag., v.112, p.257-270.

Logan, W.E., 1845. A section of the Nova Scotia coal measures as developed at the Joggins, on the Bay of Fundy, in descending order, from the neighbourhood of the West Ragged Reef to Minudie, reduced to vertical thickness: Rep. Prog. Geol. Surv. Canada 1843, Appendix, 92-153.

Lyell, C., 1843. On the coal-formation of Nova Scotia, and on the age and relative position of the gypsum and accompanying marine limestones: Proc. Geol. Soc. London, v.4, p.184-186.

, and Dawson, J.W., 1853. On the remains of a reptile (Dendrepeton Acadianum Wyman and Owen) and of a land shell discovered in the coal measures of Nova Scotia: Quart. J. Geol. Soc. London, v.9, p.58-63.

Mack, G.H., and Rasmussen, K.A., 1984. Alluvial fan sedimentation of the Cutler Formation (Permo-Pennsylvanian) near Gateway Colorado: Geol. Soc. Am. Bull., v.95, p.109-116.

Mader, D., and Teyssen, T., 1985. Paleoenvironmental intepretation of fluvial red beds by statistical analysis of paleocurrent data: examples from the Bundsandstein (Lower Triassic) of the Eifel and Bavaria in the German Basin (Middle Europe): Sedim. Geol., v.41, p.1-74.

Mardia, K.V., 1972. Statistics of Directional Data: Academic Press, London, p.357.

Martini, I.P., and Salas, C.J., 1983. Depositional characteristics of the Whirlpool Sandstone, Lower Silurian: Ont. Geol. Surv. Open File Report 5363, p.121.

Matthes, G., 1947. Macroturbulence in natural streams: Trans. Am. Geophy. Union, v.28, p.255-261.

McBride, E.F., 1962. Flysch and associated beds of the Martinsburg Formation (Ordovician), central Appalachians: J. Sedim. Petrol., v.32, p.39-92.

______, 1963. A classification of common sandstones: J. Sedim. Petrol., v.33, p.664-669.

McDonald, D.I.M., and, Jefferson, T.H., 1985. Orientation studies of waterlogged wood: a paleocurrent indicator?: J. Sedim. Petrol., v.55, p.235-239.

McLean, J.R., and Jerykiewicz, T., 1978. Cyclicity, tectonics, and coal: some aspects of fluvial sedimentology in the Brazeau-Paskapoo Formations, Coal Valley Area, Alberta, Canada: in Fluvial Sedimentology, ed. A.D. Miall, Can. Soc. Petrol. Geol. Mem.5, p.441-468.

McManus, D.A., 1963. A criticism of certain usage of the phi notation: J. Sedim. Petrol., v.33, p.670-674.

Miall, A.D., 1973. Markov chain analysis applied to an ancient alluvial plain succession: Sedimen., v.20, p.347-364.

_, 1974. Paleocurrent analysis of alluvial sediments: a discussion of directional variance and vector magnitude: J. Sedimen. Geol., v.44, p.1174-1185.

_, 1976. Paleocurrent and paleohydrologic analysis of some vertical profiles through a Cretaceous braided stream deposit, Banks Island, Arctic Canada: Sedimen., v.23, p.459-483.

_, 1977. A review of the braided river depositional environment: Earth Sci. Revs., v.13, p.1-62.

_, 1978. Lithofacies types and vertical profile models in braided river deposits: a summary. in Fluvial Sedimentology, ed. A.D. Miall, Mem. Can. Soc. Petrol. Geol., v.5, p.597-604.

_, 1980. Cyclicity and the facies model concept in fluvial deposits: Bull. Can. Pet. Geol., v.28, p.59-80.

_, 1981. Alluvial sedimentary basins: tectonic setting and basin architecture. in Sedimentation and Tectonics in Alluvial Basins, ed. A.D. Miall, Geol. Ass. Can. Spec. Paper 23, p.1-33.

_, 1985. Variations in fluvial style in the Lower Cenozoic synorogenic sediments of the Canadian Arctic Islands: Sedim. Geol., v.38, p.499-523.

Middleton, G.V., 1976. Hydraulic interpretation of sand size distributions: J. Geol., v.84, p.405-426.

_, 1977. Introduction. in Hydraulic Interpretation of Primary Sedimentary Structures, ed. G.V. Middleton, Soc. Econ. Paleon. Mineral. Reprint Series 4, p.1-15.

_, 1978. Facies. in Encyclopedia of Sedimentology, eds. R.W. Fairbridge and J. Bourgeouis, Dowden Hutchinson and Ross Pub. Stroudsburg, p.323-325.

_, Rutka, M.A., and Salas, C.J., 1985. Braided fluvial origin of the Whirlpool Sandstone (Lower Silurian) Ontario: Third Int. Fluvial Sedim. Conf. (abs.), p.29.

_, Salas, C.J., and Martini, I.P., 1983. Whirlpool Sandstone (Silurian) of southern Ontario, a braided river deposit?: Geol. Soc. Am., (abs.), v.15.

, and Southard, J.B., 1984. Mechanics of sediment movement: Soc. Econ. Paleon. Mineral. Short Course 3, 2nd ed.

Mills, H.H., 1984. Clast orientation in Mount St. Helens debris-flow deposits, north fork Toutle River, Washington: J. Sedim. Petrol., v.54, p.626-634.

Morris, W.A., 1976. Transcurrent motion determined paleomagnetically in the northern Appalachians and Caledonides and the Acadian Orogeny: Can. J. Earth Sci, v.13, p.1236-1243.

Muir, A.D., and Rust, B.R., 1982. Sedimentology of a lower Devonian coastal alluvial fan complex: the Snowblind Bay Formation of Cornwallis Island, Northwest Territories, Canada: Can. Soc. Petrol. Geol. Bull., v.30, p.245-263.

Nami, M., and Leeder, M.R., 1978. Changing channel morphology and magnitude in the Scalby Formation (M. Jurassic) of Yorkshire, England: in Fluvial Sedimentology, ed. A.D. Miall, Can. Soc. Petrol. Geol. Mem.5, p.431-440.

Nanson, G.C., and Rust, B.R., 1985. Channel patterns and mud deposition in an arid-zone river: Cooper Creek, Central Australia: Third Int. Fluvial Sedim. Conf. (abs.), p.31.

Nemec, W., and Steel, R.J., 1984. Alluvial and coastal conglomerates: their significant features and some comments on gravelly mass-flow deposits: in Sedimentology of gravels and Conglomerates, eds. E.H. Koster and R.J. Steel, Can. Soc. Petrol. Geol. Mem.10, p.1-31.

Pearce, T.H., 1971. Short distance fluvial rounding of volcanic detritus: J. Sedim. Petrol., v.41, p.1069-1072.

Peel, B., 1972. Steamboats on the Saskaktchewan: Prairie Books, Saskatoon, p.238.

Pittman, E.D., and Ovenshine, A.T., 1967. Pebble morphology in the Merced River (California): Sedim. Geol., v.2, p.125-140.

Poole, W.H., 1967. Tectonic evolution of the Appalachian region of Canada in Geology of the Atlantic Region, eds. E.R.W. Neale and H. Williams, Geol. Ass. Can. Spec. Paper 4, p.9-51.

Potter, P.E., and Sheidegger, A.E., 1966. Bed thickness and grain size: graded beds: Sedimen., v.7, p.233-240.

Powers, D.W., and Easterling, R.G., 1982. Improved methodology for using embedded markov chains to describe cyclical sediments: J. Sedimen. Petrol., v.52, p.913-923.

Powers, M.C., 1953. A new roundness scale for sedimentary particles: J. Sedim. Petrol., v.23, p.117-119.

Press, F. and Seiver, R., 1978. Earth: 2nd Ed. W.H. Freeman and Co., San Fransisco, p.649.

Rast, N., and Grant, R.J., 1973. The Variscan front in southern New Brunswick: Am. J. Sci., v.273, p.572-579.

_____, Kennedy, M.J., and Blackwood, R.F., 1976. Comparison of some tectonostratigraphic zones in the Appalachians of Newfoundland and New Brunswick: Can. J. Earth Sci., v.13, p.868-875.

Reading, H.G., 1980. Characteristics and recognition of strike-slip fault systems: in Sedimentation in Oblique-Slip Mobile Zones, eds. P.F. Ballance and H.G. Reading, Spec. Pub. Int. Ass. Sedim. 4, p.7-26.

Ruitenberg, A.A., Venugopal, D.V., Giles, P.S., 1973. Fundy Cataclastic Zone: evidence for post-Acadian penetrative deformation: Geol. Soc. Am. Bull., v.84, p.3029-3044.

Russel, R.D., 1939. Effects of transportation on sedimentary particles: in Recent Marine Sediments, ed. P.D. Trask, Am. Ass. Petrol. Geol., p.32-47.

Rust, B.R., 1972. Structure and process in a braided river: Sedimen., v.18, p.221-246.

_____, 1978a. A classification of alluvial channel systems: in Fluvial Sedimentology, ed. A.D. Miall, Can. Soc. Petrol. Geol. Mem.5, p.187-198.

_____, 1978b. Depositional models for braided alluvium: in Fluvial Sedimentology, ed. A.D. Miall, Mem. Can Soc. Petrol. Geol., v.5, p.605-625.

_____, 1981a. Alluvial deposits and tectonic style: Devonian and Carboniferous successions in eastern Gaspé: in Sedimentation and Tectonics in Alluvial Basins, ed. A.D. Miall, Geol. Ass. Can. Spec. Paper 23, p.49-76.

_____, 1981b. Sedimentation in an arid-zone anastomosing fluvial system: Cooper's Creek, Central Australia: J. Sed. Petrol., v.51, p.745-755.

_____, 1984a. Proximal braidplain deposits in the Middle Devonian Malbaie Formation of eastern Gaspé, Quebec, Canada: Sedim., v.31, p.675-695.

, 1984b. The Cannes de Roche Formation: Carboniferous alluvial deposits in eastern Gaspé, Canada: Comptes Rendus, 12th Int. Carb. Cong., v.3, p.72-84.

, and Jones, B.G., 1985., Hawkesbury Sandstone of New South Wales, Australia: Triassic analogue for a large braided river deposit: (pers. comm.)

, Gibling, M.R., and Legun, A.S., 1984. Coal deposition in an anastomosing-fluvial system: the Pennsylvanian Cumberland Group south of Joggins, Nova Scotia, Canada. in Spec. Publs. Int. Ass. Sed., v.7, p.105-120.

, and Koster, E., 1984. Coarse alluvial deposits: in Facies Models, ed. R.G. Walker, Geoscience Reprint Series 1, p.53-69.

, and Legun, A,S., 1983. Modern anastomosing deposits in arid Central Australia, and a Carboniferous analogue in New Brunswick, Canada: in Modern and Ancient Fluvial Systems, eds. J.D. Collinson, and J. Lewin, Spec. Pub. Int. Ass. Sedim. 6, p.385-392.

Salas, C.J., and Rust, B.R., 1985. Distal gravelly braidplain deposits, the Pennsylvanian Cumberland Group, southwest of Sand River, Nova Scotia: Geol. Ass. Can. (abs.), p.A53.

Schenk, P.E.; 1975. Paleozoic evolution of African Nova Scotia - polar and deep to equatorial and continental: Inter. Congr. Sed. IXth, p.17-24.

, 1978. Synthesis of the Canadian Appalachians: Geol. Surv. Canada Paper 78-13, p.111-136.

Schumm, S.A., 1968. Speculations concerning paleohydrologic controls of terrestrial sedimentation: Geol. Soc. Am. Bull., v.70, p.1573-1588.

, and Stevens, M.A., 1973. Abrasion in place: a mechanism for rounding and size reduction of coarse sediments in rivers: Geol., v.1, p.37-40.

Schwarzacher, W., 1953. Cross-bedding and grain size in the Lower Cretaceous sands of east Anglia: Geol. Mag., v.90, p.322-330.

Scotese, C.R., Rambach, R.K., Barton, C., Van der Voo, R., and Zeigler, A.M., 1979. Paleozoic base maps: J. Geol., v.87, p.217-277.

Selley R.C., 1968. A classification of paleocurrent models: J. Geol., v.76, p.99-110.

_____, 1970. Studies of sequence in sediments using a simple mathematical device: Geol. Soc. London Quart. J., v.125, p.557-581.

Sengor, A.M.C., 1979. The North Anatolian transform fault: its age, offset, and tectonic significance: J. Geol. Soc. London, v.136., p.269-282.

Shaw, W.S., 1951. The Cumberland basin of deposition: Mass. Inst. Tech. unpub. Ph.D., 148p.

Smith, D.G., 1980. Sedimentation in anastomosed river systems: examples from alluvial valleys near Banff, Alberta: J. Sedim. Petrol., v.50, p.157-164.

_____, 1983. Anastomosed fluvial deposits: modern examples from western Canada: in Modern and ancient fluvial systems, eds. J.D. Collinson and J. Lewin, Int. Ass. Sedim. Spec. Pub. 6, p.155-168.

_____, and Putnam, P.E., 1980. Anastomosed river deposits: modern and ancient examples in Alberta, Canada: Can. J. Earth Sci., v.17, p.1396-1406.

_____, and Smith, N.D., 1980. Sedimentation in anastomosed river systems: examples from alluvial valleys near Banff, Alberta: J. Sedim. Petrol., v.50, p.157-164.

Smith, N.D., 1970. The braided stream depositional environment: a comparison of the Platte River with some Silurian clastic rocks, north-central Appalachians: Geol. Soc. Am. Bull., v.81, p.2993-3014.

_____, 1972. Some sedimentological aspects of planar cross-stratification in a sandy braided river: J. Sedim. Petrol., v.42, p.624-634.

Sneed, E.D., and Folk, R.L., 1958. Pebbles in the Lower Colorado River, Texas, a study in particle morphogenesis: J. Geol., v.66, p.114-150.

Steel, R., 1974. New Red Sandstone floodplain and piedmont sedimentation in the Hebridean province, Scotland. J. Sedim. Petrol., v.44, p.336-357.

_____, and Gloppen, T.R., 1980. Late Caledonian (Devonian) basin formation, western Norway: signs of strike-slip tectonics during infilling: in Sedimentation in Oblique-Slip Mobile Zones, eds. P.F. Ballance and H.G. Reading, Spec. Pub. Int. Ass. Sedim. 4, p.79-103.

_____, Maehle, S., Nilsen, H., Roe, S.L. and Spinnangr, A., 1977. Coarsening upward cycles in the alluvium of Hornelen Basin (Devonian), Norway: sedimentary response to tectonic events: Geol. Soc. Am. Bull., v.88, p.1124-

1134.

, and Thompson, D.B., 1983. Structures and textures in Triassic braided stream conglomerates ("Bunter Pebble Beds") in the Sherwood Sandstone Group, North Staffordshire, England: Sedimen., v.30, p.341-367.

Stephens, M.A., 1969. Tests for randomness of directions against two circular alternatives: J. Amer. Statis. Ass., v.64, p.280-289.

Surdam, R.C., and Wolfbauer, C.A., 1975. Green River Formation, Wyoming: a playa-lake complex: Geol. Soc. Am. Bull., v.86, p.335-345.

Tandon, S.K., Kumar, P., and Singh, P., 1985. Syntectonic controls of paleoflow reversals and variability: sediment-vector sequences in the late orogenic Siwalik Basin, Panjab Sub-Himalaya, India: Sedim. Geol., v.41, p.97-112.

Van der Voo, R., French, A.N., and French, R.B., 1979. A paleomagnetic pole position from the folded Upper Devonian Catskill redbeds, and its tectonic implications: Geology, v.7, p.345-348.

, and Scotese C., 1981. Paleomagnetic evidence for a large (approximately 2000km) sinistral offset along the Great Glen fault during Carboniferous time: Geology, v.9, p.583-589.

Visser, C.F., and Johnson, G.D., 1978. Tectonic control of Late Pliocene molasse sedimentation in a portion of the Jhelum re-entrant, Pakistan: Geol. Rund., v.67, p.15-37.

Walker, R.G., 1984. General introduction: facies, facies sequences and facies models: in Facies Models, ed. R.G. Walker, Geoscience Canada Reprint Series 1, p.1-9.

, and Cant, D.J., 1984. Sandy fluvial systems: in Facies Models, ed. R.G. Walker, Geoscience Series Reprint Series 1, p.71-89.

Way, J.H., 1968. Bed thickness analysis of some Carboniferous fluvial sedimentary rocks near Joggins, Nova Scotia: Jour. Sed. Petrol., v. 38, p.424-433.

Webb, G.A., 1963. Occurrence and exploration significance of strike-slip faults in southern New Brunswick: Am. Ass. Petrol. Geol. Bull., v.47, p.1904-1927.

, 1969. Paleozoic wrench faults in the Canadian Appalachians: Mem. Am. Ass. Petrol. Geol., v.12, p.754-786.

Whitaker, J.H. McD., 1973. "Guttercasts" a new name for scour-and-fill structures: with examples from the Llandoverian of Rjngerike and Malnoya, southern Norway: Norsk Geol. Tidd., v.53, p.403-417.

Williams, H., 1964. The Appalachians in Northeastern Newfoundland - a two-sided symmetrical system: Am. J. Sci., v.262, p.1137-1158.

_____, 1976. Tectonic-stratigraphic subdivisions of the Appalachian Orogen (abs.): Geol. Soc. Am., v.8, p.300.

_____, 1978. Tectonic-lithofacies map of the Appalachain Orogen, Map 1, Memorial University of Newfounland.

_____, 1979. Appalachian orogen in Canada: Can. J. Earth Sci., v.16, p.792-807.

Williams, P.F., and Rust,B.R., 1969. The sedimentology of a braided river: J. Sedim. Petrol., v.39, p.649-679.

Zaitlin, B.A., and Rust, B.R., 1983. A spectrum of alluvial deposits in the Lower Carboniferous Bonaventure Formation of western Chaleur Bay area, Gaspe and New Brunswick, Canada: Can. J. Earth Sci., v.20, p.1098-1110.

Zingg, T., 1935. Beitrage zur schotteranalyse: Schweiz. Min. Pet. Mitt., v.15, p.39-140.

APPENDIX 1

LOCATION OF SAMPLES

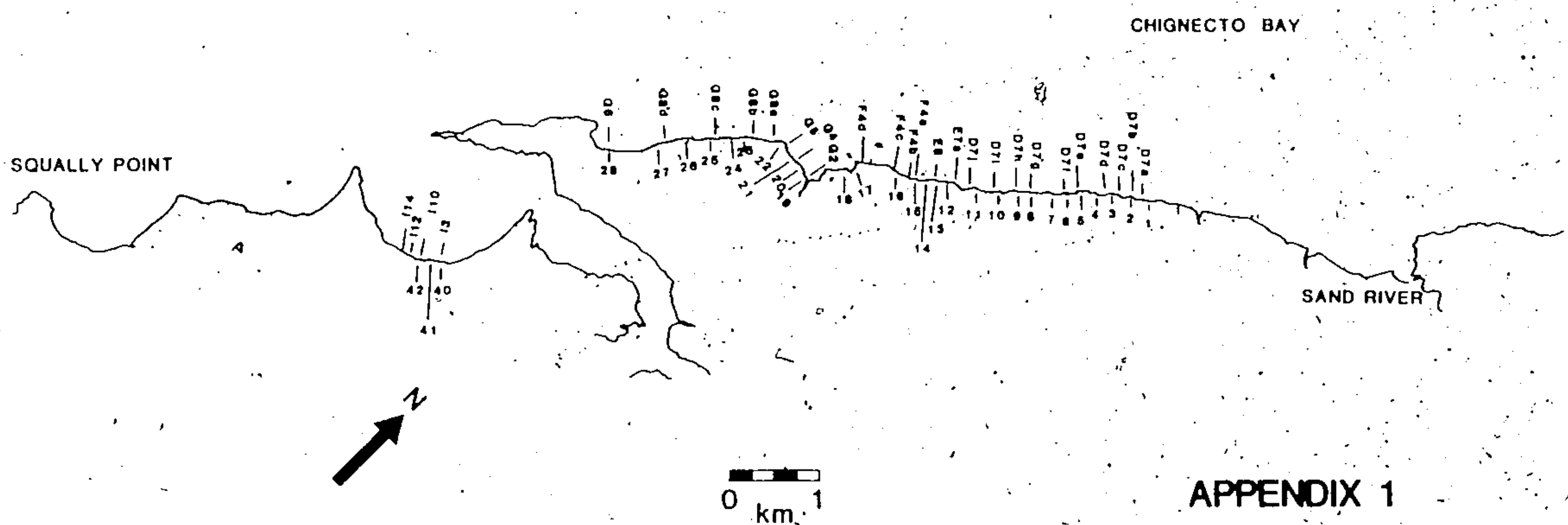

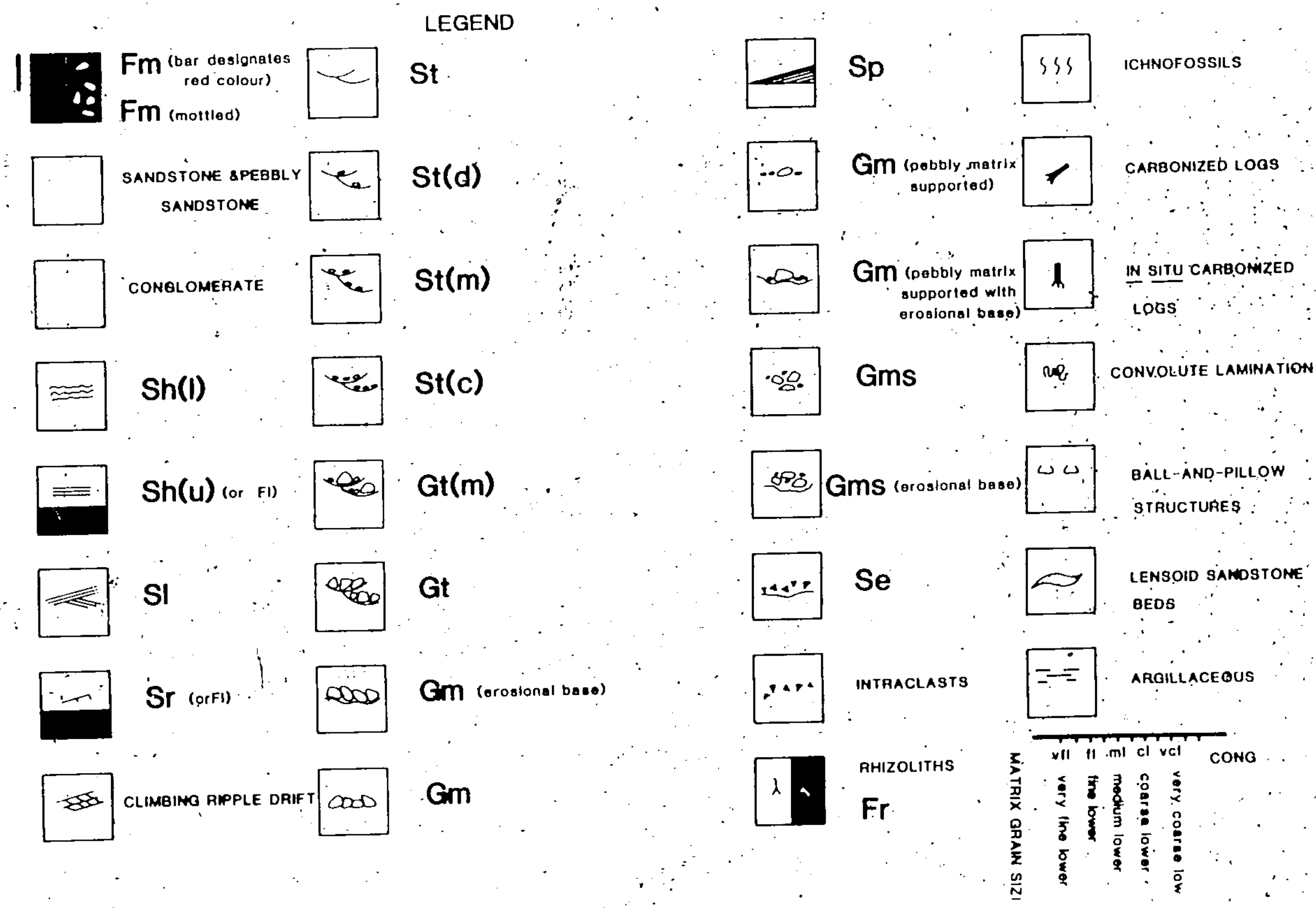
LEGEND
Fm (bar designates red colour)
Fm (mottled)
SANDSTONE &PEBBLY SANDSTONE
CONGLOMERATE
Sh(l)
Sh(u) (or Fl)
Sl
Sr (orFl)
CLIMBING RIPPLE DRIFT
St
St(d)
St(m)
St(c)
Gt(m)
Gt
Gm (erosional base)
Gm
Sp
Gm (pebbly matrix supported)
Gm (pebbly matrix supported with erosional base)
Gms
Gms (erosional base)
Se
INTRACLASTS
RHIZOLITHS
Fr
ICHNOFOSSILS
CARBONIZED LOGS
IN SITU CARBONIZED LOGS
CONVOLUTE LAMINATION
BALL-AND-PILLOW STRUCTURES
LENSOID SANDSTONE BEDS
ARGILLACEOUS
MATRIX GRAIN SIZI
vfl very fine lower
fl fine lower
ml medium lower
cl coarse lower
vcl very coarse low
CONG

APPENDIX 2

SECTION 01

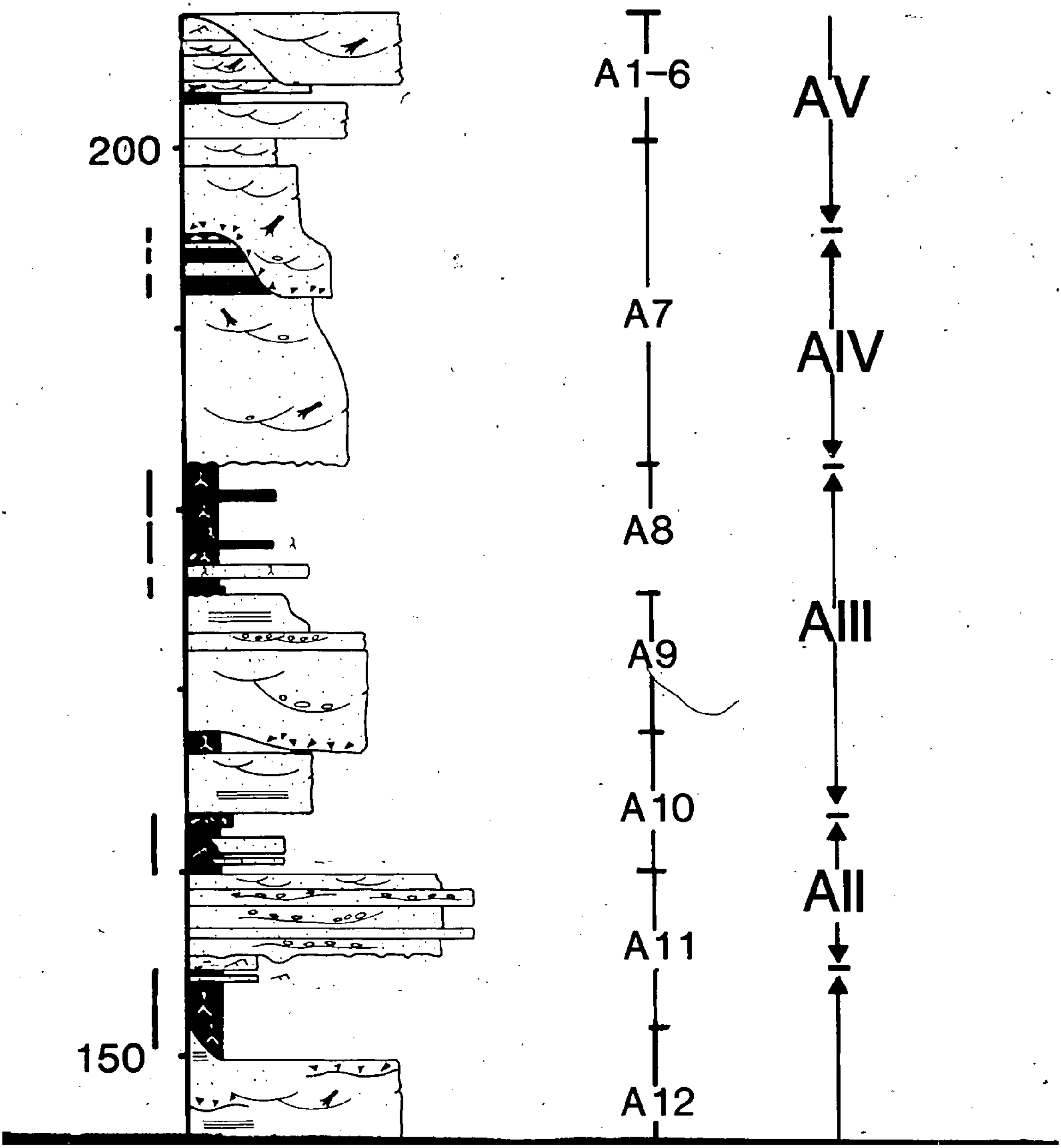

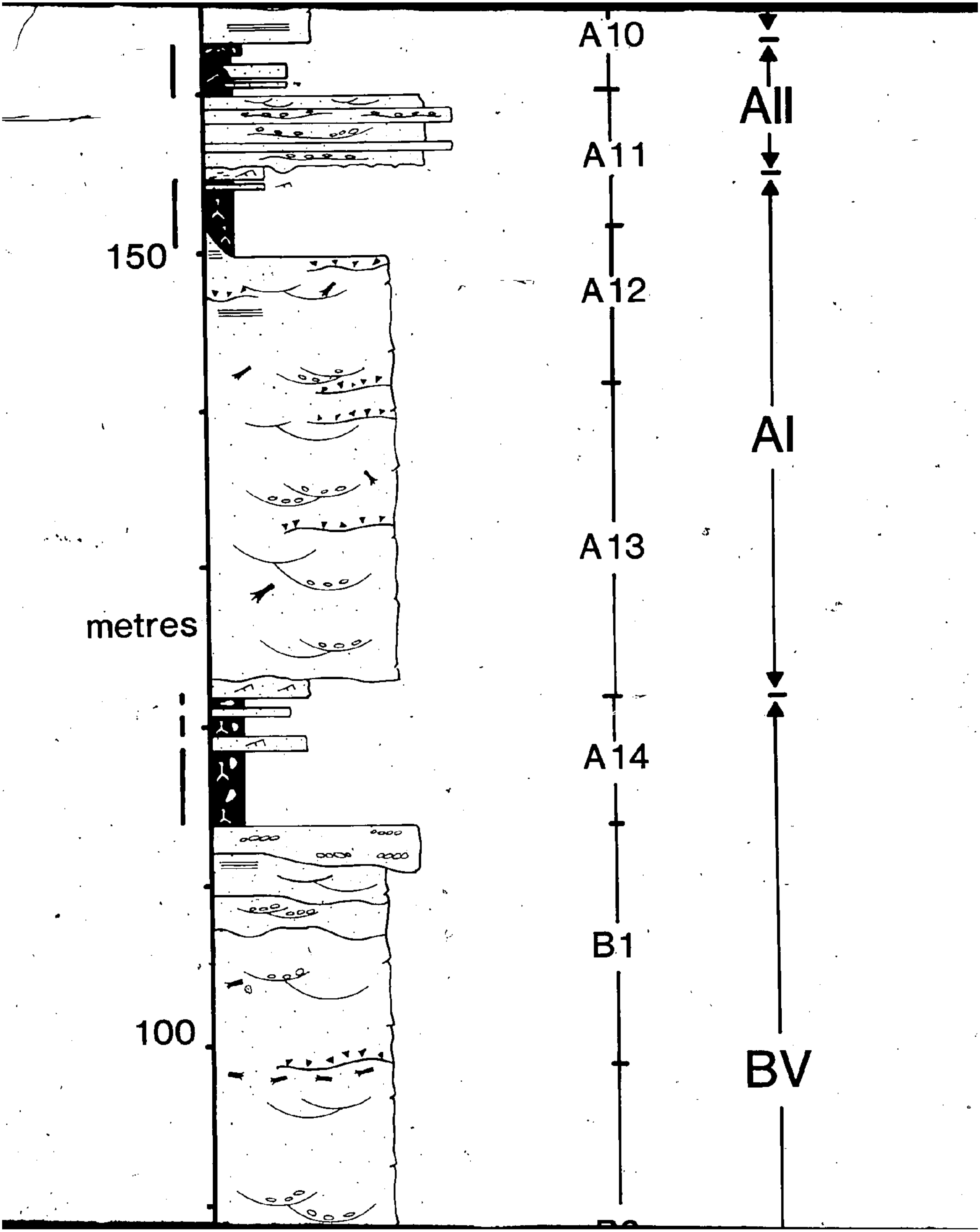
A10
AII
A11
150
A12
AI
A13
metres
A14
B1
100
BV

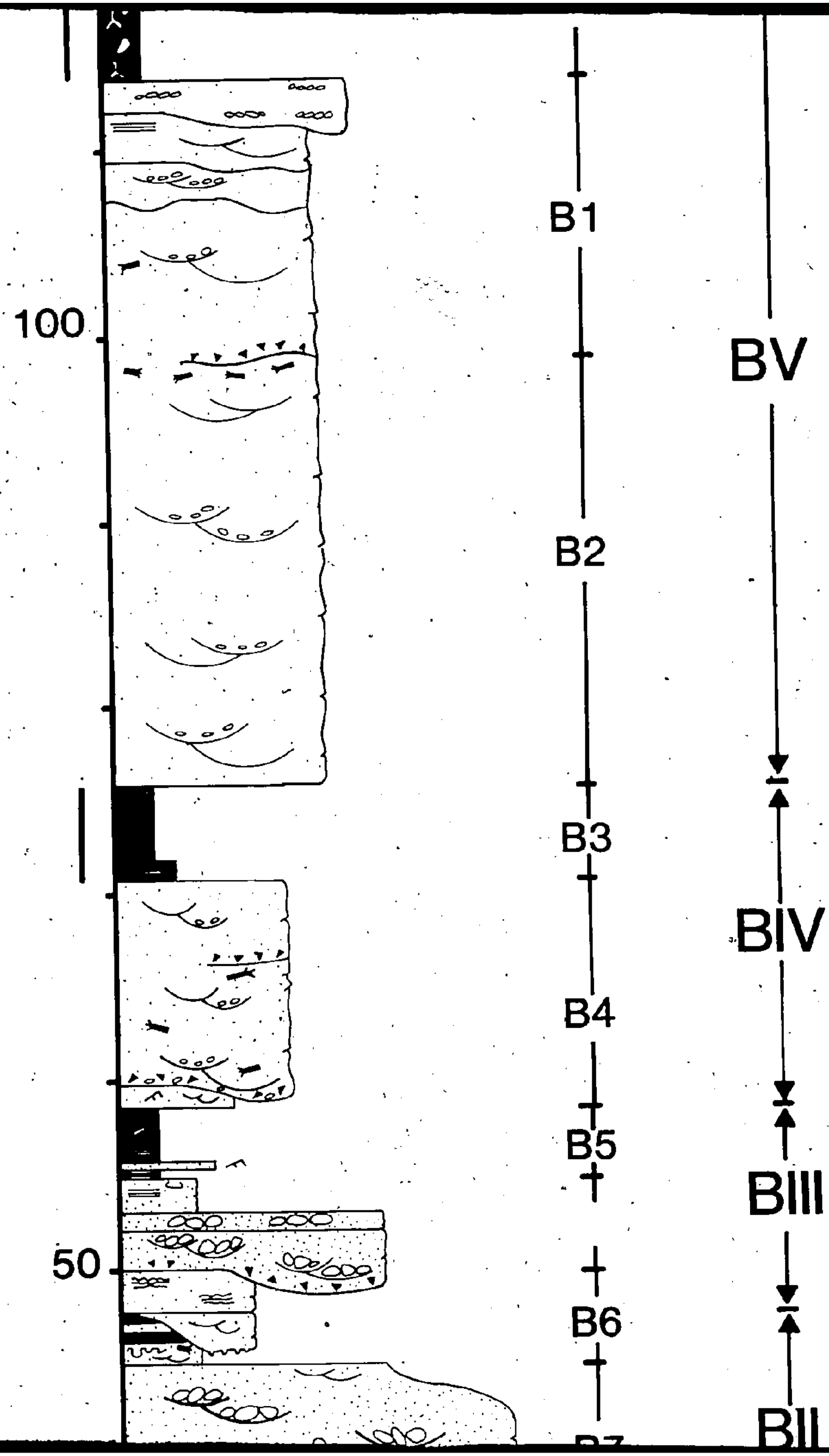

100
50
B1
B2
B3
B4
B5
B6
BV
BIV
BIII
BII

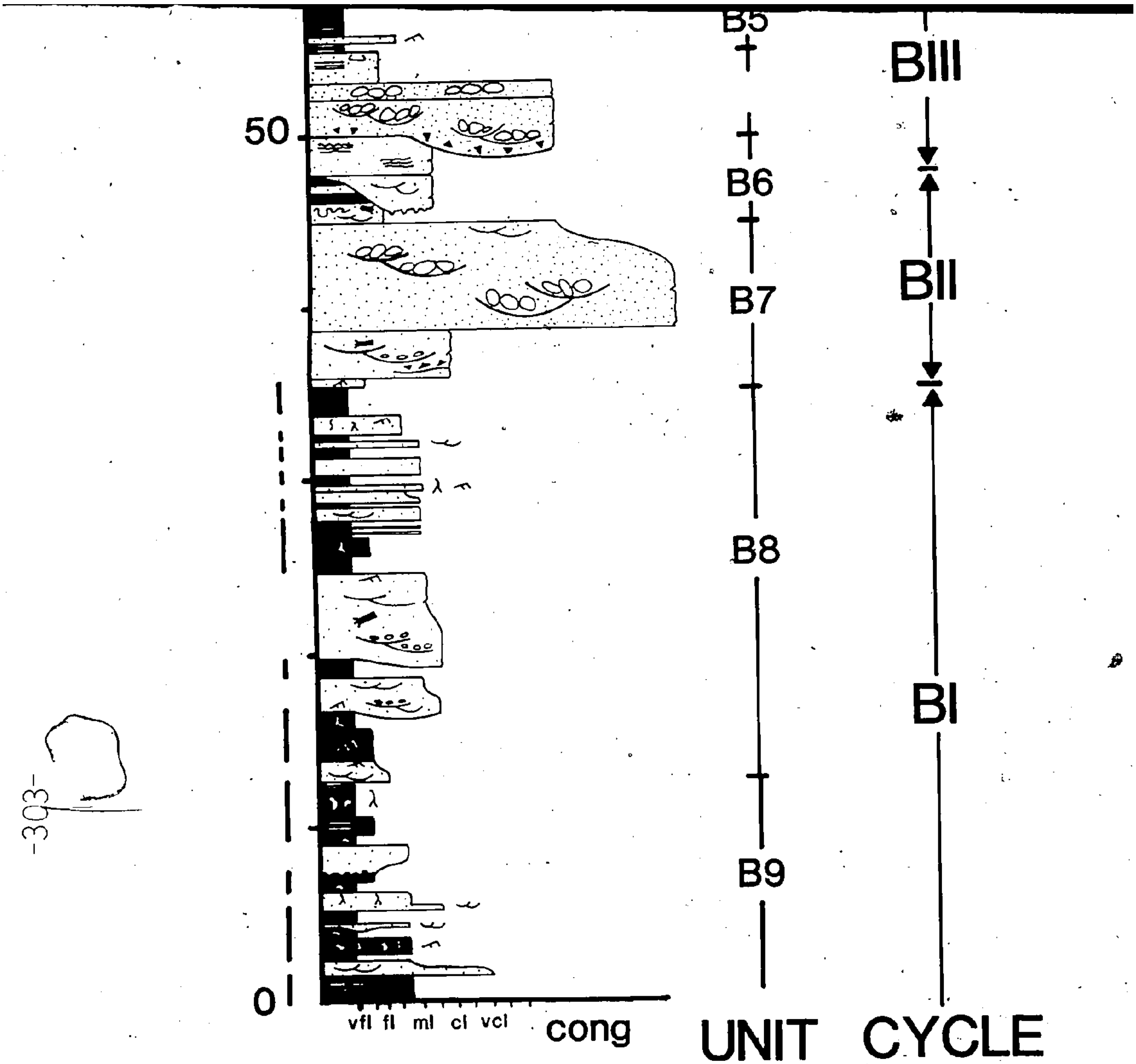
B5
BIII
50
B6
B7
BII
B8
BI
B9
0
vfl fl ml cl vcl
cong
UNIT
CYCLE

APPENDIX 3

SECTION 02

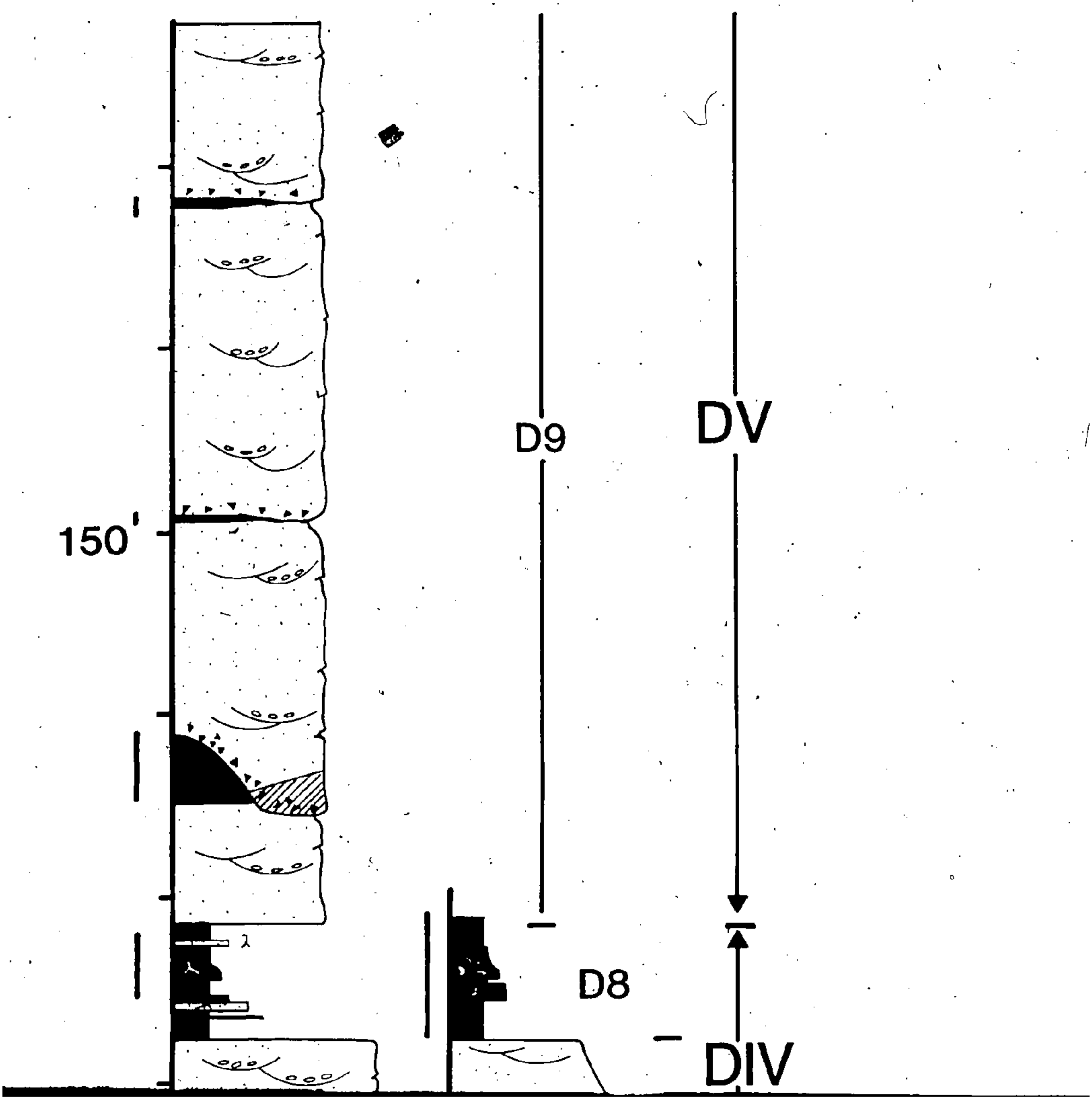

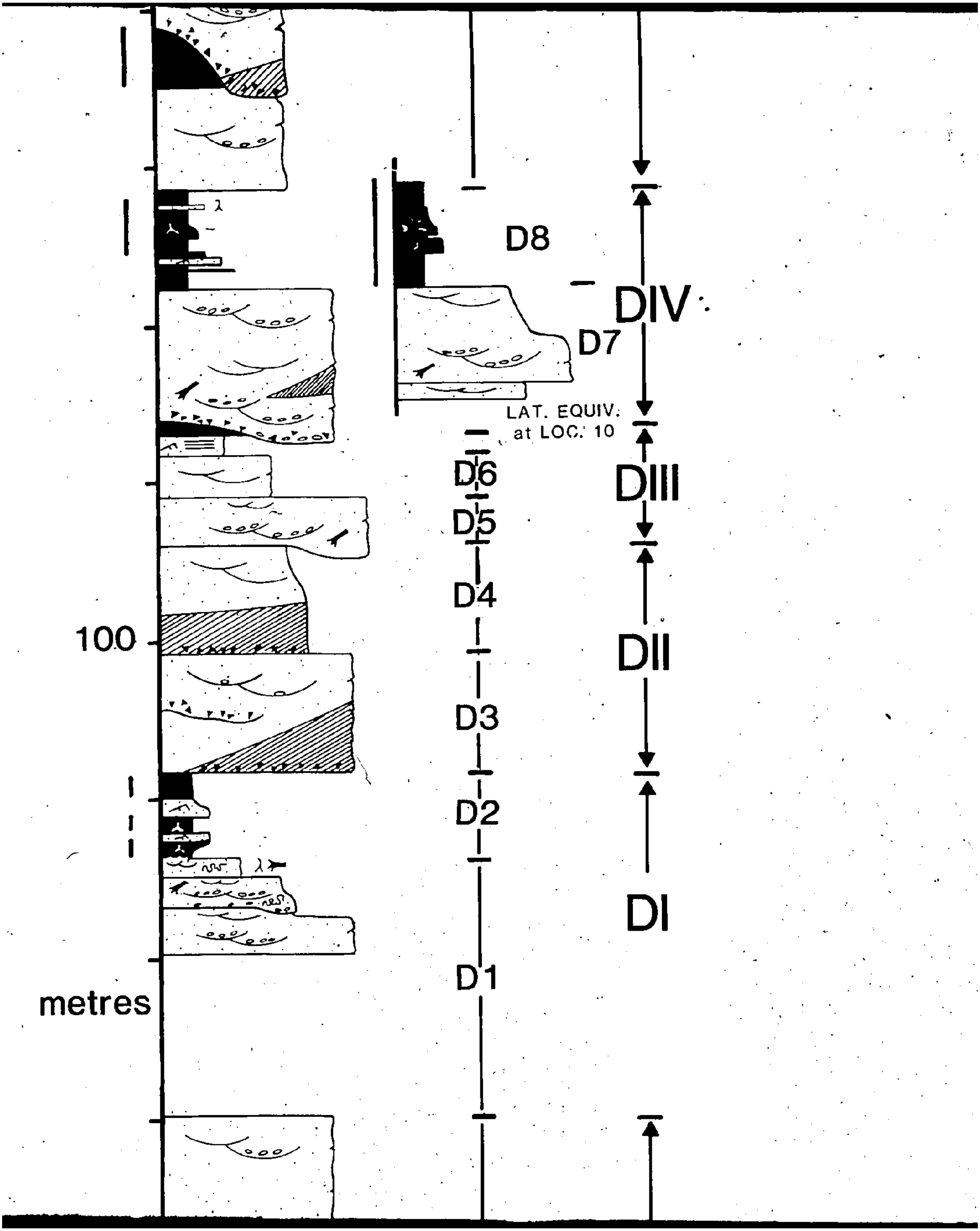

100
metres
D8
D7
LAT. EQUIV. at LOC. 10
D6
D5
D4
D3
D2
D1
DIV
DIII
DII
DI

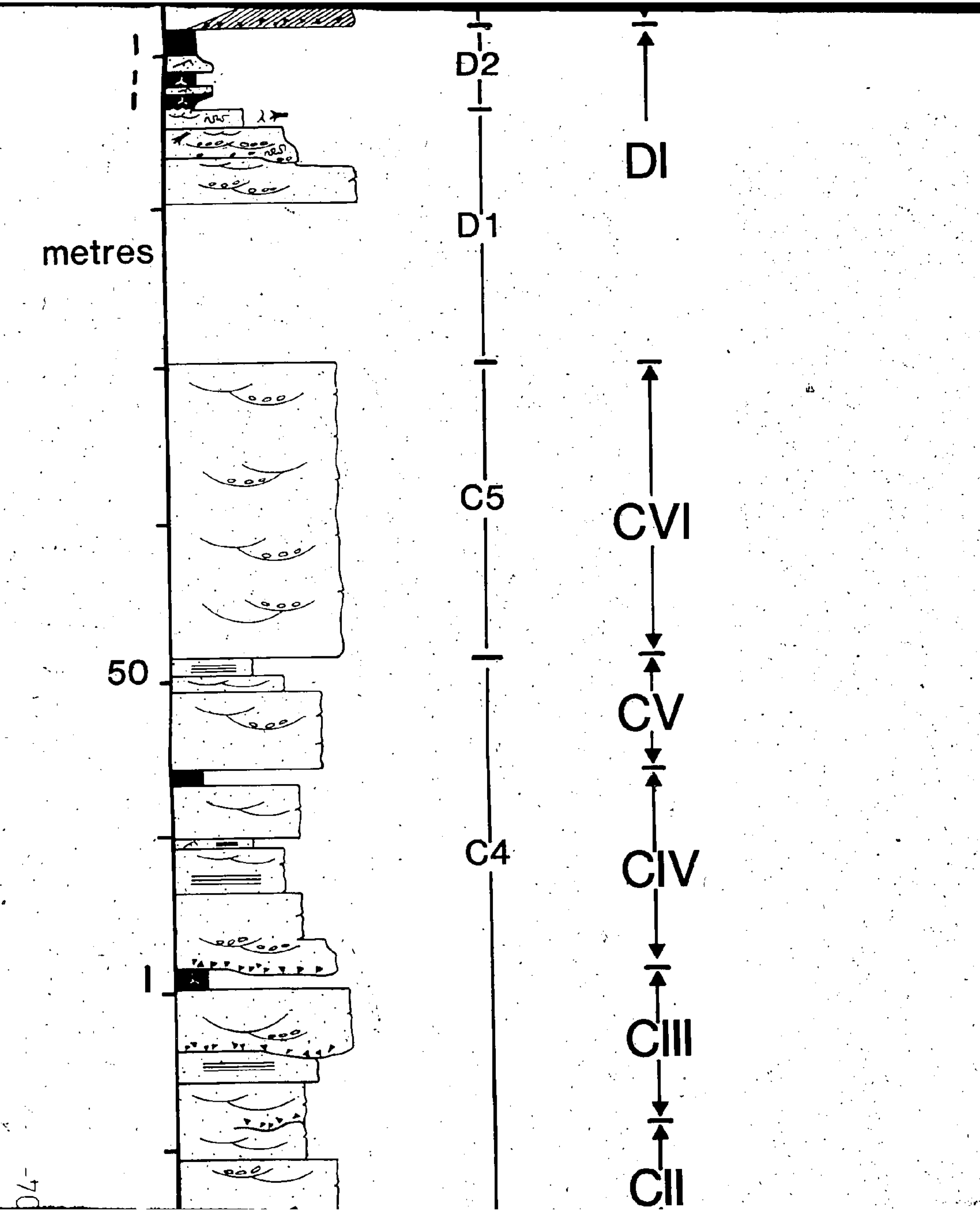

metres
50
D2
D1
C5
C4
DI
CVI
CV
CIV
CIII
CII

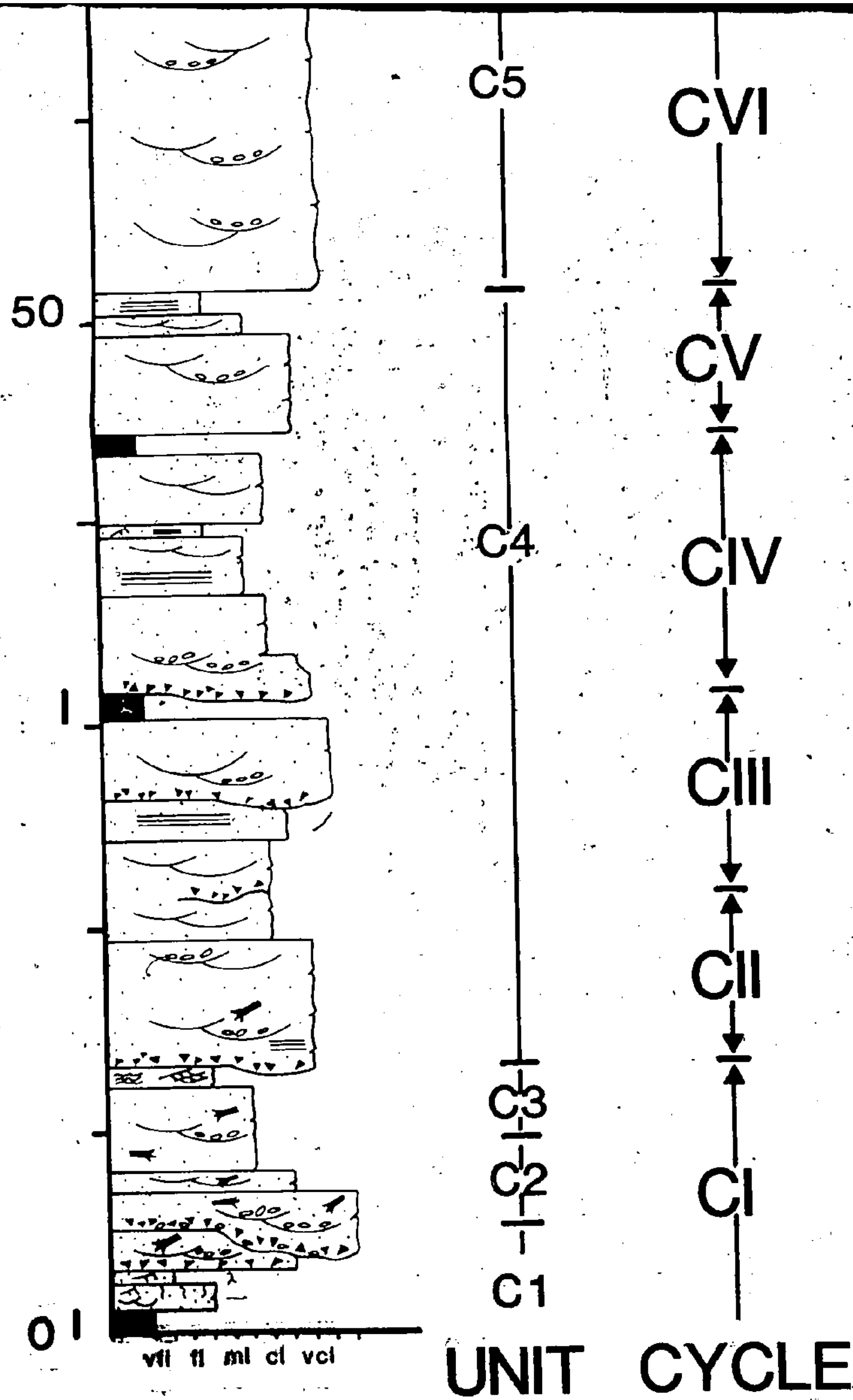
C5
CVI
50
CV
C4
CIV
CIII
CII
C3
C2
CI
C1
0
vfl fl ml cl vcl
UNIT
CYCLE

APPENDIX 4

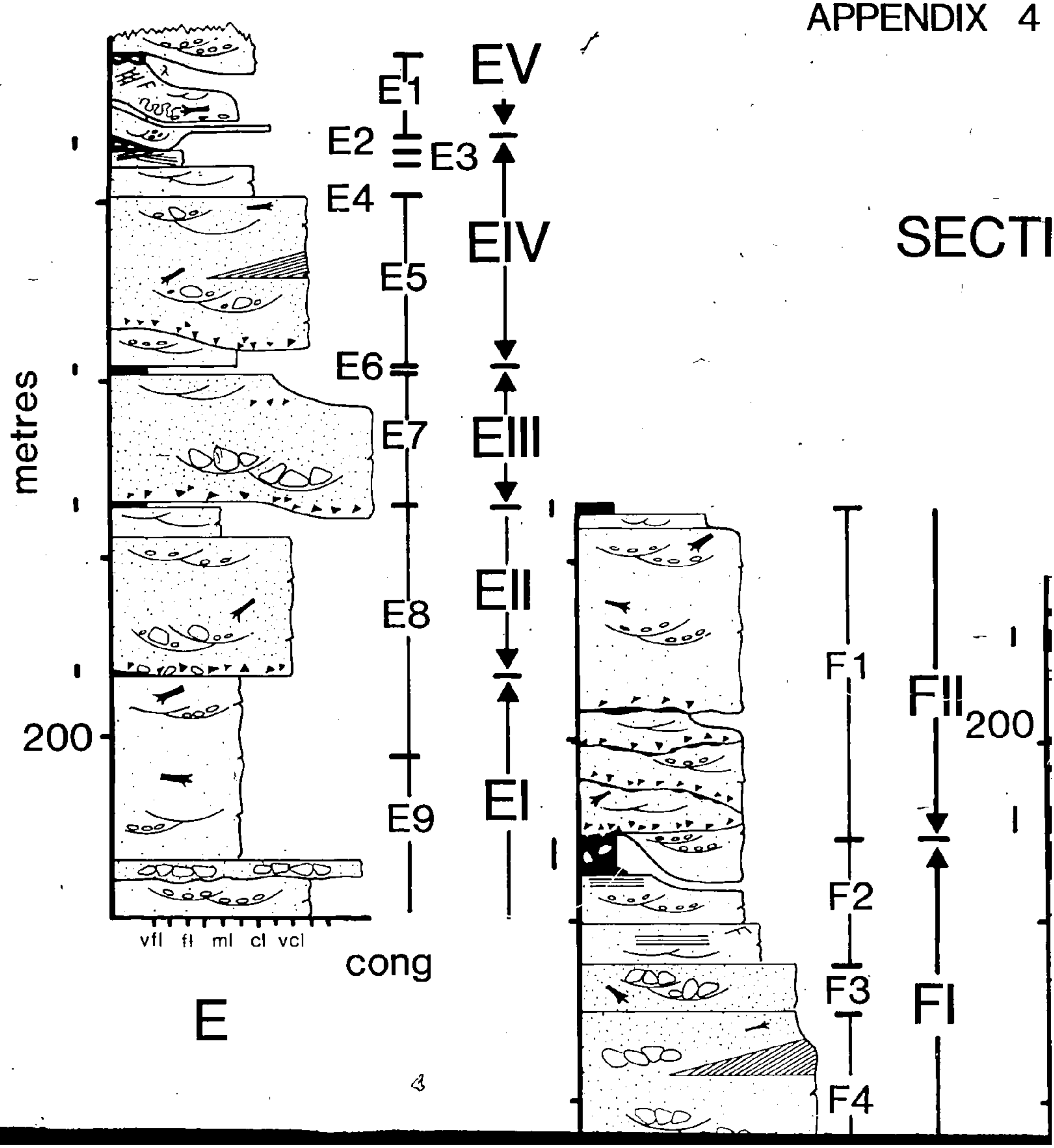
SECTI
metres
200
vfl fl ml cl vcl
cong
E
E1
E2
E3
E4
E5
E6
E7
E8
E9
EV
EIV
EIII
EII
EI
F1
F2
F3
F4
FII
FI
200

APPENDIX 4

SECTION 03

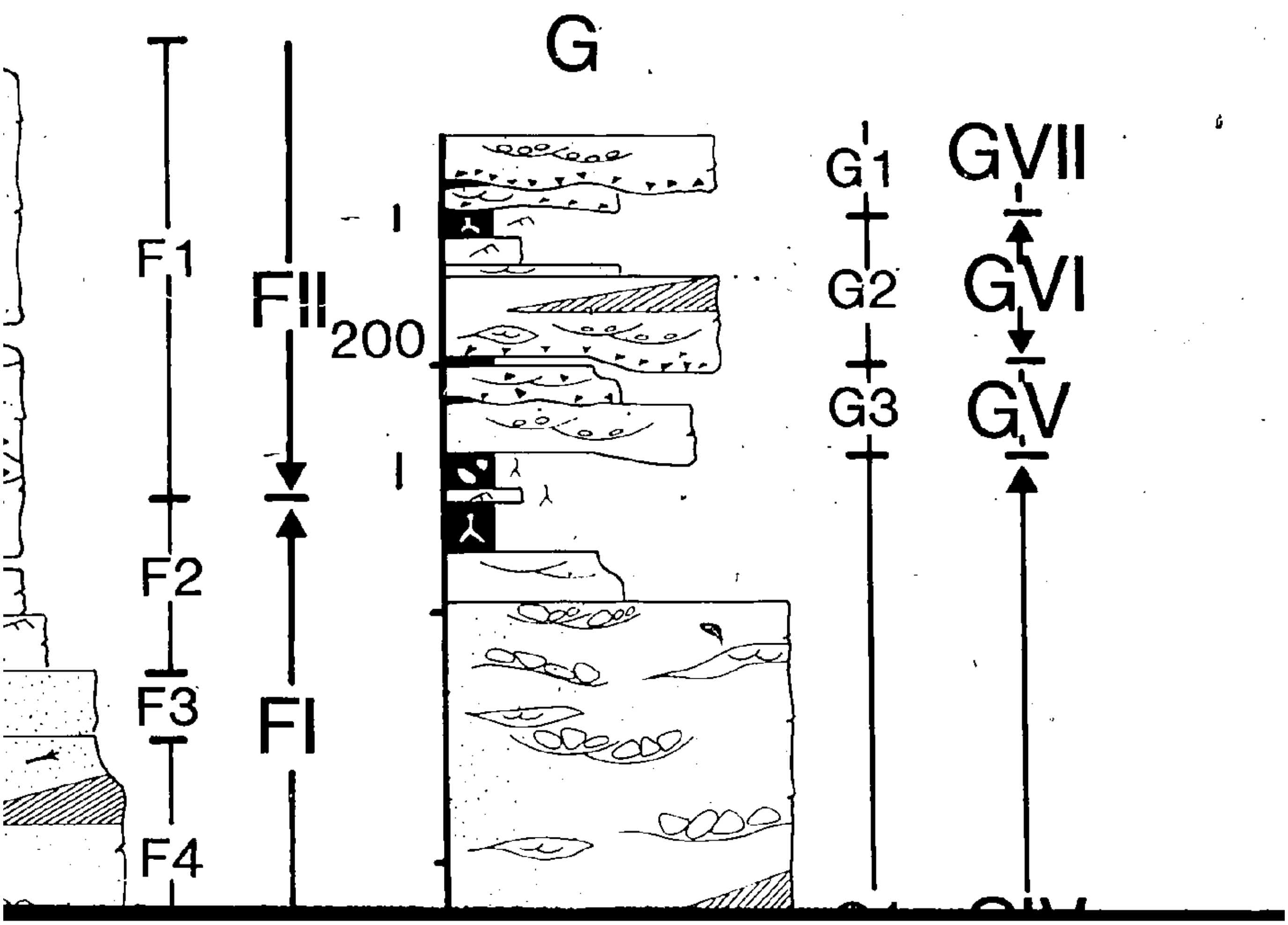

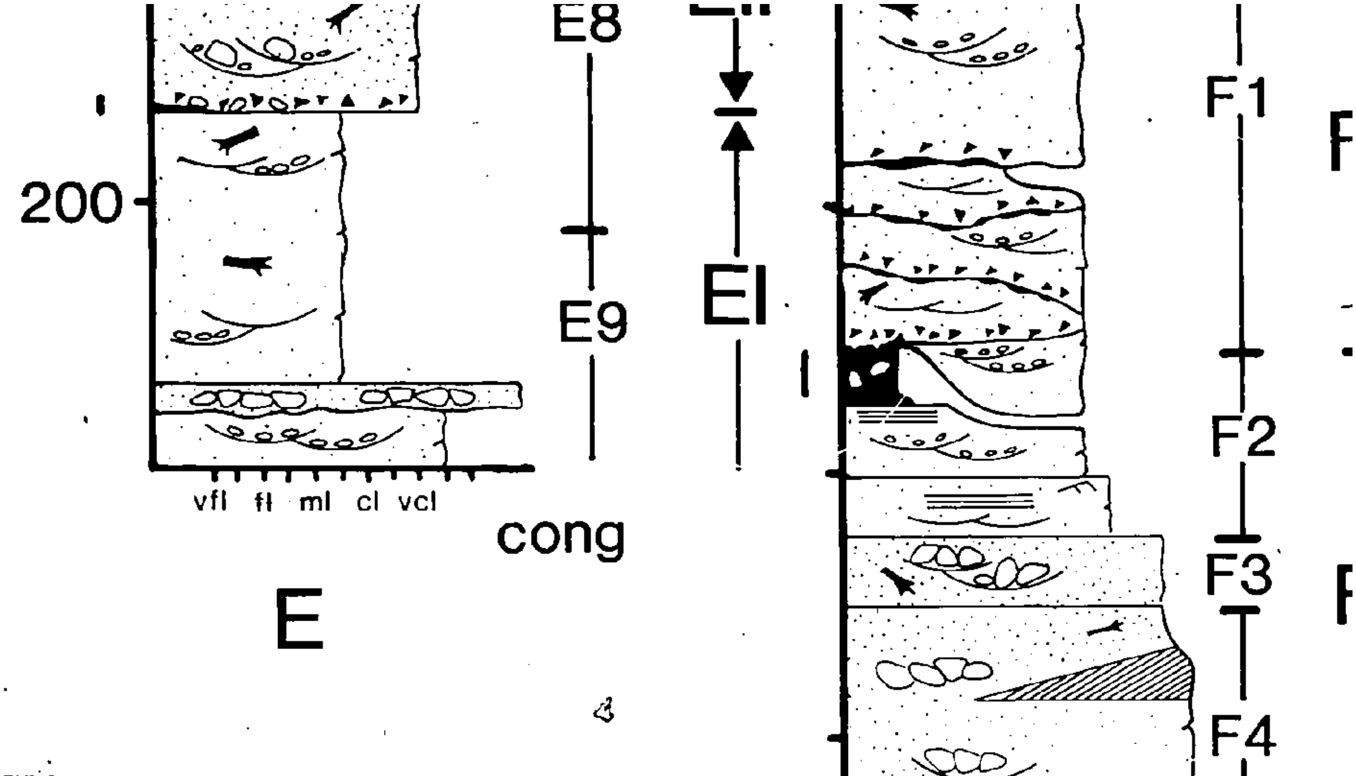

E8
200
E9
EI
I
F1
F2
F3
F4
vfl fl ml cl vcl
cong
E

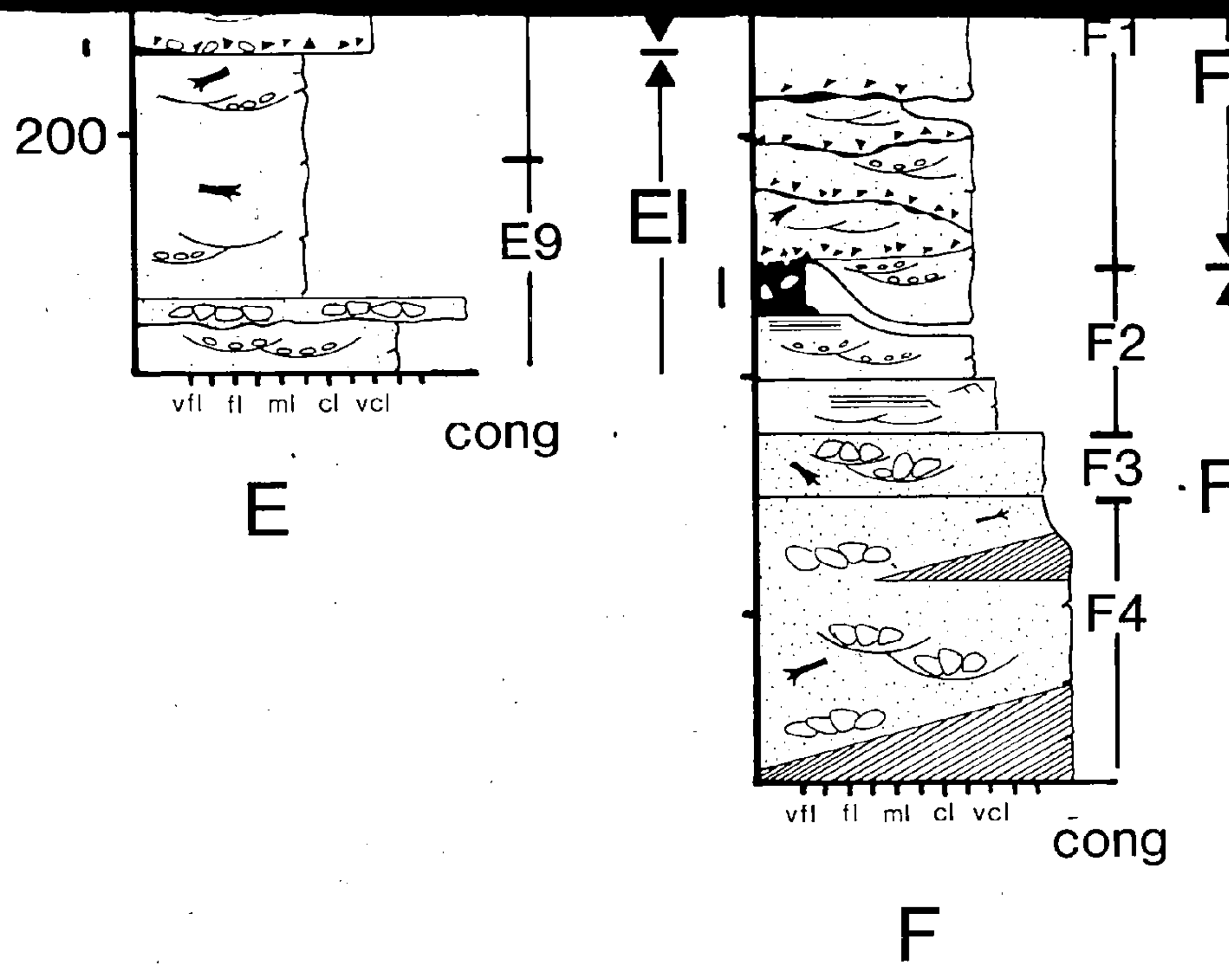

200
E9
EI
I
F1
F2
F3
F4
F
vfl fl ml cl vcl
cong
E
F

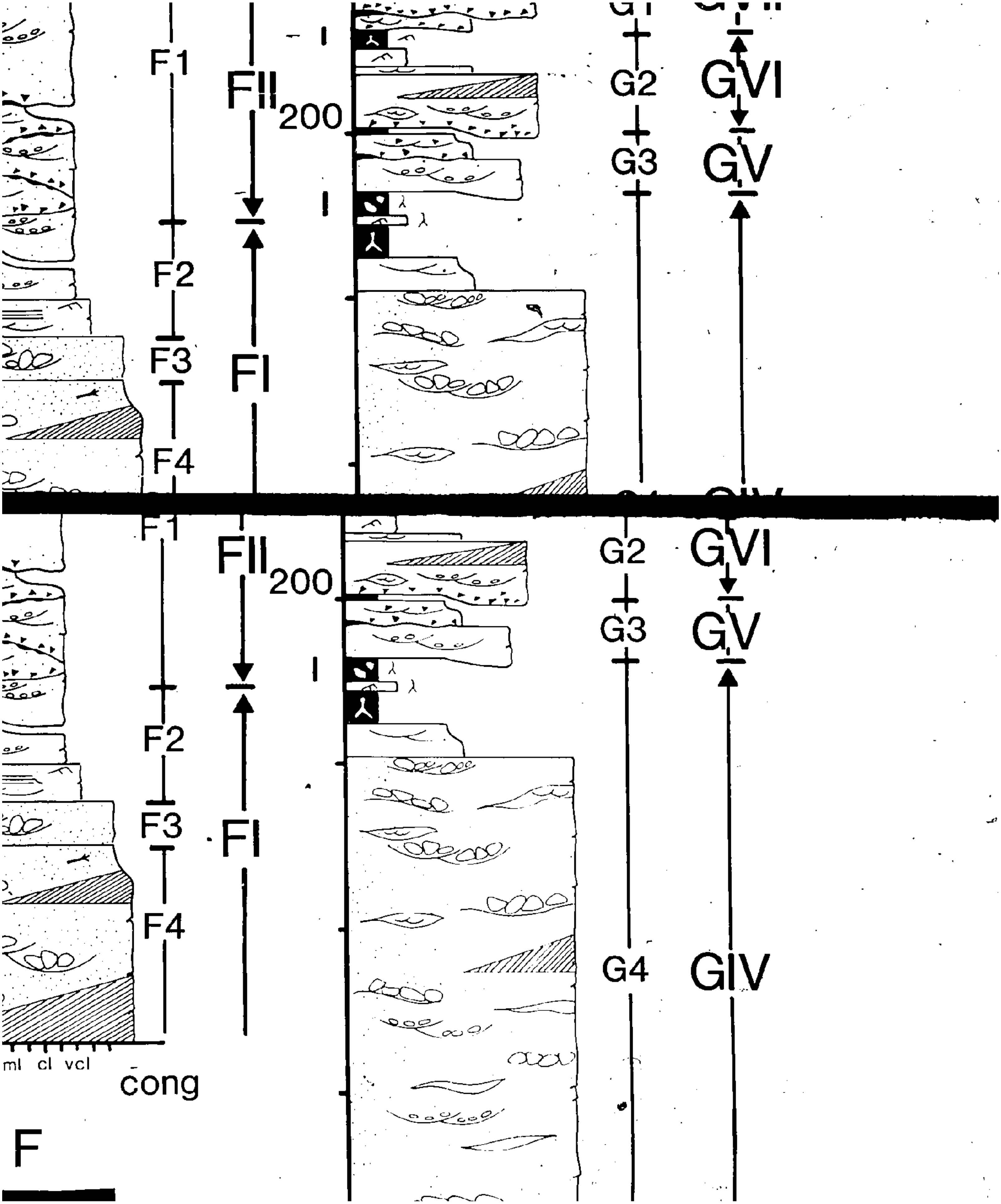
F1
FII
200
F2
F3
FI
F4
G2
GVI
G3
GV
G4
GIV
ml cl vcl
cong
F

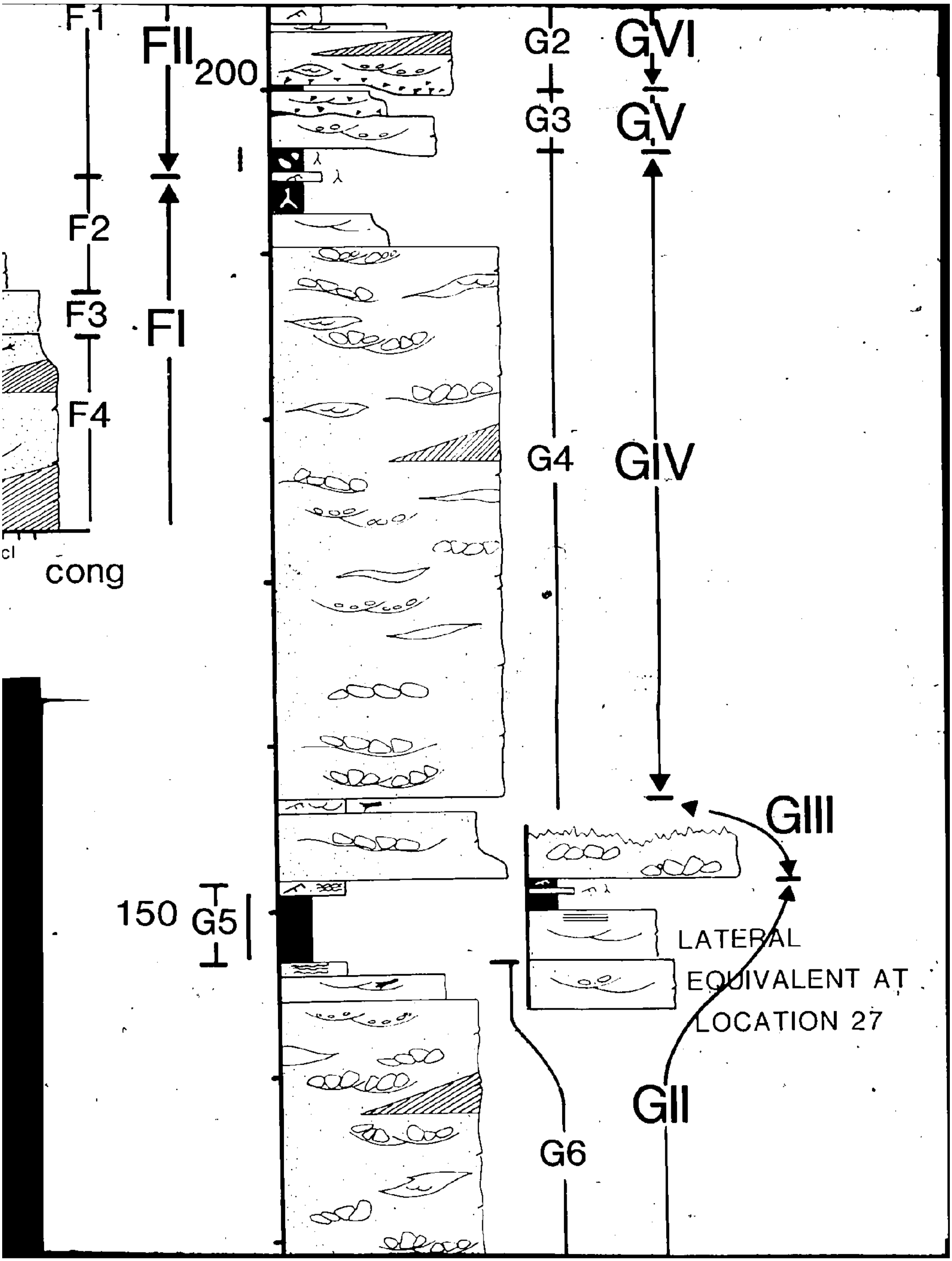

F1
FII
200
F2
F3
FI
F4
cl
cong
G2
GVI
G3
GV
G4
GIV
GIII
150
G5
LATERAL
EQUIVALENT AT
LOCATION 27
GII
G6

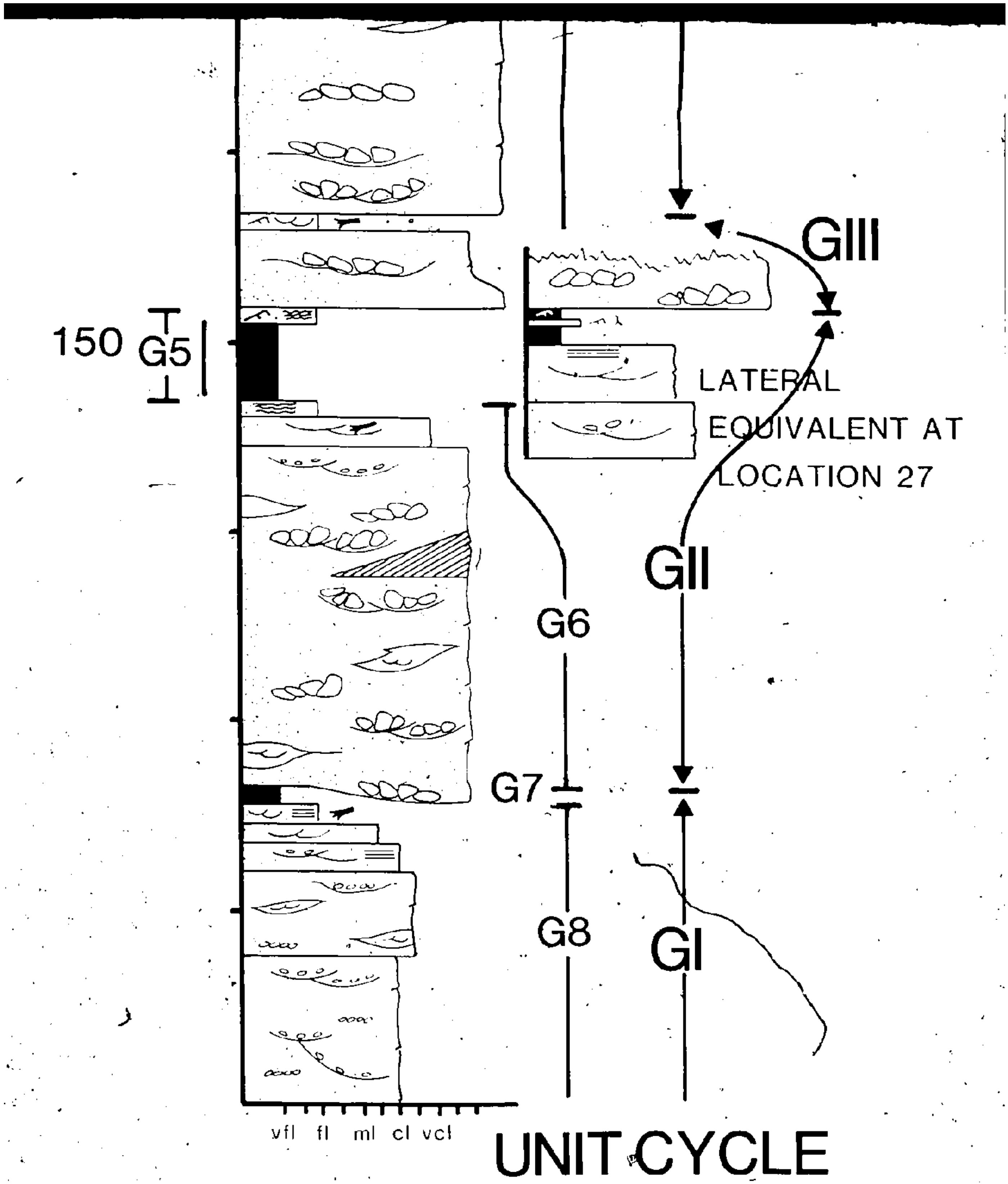

150
G5
GIII
LATERAL
EQUIVALENT AT
LOCATION 27
GII
G6
G7
G8
GI
vfl fl ml cl vcl
UNIT CYCLE

APPENDIX 5

SECTION 03 SUBSECTION H

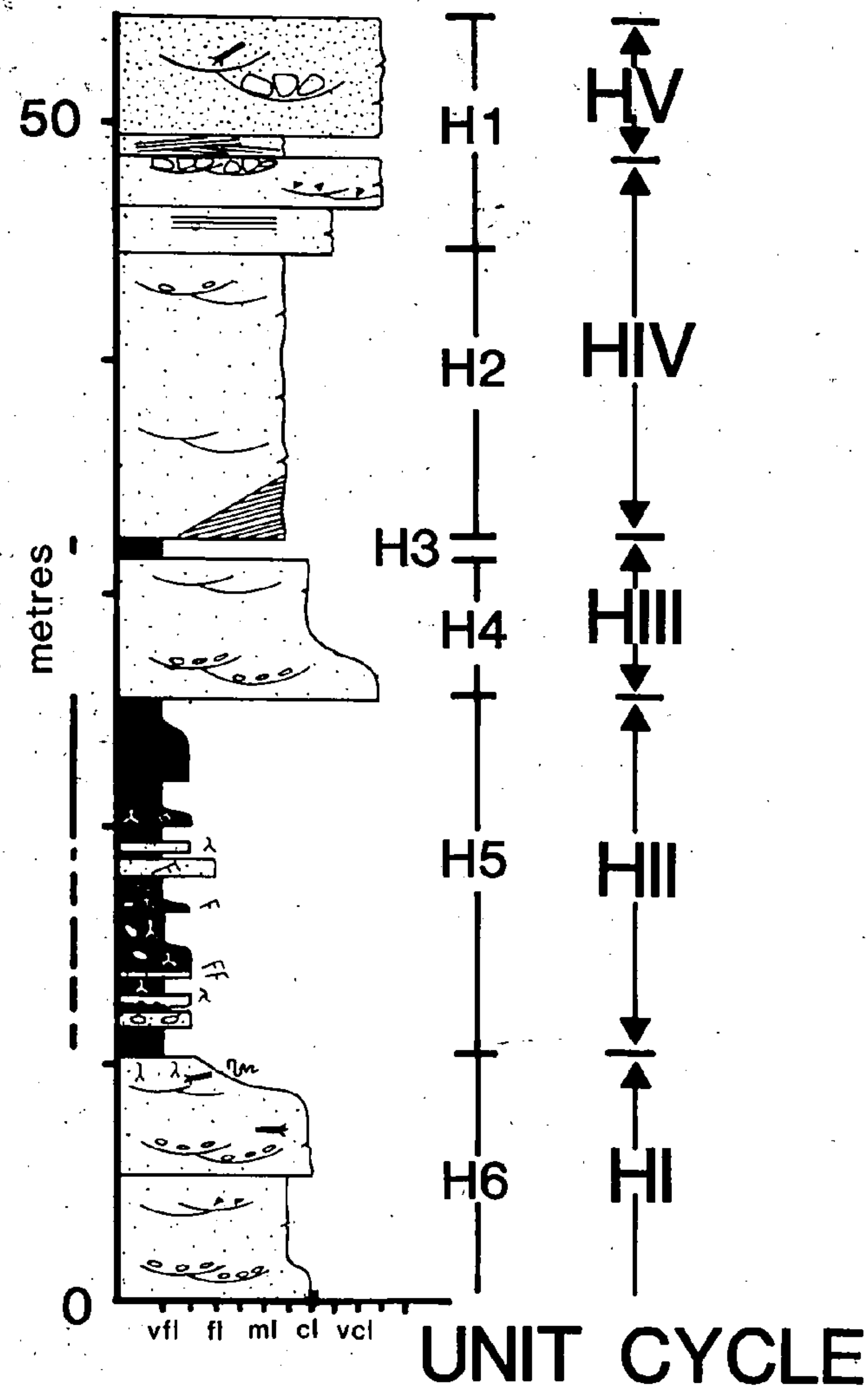

APPENDIX 6

SUBSECTIONS IJ

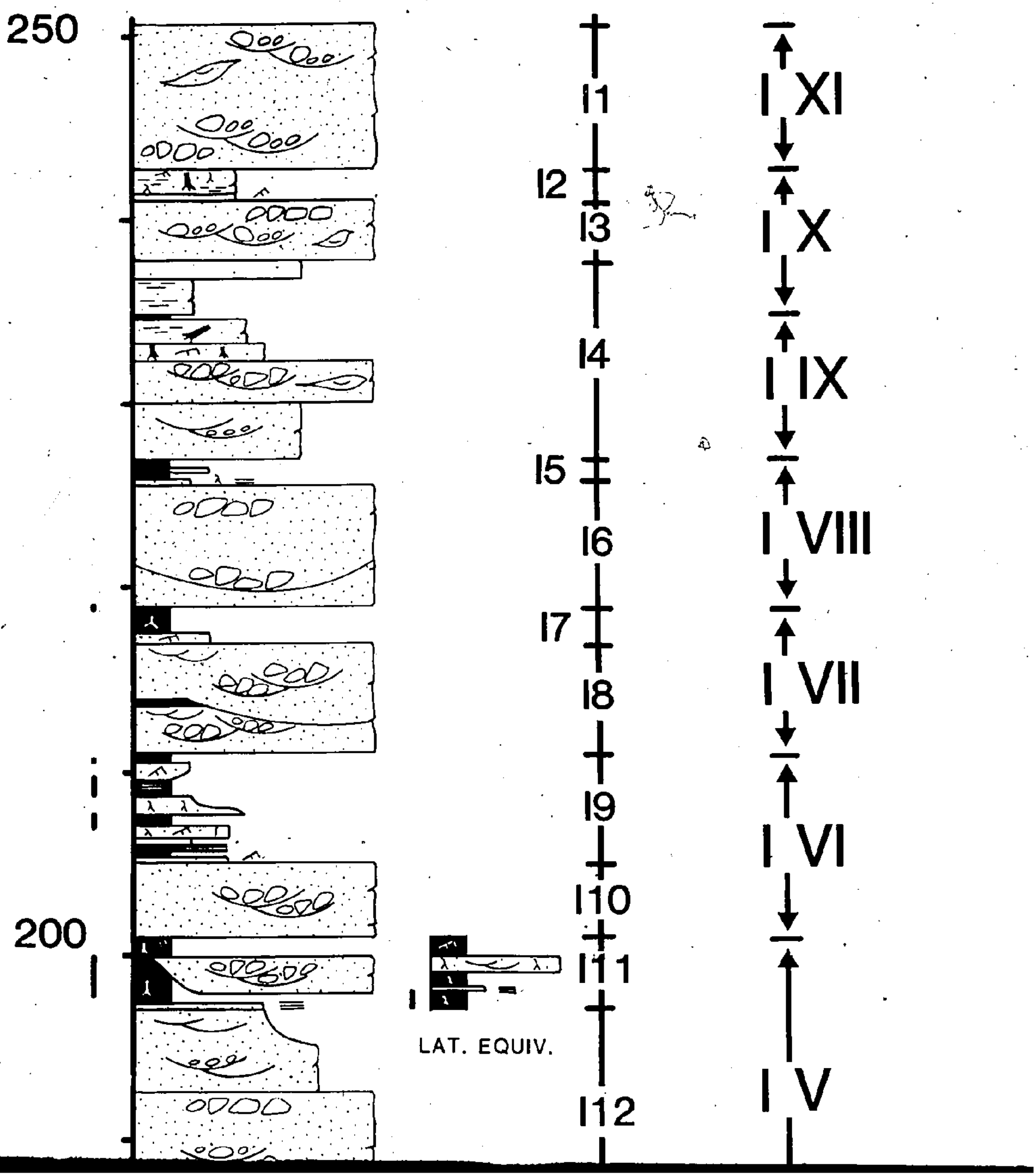

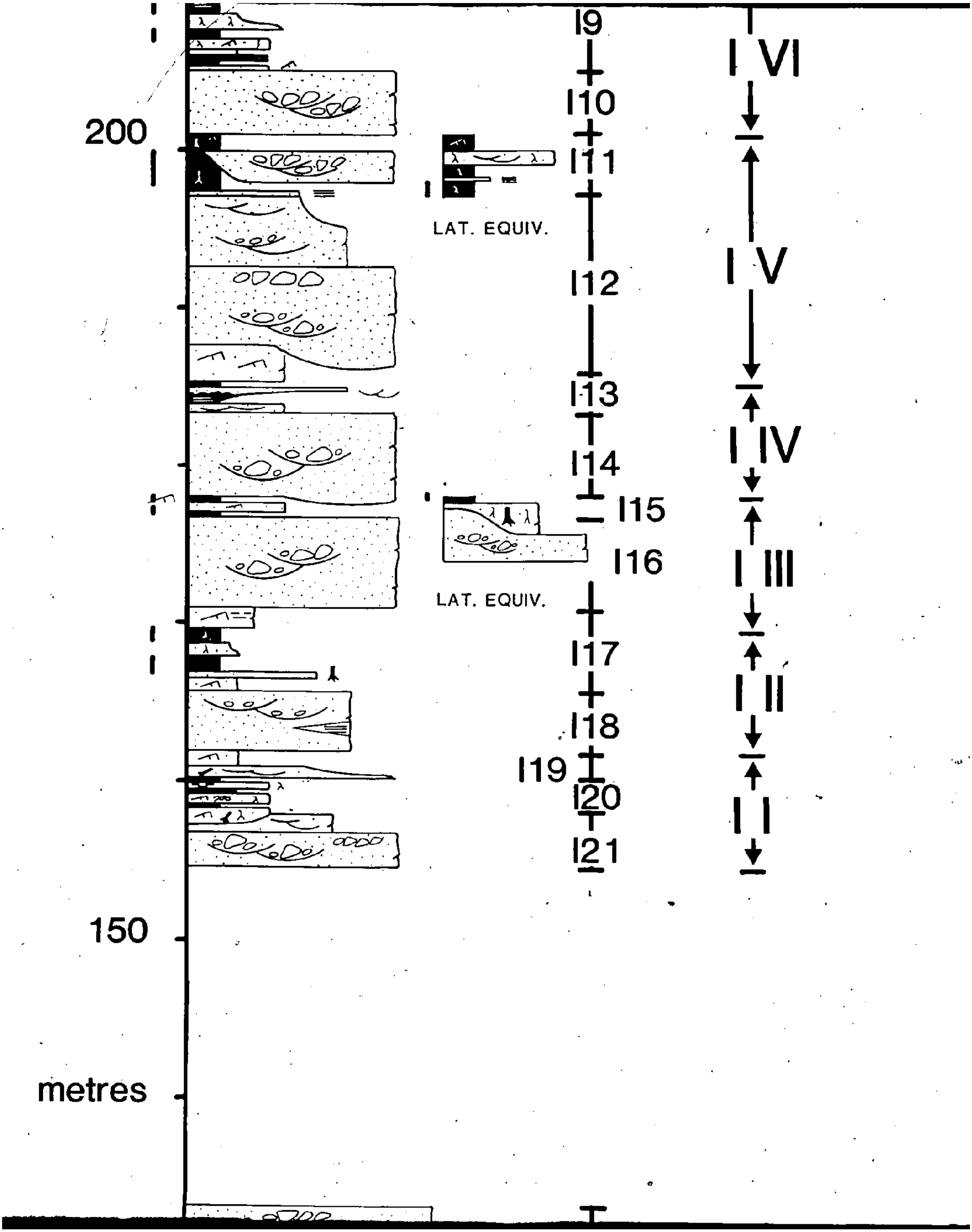

200
150
metres
LAT. EQUIV.
LAT. EQUIV.
I9
I10
I11
I12
I13
I14
I15
I16
I17
I18
I19
I20
I21
I VI
I V
I IV
I III
I II
I I

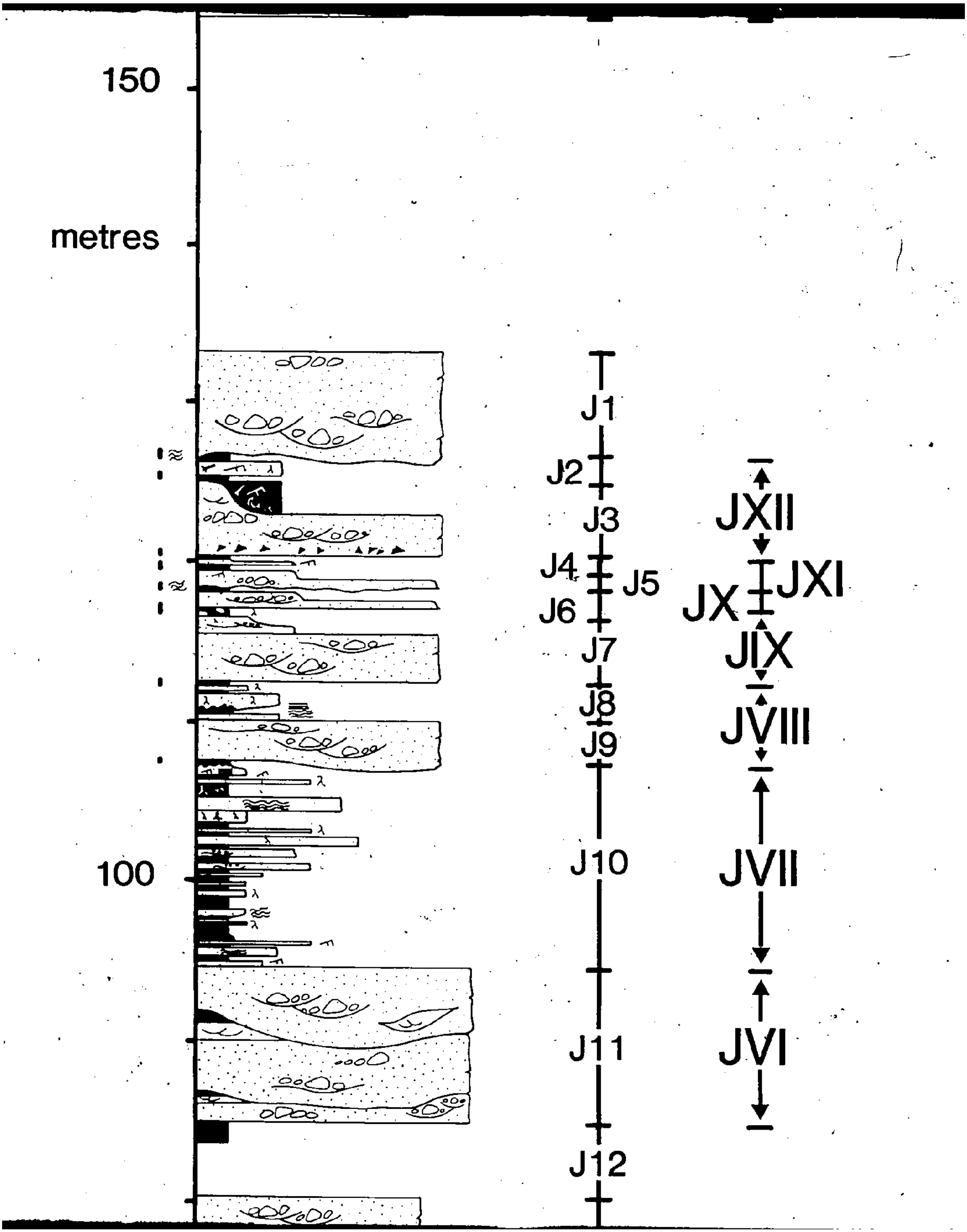
150
metres
100
J1
J2
J3
J4
J5
J6
J7
J8
J9
J10
J11
J12
JXII
JXI
JX
JIX
JVIII
JVII
JVI

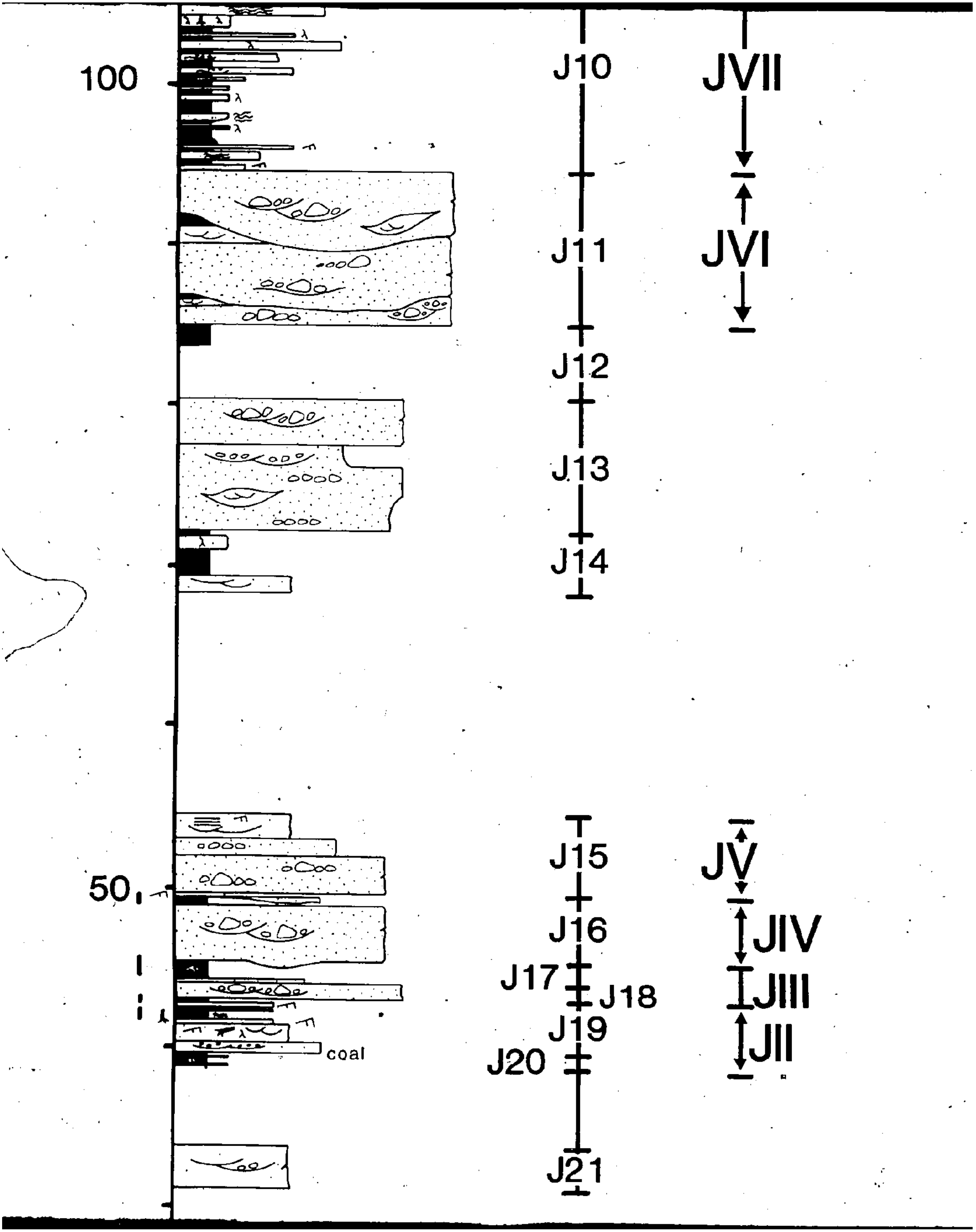

100
50
coal
J10
J11
J12
J13
J14
J15
J16
J17
J18
J19
J20
J21
JVII
JVI
JV
JIV
JIII
JII

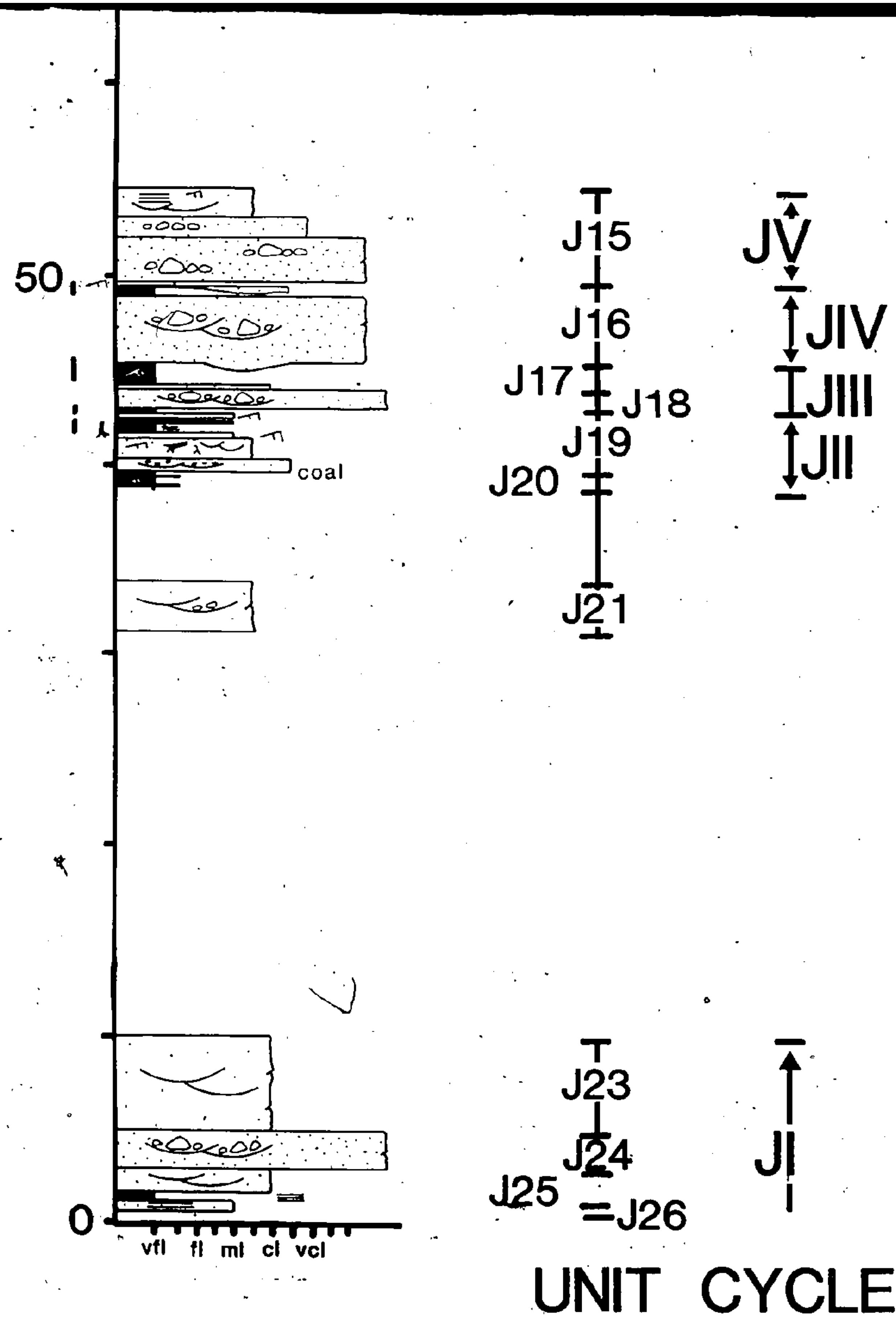
50
0
coal
vfl
fl
ml
cl
vcl
J15
J16
J17
J18
J19
J20
J21
J23
J24
J25
J26
JV
JIV
JIII
JII
JI
UNIT
CYCLE

APPENDIX 7

SUBSECTIONS K,L

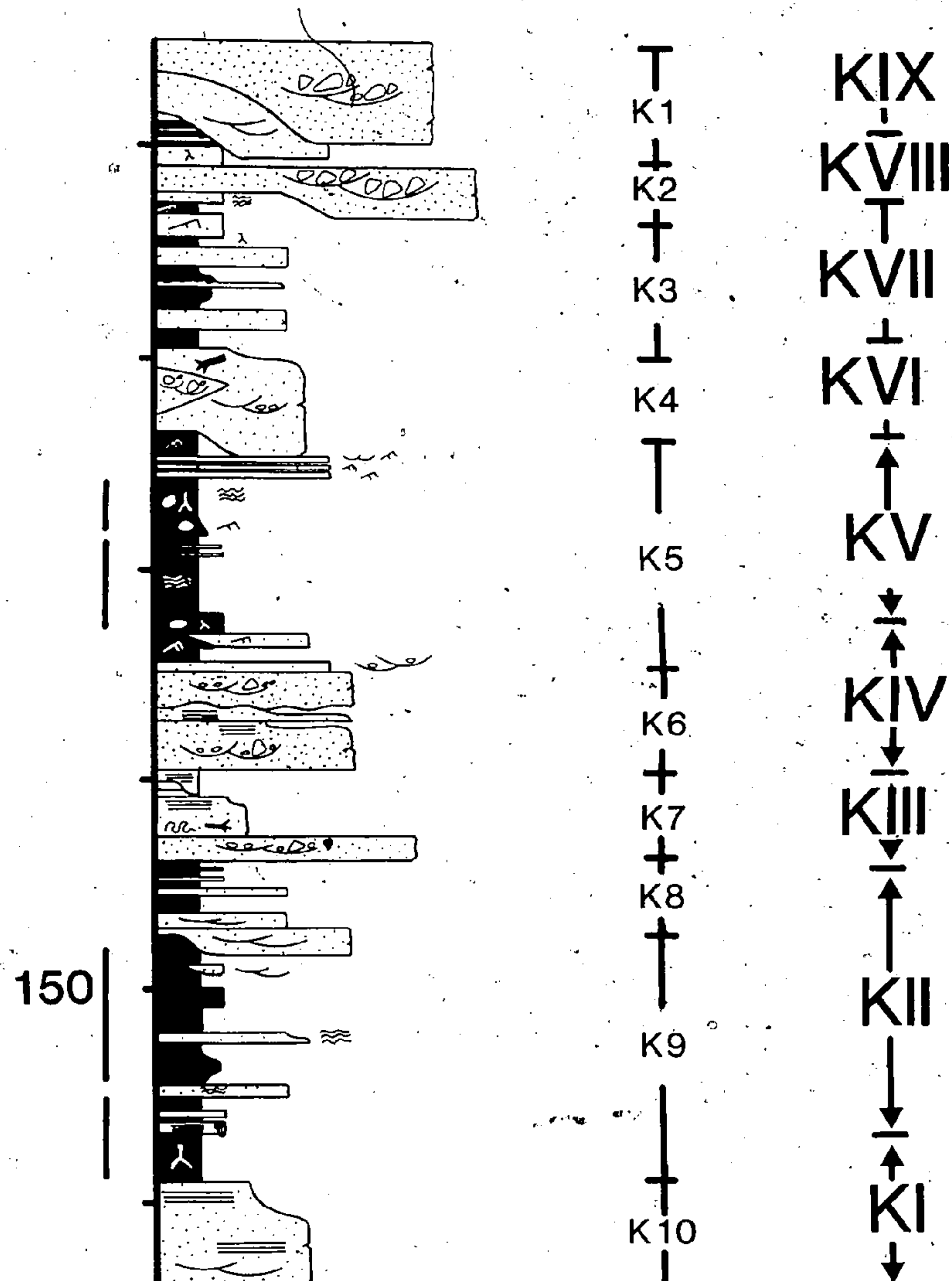

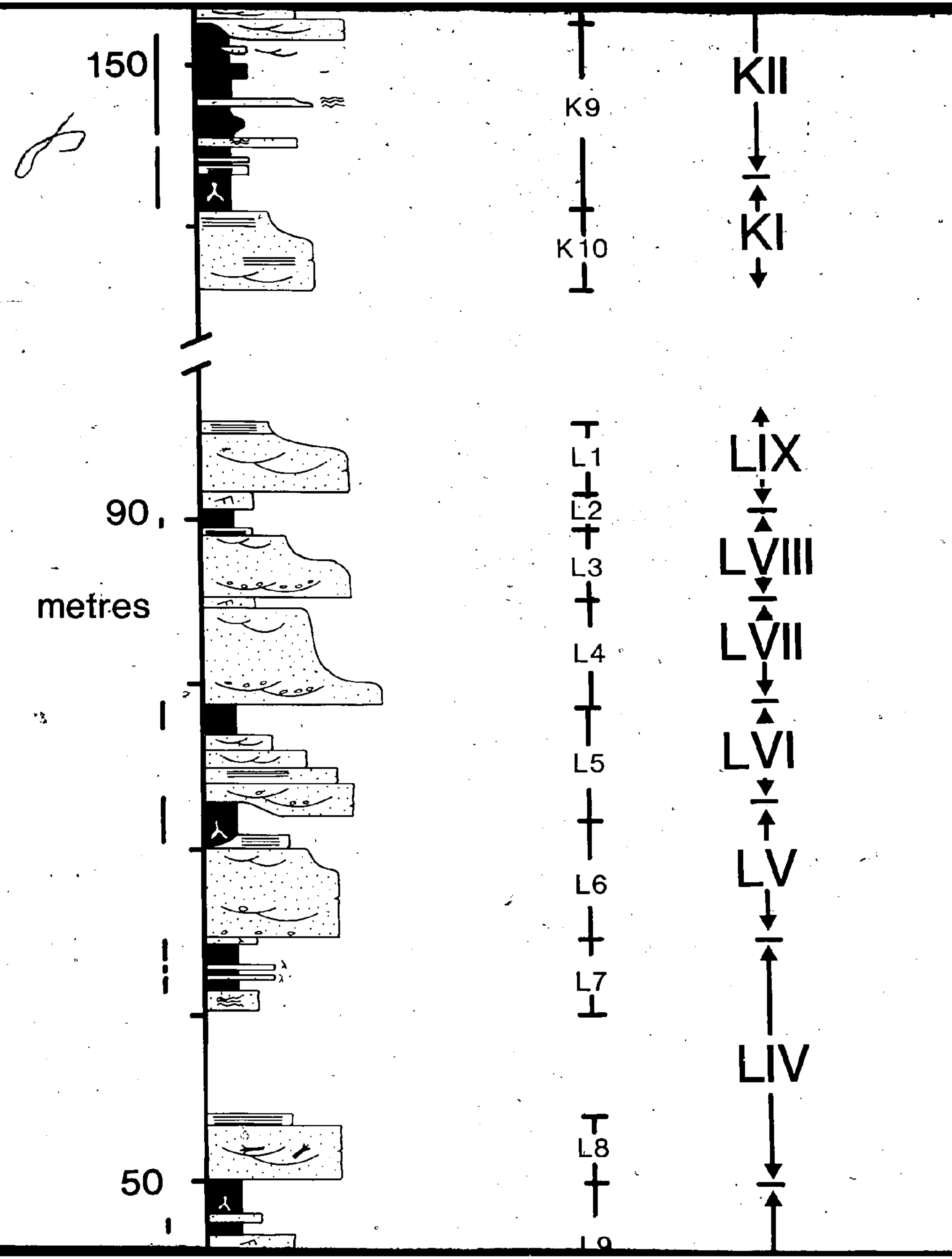

150
90
metres
50
K9
K10
L1
L2
L3
L4
L5
L6
L7
L8
KII
KI
LIX
LVIII
LVII
LVI
LV
LIV

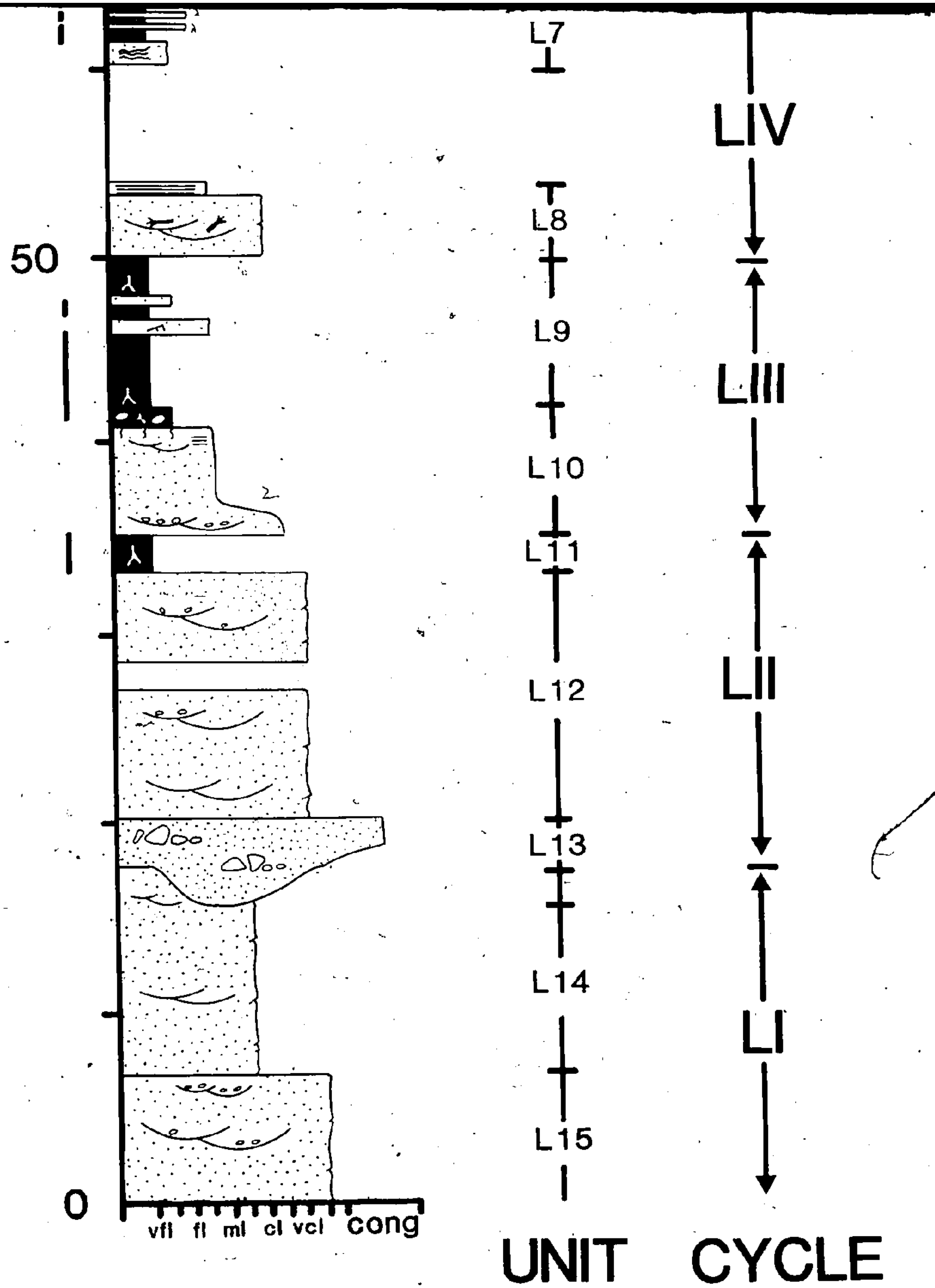

50
0
vfl fl ml cl vcl cong
L7
L8
L9
L10
L11
L12
L13
L14
L15
LIV
LIII
LII
LI
UNIT
CYCLE

APPENDIX 8

SUBSECTION M

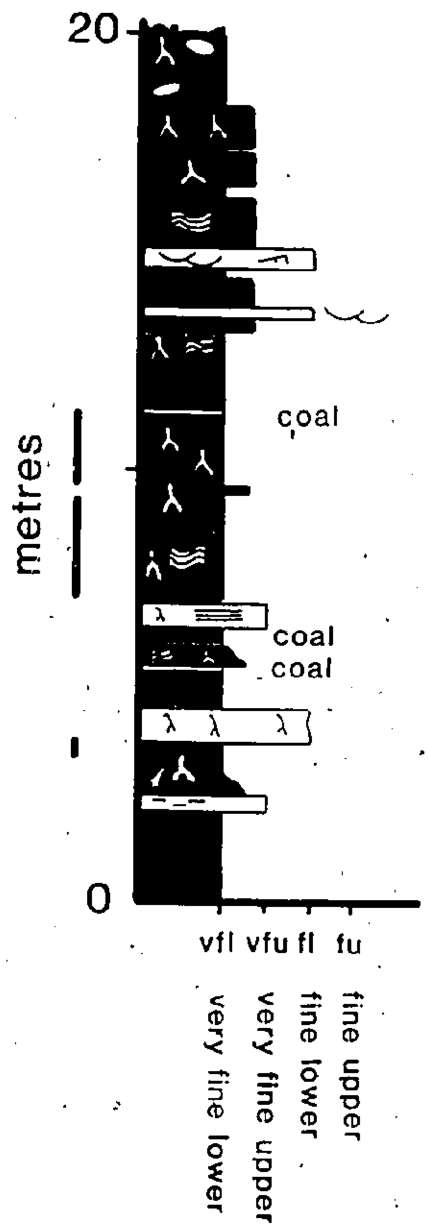

APPENDIX 9

SUBSECTION N

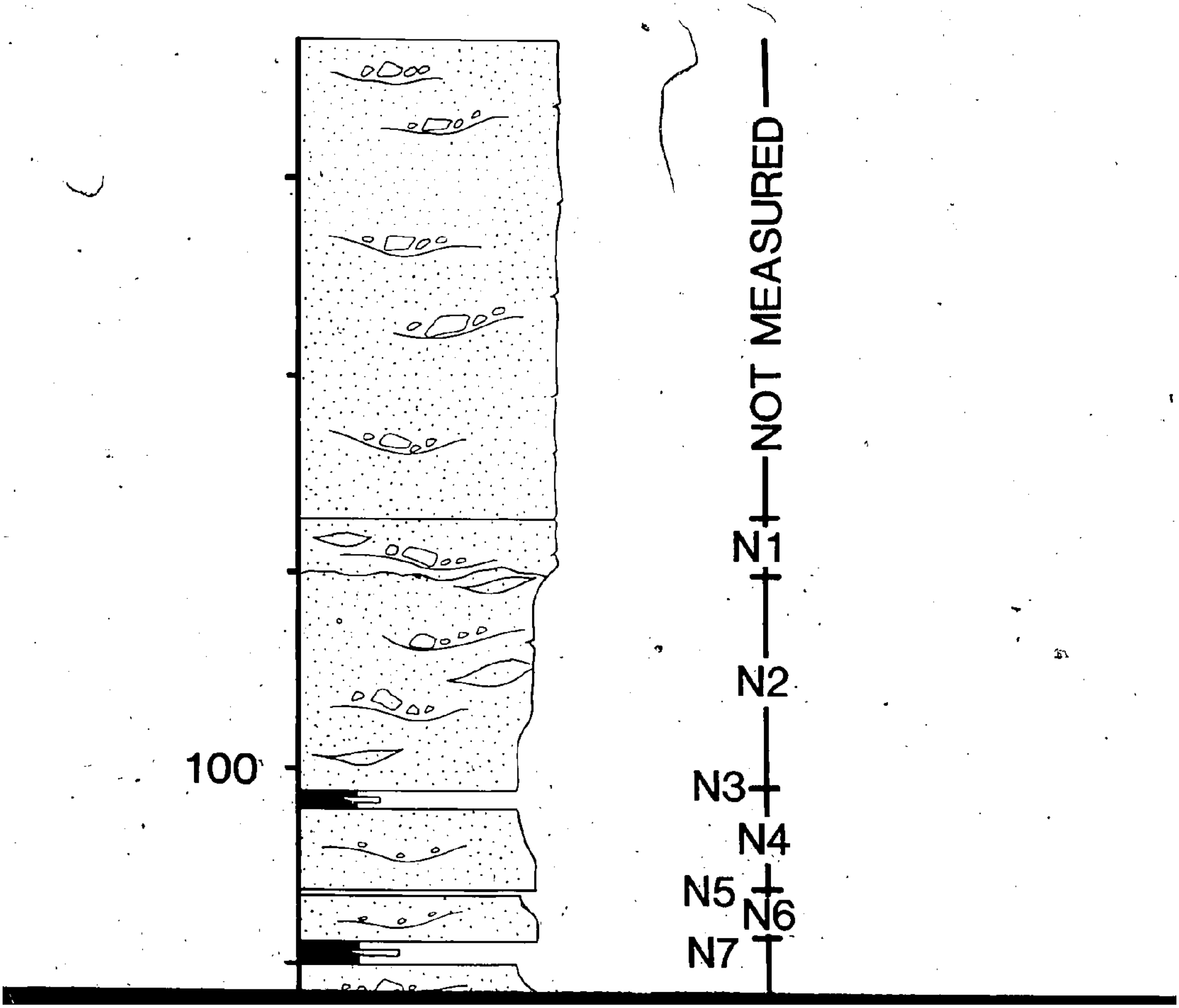

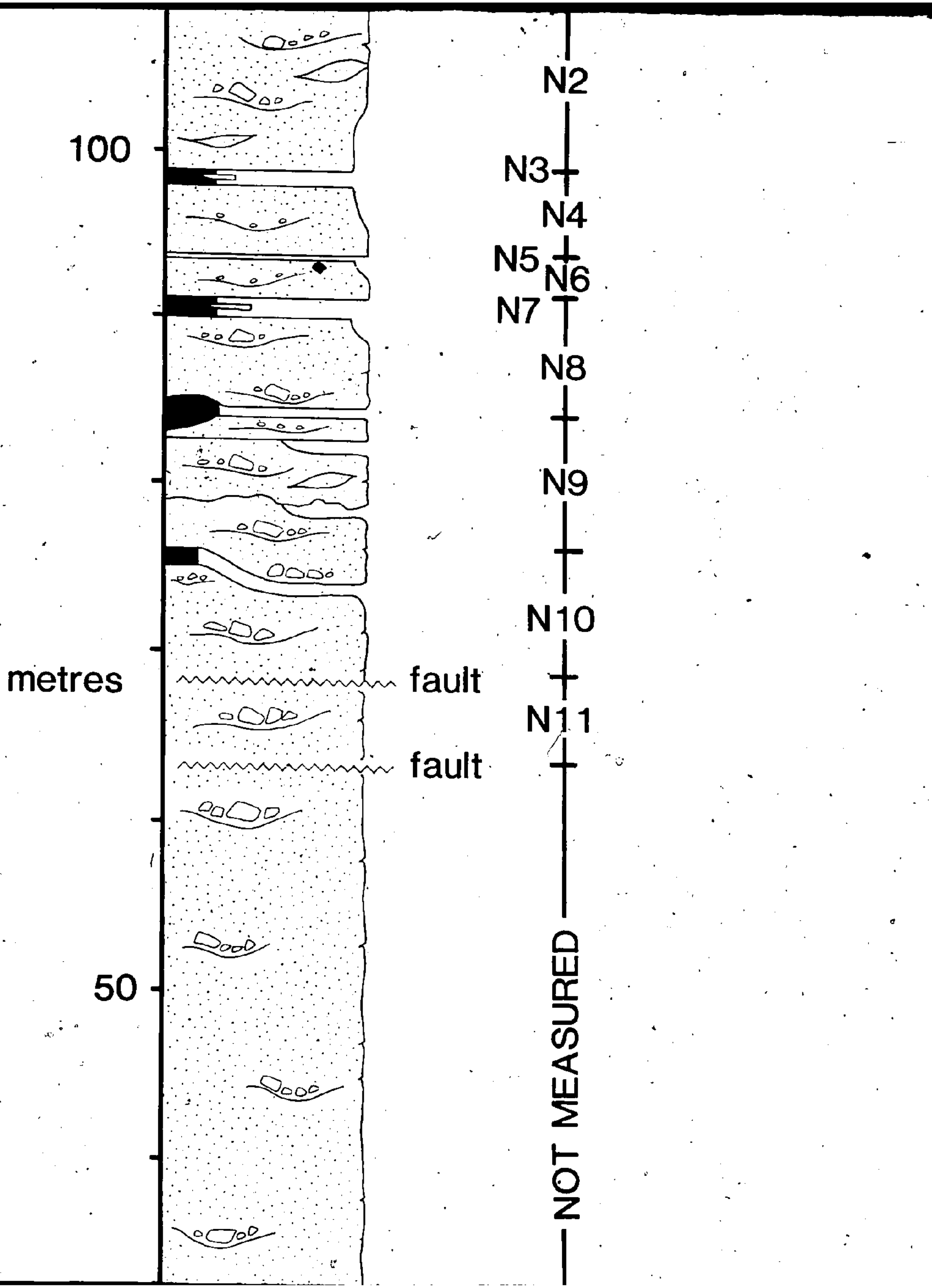

100
50
metres
fault
fault
N2
N3
N4
N5
N6
N7
N8
N9
N10
N11
NOT MEASURED

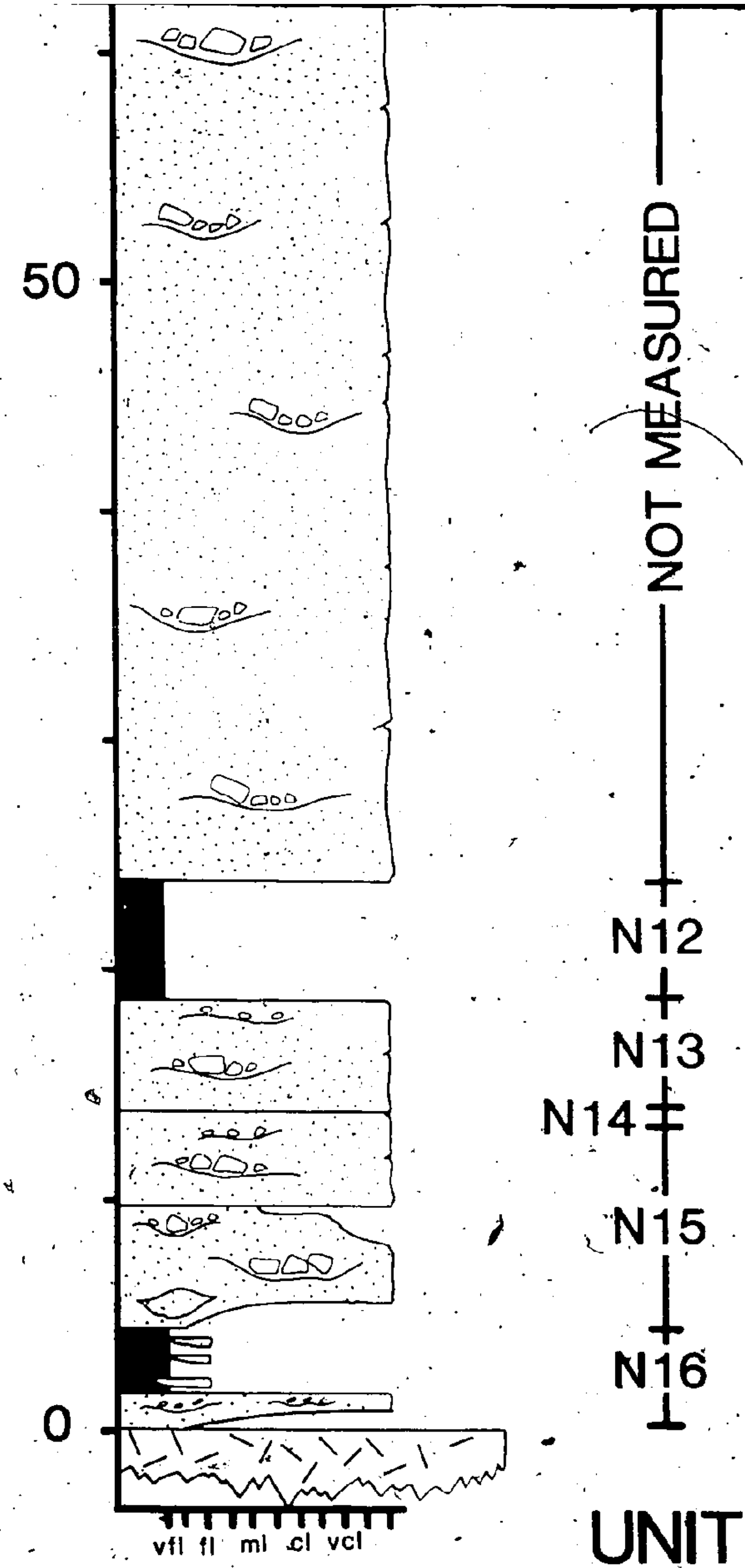
50
0
vfl fl ml cl vcl
NOT MEASURED
N12
N13
N14
N15
N16
UNIT

APPENDIX 10: PREFERRED FACIES TRANSITIONS

SECTION 01

TOTAL NUMBER OF FACIES TRANSITIONS: 75

OBSERVED TRANSITIONS:

	Se	F	Sr	Sh	St(m)	St(c)	Gt	Gm/Gt	Gm	Sm
Se	-	3	0	2	9	5	1	0	0	0
F	4	-	4	1	2	1	0	0	0	0
Sr	1	0	-	0	0	3	3	0	0	0
Sh	4	3	0	-	0	0	0	0	0	0
St(m)	6	3	1	2	-	3	0	0	0	0
St(c)	5	1	0	3	2	-	1	0	0	0
Gt	0	0	0	0	1	0	-	0	1	0
Gm/Gt	0	0	0	0	0	0	0	-	0	0
Gm	0	0	0	1	0	0	0	0	-	0
Sm	0	0	0	0	0	0	0	0	0	-

OBSERVED MINUS RANDOM TRANSITIONS PROBABILITY:

	Se	F	Sr	Sh	St(m)	St(c)	Gt	Gm/Gt	Gm	Sm
Se	0.0	-0.03	-0.08	-0.05	0.13	0.03	0.01	0.0	-0.01	0.0
F	-0.02	0.0	0.26	-0.04	-0.08	-0.09	-0.02	0.0	-0.01	0.0
Sr	-0.08	-0.13	0.0	-0.11	-0.22	0.59	-0.02	0.0	-0.01	0.0
Sh	0.09	0.19	-0.06	0.0	-0.01	-0.17	-0.02	0.0	-0.01	0.0
St(m)	0.00	0.04	-0.00	-0.00	0.0	0.00	-0.02	0.0	-0.01	0.0
St(c)	0.05	-0.06	-0.06	0.12	-0.08	0.0	0.05	0.0	-0.01	0.0
Gt	-0.31	-0.12	-0.05	-0.11	0.28	-0.15	0.0	0.0	0.48	0.0
Gm/Gt	0.0	0.0	0.0	0.0	0.0	0.0	0.0	0.0	0.0	0.0
Gm	-0.31	-0.12	-0.05	0.89	-0.21	-0.15	-0.02	0.0	0.0	0.0
Sm	0.0	0.0	0.0	0.0	0.0	0.0	0.0	0.0	0.0	0.0

BINOMIAL PROBABILTY

	Se	F	Sr	Sh	St(m)	St(c)	Gt	Gm/Gt	Gm	Sm
Se	-	-	-	-	0.141	0.458	0.478	-	-	-
F	-	-	0.005	-	-	-	-	-	-	-
Sr	-	-	-	-	-	0.014	-	-	-	-
Sh	-	0.122	-	-	-	-	-	-	-	-
St(m)	0.389	0.439	-	-	-	0.575	-	-	-	-
St(c)	0.584	-	-	0.188	-	-	0.271	-	-	-
Gt	0.463	-	-	-	0.392	-	-	-	0.002	-
Gm/Gt	-	-	-	-	-	-	-	-	-	-
Gm	-	-	-	0.109	-	-	-	-	-	-
Sm	-	-	-	-	-	-	-	-	-	-

SECTION 02

TOTAL NUMBER OF FACIES TRANSITIONS: 65

OBSERVED TRANSITIONS:

	Se	F	Sr	Sh	St(m)	St(c)	Gt	Gm/Gt	Gm	Sm
Se	-	0	0	0	2	2	0	0	0	0
F	3	-	1	0	0	3	0	0	0	0
Sr	2	1	-	2	1	0	0	0	0	0
Sh	2	0	3	-	2	1	0	0	0	0
St(m)	0	5	2	2	3	-	1	0	0	0
St(c)	2	0	3	0	3	9	-	0	0	0
Gt	0	0	0	0	0	0	0	-	0	0
Gm/Gt	0	0	0	0	0	0	0	0	-	0
Gm	0	0	0	0	0	0	0	0	0	-
Sm	0	0	0	0	0	0	0	0	0	0

OBSERVED MINUS RANDOM PROBABILITY:

	Se	F	Sr	Sh	St(m)	St(c)	Gt	Gm/Gt	Gm	Sm
Se	-	-0.10	-0.10	-0.14	-0.13	0.47	0.0	0.0	0.0	0.0
F	0.19	0.0	0.05	-0.12	-0.23	0.10	0.0	0.0	0.0	0.0
Sr	0.09	0.07	0.0	0.21	-0.06	-0.32	0.0	0.0	0.0	0.0
Sh	0.00	-0.05	0.28	0.0	0.09	-0.20	0.0	0.0	0.0	0.0
St(m)	0.10	0.05	0.09	0.0	-0.29	0.0	0.0	0.0	0.0	0.0
St(c)	-0.19	0.0	-0.11	0.02	0.22	0.0	0.0	0.0	0.0	0.0
Gt	0.0	0.0	0.0	0.0	0.0	0.0	0.0	0.0	0.0	0.0
Gm/Gt	0.0	0.0	0.0	0.0	0.0	0.0	0.0	0.0	0.0	0.0
Gm	0.0	0.0	0.0	0.0	0.0	0.0	0.0	0.0	0.0	0.0
Sm	0.0	0.0	0.0	0.0	0.0	0.0	0.0	0.0	0.0	0.0

BINOMIAL PROBABILITY:

	Se	F	Sr	Sh	St(m)	St(c)	Gt	Gm/Gt	Gm	Sm
Se	-	-	-	-	-	0.000	-	-	-	-
F	0.219	-	0.471	-	-	0.401	-	-	-	-
Sr	0.440	0.425	-	0.156	-	-	-	-	-	-
Sh	0.623	-	0.029	-	0.610	-	-	-	-	-
St(m)	0.284	0.393	0.388	0.270	-	-	-	-	-	-
St(c)	-	0.310	-	0.508	0.045	-	-	-	-	-
Gt	-	-	-	-	-	-	-	-	-	-
Gm/Gt	-	-	-	-	-	-	-	-	-	-
Gm	-	-	-	-	-	-	-	-	-	-
Sm	-	-	-	-	-	-	-	-	-	-

SECTION 03

TOTAL NUMBER OF FACIES TRANSITIONS: 78

OBSERVED TRANSITIONS:

	Se	F	Sr	Sh	St(m)	St(c)	Gt	Gm/Gt	Gm	Sm
Se	-	1	0	0	4	7	4	0	1	0
F	11	-	1	1	0	0	0	1	0	0
Sr	1	2	-	0	0	1	0	0	0	0
Sh	0	4	1	-	1	0	0	0	1	0
St(m)	3	4	2	5	-	0	0	1	0	0
St(c)	2	2	0	1	3	-	1	1	0	0
Gt	0	0	0	0	4	1	-	0	0	0
Gm/Gt	1	0	0	0	2	1	0	-	0	0
Gm	0	0	0	0	1	1	0	0	-	0
Sm	0	0	0	0	0	0	0	0	0	-

OBSERVED MINUS RANDOM PROBABILTY:

	Se	F	Sr	Sh	St(m)	St(c)	Gt	Gm/Gt	Gm	Se
Se	-	-0.16	-0.06	-0.10	-0.03	0.23	0.15	-0.04	0.03	0.0
F	0.47	-	0.01	-0.02	-0.24	-0.16	-0.06	0.03	-0.02	0.0
Sr	-0.01	0.32	-	-0.08	-0.21	0.10	-0.05	-0.03	-0.02	0.0
Sh	-0.27	0.38	0.09	-	-0.07	-0.14	-0.06	-0.03	0.11	0.0
St(m)	-0.11	0.05	0.07	0.23	-	-0.16	-0.07	0.02	-0.02	0.0
St(c)	-0.09	0.003	-0.05	0.006	0.06	-	0.03	0.06	-0.02	0.0
Gt	-0.27	-0.18	-0.04	-0.08	0.58	0.05	-	-0.03	-0.02	0.0
Gm/Gt	-0.01	-0.17	-0.04	-0.08	0.29	0.11	-0.05	-	-0.02	0.0
Gm	-0.21	-0.17	-0.04	-0.08	0.29	0.36	-0.05	-0.03	-	0.0
Se	0.0	0.0	0.0	0.0	0.0	0.0	0.0	0.0	0.0	-

BINOMIAL PROBABILITY:

	Se	F	Sr	Sh	St(m)	St(c)	Gt	Gm/Gt	Gm	Sm
Se	-	-	-	-	-	0.023	0.037	-	0.394	-
F	0.00	-	0.540	-	-	-	-	0.444	-	-
Sr	-	0.148	-	-	-	0.456	-	-	-	-
Sh	-	0.026	0.297	-	-	-	-	-	0.156	-
St(m)	-	0.401	0.204	0.014	-	-	-	0.475	-	-
St(c)	-	0.615	-	0.627	0.423	-	0.495	0.328	-	-
Gt	-	-	-	-	0.009	0.538	-	-	-	-
Gm/Gt	-	-	-	-	0.193	0.450	-	-	-	-
Gm	-	-	-	-	0.370	0.255	-	-	-	-
Sm	-	-	-	-	-	-	-	-	-	-

SECTION 01/02 HETEROLITHIC FACIES ASSOCIATION

TOTAL NUMBER OF FACIES TRANSITIONS: 73

OBSERVED TRANSITIONS:

	Fm(m)	Fm(g)	Fm(r)	Fr	Fl	Sh	Sr	Sm	CM
Fm(m)	-	2	0	1	0	0	0	1	2
Fm(g)	0	-	1	1	0	0	1	2	8
Fm(r)	3	4	-	2	0	0	2	2	2
Fr	0	0	3	-	1	0	2	1	0
Fl	0	2	1	0	-	0	4	0	0
Sh	0	0	0	0	0	-	0	0	0
Sr	0	0	5	1	2	0	-	0	0
Sm	2	2	1	1	0	0	0	-	0
CM	1	3	3	1	3	0	0	0	-

OBSERVED MINUS RANDOM TRANSITIONS:

	Fm(m)	Fm(g)	Fm(r)	Fr	Fl	Sh	Sr	Sm	CM
Fm(m)	-	0.13	-0.22	0.07	-0.08	0.0	-0.12	0.08	0.15
Fm(g)	-0.09	-	-0.18	-0.03	-0.09	0.0	-0.06	0.06	0.41
Fm(r)	0.10	0.03	-	0.01	-0.09	0.0	-0.01	0.03	-0.07
Fr	-0.08	-0.02	0.19	-	0.05	0.0	0.15	0.06	-0.18
Fl	-0.08	0.08	-0.08	-0.09	-	0.0	0.44	-0.08	-0.18
Sh	0.0	0.0	0.0	0.0	0.0	-	0.0	0.0	0.0
Sr	-0.08	-0.21	0.38	0.02	0.16	0.0	-	-0.08	-0.18
Sm	0.25	0.13	-0.06	0.07	-0.083	0.0	-0.12	-	-0.18
CM	0.0	0.04	0.02	-0.17	0.18	0.0	-0.14	-0.09	-

BINOMIAL PROBABILITY:

	Fm(m)	Fm(g)	Fm(r)	Fr	Fl	Sh	Sr	Sm	CM
Fm(m)	-	0.350	-	0.458	-	-	-	0.402	0.296
Fm(g)	-	-	-	-	-	-	-	0.344	0.001
Fm(r)	0.169	0.491	-	0.523	-	-	-	0.429	-
Fr	-	-	0.205	-	0.459	-	0.007	0.455	-
Fl	-	0.432	-	-	-	-	-	-	-
Sh	-	-	-	-	-	-	-	-	-
Sr	-	-	0.023	0.577	0.149	-	-	-	-
Sm	0.081	0.350	-	0.458	-	-	-	-	-
CM	-	0.462	0.551	-	0.075	-	-	-	-

APPENDIX 11: PALEOCURRENT DATA

CYCLE	UNIT	STR	READINGS
AV	1	LOGS	35,41
	2	TXB	02
	3	LOGS	35,89,61
		TXB	11,41,55
	4	TXB	87
AIV	7	TXB	21,20,46,54,35,53,40,33,33,40,27,07,43,32
		PL	32
		LOG	104,114,153,114,94
AIII	9	TXB	131,118,117,104,138,114,106,104,02,79,85, 78,78,121,121,145,70,100,146,89,135,119,122 130
		CHANNEL	130
		LOGS	02,108,72,92,44,65,61,06
AII	11	LOGS	174,179,147,38,30,11,18,54,03,03
		TXB	44,89,06,99,89,86
		SOLES	302
		RUNNELS	142
AI	13	TXB	101,138,151,91,32,151,86,100,132,126,137, 151,160,107,90
		PL	39,29
		LOGS	72,42,171,70,38,60,44,40,64,82,116
	lower parts:	PL	05,59,29
		LOGS	09,59,29
	14	TXB	321,12,48,19,18,90,130,122,138
BV	1	TXB	314,195
		LOGS	104,95,116,116,71,92
		PL	142
	2	TXB	81,112,90,89,68,28,70,84,74,90,100
		LOGS	178,05,350,14,0,81,108,111
BIV	4	TXB	110,103,107,105,121,106,92,90
		LOGS	132,0,156,178,85,85,104,137,145,143
		SOLE	388,119
BIII	5	RXL	157
BII	7	TXB	106
	8	TXB	86,110,107
		LOGS	160,13,160,171,157,02,132,174
BI	9	TXB	115,124,142
CI	1	PL	26,30,31
		RXL	207
		TXB	127,39,40,35,39,34,85,104,125,110,59,25,102 52,10,36,124,136,116

			LOGS	152,153,171,29,148,28,84
CII-V	2		LOGS	48,164,138,179
	4		TXB	10,23,16,159,135,59,54,26,109,52,95,69,90
			LOGS	163,147,157,163,25
CV	5		TXB	62,115,181,115,121,171,95,125,179,115,151
			PL	171
DI	1		TXB	119,212,206,55,01
			LOGS	163,147,157,163,26
DII	3		TXB	94,163,107
			CHANNEL	154
			SOLES	90
	4		TXB	143
DIII	5		TXB	179,95,95,126,109,128,76,181,88,144,169,168,211, 88,144,169,168,211,159
			LOGS	129,156,126,13,153,130
DIV	7		TXB	81,125,66,98,124,91,58,104,78,179
			LOGS	137,165
		N of Fall D. Bk.	TXB	230,218,228,223,193,185,240
		S of Fall D. Bk.	TXB(U)	44,30,351,0,09
			TXB(M)	62,47,78,96,100,77,121,161, 142,122,162, 125,137,150,121,115,61
			CHANNELS	140
			LOGS	105,107,110,141,112,160,150
		at loc. 1	TXB(U)	51,62,71,63,99,100,62,56,77,43,67,56
		at loc. 2	TXB(U)	90,97,111,97,93,24,92,41
			TXB(M)	86,111,132,106,123,122,125,72,132,77,103
		at loc. 3	TXB(U)	75,80,110,133,101,62,82,110,06,60,95,70
			TXB(M)	115,113,90,71,60,73
		at loc. 7	TXB(U)	80,80,56,52
			TXB(M)	56,52
		at loc.10	TXB(U)	85,83,79
			TXB(M)	93,96,93,85,96,47,105,86
			TXB(L)	21,21
DV	9	at loc.10	SOLE	100,101,73,93,93,97
			CHANNEL	96
			LOGS	82,161,06,01,21,26,06,21,25,06,21,26,177,201 191,104,206
		at loc.10-11	LOGS	159,139,121,145,127,137,11,91,204,195,21,161, 174,121,161,116
		at loc. 9	TXB	141,81,73,79,83,111,110,128
		at loc.3-4	TXB	93,60,60,28,40,22,45
		at loc.7	TXB	70,61,72,73,75,71,85
			LOGS	141,140,158,161,131,152,162,162,150,132,144, 150,140,140,141,125,126,120,150,137,145,151, 154,150,160,147,163,151,130,151,142,162,01,127 115,162,109,81,88,150,141

EV	1	TXB	255,282,165,
		PL	171,155,165,166,172,130
EIV	3	PL	160
	5	PL	102,255,32,25,62
		TXB	82,85,69,0
		LOGS	129,149,148,148,06,149,132,137,158,146
EIII	7	PL	255
		TXB	72
EII	8	TXB	79,99,129,129,125,92,63,100,126,76,41,56
EI	9	TXB	104,124,128,119,220,159,174,181,159,65,99,79, 42
FII	2	SOLE	66,18
		HARROWS	113,113
		TXB	92,52,45,54,59,120,95,52,
	1	TXB	76,52,52,62,62,46,106,86
FI	4	TXB	70,77,67,100,141,108,93,72,61,54,55,60,60,67, 72,72,71,213,108,72,233,226,77,109
		LOGS	165,155,0,165,178,18,161,168,165,164,155,140
	5	LOGS	65,65,70,70,70,90,95,100,101,101,100,95,105, 65,65,70,30,55,24,72,61,50.46,61,46
GVI	2	TXB	109,92
GV	3	SOLE	41,30,35
GIV	4	TXB	132,72,84,74,132,51,118,118,144,143,146,74, 131,205,112,112,113,121,102,63,140,128,147, 154
GII	6	TXB	63,104,126,114,94,110,88,99,84,67,72,19,180, 77,04,03,20,46,80,74,94,37,20,29
		PL	66,106
		LOGS	188,162,168,~~178,168~~,144,166,144,149,147,168, 194,126,170,125,140,171,313,165,250,86,71,66 117,140,147,112,149,115,137,140,05,357
HV	1	PL	63
		TXB	107,63,72,72,61,79,63
HIV	2	TXB	68,70
		LOGS	187,20,183,150,188,173,172,154,154,200,179, 304,25,196,112,127,80,278,117,128,158,149, 125
HIII	4	PL	76
		RXL	42

HI	6	TXB	124,114,165,21,96,85,140,25,89,57,66
		PL	33,31,26,33,40,32,135
		SOLE	56
		LOGS	99,102,145,102,66,63,181
I XI	1	TXB	74
I X	3	TXB	76
I VIII	6	Gm	61
		TXB	65
I VII	8	CHANNEL	135
		TXB	26,28
I VI	10	TXB	53,48,354,73,27,27,345,89,58,30
I V	11	TXB	32,30
I IV	13	TXB	64
	14	TXB	84,138,73,130
I III	16	TXB	46,65,27
I II	18	TXB	85,23,22,20,02
I I	21	TXB	42,26,78,43,31,20,27,55,70
JXII	1	TXB	39,46,26
JIX	7	TXB	60,16,22
JVII	9	TXB	106
JVI	11	TXB	0
	14	TXB	80
JV	15	PL	06,09
JIV	16	TXB	75
	21	TXB	105,71,82,06
JI	22	PL	144
	23	TXB	57,71,218
	27	PL	104,124
		TXB	29,21,28,28,41,44,62,05,60
KVIII	2	TXB	51,32,25,
		Gm	14,345
K VI	4	TXB	57.329,315,72,102,26,312,32,89
KIV	6	TXB	101,25,37,23,54,61
KIII	7	TXB	54,103

LIX	1 and 2	TXB	126,150,96,101,106,51,120,121,152,128,112, 112,122,146,96,120,129,116,109,125,151,96, 111
LVI	5	~~TXB~~	02,16,75,57,06,26,49,160,49
LV	6	TXB	102,109,140,139,63,109,125,96,51,115,142,126 139,111,105,119,152,123,149,162,179
		PL	135,107,141,126,138,66,79,40,179
LIII	10	TXB	119,111,130,133,150
		PB	129
LII	12	TXB	90,130,79,60,57
	13	TXB	80,60
LI	14	TXB	52,31,36,56,30,43,63,58,48,63,96,57,09,53, 58,19,73,60
		TXB	92,167,179,147,132,105,172,144,104,118,120, 144,160,182,145,174,125,142,130,142,152

legend seen in Appendix 12

APPENDIX 12: COMPUTED PALEOCURRENT DATA

CYCLE	UNIT	STR	$\bar{0}$	R	L	P	N	S_0	SIG
AV		LOGS	51.8	4.68	93.6	0.987	5	9.3	**
		TXB	38.7	4.31	86.2	0.975	5	31.2	*
A1V	7	TXB	34.6	13.6	97.6	1.00	14	12.6	***
		LOGS	115.4	4.70	94.0	0.988	5	20.1	**
		PL	32						
A111	9a	TXB	103.0	14.58	85.8	1.00	17	31.7	***
	9[illegible]	TXB	89.4	5.83	97.1	0.99	6	13.9	***
		LOGS	56.9	6.57	82.3	0.995	8	35.8	**
		CHANNEL	130.				1		
A111a	10	TXB	130.						
A11	11	LOGS	43.7	4.62	46.2	0.881	10	71.1	
		TXB	77.0	4.19	83.9	0.970	5	33.9	***
		SOLES	302						
		RUNNELS	142						
A1	13	TXB	118.4	12.68	89.57	1.00	15	33.1	***
		LOGS	68.2	8.96	81.5	0.999	11	36.6	***
		PL	34.0	1.99	99.6	0.862	2	5.1	*
	14	TXB	53.7	5.66	56.6	0.959	10	61.0	*
		LOGS	32.2	2.81	93.6	0.928	3	20.8	***
		PL	13.4	4.98	99.67	0.993	5	4.7	***
	TOTAL	TXB	99.8	15.94	63.8	1.00	25	54.2	
		LOGS	59.8	11.35	81.1	0.999	14	37.0	***
		PL	19.2	6.88	98.4	0.998	7	10.2	***
BV	1a	TXB	254.5	1.01	50.7	0.40	2	66.7	
		LOGS	111.7	4.46	63.8	0.941	7	54.2	*
		SOLE	338						
		RXL	157						
	2	TXB	81.0	10.3	93.7	0.999	11	20.7	***
		LOGS	60.7	4.63	51.5	0.908	9	65.9	*
	TOTAL	TXB	81.7	9.30	71.6	0.998	13	46.8	***
		LOGS	78.5	9.03	64.5	0.997	14	53.6	**
B1V	4	TXB	120.3	7.44	92.9	0.999	8	21.9	**
		LOGS	123.7	7.2	72.1	0.994	10	46.3	**
		SOLE	228.5	0.66	33.3	.199	2	84.9	
B111	5	RXL	157						
B11	8	TXB	115.6	15.6	87.0	1.00	18	30.2	***
		LOGS	120.6	7.6	58.8	.988	13	59.0	**
B1	9b	TXB	126.9	2.94	98.0	.944	3	11.5	**

CI	1	PL	29.0	2.99	99.9	0.95	3	2.6	**
		RXL	207				1		
		TXB	37.4	4.99	99.9	1.00	5	2.56	***
		LOGS	107.9	2.76	39.6	0.66	7	77.9	
	2	LOGS	140.0	2.65	66.3	0.83	4	51.9	
		TXB	85.2	9.99	76.8	1.00	13	41.6	***
	TOTAL	LOGS	123.6	5.21	47.4	0.92	11	69.9	*
CII,III IV,V	4	TXB	57.2	2.26	45.3	0.64	5	72.0	
		LOGS	144.9	3.37	67.6	0.89	5	50.6	
CVI	5	TXB	130.1	9.0	82.2	0.99	11	35.8	***
		PL	171				1		
DI		TXB	156.3	1.8	45.2	0.56	4	72.1	
		LOGS	149						
DII	3	TXB	120.4	2.6	86.8	0.89	3	30.4	*
		CHANNEL	154				1		
		FLUTES	90				1		
	4	TXB	143				1		
	TOTAL	TXB	126.6	3.54	88.7	0.96	4	28.0	*
DIII	5	TXB	122.9	7.49	83.3	0.99	9	34.6	***
		LOGS	128.0	4.36	72.7	0.96	6	45.7	*
	5b	TXB	157.9	4.88	81.3	0.98	6	36.8	***
	TOTAL	TXB	136.6	11.8	78.8	0.99	15	39.5	***
DIVa	7	TXB	98.3	8.46	84.6	0.99	10	33.1	***
		LOGS	151	1.94	97.0	0.85	2	14.1	*
N. of Fall D.		TXB	216.1	16.3	94.7	0.98	7	18.8	***
S. of Fall D.		TXB(U)	14.6	4.71	94.2	0.98	5	19.7	**
		TXB(U)	111.5	15.1	83.7	1.00	18	34.1	***
		CHANNEL	140				1		
		LOGS	117.9	6.09	87.0	0.99	7	30.2	**
	at loc.1	TXB(U)	67.0	11.5	95.8	1.00	12	16.7	***
	at loc.2	TXB(U)	82.0	7.04	88.0	0.99	8	28.9	***
		TXB(M)	108.3	10.3	93.7	0.99	11	20.6	***
	at loc.3	TXB(U)	83.1	10.3	86.6	0.99	12	30.7	***
		TXB(M)	86.8	5.66	93.3	0.99	6	21.3	**
	at loc.7	TXB(U)	67.0	3.89	97.4	0.98	4	13.1	*
		TXB(M)	54.0	1.99	99.9	0.86	2	2.6	*
	at loc.10	TXB(U)	82.3	2.99	99.9	0.94	3	2.6	*
		TXB(M)	88.0	7.68	96.0	0.99	8	16.3	***
		TXB(L)	21.0	2.00	100	0.86	2	0	**
	TOTAL	TXB(U)	69.0	38.9	88.4	1.00	44	28.4	***
	TOTAL	TXB(M)	100.3	39.3	87.4	1.00	45	29.7	***
	TOTAL	TXB	89.8	80.2	74.3	1.00	108	38.0	***
	TOTAL	LOGS	131.8	8.3	92.4	0.99	9	22.7	***
DV 9	at loc.3-4	TXB	49.3	6.49	92.7	0.97	7	22.3	***
	at loc.7	TXB	72.4	6.95	99.3	0.99	7	6.9	***
		LOGS	144.9	24.4	90.6	1.00	27	25.4	***
	at loc.9	LOGS	132.1	12.9	80.8	1.00	16	37.3	***

		TXB	100.4	7.33	91.6	0.99	8	23.9	***
	at loc.10	SOLES	92.9	6.92	98.8	0.99	7	8.9	***
		CHANNEL	96				1		
	at loc.10-11	LOGS	145.8	12.8	75.4	0.99	17	43.0	***
		LOGS	50.5	6.2	34.4	0.82	18	83.6	
		TOTAL TXB	75.0	19.4	88.3	1.00	22	28.6	***
		TOTAL LOGS	134.7	50.2	64.4	1.00	78	53.7	***
EV	1	TXB	169.2	5.35	76.4	0.983	7	42.0	**
EIV	3	PL	160				1		
	5	TXB	67.4	7.62	7.62	0.997	10	42.2	*
		PL	88.5	0.47	23.3	0.10	2	99.2	
		LOGS	139.3	8.17	81.7	0.99	10	36.4	***
EIII	7	PL	75				1		
		TXB	72				1		
EII	8	TXB	93.1	10.4	87.4	1.00	12	29.7	***
EI	9	TXB	126.6	8.9	68.7	0.99	13	49.6	**
		LOGS	142.0	8.0	80.2	0.9	10	38.0	***
FII	1	TXB	67.4	7.56	94.6	0.999	8	19.1	***
	2	SOLES	42.0	1.82	91.3	0.81	2	24.4	*
		HARROWS	113.0	2.00	100.0	0.87	2	0.00	*
		TXB	70.4	7.23	90.3	0.999	8	25.9	**
FI	4	TXB	85.0	16.2	70.5	1.00	23	47.8	***
		LOGS	155.2	8.15	67.9	0.99	12	50.3	**
	1 at loc.18	LOGS	71.5	24.1	92.8	1.00	26	22.1	***
GVI	2	TXB	100.5	1.97	98.9	0.86	2	8.5	**
	3	TXB	35.3	2.99	99.7	0.949	3	4.44	***
GIV	4	TXB	188.8	20.9	83.7	1.00	25	34.1	***
GI	7	SOLES	93				1		
	8	TXB	82.3	70.0	88.6	1.00	79	28.1	***
		LOGS	158.0	38.4	85.4	1.00	45	32.1	***
		PL	03				1		
GII	6	TXB	94.9	9.45	94.5	0.99	10	19.2	***
at Carrying C.		TXB	47.7	10.5	73.4	0.99	14	45.0	***
		LOGS	144.4	22.1	67.3	1.00	33	50.9	***
		TOTAL TXB	69.9	18.3	65.5	1.00	28	52.6	***
		PL	86.0	1.87	93.9	0.829	2	20.3	**
HV	1	TXB	74.3	7.76	97.0	0.99	8	14.1	***
		PL	63				1		
HIV	2	TXB	69.0	1.99	99.9	0.87	2	2.5	**
		LOGS	154.7	13.5	58.7	0.99	23	59.1	***
HIII	4	PL	76				1		
		RXL	42				1		

HI	6	TXB	89.3	8.16	74.2	0.99	11	44.2	**
		PL	42.1	5.85	83.5	0.99	7	34.3	**
		SOLE	56				1		
		LOGS	95.6	5.45	77.9	0.98	7	40.4	**
I XI	1	TXB	74				1		
I X	3	TXB	76				1		
I VIII	6	Gm	61				1		
		TXB	65				1		
I VII	8	CHANNEL	135				1		
		TXB	27.0	2.00	99.9	0.865	2	2.56	***
I VI	10	TXB	40.3	7.63	84.8	0.99	9	32.8	***
I V	11	TXB	31.0	1.99	99.9	0.86	2	2.6	**
I IV	13	TXB	64				1		
		TXB	106.2	3.52	88.1	0.96	4	28.8	**
		TOTAL TXB	97.3	4.32	86.4	0.98	5	30.9	*
I III	16	TXB	36.5	1.97	98.6	0.857	2	9.62	***
I II	18	TXB	28.9	4.42	88.5	0.980	5	28.3	***
I I	21	TXB	43.3	8.5	94.4	0.99	9	19.4	***
TOTAL FOR I			53.2	25.5	85.3	1.00	30	32.2	***
JXII	1	TXB	37.0	2.96	98.9	0.99	3	8.5	**
JIX	7	TXB	32.4	2.83	94.3	0.931	3	19.6	***
JVI	11	TXB	0				1		
	14	TXB	80				1		
JIV	15	TXB	7.5	1.99	99.9	0.864	2	2.56	
	16	TXB	75				1		
	21	TXB	68.2	3.23	80.9	0.93	4	37.2	*
JI	22	PL	144				1		
	23	TXB	85.9	1.17	39.0	0.36	3	78.5	*
	27	PL	114.0	1.96	98.4	0.86	2	10.2	*
		TXB	35.3	8.59	95.5	0.99	9	17.3	***
		TOTAL TXB	40.8	9.38	78.1	0.99	12	40.2	***
		TOTAL TXB	124.0	2.87	95.9	0.94	3	16.5	
	TOTAL TXB FOR I		47.4	18.6	81.0	1.00	23	37.1	***
	2	TXB	21.6	4.64	92.9	0.987	5	21.9	***
KVI	4	TXB	25.2	4.53	56.6	0.923	8	61.1	*

KIV	6	TXB	49.2	5.38	89.6	0.99	6	26.8	**
KIII	7	TXB	78.5	1.81	90.9	0.80	2	25.0	**
KI	10	PL	65.0	4.94	98.9	0.99	5	8.5	**
		TXB	73.9	20.4	81.5	1.00	25	36.6	***
TOTAL TXB FOR K			69.0	28.1	82.8	1.00	34	35.1	***
LIX	1 and 2	TXB	117.8	24.4	93.8	1.00	26	20.3	***
LV	6	TXB	134.4	15.4	95.9	1.00	16	16.5	***
		PL	127.8	2.9	96.7	0.94	3	14[illegible]	**
LIII	10	TXB	128.3	4.86	97.3	0.99	5	13.3	**
		PL	129				1		
LII	12	TXB	82.4	4.49	89.8	0.98	7	23.6	**
	13	TXB	70.0	1.96	98.4	0.86	2	10.3	*
LI	14	TXB	50.2	16.9	94.3	1.00	18	19.6	***
	15	TXB	141.8	19.1	90.9	1.00	21	25.0	***
	TOTAL	TXB	99.5	25.2	64.6	1.00	39	53.5	***
TOTAL TXB FOR L			106.7	67.1	77.9	1.00	86	51.2	***

STR = sedimentary structure
$\bar{\emptyset}$ = paleocurrent in degrees
R = vector length
L = vector magnitude in percent
N = number of observations
S_0 = standard deviation
SIG = statistical significance
(U) = upper part of unit
(M) = middle part of unit
(L) = lower part of unit
TXB = trough crossbedding
RXL = ripple cross-lamination
PL = parting lineation
* = significant at 0.10
** = significant at 0.01
*** = significant at 0.001

APPENDIX 13: MEAN CLAST SIZE

UNIT	MEAN 100 (CM) A	SD	SN	N	MPS (CM) A	SD
A7	1.35	0.440	0.302	100	2.15	0.65
A9	1.42	0.529	0.328	100	3.33	-
A11	1.88	0.963	0.512	100	6.61	-
A13	1.70	0.670	0.394	100		
A14	2.14	0.891	0.416	100	4.43	-
B1	2.26	0.62	0.278	100		
B4	1.88	0.936	0.498	100	9.95	-
B6	1.78	0.829	0.466	100		
B8	3.04	1.26	0.498	102	12.5	-
C1	1.64	0.769	0.469	50		
C4	1.76	0.849	0.482	50		
C5	2.40	1.27	0.529	50		
D1	2.53	1.26	0.498	50	4.72	-
D3	2.50	0.87	0.348	102	6.56	-
D5a	2.31	0.79	0.342	101	7.55	1.30
D5b	2.77	0.97	0.350	101	8.85	1.33
D5c	1.57	0.49	0.312	100		
D5d	2.16	0.97	0.449	100		
D5e	1.66	0.66	0.398	100		
D7a	1.86	0.77	0.414	105	6.5	0.94
D7b	1.93	0.85	0.440	100	7.34	1.57
D7c	2.58	1.03	0.399	65	7.71	1.25
D7d	2.04	0.99	0.485	100	6.34	1.17
D7e	2.57	1.24	0.482	100	8.12	0,87
D7f	2.64	1.41	0.534	100	13.3	3.7
D7g	2.65	1.38	0.521	100	9.73	1.64
D7h	2.33	1.18	0.506	100	9.33	1.26
D7i	2.42	1.44	0.595	100	9.61	1.22
D7j	2.66	1.38	0.505	100	8.56	1.11
D9	1.74	0.793	0.456	50		
E5	2.10	1.11	0.529	100		
E7	2.79	1.41	0.505	100	10.2	1.83
E8	2.33	1.34	0.575	100		
E9	2.51	1.31	0.522	100	12.9	2.11
F1	1.97	1.05	0.533	50		
F3	2.87	1.60	0.557	50		
F4a	2.37	1.93	0.814	93	9.87	1.24
F4b	2.18	1.37	0.628	100	12.4	1.85
F4bi	2.71	1.67	0.616	100	14.6	2.12
F4c	3.60	2.68	0.744	100	14.5	3.7
F4d	3.14	2.14	0.628	100	17.8	3.98
G1	2.29	1.41	0.616	50		
G2	2.87	1.47	0.512	99	9.72	1.00
G3	1.88	0.734	0.390	50		
G4	3.37	1.97	0.585	99	15.8	2.66
G4	2.24	1.03	0.460	50		
G6a	2.86	1.61	0.563	100	10.9	1.14
G6b	4.57	2.71	0.593	100	13.8	1.97
G8a	2.84	2.12	0.746	100	14.2	3.15
G8b	2.47	1.69	0.684	100	11.6	2.81

G8c	3.23	1.47	0.455	100	12.6	1.78
G8d	3.11	1.70	0.547	100	15.0	2.3
H2	2.39	1.35	0.565	100	9.05	0.76
I3	3.52	1.75	0.497	100	17.1	2.85
I4	2.45	1.44	0.588	50		
I5	3.27	2.18	0.667	50		
I8	2.82	1.57	0.557	100		
I10	3.25	1.82	0.560	100	17.83	2.09
I12	2.87	1.50	0.523	100	11.4	1.9
I14	3.53	1.97	0.558	100	19.9	5.26
I16	3.24	1.92	0.593	100	14.9	2.07
I18	2.76	1.48	0.536	100	10.0	8.82
I21	2.99	2.13	0.712	100	11.8	1.99
J1	2.70	1.34	0.496	100	14.8	3.09
J3	3.14	1.71	0.545	100	11.1	1.77
J7	2.39	1.25	0.523	50		
J9	2.61	1.34	0.513	50		
J11	2.65	1.47	0.555	75	9.35	1.70
J15	2.30	1.10	0.478	50		
J16	3.67	2.55	0.695	100	18.5	3.16
J18	2.45	1.59	0.649	50		
J19	1.68	0.686	0.408	50		
K2	2.58	1.41	0.547	100	9.67	1.82
K2	1.96	1.02	0.502	50		
K4	2.05	0.987	0.481	50		
K6	2.67	1.37	0.513	100	9.32	1.17
K7	2.20	1.12	0.509	50		
L12	2.11	1.14	0.540	100	5.96	1.35
L13	2.61	1.36	0.521	100	9.68	1.2
L15	2.14	1.12	0.549	100	8.64	1.04
N1	3.75	2.20	0.587	100	14.3	3.07
N2a	3.26	2.53	0.776	100	16.1	2.07
N2b	2.52	1.23	0.488	100	10.1	1.71
N4	2.89	1.27	0.439	100	11.0	1.05
N8a	3.67	2.27	0.619	100	13.52	2.62
N8b	2.95	1.97	0.668	100	25.0	6.63
N8c	2.79	1.76	0.631	100	17.9	2.09
N15	2.51	1.09	0.434	100		

A = length of apparent a axis

S_D = standard deviation

S_N = normalized standard deviation

N = number of observations

APPENDIX 14: CLAST/MATRIX PERCENTAGE FOR VARIOUS UNITS

UNIT/LOC.	MATRIX %	CLAST %	S_D	N
D3	69.3	30.7	10.7	731
D4	26.8	75.3	12.2	837
D5a	45.3	54.6	18.3	889
D5b	71.9	28.1	15.3	1070
D5 (total)	59.8	40.1	19.7	1959
D7a at 2	85.4	14.5	-	246
D7b at 9	64.9	35.1	-	259
D7d at 3	49.6	50.4	-	224
D7e at 5	43.2	56.8	-	227
D7f	43.8	56.1	10.1	928
D7g	35.8	64.2	2.9	463
D7h at 9	58.4	41.6	-	257
D7 (total)	50.4	49.6	16.0	2374
E7 at 11	56.4	43.6	-	220
E9	52.1	47.9	-	219
F4	63.1	36.6	9.6	651
G6	35.7	64.3	6.5	409
L13	80.1	19.9	-	206
N3	49.8	50.2	-	201
N8b	54.6	45.3	-	637
N10	60.3	39.8	7.5	416
N13	44.7	25.3	3.9	667

MATRIX is defined as pebbles <0.01m

S_D = standard deviation

N = number of point counts from photographs

LOC. = location

APPENDIX 15: LITHOTYPE PERCENTAGES FOR CLASTS

UNIT	SYN	GRAN	GNS	RHY	QTZT	SST	MDST	PHY	OTH
A11	4.0	18.8	2.0	8.9	52.8	2.0	-	-	-
A14a	8.0	8.0	12.5	3.0	40.2	18.7	-	-	-
A14b	20.0	6.3	15.0	1.3	6.3	45.1	-	-	-
A14c	13.0	13.0	7.8	3.5	10.4	48.4	-	-	-
B1	9.0	9.0	2.0	-	15.0	58.0	5.0	-	-
B4	8.3	-	2.1	1.0	12.5	68.8	1.0	-	-
B8	5.6	1.1	0.7	0.7	31.0	56.0	1.1	-	-
D3	20.6	2.9	3.9	-	30.9	34.3	2.0	2.0	-
D5a	10.9	18.8	5.9	-	40.6	20.8	-	-	-
D5b	4.0	18.8	5.9	-	25.7	44.6	-	-	-
D5c	12.0	37.0	2.0	-	20.0	27.0	-	-	-
D5d	5.0	17.0	2.0	-	26.0	47.0	-	1.0	-
D5e	5.0	19.0	3.0	-	39.0	32.0	1.0	-	-
D7a	13.5	19.2	4.8	1.0	43.3	14.6	-	-	-
D7b	17.0	12.0	6.0	3.0	43.0	14.0	-	-	-
D7c	15.4	26.2	3.1	-	38.5	10.7	-	-	-
D7d	22.0	9.0	1.0	-	47.0	19.0	1.0	-	-
D7e	13.0	14.0	3.0	1.0	28.0	40.0	-	-	-
D7f	11.0	0.9	6.0	1.0	32.0	34.0	4.0	-	-
D7g	7.0	20.0	2.0	-	36.0	23.0	6.0	2.0	-
D7h	8.0	20.0	2.0	-	32.0	22.0	7.0	1.0	-
D7i	6.0	13.0	5.0	-	29.0	39.0	2.0	-	-
D7j	14.0	5.0	-	1.0	51.0	18.6	4.0	-	-
E7	19.0	8.0	1.0	4.0	34.0	30.0	2.0	-	-
E9	5.0	6.0	3.0	36.0	40.0	6.0	-	-	-
F4a	5.4	3.3	2.2	-	54.3	27.2	-	-	-
F4bi	12.0	7.0	1.0	-	44.0	30.0	7.0	-	-
F4bii	10.0	5.0	3.0	-	35.0	33.0	6.0	-	-
F4c	8.0	5.0	-	-	29.0	47.0	8.0	-	-
F4d	6.0	2.0	1.0	-	45.0	32.0	2.0	-	-
G2	14.0	17.0	4.0	-	31.0	24.0	1.0	5.0	-
G4	8.0	11.0	1.0	-	39.0	33.0	4.0	1.0	-
G6a	13.0	16.0	2.0	-	30.0	31.0	1.0	6.0	-
G6b	3.0	5.0	-	-	32.0	47.0	-	10.0	-
G8a	7.0	-	1.0	2.0	53.0	33.0	-	-	-
G8b	3.0	5.0	2.0	-	38.0	45.0	2.0	-	-
G8c	13.0	8.0	3.0	1.0	35.0	35.0	2.0	1.0	-
G8d	7.0	6.0	2.0	-	31.0	48.0	-	-	-
H2	10.0	2.0	3.0	-	60.0	28.0	5.0	-	-
I3	6.0	12.0	2.0	4.0	36.0	23.0	3.0	23.0	9.0
I10	8.0	16.0	1.0	1.0	48.0	16.0	-	5.0	5.0
I12	11.0	17.2	2.0	1.0	32.0	22.0	4.0	2.0	8.0
I14	7.0	10.0	4.0	-	30.0	23.0	-	8.0	21.0
I16	9.0	1.0	3.0	-	24.0	11.0	-	17.0	31.0
I18	17.0	5.0	1.0	1.0	38.0	8.0	5.0	9.0	14.0
I21	12.0	9.0	2.0	-	38.0	14.0	1.0	9.0	14.0
J1	12.0	6.0	3.0	-	26.0	19.0	5.0	11.0	18.0
J3	15.0	12.0	4.0	-	27.0	17.0	1.0	12.0	7.0
J11	29.3	1.3	-	2.6	24.0	13.2	2.7	10.6	16.0
J16	14.0	3.0	-	-	40.0	12.0	2.0	9.0	18.0
K2	14.0	2.0	-	1.0	63.0	10.0	1.0	2.0	6.0

K6	13.0	1.0	-	-	58.0	8.0	1.0	12.0	5.0
L12	92.0	-	-	-	7.0	-	-	-	1.0
L13	37.0	3.0	1.0	1.0	21.0	26.0	1.0	-	7.0
L15	39.0	3.0	1.0	-	32.0	22.0	1.0	-	1.0
N1	43.0	28.0	14.0	1.0	-	-	2.0	4.0	8.0
N2a	71.0	18.0	3.0	-	-	-	2.0	4.0	2.0
N2b	39.0	3.0	1.0	-	32.0	22.0	1.0	-	1.0
N4	70.0	23.0	2.0	-	-	-	-	5.0	-
N8a	56.0	28.0	5.0	-	3.0	1.0	-	5.0	-
N8b	40.0	43.0	9.0	-	-	-	1.0	2.0	5.0
N8c	34.0	51.0	11.0	-	-	-	-	-	-

SYN = syenite
GRAN = granite
GNS = gneiss
RHY = rhyolite
QTZT = quartzite
SST = sandstone
MDST = mudstone
PHY = phyllite
OTH = others

APPENDIX 16: PETROGRAPHIC RESULTS (%)

UNIT	1	2	3	4	5	6	7	8	9	10	11	12
A1	58.0	4.6	7.0	5.3	0.3	0.3	-	0.6	0.6	1.3	21.6	-
A2	42.3	9.0	5.3	7.3	4.3	5.0	3.6	7.3	8.6	0.3	1.6	-
A3	48.6	6.0	6.6	3.0	5.3	4.6	3.3	9.3	9.0	-	4.0	-
A7	52.6	3.0	9.3	1.6	3.6	3.6	5.3	0.6	10.0	10.3	0.6	2.6
A9	57.6	5.6	6.3	2.3	4.0	0.6	1.3	14.0	6.3	0.6	1.0	-
A11	32.3	12.3	5.6	2.6	5.0	1.0	4.3	21.6	13.0	-	0.6	-
A13	42.0	7.3	5.0	1.0	1.3	0.3	-	25.6	7.6	-	2.6	-
A14c	24.0	5.0	4.0	0.6	4.0	0.6	1.3	15.0	19.0	-	-	20.3
B1	45.3	4.3	7.3	0.6	2.0	0.3	1.0	8.0	17.3	-	7.3	-
B1a	24.3	16.3	1.6	2.0	20.3	1.0	0.3	22.0	7.3	-	4.3	-
B1b	53.6	4.0	4.0	2.3	0.3	0.3	0.3	19.6	10.6	-	1.0	-
B5	35.3	-	3.6	-	-	-	-	-	-	5.0	55.0	-
B9i	43.3	1.6	1.3	0.6	-	-	-	4.6	0.3	0.6	47.3	-
B9ii	44.0	7.0	6.0	-	0.6	0.6	0.3	7.0	1.3	-	6.3	20.3
D1	48.3	9.3	10.3	1.0	-	0.3	0.6	14.6	7.0	-	2.3	-
D7	61.6	8.0	1.3	0.3	-	0.3	-	13.3	4.0	1.0	5.3	-
D3	26.0	10.0	10.6	1.0	-	0.6	4.0	19.3	19.0	0.6	0.6	
D5	61.3	6.3	5.6	0.6	-	0.3	0.6	12.6	6.0	0.6	2.6	-
D2	58.6	1.0	12.3	0.3	-	-	-	1.0	-	0.6	26.0	-
D8	53.6	4.0	7.3	1.6	-	3.6	0.3	6.0	1.3	20.3	-	-
D7	39.6	11.0	4.3	1.0	6.3	1.6	6.3	20.0	4.6	-	1.6	-
E1	54.6	6.0	6.0	2.3	-	0.3	-	13.0	2.6	1.3	13.3	-
E5	51.3	6.0	3.6	1.0	1.6	0.3	20.0	1.0	-	6.6	-	-
E3	47.6	-	5.0	-	-	-	-	-	-	-	46.6	-
E3	60.0	5.6	3.6	2.3	-	0.3	-	13.6	1.0	-	13.3	-
F1	31.0	8.6	6.6	1.3	8.3	-	4.0	24.6	7.3	-	6.6	-
F3	29.6	6.3	2.3	1.0	11.3	2.0	0.6	30.3	3.3	-	12.0	-
G4b	48.0	5.6	2.3	1.0	0.3	11.3	13.9	2.6	-	10.0	1.0	-
G1	51.0	10.3	7.6	1.3	0.6	0.3	-	13.0	3.3	0.3	7.3	-
G3	30.6	12.0	12.0	2.6	3.0	2.0	0.6	21.0	6.3	0.6	4.3	-
G6	29.3	14.3	5.3	2.3	8.6	-	5.3	18.3	7.3	0.6	4.0	-
H1	59.0	3.3	8.6	3.6	-	-	-	10.0	2.3	-	11.3	-
H5	52.6	0.3	4.0	1.0	-	-	-	1.3	-	2.5	38.0	-
H2	54.6	5.6	6.3	2.3	-	-	-	13.3	2.3	0.6	11.3	-
H4	62.3	7.6	5.0	4.3	0.3	-	0.6	5.6	-	-	10.0	-
H4	53.3	5.3	8.6	2.3	0.3	0.3	0.3	12.6	1.0	0.6	5.3	-
H5	49.6	9.3	6.3	5.3	-	0.6	-	11.6	5.3	-	7.0	-
H6	51.0	6.0	10.6	3.6	0.6	-	0.3	11.0	1.3	-	15.0	-
I2	40.5	5.8	12.6	1.9	1.8	0.9	0.9	9.1	2.7	1.8	26.7	-
I6	21.3	12.6	11.3	2.3	2.3	2.0	2.3	24.3	7.3	-	13.3	-
I18	21.3	11.6	11.3	4.0	2.6	1.3	3.3	28.0	5.0	0.3	10.3	-
I12	8.0	9.0	4.3	0.6	20.3	1.0	4.3	26.0	17.3	-	8.0	-
J1	11.3	8.3	4.6	2.6	6.3	0.6	11.3	22.3	10.0	-	6.6	-
J2	30.0	6.3	15.3	7.0	1.3	1.3	0.3	27.0	2.0	0.3	8.0	-
J4	30.6	2.3	15.0	5.0	0.3	1.3	1.0	32.0	3.3	-	8.3	-
J6	8.6	8.3	6.0	1.0	8.0	1.3	13.0	28.6	10.6	-	1.6	-
J15	53.6	6.3	6.3	2.0	0.6	1.0	0.3	13.3	1.0	-	10.6	-
J19	11.6	6.6	4.0	2.0	6.6	2.3	9.0	29.6	11.0	-	7.6	1.3
J21	48.3	4.0	6.3	4.6	3.0	1.3	4.3	19.3	1.6	-	2.0	
K6	4.6	6.6	2.6	-	5.3	0.6	9.3	20.6	22.0	-	1.3	26.0
K9	19.6	5.0	6.6	2.3	-	-	1.6	15.6	4.6	0.3	43.6	-

N1	7.3	5.6	21.0	4.6	8.0	2.3	10.0	0.6	-	-	40.3	-
N2	7.3	9.3	13.3	4.0	19.6	1.0	28.3	1.6	-	-	13.6	-
N4	14.3	8.0	14.0	10.0	12.0	1.3	18.0	1.0	-	-	18.3	-
N9	12.3	12.0	11.6	3.6	16.6	3.6	18.3	1.6	-	-	11.6	-
N9	14.6	5.6	13.0	3.6	27.6	1.0	1.6	7.0	-	-	20.6	-
N10	16.3	1.3	20.6	3.3	11.6	2.3	1.3	11.3	0.6	-	31.0	-

1 = Q_{mcxl} : microcrystalline quartz

2 = Q_{pcxl} : polycrystalline quartz

3 = F_k : potassic feldspar

4 = F_p : sodic feldspar

5 = IRF: igneous rock fragment

6 = MRF 1: type 1 metamorphic rock fragments

7 = MRF 2: type 2 metamorphic rock fragments

8 = SRF 1: type 1 sedimentary rock fragments

9 = SRF 2: type 2 sedimentary rock fragments

10 = heavy minerals

11 = matrix (includes porosity)

12 = secondary calcite

APPENDIX 17: GLOSSARY FOR TERMINOLOGY USED IN THE TEXT

Clast-supported conglomerate: A clastic rock with 50% (or more) of clasts greater than 1.0cm.

Clast: a rock particle with "A" axis greater than 1.0cm.

High order channel: Large channels within the braided fluvial system usually characterized by coarser bedload (eg. gravels) and deeper/wider channels.

Lithofacies unit: A unit of rock comprising a specific lithofacies.

Low order channels: Small channels within a braided fluvial system often characterized by shallow channels and fine-grained bedload (eg. sands).

Matrix-supported conglomerates: A clastic rock with less than 50% clasts (larger than 1.0cm).

Pebble: A rock particle larger than granule size but smaller than 1.0cm.

Pebbly clast-supported sandstones: A clastic rock comprising greater than 50% pebbles (up to 1.0cm).

Pebbly matrix: Matrix within a conglomerate which is larger than coarse granule size and smaller than 1.0cm.

Pebbly matrix-supported sandstones: A clastic rock with less than 50% pebbles (less than 1.0cm).

Pebbly sandstone: A clastic rock comprising clasts ranging in size between very fine sand to 1.0cm.

Stratigraphic Unit: A stratum of rock defined on the basis of its lithological characteristics.